Evidence-Based Complementary and Alternative Medicine

The Role and Mechanism of Electroacupuncture for Neurological Diseases

Lead Guest Editor: Feng Zhang
Guest Editors: Yuchuan Ding, Peng-Yue Zhang, and Wei-Lin Liu

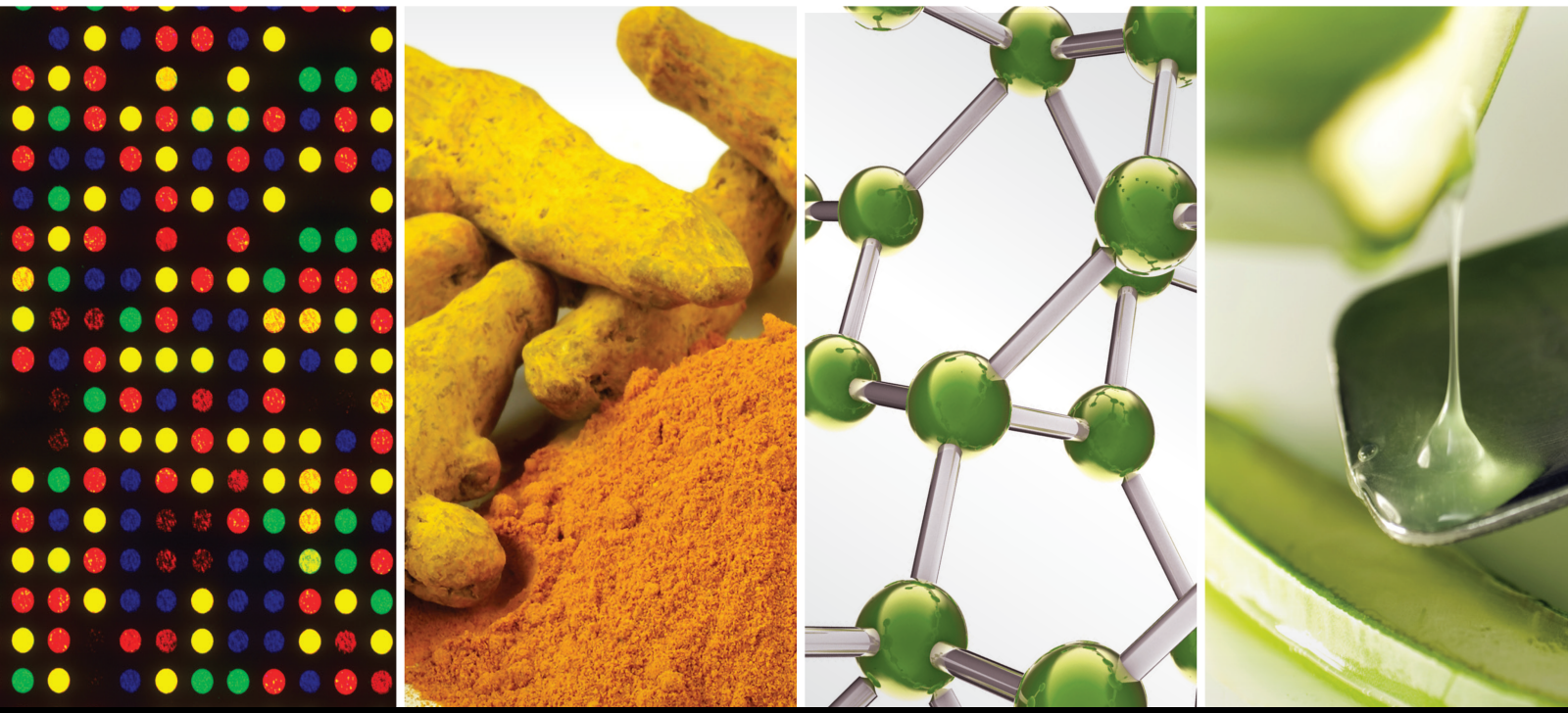

The Role and Mechanism of Electroacupuncture for Neurological Diseases

Evidence-Based Complementary and Alternative Medicine

The Role and Mechanism of Electroacupuncture for Neurological Diseases

Lead Guest Editor: Feng Zhang
Guest Editors: Yuchuan Ding, Peng-Yue Zhang, and Wei-Lin Liu

Chief Editor

Associate Editors

Academic Editors

Contents

Hindawi
Evidence-Based Complementary and Alternative Medicine
Volume 2021, Article ID 8837625, 18 pages
https://doi.org/10.1155/2021/8837625

Review Article

The Effectiveness of Acupuncture for Dysphagia after Stroke: A Systematic Review and Meta-Analysis

Lida Zhong,[1] **Jing Wang**,[1] **Fang Li**,[1] **Xiao Bao**,[1] **Huiyu Liu**,[1] **and Pu Wang**[2]

[1]*Department of Rehabilitation Medicine, Yuebei People's Hospital, Shaoguan, Guangdong 512026, China*
[2]*Department of Rehabilitation Medicine, The Seventh Affiliated Hospital Sun Yat-sen University, Shenzhen, Guangdong 518107, China*

Correspondence should be addressed to Huiyu Liu; liuhuiyudoctor@sohu.com and Pu Wang; wangpu_03@126.com

Received 27 August 2020; Revised 10 October 2020; Accepted 7 January 2021; Published 19 January 2021

Academic Editor: Feng Zhang

Objectives. This study reviewed and evaluated existing evidence of the efficacy of acupuncture as a clinical treatment for dysphagia after stroke. *Methods*. Five English and four Chinese databases were searched from inception to March 2020. All randomized controlled trials (RCTs) incorporating acupuncture or acupuncture combined with other interventions for the treatment of dysphagia after stroke were enrolled. All data were independently assessed and extracted by two authors. The bias risk assessment recommended by the Cochrane Collaboration's tool was used to assess the quality of the selected studies. This meta-analysis was conducted by using RevMan 5.3. Pooled analyses were calculated by the mean difference (MD) and 95% confidence interval (CI). Heterogeneity was assessed by the I^2 test. *Results*. Thirty-five studies involving 3024 patients were analyzed. The meta-analysis showed that the therapeutic efficacy of acupuncture combined with other interventions was better than that of the control group for the standardized swallowing assessment (SSA) score (MD = −3.78, 95% CI: −4.64 to −2.91, $P < 0.00001$), Ichiro Fujishima rating scale (IFRS) score (MD = 1.68, 95% CI: 1.16 to 2.20, $P < 0.00001$), videofluoroscopic swallowing study (VFSS) score (MD = 2.26, 95% CI: 1.77 to 2.74, $P < 0.00001$), and water swallowing test (WST) score (MD = −1.21, 95% CI: −1.85 to −0.57, $P = 0.0002$). In studies reporting adverse effects, no serious outcome from an adverse event was confirmed. *Conclusion*. This systematic review indicated that acupuncture could be an effective therapy for treating dysphagia after stroke although stricter evaluation standards and rigorously designed RCTs are needed.

1. Introduction

Dysphagia is one of the most common poststroke sequelae, accounting for 27 to 64% of stroke patients [1], and is often associated with malnutrition, pneumonia, and dehydration [2]. The previous study [3] has shown that dysphagia after stroke affects quality of life, carries increased risks of mortality and dependency, prolongs hospital stays, increases healthcare costs, and often leads to discharge from the hospital to a care home. Therefore, to accelerate the recovery of swallowing function and reduce these risks, it is very important to find an effective treatment for dysphagia.

At present, there are many treatments for dysphagia, such as behavioral interventions, drug therapy, physical stimulation, and transcranial magnetic stimulation. Some of these treatments have made considerable progress [4]. However, clinical evidence to establish their roles in the management of poststroke dysphagia is limited [4], and there is no clear treatment for dysphagia.

Acupuncture, as a form of alternative medicine, is a traditional treatment that is clinically effective for neurological diseases [5, 6]. Acupuncture treatment exerts therapeutic effects by inserting a needle at specific acupoints on the body surface with stimulation delivery via manual rotation or electric pulses [7–9]. Some randomized controlled trials (RCTs) [10, 11] have shown that acupuncture may reduce the proportion of participants with dysphagia at the end of the trial. However, despite the high heterogeneity, the latest updated Cochrane review [12] on swallowing therapy, which included an analysis of acupuncture, failed to show

improvement in swallowing ability. There is still a lack of high-quality research on acupuncture treatment of dysphagia [12], and many clinical studies are still in the preliminary stage, with great differences in the acupuncture methods and the selection of acupoints in the research, leading to the inconclusive conclusion of acupuncture treatment for dysphagia.

This systematic review and meta-analysis aimed to evaluate the potential availability and safety of acupuncture for poststroke dysphagia.

2. Methods

The protocol was registered on the International Platform of Registered Systematic Review and Meta-analysis Protocols (INPLASY2020100036), and it was conducted according to the preferred reporting items for systematic reviews and meta-analysis (PRISMA): The PRISMA Statement [13].

2.1. Search Strategy. We searched the following databases from their inception until March 2020: EMBASE (via Ovid), MEDLINE (via Ovid), the Cochrane library (via Ovid), PubMed (via website), ScienceDirect (via website), China National Knowledge Infrastructure (CNKI) (via website), China Biology Medicine disc (CBMdisc) (via website), China Science and Technology Journal Database (VIP) (via website), and Wanfang Data (via website). Manual searches of relevant references were also conducted. The search terms were ("dysphagia," "swallowing disorders," "deglutition disorders," or "swallowing dysfunction") and ("stroke," "cerebral apoplexy," or "cerebrovascular accident") and ("acupuncture," "needling," "electroacupuncture," or "warm acupuncture").

2.2. Inclusion and Exclusion Criteria

2.2.1. Types of Studies. All RCTs of acupuncture for dysphagia after stroke were selected and excluded nonrandomized studies, observational studies, animal studies, qualitative studies, and letters.

2.2.2. Types of Participants. All patients conformed to the explicit clinical diagnosis criteria of stroke and dysphagia: (1) the participants were clinically diagnosed with ischemic or hemorrhagic stroke by computerized tomography or magnetic resonance imaging; (2) dysphagia was diagnosed using a clinical bedside swallowing assessment, a videofluoroscopic swallowing study (VFSS), or a fiberoptic endoscopic examination of swallowing (FEES).

2.2.3. Types of Interventions. For the intervention in experimental trials, acupuncture alone or acupuncture combined with other interventions was included, and other interventions included behavioral interventions, drug therapy, and electrical stimulation. The interventions should be the same between experimental and control trials, except for acupuncture in the experimental trials.

2.2.4. Types of Outcome Measures. The clinical symptoms had obviously improved with specific evaluation standards, such as (1) Watian swallowing test (WST) [14], (2) standardized swallowing assessment (SSA) [15–17], (3) penetration-aspiration scale (PAS) [18], and (4) functional oral intake scale (FOIS) [19], or by using an objective index, such as (1) VFSS [20] and (2) endoscopic evaluation of swallowing [21], as the efficacy evaluation criterion.

2.3. Data Extraction. Data were extracted by three review authors (Lida Zhong, Jing Wang, and Fang Li) independently using a standardized form after evaluation. Disagreements were resolved with the assistance from a fourth author (Pu Wang), if necessary. Data extracted included the surname of the first author, year of publication, intervention used in the acupuncture and control groups, evaluation time, outcomes, conclusions, follow-up duration, and adverse effects.

2.4. Risk of Bias Assessment. The included RCTs were assessed according to the Cochrane risk of bias assessment tool [22], and this process was carried out independently by the two review authors (Lida Zhong and Jing Wang). Quality was assessed as having a low, an unclear, or a high risk of bias according to seven criteria: (1) random allocation method (selection bias); (2) allocation concealment (selection bias); (3) blinding of assessors (performance bias); (4) blinding of outcome assessment (detection bias); (5) integrity of data results (attrition bias); (6) selective reporting (reporting bias); and (7) other sources of bias. Any disagreements that arouse at any stage between the two reviews were resolved through discussion with a third author (Pu Wang).

2.5. Statistical Analysis. All statistical analyses were performed using RevMan 5.3 (http://ims.cochrane.org/revman). For dichotomous variables, the relative risk (RR) with its 95% confidence interval (CI) was calculated. For continuous variables, the mean difference (MD) and standardized mean difference (SMD) with their 95% CIs were calculated. The heterogeneity between each group was tested by Cochran's Q statistic and the I^2 test [23]. Studies with an I^2 of 25% to 50% were considered to have low heterogeneity, and I^2 values of 50% to 75% and >75% were considered indicative of moderate and high levels of heterogeneity, respectively. Fixed-effect models were used to combine studies if the I^2 test was not significant (P for heterogeneity<0.1). Otherwise, random-effect models were used. $P < 0.05$ was considered statistically significant for the between-group difference. If substantial heterogeneity was detected, we looked for reasonable explanations, and subgroup analysis or sensitivity analysis could be applied to explore the causes of heterogeneity. If the sources of heterogeneity could not be determined, a descriptive analysis was adopted.

3. Results

3.1. Study Selection. The PRISMA flow diagram of the literature search and the results are shown in Figure 1. These

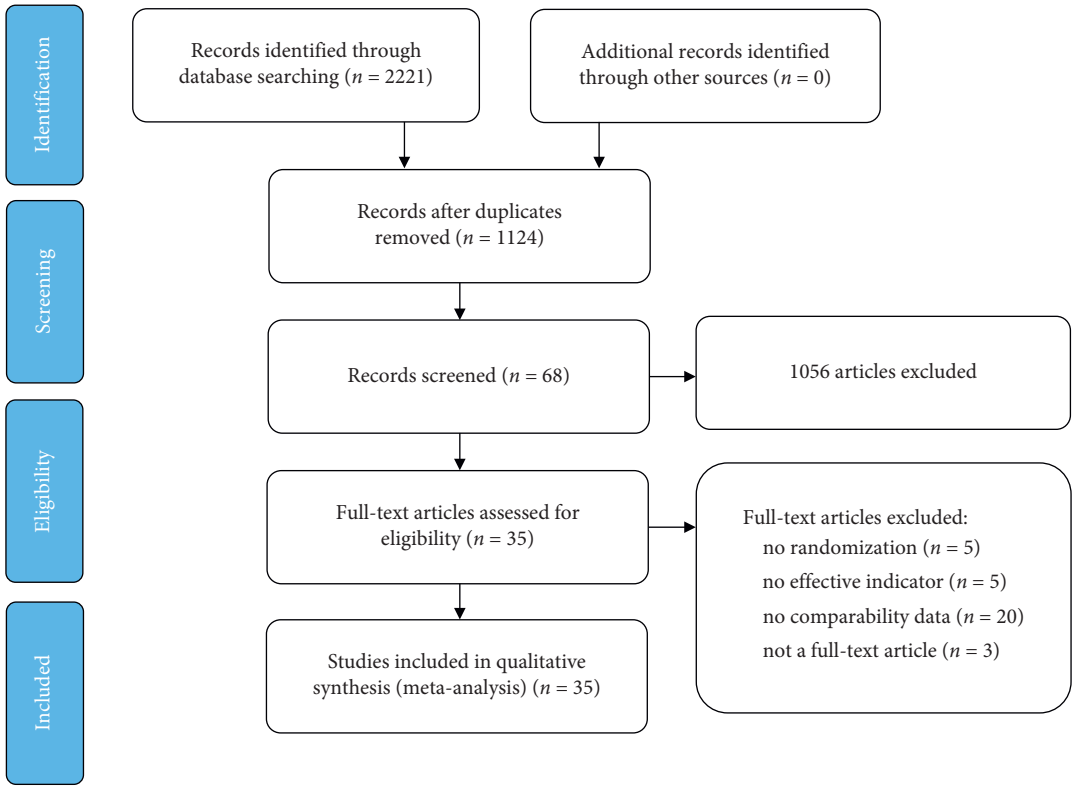

Figure 1: Flow diagram for the selection of the included studies.

studies were screened for eligibility using the detailed participant, intervention, comparison, and outcome (PICO) criteria. The initial search of computerized databases retrieved a total of 2221 articles. After removing duplicates, 1124 articles were found, of which 68 records were subjected to a full-text review. We excluded 33 articles for the following reasons: no randomization ($n = 5$), no effective indicator ($n = 5$), no comparability data ($n = 20$), and not a full-text article ($n = 3$). Finally, 35 RCTs were included in this review.

3.2. Description of Studies. The characteristics of the included studies in this review are shown in Table 1. Among the 35 included studies, all the studies were conducted in China. Nine of thirty-five articles [24, 26–28, 31, 32, 35, 38, 41] were reported in an English database, and the remaining were reported in a Chinese database. Overall, 35 eligible studies involved 3024 participants diagnosed with dysphagia after stroke, and they were published between 2006 and 2020. All trials compared acupuncture with a swallowing treatment. In these trials, the frequency of acupuncture intervention was at least three times a week for more than two weeks in duration. Three studies [28, 32, 49] reported adverse events, and four studies [25, 28, 31, 40] reported dropouts.

3.3. Assessment for Risk of Bias. The details of the overall risk of bias across the 35 RCTs are provided in Table 2. Of the 35 included studies, the randomization procedure was reported in adequate detail in all studies. One trial [28] clearly reported the allocation concealment, the blinding of participants and personnel, and the blinding of outcome assessment; other descriptions in the other studies were unclear. Four trials [25, 28, 31, 40] excluded dropout participants for the data analysis, which may increase the risk of attrition bias. All the studies clearly described the selective reporting. In total, 4 out of 35 studies (11.43%) were judged as having a high risk of bias because one of the main aspects of the bias assessments was high (Figures 2 and 3).

3.4. Standard Swallowing Assessment (SSA). There were 13 studies that used the SSA as the effective evaluation standard with continuous data. The meta-analysis showed a MD with high heterogeneity ($I^2 = 80\%$). Therefore, the random-effect model was used (Figure 4), and we performed a subgroup analysis according to the course of the disease. Heterogeneity was found to remain unaltered although no source for it was identified. Meanwhile, the meta-analysis results showed significant differences in SSA scores in dysphagia between the acupuncture and control groups. The acupuncture group had lower SSA scores than the control group (MD = −3.78, 95% CI: −4.64 to −2.91, $P < 0.00001$) (Figure 4).

3.5. Ichiro Fujishima Rating Scale (IFRS). Twelve studies used the Ichiro Fujishima rating scale as the evaluation standard. The meta-analysis indicated that the acupuncture group had obviously improved IFRS scores (MD = 1.68, 95%

Table 1: Characteristics of included studies.

Reference	Participants	Intervention	Acupoints	Outcome measures	Main conclusion
Wang et al. [24]	G1 (50): 62.14 ± 12.14 G2 (50): 62.37 ± 5.34	G1: A + ST, G2: ST, F: 3 times/week, D: 4 weeks	GB20, GB12, BL10, RN23, ST5, ST40, EX-HN12, EX-HNl3	WST + IFRS	1 WST (G1 < G2) 2 IFRS (G1 > G2)
Jiang et al. [25]	G1 (65): 60 ± 10 G2 (65): 60 ± 9	G1: A + ST + NEST, G2: ST + NEST, F: 5 times/ week, D: 4 weeks	Shesanzhen (extra)	HAMA + HAMD + SSA + sEMG	G1 < G2 in all outcomes
Wu et al. [26]	G1 (65): 44.00 ± 2.92 G2 (63): 44.35 ± 2.60	G1: A + ST, G2: ST, F: 5 times/week, D: 6 weeks	EX-HN1, GV20, EX-HN5, GB20, CV23	IFRS	IFRS (G1 > G2)
Wei et al. (2015) [27]	G1 (50): 61.50 ± 4.2 G2 (50): 62.50 ± 4.90	G1: A + ST, G2: ST, F: 7 times/week, D: 2 weeks	RN23, RN22, EX-HN12, EX-HNl3, LI4, PC6, ST36	VFSS + MBI + FIM	G1 > G2 in all outcomes
Xia et al. [28]	G1 (67): 67±9 G2 (63): 66 ± 10	G1: A + ST, G2: ST, F: 6 times/week, D: 6 weeks	PC6, DU26, SP6, HT1, LU5, BL40, GV20, GB20, CV23, Jialianquan (extra), EX-HN12, EX-HNl3	VFSS + SSA + BI + SWAL-QOL	1 SSA (G1 < G2) 2 G1 > G2 in other outcomes
Zeng et al. [29]	G1 (25): 58.01 ± 10.74 G2 (25): 57.98 ± 11.82	G1: A + ST, G2: ST, F: 7 times/week, D: 4 weeks	SJ17, GB12, Ex-HN14, SI17, RN22, ST9, Toupizhen (extra), RN23, EX-HN12, EX-HNl3, Tunyan (extra), Tiyan (extra), ST4, ST6, DU26, RN24	IFRS	IFRS (G1 > G2)
Chang et al. [30]	G1 (38): 46 ± 10 G2 (36): 44 ± 11	G1: A + BT + NEST, G2: BT + NEST, F: 6 times/week, D: 4 weeks	GV20, RN23, EX-HN12, EX-HNl3, Toupizhen (extra)	IFRS	IFRS (G1 > G2)
Chen et al. [31]	G1 (50): 67 ± 11 G2 (50): 67 ± 10	G1: A + ST, G2: ST, F: 6 times/week, D: 8 weeks	GB20, Ex-HN14, Gongxue (extra), Zhiqiang (extra), Tunyan (extra), Fayin (extra), RN23, EX-HN12, EX-HNl3	RSST + WST + SSA	1 WST (G1 < G2) 2 RSST (G1 > G2) 3 SSA (G1 < G2)
Feng et al. [32]	G1 (30): 60 ± 12 G2 (30): 58 ± 12	G1: A + ST, G2: ST, F: 7 times/week, D:3 weeks	RN23, SJ17, GB12, GB20, DU16, DU15, ST5, EX-HN12, EX-HNl3, Shezhen (extra)	VFSS + WST	1 WST (G1 < G2) 2 VFSS (G1 > G2)
Guo et al. [33]	G1 (50): 66.21 ± 8.03 G2 (50): 65.91 ± 7.85	G1: A + ST, G2: ST, F: 6 times/week, D: 4 weeks	DU15, DU16, BL10, Zhiqiang (extra), RN23	SSA + WST + BI	1 WST (G1 < G2) 2 BI (G1 > G2) 3 SSA (G1 < G2)
He et al. [34]	G1 (60): 62.16 ± 7.04 G2 (60): 61.83 ± 6.81	G1: A + ST, G2: ST, F: 5 times/week, D: 8 weeks	GB20, SJ17, RN23	SSA + WST + BI	1 WST (G1 < G2) 2 BI (G1 > G2) 3 SSA (G1 < G2)
Li et al. [35]	G1 (42): 57.4 ± 4.8 G2 (42): 57.4 ± 4.8	G1: A + BT + ST, G2: BT + ST, F: 6 times/ week, D: 4 weeks	Shezhen (extra)	VFSS	VFSS (G1 > G2)

Table 1: Continued.

Reference	Participants	Intervention	Acupoints	Outcome measures	Main conclusion
Li et al. [36]	G1 (50): 42.6 ± 2.3 G2 (50): 42.5 ± 2.2	G1: A + ST, G2: ST, F: 7 times/week, D: 3 weeks	GB20, Ex-HN14, Gongxue (extra), Zhiqiang (extra), Tunyan (extra) RN23, EX-HN12, EX-HNl3	IFRS + WST	1 WST (G1 < G2) 2 IFRS (G1 > G2)
Li and Gu [37]	G1 (40): 61.9 ± 7.9 G2 (40): 63.6 ± 6.9	G1: A + BT + ST, G2: BT + ST, F: 6 times/week, D: 4 weeks	GB20, DU16, HT5, LR3	PAS + SSA + WST	G1 < G2 in all outcomes
Liu et al. [38]	G1 (36): 57.6 ± 8.2 G2 (36): 58.5 ± 8.7	G1: A + BT, G2: BT, F: 6 times/week, D: 8 weeks	GB20, Ex-HN14, CV23, Ex-HN12, Ex-HN13, SP6, LR3, ST40, LI4	WST	WST (G1 < G2)
Qiao et al. [39]	G1 (43): 52.27 ± 10.45 G2 (43): 52.86 ± 10.72	G1: A + BT + ST, G2: BT + ST, F: 3 times/week, D: 2 weeks	GB20, DU16, EX-HN15, RN23, Jialianquan (extra), EX-HN12, EX-HNl3, LI4, LR3, HT5	IFRS + WST	1 WST (G1 < 2) 2 IFRS (G1 > G2)
Wang et al. [40]	G1 (35): 64 + 8 G2 (35): 65 ± 9	G1: A + ST, G2: ST, F: 5 times/week, D: 3 weeks	Shesanzhen (extra)	SSA + WST + SWAL-QOL	1 WST (G1 < G2) 2 SWAL-QOL (G1 > G2) 3 SSA (G1 < G2)
Wang [41]	G1 (30): 57.6 ± 9.1 G2 (30): 59.6 ± 8.9	G1: A + BT + NEST, G2: BT + NEST, F: 7 times/week, D: 2 weeks	RN23, Jialianquan (extra), HT5, DU20, Zuqianjin (extra), Zuwujin (extra)	WST	WST (G1 < G2)
Xu [42]	G1 (38): 62.74 ± 5.19 G2 (38): 63.19 ± 4.38	G1: A + BT, G2: BT, F: 5 times/week, D: 4 weeks	GB20, BL10, DU16, RN23, EX-HN12, EX-HNl3, PC6, HT5, SP6, ST36, RN12, BL23, SP3, KI3	WST	WST (G1 < G2)
Yang et al. [43]	G1 (30): 65.8 G2 (30): 67.3	G1: A + BT, G2: BT, F: 5 times/week, D: 2 weeks	GV20, SJ17, RN23, SP6, ST36	WST	WST (G1 < G2)
Yu et al. [44]	G1 (40): 63 ± 10 G2 (38): 64 ± 11	G1: A + ST, G2: ST, F: 7 times/week, D: 3 weeks	DU26, LI4, DU15, DU16, GB20, RN23	IFRS + WST	1 WST (G1 < G2) 2 IFRS (G1 > G2)
Zhu [45]	G1 (50): 65.05 ± 8.99 G2 (48): 64.03 ± 9.83	G1: A + BT + ST, G2: BT + ST, F: 6 times/week, D: 4 weeks	GB20, GB12, SJ17, Shanglianquan (extra), ST9	SSA + SWAL-QOL	1 SWAL-QOL (G1 > G2) 2 SSA (G1 < G2)
Zhou et al. [46]	G1 (34): 59.90 ± 3.87 G2 (34): 60.43 ± 4.07	G1: A + ST + NEST, G2: ST + NEST, F: 6 times/week, D: 4 weeks	Toupizhen (extra)	SSA + SWAL-QOL + CT7R	1 SSA (G1 < G2) 2 G1 > G2 in other outcomes 1 CT7R (G1 > G2)
Zhou et al. [47]	G1 (30): 68.30 ± 13.84 G2 (30): 70.26 ± 11.97	G1: A + ST + NEST, G2: ST + NEST, F: 6 times/week, D: 2 weeks	Toupizhen (extra)	SSA + VFSS + WST + CT7R	2 VFSS (G1 > G2) 3 SSA (G1 < G2) 4 WST (G1 < G2)

Table 1: Continued.

Reference	Participants	Intervention	Acupoints	Outcome measures	Main conclusion
Zhi et al. [48]	G1 (39): 63.16 ± 6.92 G2 (39): 62.78 ± 6.78	G1: A + BT + ST, G2: BT + ST, F: 6 times/week, D: 12 weeks	RN23, Jialianquan (extra), EX-HN12, EX-HNl3, Shexiaxue (extra)	WST + GUSS + BI + FMA	1 WST (G1 < G2) 2 G1 > G2 in other outcomes
Zhang and Li [49]	G1 (46): 66.2 ± 7.4 G2 (46): 67.5 ± 6.7	G1: A + ST + NEST, G2: ST + NEST, F: 7 times/week, D: 4 weeks	RN23, Tunyan (extra), Toupizhen (extra)	VFSS + WST + IFRS	1 WST (G1 < G2) 2 VFSS (G1 > G2) 3 IFRS (G1 > G2)
Zhang et al. [50]	G1 (19): 64.10 ± 8.20 G2 (18): 65.58 ± 10.64	G1: A + rTMS + BT, G2: rTMS + BT, F: 6 times/week, D: 4 weeks	DU20, EX-HN1, ST8, DU16, GB20, RN23, Jialianquan (extra), ST4, ST6, ST7	MBSImP + OTT	G1 < G2 in all outcomes
Zhang et al. [51]	G1 (87): 64.61 ± 9.70 G2 (87): 63.86 ± 10.55	G1: A + ST, G2: ST, F: 3 times/week, D: 8 weeks	DU16, GB20, RN23, Jialianquan (extra), EX-HN15, EX-HN12, EX-HNl3, HT5, LR3, LI4	IFRS + WST	1 WST (G1 < G2) 2 IFRS (G1 > G2)
Zhang and Yin [52]	G1 (62): 70 ± 1 G2 (56): 68 ± 2	G1: A + ST, G2: ST, F: 5 times/week, D: 4 weeks	Shenguan (extra), KI3, LR3	SSA + WST + IFRS	1 WST (G1 < G2) 2 SSA (G1 < G2) 3 IFRS (G1 > G2)
Zhang et al. [53]	G1 (20): 58.3 ± 10.1 G2 (20): 58.2 ± 10.1	G1: A + ST + NEST, G2: ST + NEST, F: 5 times/week, D: 4 weeks	Tunyan (extra), RN23, DU16, SJ17, EX-HN12, EX-HNl3	VFSS + sEMG	1 VFSS (G1 > G2) 2 sEMG (G1 < G2)
Yin et al. [54]	G1 (18): 69.52 ± 6.01 G2 (20): 65.41 ± 7.01	G1: A + ST + NEST, G2: ST + NEST, F: 5 times/week, D: 3 weeks	ST9, RN22, RN23, EX-HN12, EX-HNl3	IFRS + WST	1 WST (G1 < G2) 2 IFRS (G1 > G2)
Gao et al. [55]	G1 (30): 64 ± 5 G2 (30): 65 ± 5	G1: A + BT + ST, G2: BT + ST, F: 5 times/week, D: 4 weeks	DU16, BL10, GB12, RN23, Jialianquan (extra), EX-HN12, EX-HNl3	VFSS + SSA + sEMG	1 VFSS (G1 > G2) 2 sEMG (G1 < G2) 3 SSA (G1 < G2)
Dong [56]	G1 (60): 55.3 ± 6.4 G2 (60): 55.3 ± 6.4	G1: A + ST, G2: ST, F: 5 times/week, D: 2 weeks	EX-HN12, EX-HNl3, DU16, DU15, RN23	VFSS + WST	1 WST (G1 < G2) 2 VFSS (G1 > G2)
Deng et al. [57]	G1 (53): 59.2 ± 11.6 G2 (52): 59.8 ± 13.2	G1: A + ST + NEST, G2: ST + NEST, F: 5 times/week, D: 3 weeks	PC6, DU26, SP6, GB20, SJ17, GB12, Yanhoubi (extra), RN23	WST + SSA	1 WST (G1 < G2) 2 SSA (G1 < G2)
Zhu et al. [58]	G1 (35): 54.97 ± 5.10 G2 (35): 56.26 ± 6.17	G1: A + BT + ST, G2: BT + ST, F: 6 times/week, D: 2 weeks	Yushizhen (extra), LI15, LI11, LI10, SJ5, SJ3, LI4, ST32, GB34, ST36, ST40, GB40, LR3, SP6	IFRS + WST	1 WST (G1 < G2) 2 IFRS (G1 > G2)

G1 > G2/G1 < G2 indicates that the difference between the two groups was statistically significant, $P < 0.05$; G1 = G2 indicates that no significant differences were noted between the two groups, $P \geq 0.05$. G: group; G1: experimental group; G2: control group; A: acupuncture; ST: swallowing treatment; BT: basic treatment; NEST: neuromuscular electrical stimulation; rTMS: repetitive transcranial magnetic stimulation; F: frequency; D: duration; WST: Watian swallowing test; SSA: standard swallowing assessment; VFSS: videofluoroscopic swallowing study; IFRS: Ichiro Fujishima rating scale; SWAL-QOL: swallow quality-of-life questionnaire; BI: Barthel index; FMA: Fugl–Meyer assessment; CT7R: Caiteng 7 rank; sEMG: surface electromyography; HAMA: Hamilton anxiety scale; HAMD: Hamilton depression scale; RSST: repetitive saliva swallowing test; MBSImP: modified barium swallow impairment profile; OTT: oral transit time.

Table 2: The risk of bias assessment.

Reference	Randomization	Allocation concealment	Blinding	Incomplete data	Selective report	Other bias
Wang et al. [24]	Low risk Randomized by random number table	Unclear risk Allocation schedule was not mentioned	Unclear risk Blinding unclear	Low risk None lost to follow-up	Low risk All outcomes reported	Unclear risk
Jiang et al. [25]	Low risk Randomized by random number table	Unclear risk Allocation schedule was not mentioned	Unclear risk Blinding unclear	High risk 10 participants dropout	Low risk All outcomes reported	Unclear risk
Wu et al. [26]	Low risk Randomized by random number table	Unclear risk Allocation schedule was not mentioned	Unclear risk Blinding unclear	Low risk None lost to follow-up	Low risk All outcomes reported	Unclear risk
Wei et al. [27]	Low risk Randomized by random number table	Unclear risk Allocation schedule was not mentioned	Unclear risk Blinding unclear	Low risk None lost to follow-up	Low risk All outcomes reported	Unclear risk
Xia et al. [28]	Low risk Randomized by random number table	Low risk Automated assignment system	Low risk Participants and outcome assessors blinded	High risk 14 participants dropout	Low risk All outcomes reported	Unclear risk
Zeng et al. [29]	Low risk Randomized by random number table	Unclear risk Allocation schedule was not mentioned	Unclear risk Blinding unclear	Low risk None lost to follow-up	Low risk All outcomes reported	Unclear risk
Chang et al. [30]	Low risk Randomized by random number table.	Unclear risk Allocation schedule was not mentioned	Unclear risk Blinding unclear	Low risk None lost to follow-up	Low risk All outcomes reported	Unclear risk
Chen et al. [31]	Low risk Randomized by random number table	Unclear risk Allocation schedule was not mentioned	Unclear risk Blinding unclear	High risk 3 participants dropout	Low risk All outcomes reported	Unclear risk
Feng et al. [32]	Low risk Randomized by random number table	Unclear risk Allocation schedule was not mentioned	Unclear risk Blinding unclear	Low risk None lost to follow-up	Low risk All outcomes reported	Unclear risk
Guo et al. [33]	Low risk Randomized by random number table	Unclear risk Allocation schedule was not mentioned	Unclear risk Blinding unclear	Low risk None lost to follow-up	Low risk All outcomes reported	Unclear risk
He et al. [34]	Low risk Randomized by random number table	Unclear risk Allocation schedule was not mentioned	Unclear risk Blinding unclear	Low risk None lost to follow-up	Low risk All outcomes reported	Unclear risk
Li et al. [35]	Low risk Randomized by random number table	Unclear risk Allocation schedule was not mentioned	Unclear risk Blinding unclear	Low risk None lost to follow-up	Low risk All outcomes reported	Unclear risk
Li et al. [36]	Low risk Randomized by random number table	Unclear risk Allocation schedule was not mentioned	Unclear risk Blinding unclear	Low risk None lost to follow-up	Low risk All outcomes reported	Unclear risk
Li and Gu [37]	Low risk Randomized by random number table	Unclear risk Allocation schedule was not mentioned	Unclear risk Blinding unclear	Low risk None lost to follow-up	Low risk All outcomes reported	Unclear risk
Liu et al. [38]	Low risk Randomized by random number table	Unclear risk Allocation schedule was not mentioned	Unclear risk Blinding unclear	Low risk None lost to follow-up	Low risk All outcomes reported	Unclear risk
Qiao et al. [39]	Low risk Randomized by random number table	Unclear risk Allocation schedule was not mentioned	Unclear risk Blinding unclear	Low risk None lost to follow-up	Low risk All outcomes reported	Unclear risk
Wang et al. [40]	Low risk Randomized by random number table	Unclear risk Allocation schedule was not mentioned	Unclear risk Blinding unclear	High risk 8 participants dropout	Low risk All outcomes reported	Unclear risk
Wang [41]	Low risk Randomized by random number table	Unclear risk Allocation schedule was not mentioned	Unclear risk Blinding unclear	Low risk None lost to follow-up	Low risk All outcomes reported	Unclear risk
Xu [42]	Low risk Randomized by random number table	Unclear risk Allocation schedule was not mentioned	Unclear risk Blinding unclear	Low risk None lost to follow-up	Low risk All outcomes reported	Unclear risk
Yang et al. [43]	Low risk. Randomized by random number table.	Unclear risk. Allocation schedule was not mentioned.	Unclear risk. Blinding unclear.	Low risk. None lost to follow-up	Low risk. All outcomes reported	Unclear risk

Table 2: Continued.

Reference	Randomization	Allocation concealment	Blinding	Incomplete data	Selective report	Other bias
Yu et al. [44]	Low risk Randomized by random number table	Unclear risk Allocation schedule was not mentioned	Unclear risk Blinding unclear	Low risk None lost to follow-up	Low risk All outcomes reported	Unclear risk
Zhu [45]	Low risk Randomized by random number table	Unclear risk Allocation schedule was not mentioned	Unclear risk Blinding unclear	Low risk None lost to follow-up	Low risk All outcomes reported	Unclear risk
Zhou et al. [46]	Low risk Randomized by random number table	Unclear risk Allocation schedule was not mentioned	Unclear risk Blinding unclear	Low risk None lost to follow-up	Low risk All outcomes reported	Unclear risk
Zhou et al. [47]	Low risk Randomized by random number table	Unclear risk Allocation schedule was not mentioned	Unclear risk Blinding unclear	Low risk None lost to follow-up	Low risk All outcomes reported	Unclear risk
Zhi et al. [48]	Low risk Randomized by random number table	Unclear risk Allocation schedule was not mentioned	Unclear risk Blinding unclear	Low risk None lost to follow-up	Low risk All outcomes reported	Unclear risk
Zhang and Li [49]	Low risk Randomized by random number table	Unclear risk Allocation schedule was not mentioned	Unclear risk Blinding unclear	Low risk None lost to follow-up	Low risk All outcomes reported	Unclear risk
Zhang et al. [50]	Low risk Randomized by random number table	Unclear risk Allocation schedule was not mentioned	Unclear risk Blinding unclear	Low risk None lost to follow-up	Low risk All outcomes reported	Unclear risk
Zhang et al. [51]	Low risk Randomized by random number table	Unclear risk Allocation schedule was not mentioned	Unclear risk Blinding unclear	Low risk None lost to follow-up	Low risk All outcomes reported	Unclear risk
Zhang and Yin [52]	Low risk Randomized by random number table	Unclear risk Allocation schedule was not mentioned	Unclear risk Blinding unclear	Low risk None lost to follow-up	Low risk All outcomes reported	Unclear risk
Zhang et al. [53]	Low risk Randomized by random number table	Unclear risk Allocation schedule was not mentioned	Unclear risk Blinding unclear	Low risk None lost to follow-up	Low risk All outcomes reported	Unclear risk
Yin et al. [54]	Low risk Randomized by random number table	Unclear risk Allocation schedule was not mentioned	Unclear risk Blinding unclear	Low risk None lost to follow-up	Low risk All outcomes reported	Unclear risk
Gao et al. [55]	Low risk Randomized by random number table	Unclear risk Allocation schedule was not mentioned.	Unclear risk Blinding unclear	Low risk None lost to follow-up	Low risk All outcomes reported	Unclear risk
Dong [56]	Low risk Randomized by random number table	Unclear risk Allocation schedule was not mentioned	Unclear risk Blinding unclear	Low risk None lost to follow-up	Low risk All outcomes reported	Unclear risk
Deng et al. [57]	Low risk Randomized by random number table	Unclear risk Allocation schedule was not mentioned	Unclear risk Blinding unclear	Low risk None lost to follow-up	Low risk All outcomes reported	Unclear risk
Zhu et al. [58]	Low risk Randomized by random number table	Unclear risk Allocation schedule was not mentioned.	Unclear risk Blinding unclear	Low risk None lost to follow-up	Low risk All outcomes reported	Unclear risk

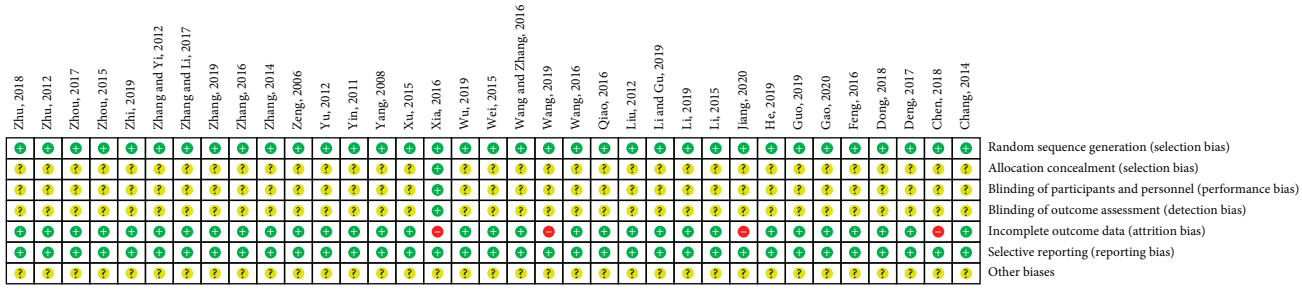

Figure 2: Potential risk of bias of each included study.

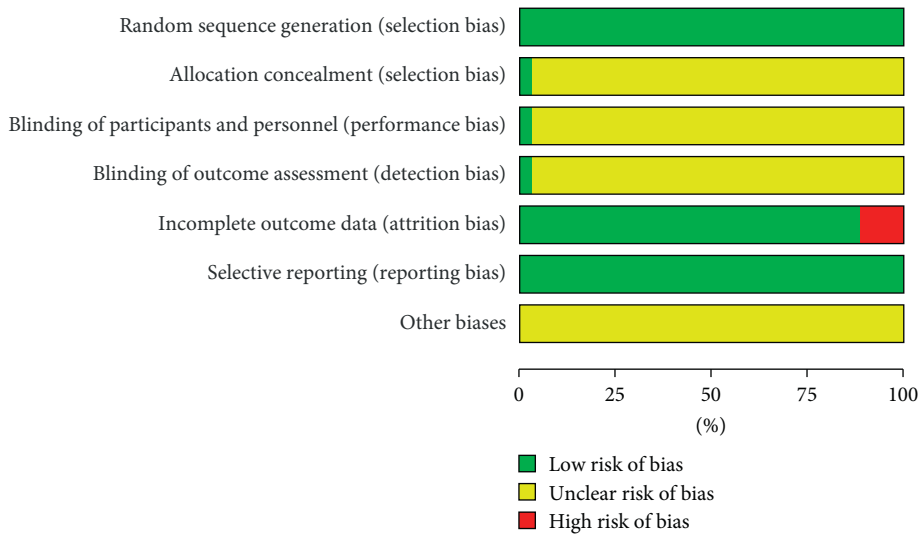

Figure 3: Summary of bias evaluation for the studies.

CI: 1.16 to 2.20, $P < 0.00001$, $I^2 = 91\%$) (Figure 5). The heterogeneity was high, and we found that the treatment durations and the acupuncture methods were different in these 12 studies, so we performed a subgroup analysis. Subgroup analysis of six articles seemed to show that electroacupuncture combined with swallowing treatment was more effective than swallowing treatment alone (MD = 1.75, 95% CI: 0.92 to 2.58, $P < 0.00001$) (Figure 6). The subgroup analysis of these six articles seemed to show that simple acupuncture combined with swallowing treatment was more effective than swallowing treatment alone (MD = 1.62, 95% CI: 0.90 to 2.34, $P < 0.00001$) (Figure 6). However, we did not find a clear source of heterogeneity for IFRS with an I^2 statistic that ranged from 75% to 96% in subgroup analyses, such as different acupuncture stimulation parameters, different acupoint selections, different needle holding times, and treatment durations.

3.6. Videofluoroscopy (VFSS). Among the included studies, 8 used videofluoroscopy to evaluate the effectiveness of the treatment with continuous data. The result exhibited a MD with medium heterogeneity ($I^2 = 81\%$). We performed a subgroup analysis, and heterogeneity was found to remain unaltered although no source for it was identified. The meta-analysis showed that acupuncture combined with swallowing treatment produced a sustained and significant improvement, as reflected in the VFSS scores in these stroke patients (MD = 2.26, 95% CI: 1.77 to 2.74, $P < 0.00001$) (Figure 7).

3.7. Watian Swallowing Test (WST). Eleven studies selected the Watian swallowing test as the evaluation standard. The meta-analysis showed a MD with high heterogeneity ($I^2 = 99\%$). We did not find a clear source of heterogeneity for WST with an I^2 statistic that ranged from 93% to 100% in subgroup analyses, such as different acupuncture stimulation parameters, different acupoint selections, different needle holding times, and treatment durations. We could see from the figure that the score of the control group was higher than that of the acupuncture group (Figure 8). This illustrated that the acupuncture group was able to lower the WST scores (MD = −1.21, 95% CI: −1.85 to −0.57, $P = 0.0002$) (Figure 8).

3.8. Acupuncture Point. The selection of acupoints was chosen mainly based on the symptoms and syndrome differentiation of traditional Chinese medicine (TCM) (Figure 9). After analysis of points adopted in these trials, we found that Fengchi (GB20), Jinjin (EX-HN12), Yuye (EX-HNl3), Lianquan (RN23), and Yifeng (SJ17) were the five points most commonly used (Figure 10).

3.9. Publication Bias. Publication bias was reported via a funnel plot (Figure 11), in which the asymmetry of the funnel plots may have arisen through heterogeneity.

3.10. Adverse Events. Three studies reported adverse events [28, 32, 49], while the remaining 32 studies did not mention adverse events. Among the 3 studies, they reported the occurrence of adverse events such as bleeding, pain, and discomfort. However, no life-threatening adverse events were noted in any of the included studies.

4. Discussion

The object of this systematic review was to evaluate the effectiveness of acupuncture in treating dysphagia after stroke. This systematic review showed that the therapeutic efficacy of acupuncture combined with other interventions was better than that of the control group in the SSA score, IFRS score, VFSS score, and WST score. In the subgroup analysis, we obtained similar results that acupuncture had a significant effect on dysphagia.

Study or subgroup	Experimental Mean	SD	Total	Control Mean	SD	Total	Weight (%)	Mean difference IV, random, 95% CI
1.2.1. SSA score								
Chen, 2018	20.58	3.51	48	23.51	4.4	49	3.8	−2.93 [−4.51, −1.35]
Deng, 2017	18.72	3.15	53	22.08	5.37	52	3.7	−3.36 [−5.05, −1.67]
Gao, 2020	25.57	1.94	30	26.7	2.18	30	4.5	−1.13 [−2.17, −0.09]
Guo, 2019	17.22	1.97	50	21.88	2.55	50	4.7	−4.66 [−5.55, −3.77]
He, 2019	18.15	2.17	60	22.68	2.89	60	4.6	−4.53 [−5.44, −3.62]
Jiang, 2020	21.32	2.5	62	25.16	2.9	58	4.6	−3.84 [−4.81, −2.87]
Li and Gu, 2019	22.7	2.99	40	24.63	2.96	40	4.2	−1.93 [−3.23, −0.63]
Wang, 2019	23.03	2.56	32	27.93	6.65	30	2.7	−4.90 [−7.44, −2.36]
Xia, 2016	21.6	4.3	61	28.1	5.8	55	3.4	−6.50 [−8.37, −4.63]
Zhang and Yi, 2012	17.11	3.69	62	19.67	4.54	56	3.9	−2.56 [−4.06, −1.06]
Zhou, 2015	23.2	4.56	30	25.57	4.69	30	2.9	−2.37 [−4.71, −0.03]
Zhou, 2017	22.57	3.1	34	27.64	3.7	34	3.8	−5.07 [−6.69, −3.45]
Zhu, 2012	19.35	5.28	50	25.53	4.95	48	3.3	−6.18 [−8.21, −4.15]
Subtotal (95% CI)			*612*			*592*	*50.0*	*−3.78 [−4.64, −2.91]*
Heterogeneity: $tau^2 = 1.90$; $chi^2 = 60.46$, $df = 12$ ($P < 0.00001$); $I^2 = 80\%$								
Test for overall effect: $Z = 8.55$ ($P < 0.00001$)								
1.2.2. SSA (2-3 weeks)								
Deng, 2017	18.72	3.15	53	22.08	5.37	52	3.7	−3.36 [−5.05, −1.67]
Wang, 2019	23.03	2.56	32	27.93	6.65	30	2.7	−4.90 [−7.44, −2.36]
Zhou, 2015	23.2	4.56	30	25.57	4.69	30	2.9	−2.37 [−4.71, −0.03]
Subtotal (95% CI)			*115*			*112*	*9.2*	*−3.45 [−4.68, −2.21]*
Heterogeneity: $tau^2 = 0.05$; $chi^2 = 2.08$, $df = 2$ ($P = 0.35$); $I^2 = 4\%$								
Test for overall effect: $Z = 5.47$ ($P < 0.00001$)								
1.2.3. SSA (4 weeks)								
Gao, 2020	25.57	1.94	30	26.7	2.18	30	4.5	−1.13 [−2.17, −0.09]
Guo, 2019	17.22	1.97	50	21.88	2.55	50	4.7	−4.66 [−5.55, −3.77]
Jiang, 2020	21.32	2.5	62	25.16	2.9	58	4.6	−3.84 [−4.81, −2.87]
Li and Gu, 2019	22.7	2.99	40	24.63	2.96	40	4.2	−1.93 [−3.23, −0.63]
Zhang and Yi, 2012	17.11	3.69	62	19.67	4.54	56	3.9	−2.56 [−4.06, −1.06]
Zhou, 2017	22.57	3.1	34	27.64	3.7	34	3.8	−5.07 [−6.69, −3.45]
Zhu, 2012	19.35	5.28	50	25.53	4.95	48	3.3	−6.18 [−8.21, −4.15]
Subtotal (95% CI)			*328*			*316*	*28.9*	*−3.54 [−4.82, −2.27]*
Heterogeneity: $tau^2 = 2.47$; $chi^2 = 43.97$, $df = 6$ ($P < 0.00001$); $I^2 = 86\%$								
Test for overall effect: $Z = 5.47$ ($P < 0.00001$)								
1.2.4. SSA (>4 weeks)								
Chen, 2018	20.58	3.51	48	23.51	4.4	49	3.8	−2.93 [−4.51, −1.35]
He, 2019	18.15	2.17	60	22.68	2.89	60	4.6	−4.53 [−5.44, −3.62]
Xia, 2016	21.6	4.3	61	28.1	5.8	55	3.4	−6.50 [−8.37, −4.63]
Subtotal (95% CI)			*169*			*164*	*11.9*	*−4.58 [−6.25, −2.91]*
Heterogeneity: $tau^2 = 1.62$; $chi^2 = 8.16$, $df = 2$ ($P = 0.02$); $I^2 = 75\%$								
Test for overall effect: $Z = 5.38$ ($P < 0.00001$)								
Total (95% CI)			*1224*			*1184*	*100.0*	*−3.77 [−4.37, −3.18]*
Heterogeneity: $tau^2 = 1.77$; $chi^2 = 120.93$, $df = 25$ ($P < 0.00001$); $I^2 = 79\%$								
Test for overall effect: $Z = 12.40$ ($P < 0.00001$)								
Test for subgroup differences: $chi^2 = 1.29$, $df = 3$ ($P = 0.73$), $I^2 = 0\%$								

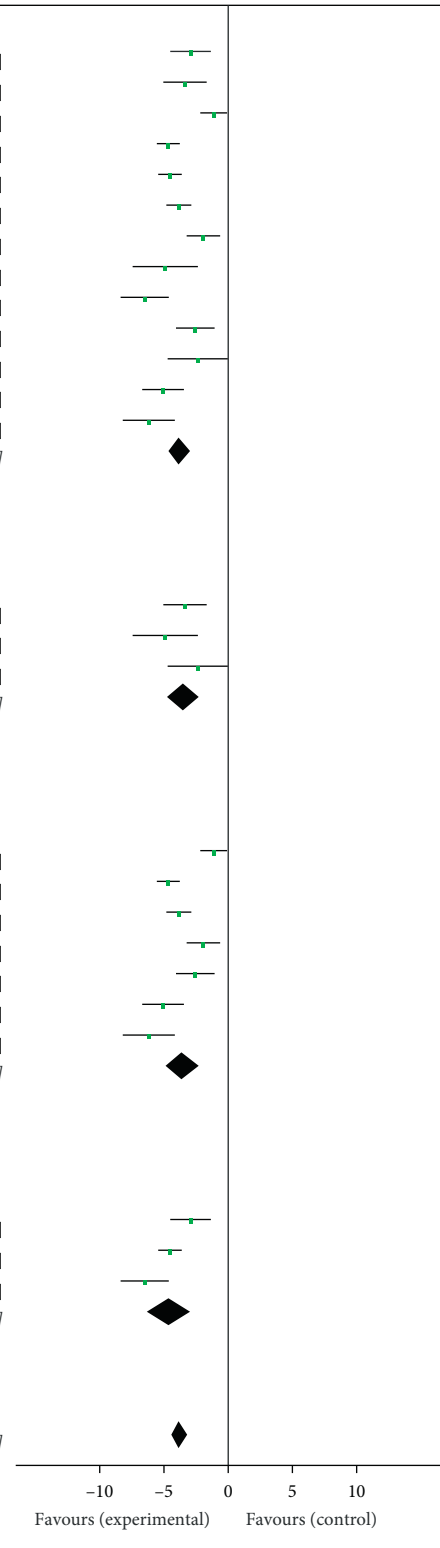

Figure 4: Forest plot of the SSA effective rate.

Study or subgroup	Experimental Mean	SD	Total	Control Mean	SD	Total	Weight (%)	Mean difference IV, random, 95% CI
2.1.1. IFRS score								
Chang, 2014	8.01	1.25	38	4.73	1.36	36	4.2	3.28 [2.68, 3.88]
Li, 2019	8.79	1.11	50	5.96	1.12	50	4.4	2.83 [2.39, 3.27]
Qiao, 2016	8.97	2.32	43	6.24	1.61	43	3.8	2.73 [1.89, 3.57]
Wang, 2016	8.24	1.34	50	6.75	2.27	50	4.0	1.49 [0.76, 2.22]
Wu, 2019	8.68	1.12	65	7.32	0.91	63	4.6	1.36 [1.01, 1.71]
Yin, 2011	8.06	1.06	18	7.1	1.29	20	3.9	0.96 [0.21, 1.71]
Yu, 2012	8.97	1.04	40	7.13	1.25	38	4.3	1.84 [1.33, 2.35]
Zeng, 2006	6.6	1.61	25	4.48	1.45	25	3.7	2.12 [1.27, 2.97]
Zhang and Li, 2017	8.12	1.13	46	7.45	1.04	46	4.4	0.67 [0.23, 1.11]
Zhang and Yi, 2012	6.73	1.16	62	5.25	1.25	56	4.4	1.48 [1.04, 1.92]
Zhang, 2014	9.03	1.186	87	8.55	1.553	87	4.5	0.48 [0.07, 0.89]
Zhu, 2018	7.71	1.76	35	6.63	1.96	35	3.7	1.08 [0.21, 1.95]
Subtotal (95% CI)			*559*			*549*	*50.0*	*1.68 [1.16, 2.20]*
Heterogeneity: $\tau^2 = 0.74$; $\chi^2 = 121.67$, $df = 11$ ($P < 0.00001$); $I^2 = 91\%$								
Test for overall effect: $Z = 6.37$ ($P < 0.00001$)								
2.1.2. IFRS score (2 weeks)								
Qiao, 2016	8.97	2.32	43	6.24	1.61	43	3.8	2.73 [1.89, 3.57]
Wang, 2016	8.24	1.34	50	6.75	2.27	50	4.0	1.49 [0.76, 2.22]
Zhu, 2018	7.71	1.76	35	6.63	1.96	35	3.7	1.08 [0.21, 1.95]
Subtotal (95% CI)			*128*			*128*	*11.4*	*1.76 [0.83, 2.70]*
Heterogeneity: $\tau^2 = 0.51$; $\chi^2 = 7.93$, $df = 2$ ($P = 0.02$); $I^2 = 75\%$								
Test for overall effect: $Z = 3.69$ ($P = 0.0002$)								
2.1.3. IFRS score (3 weeks)								
Li, 2019	8.79	1.11	50	5.96	1.12	50	4.4	2.83 [2.39, 3.27]
Yin, 2011	8.06	1.06	18	7.1	1.29	20	3.9	0.96 [0.21, 1.71]
Yu, 2012	8.97	1.04	40	7.13	1.25	38	4.3	1.84 [1.33, 2.35]
Subtotal (95% CI)			*108*			*108*	*12.7*	*1.91 [0.90, 2.93]*
Heterogeneity: $\tau^2 = 0.72$; $\chi^2 = 20.41$, $df = 2$ ($P < 0.0001$); $I^2 = 90\%$								
Test for overall effect: $Z = 3.69$ ($P = 0.0002$)								
2.1.4. IFRS score (4 weeks)								
Chang, 2014	8.01	1.25	38	4.73	1.36	36	4.2	3.28 [2.68, 3.88]
Zeng, 2006	6.6	1.61	25	4.48	1.45	25	3.7	2.12 [1.27, 2.97]
Zhang and Li, 2017	8.12	1.13	46	7.45	1.04	46	4.4	0.67 [0.23, 1.11]
Zhang, 2014	9.03	1.186	87	8.55	1.553	87	4.5	0.48 [0.07, 0.89]
Subtotal (95% CI)			*196*			*194*	*16.9*	*1.62 [0.34, 2.90]*
Heterogeneity: $\tau^2 = 1.62$; $\chi^2 = 68.56$, $df = 3$ ($P < 0.00001$); $I^2 = 96\%$								
Test for overall effect: $Z = 2.47$ ($P = 0.01$)								
2.1.5. IFRS score (>4 weeks)								
Wu, 2019	8.68	1.12	65	7.32	0.91	63	4.6	1.36 [1.01, 1.71]
Zhang and Yi, 2012	6.73	1.16	62	5.25	1.25	56	4.4	1.48 [1.04, 1.92]
Subtotal (95% CI)			*127*			*119*	*9.0*	*1.41 [1.13, 1.68]*
Heterogeneity: $\tau^2 = 0.00$; $\chi^2 = 0.18$, $df = 1$ ($P = 0.68$); $I^2 = 0\%$								
Test for overall effect: $Z = 10.05$ ($P < 0.00001$)								
Total (95% CI)			*1118*			*1098*	*100.0*	*1.68 [1.33, 2.04]*
Heterogeneity: $\tau^2 = 0.69$; $\chi^2 = 243.34$, $df = 23$ ($P < 0.00001$); $I^2 = 91\%$								
Test for overall effect: $Z = 9.27$ ($P < 0.00001$)								
Test for subgroup differences: $\chi^2 = 1.88$, $df = 4$ ($P = 0.76$), $I^2 = 0\%$								

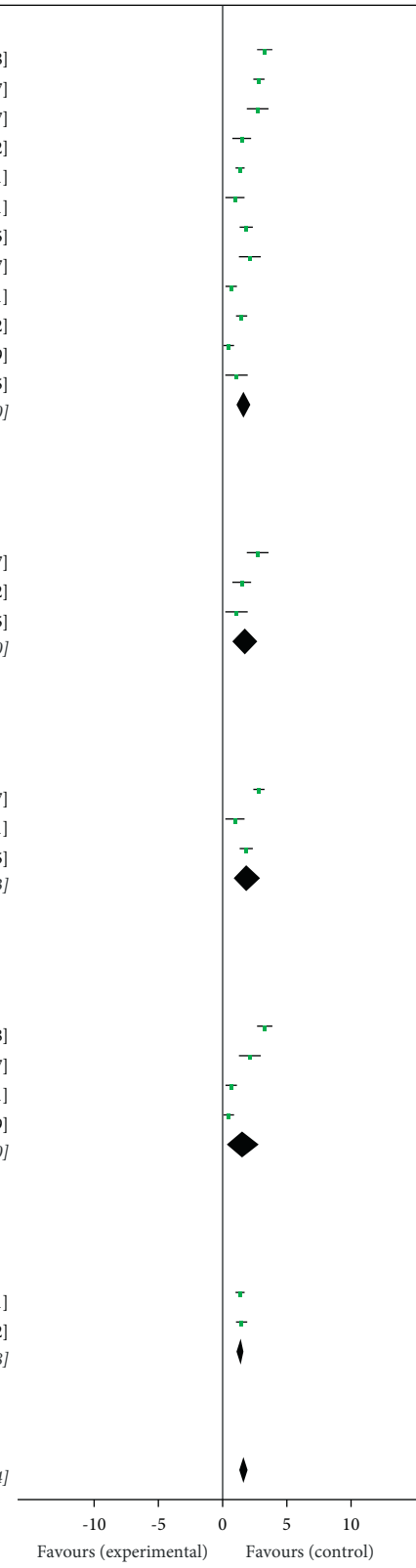

Figure 5: Forest plot of IFRS effective rate.

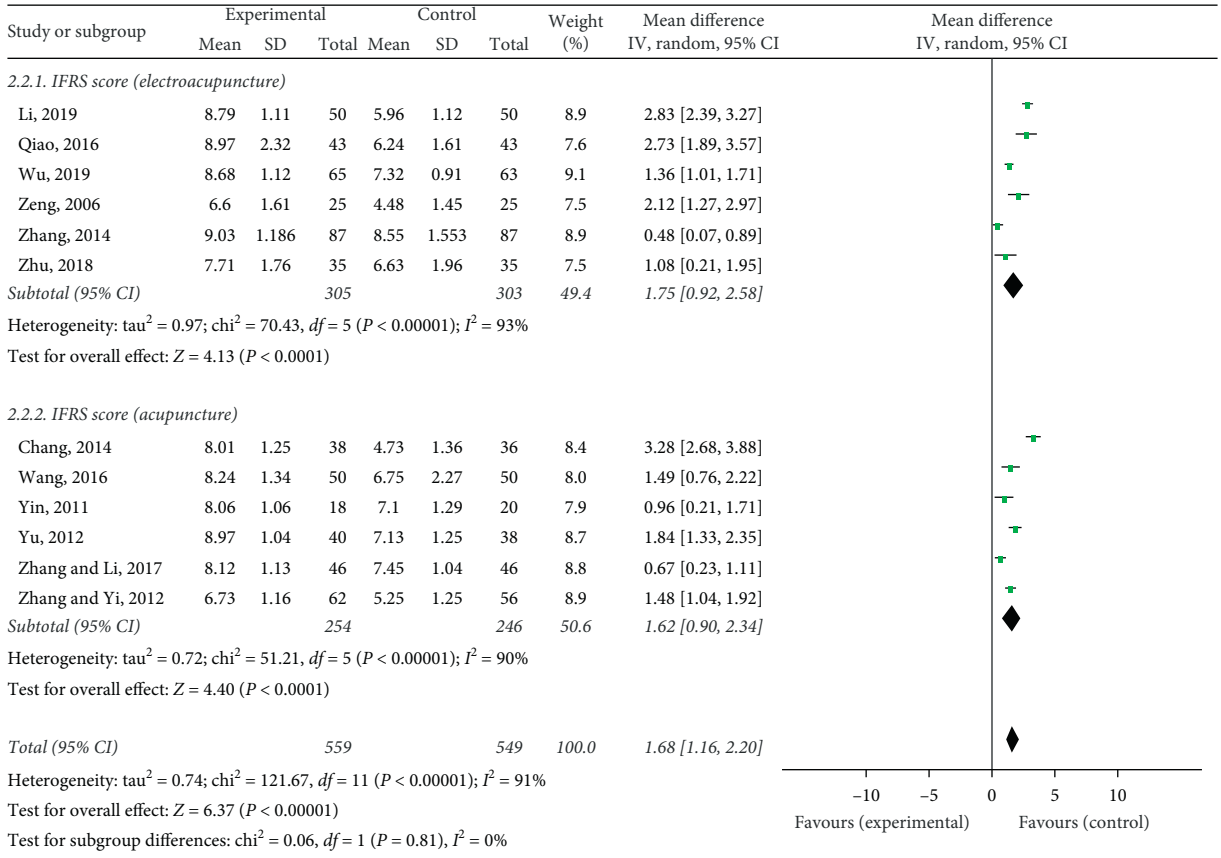

Figure 6: Forest plot of IFRS subgroup analysis.

The advantage of this systematic review was that most of the included RCTs had a low or moderate risk of bias. However, we acknowledge that there are some limitations in this review. First, a language bias may exist because all of the included trials were conducted and published by Chinese investigators. Second, in the present study, only one trial [28] reported allocation concealment, blinding of performance, and blinding of assessment; these risks of bias may affect the interpretation of the results. Finally, four trials [25, 28, 31, 40] excluded dropout participants for data analysis, which may increase the risk of attrition bias.

Poststroke dysphagia is in the category of "unsound speech and motor impairment" in TCM. It is believed in TCM that the etiology and pathogenesis of dysphagia are pathogenic wind, fire, phlegm, blood stasis, and qi deficiency, leading to the dysfunction of Zang-fu organs, reverse flow of qi and blood, obstruction of meridians and collaterals by blood stasis, and oppression of the brain marrow. The location of sickness is related to the brain, mouth, tongue, and throat. Hence, acupuncture can be used at the corresponding points to nourish yin, activate collaterals, wake up the brain, open the aperture, and remove obstruction. Some studies [59–61] showed that acupuncture therapy could improve the blood circulation in the cerebral cortex motor functional areas, promote the recovery of central nervous system function, improve the brain energy metabolism, activate the specific motor functional areas of the cerebral cortex, and promote the remodeling of brain function. This may be the main mechanism of acupuncture in treating dysphagia after stroke.

Meta-analyses showed that acupuncture could improve swallowing at different stages of treatment, and some studies [28, 34, 55] showed that the longer the acupuncture treatment lasts, the better the recovery of swallowing function, which may be related to the time it takes to remodel brain functions. However, some studies [38, 48, 51] showed that the recovery of the swallowing function after acupuncture treatment for more than 4 weeks was not as good as that after acupuncture treatment for 4 weeks, which may be related to the different evaluation criteria of the efficacy of swallowing disorders and the diversity of acupuncture treatment options. VFSS and FEES are two instrumental assessments of dysphagia and are considered the "gold standard" for swallowing assessment [62, 63]. However, only 8 studies used VFSS to evaluate the swallowing performance of the participants, and most of the studies used the WST, SSA, and IFRS. These clinical evaluation scales were subjective clinical evaluation tools based on the observation of the evaluator, which may lead to inaccurate evaluation of the treatment effect. Moreover, in the therapeutic schedule of acupuncture, acupoint selection, stimulation method, needle holding time, and treatment durations in the included studies were not identical, which may affect the outcomes. Previous studies [64–66] showed that many factors influenced the

Study or subgroup	Experimental Mean	SD	Total	Control Mean	SD	Total	Weight (%)	Mean difference IV, random, 95% CI
3.2.1. VFSS score								
Dong, 2018	8.73	1.36	60	6.47	1.32	60	7.5	2.26 [1.78, 2.74]
Feng, 2016	7.46	2.31	30	4.27	1.56	30	5.0	3.19 [2.19, 4.19]
Gao, 2020	6.93	1.05	30	5.97	1.27	30	7.0	0.96 [0.37, 1.55]
Li, 2015	7.46	1.56	42	4.27	1.51	42	6.7	3.19 [2.53, 3.85]
Wei, 2015	6.31	1.47	50	4.19	1.12	50	7.4	2.12 [1.61, 2.63]
Xia, 2016	8.6	1.9	61	5.8	1.6	55	6.8	2.80 [2.16, 3.44]
Zhang and Li, 2017	7.97	1.05	46	5.67	0.88	46	7.9	2.30 [1.90, 2.70]
Zhang, 2016	7.04	1.56	20	5.74	1.62	20	5.1	1.30 [0.31, 2.29]
Subtotal (95% CI)			*339*			*333*	*53.4*	*2.26 [1.77, 2.74]*
Heterogeneity: $tau^2 = 0.38$; $chi^2 = 36.39$, $df = 7$ ($P < 0.00001$); $I^2 = 81\%$								
Test for overall effect: $Z = 9.12$ ($P < 0.00001$)								
3.2.2. VFSS score (2-3 weeks)								
Dong, 2018	8.73	1.36	60	6.47	1.32	60	7.5	2.26 [1.78, 2.74]
Feng, 2016	7.46	2.31	30	4.27	1.56	30	5.0	3.19 [2.19, 4.19]
Wei, 2015	6.31	1.47	50	4.19	1.12	50	7.4	2.12 [1.61, 2.63]
Subtotal (95% CI)			*140*			*140*	*20.0*	*2.36 [1.89, 2.83]*
Heterogeneity: $tau^2 = 0.08$; $chi^2 = 3.56$, $df = 2$ ($P = 0.17$); $I^2 = 44\%$								
Test for overall effect: $Z = 9.86$ ($P < 0.00001$)								
3.2.3. VFSS score (4 weeks)								
Gao, 2020	6.93	1.05	30	5.97	1.27	30	7.0	0.96 [0.37, 1.55]
Li, 2015	7.46	1.56	42	4.27	1.51	42	6.7	3.19 [2.53, 3.85]
Zhang and Li, 2017	7.97	1.05	46	5.67	0.88	46	7.9	2.30 [1.90, 2.70]
Zhang, 2016	7.04	1.56	20	5.74	1.62	20	5.1	1.30 [0.31, 2.29]
Subtotal (95% CI)			*138*			*138*	*26.7*	*1.96 [1.02, 2.90]*
Heterogeneity: $tau^2 = 0.81$; $chi^2 = 28.43$, $df = 3$ ($P < 0.00001$); $I^2 = 89\%$								
Test for overall effect: $Z = 4.08$ ($P < 0.0001$)								
Total (95% CI)			*617*			*611*	*100.0*	*2.22 [1.88, 2.56]*
Heterogeneity: $tau^2 = 0.34$; $chi^2 = 69.61$, $df = 14$ ($P < 0.00001$); $I^2 = 80\%$								
Test for overall effect: $Z = 12.72$ ($P < 0.00001$)								
Test for subgroup differences: $chi^2 = 0.57$, $df = 2$ ($P = 0.75$), $I^2 = 0\%$								

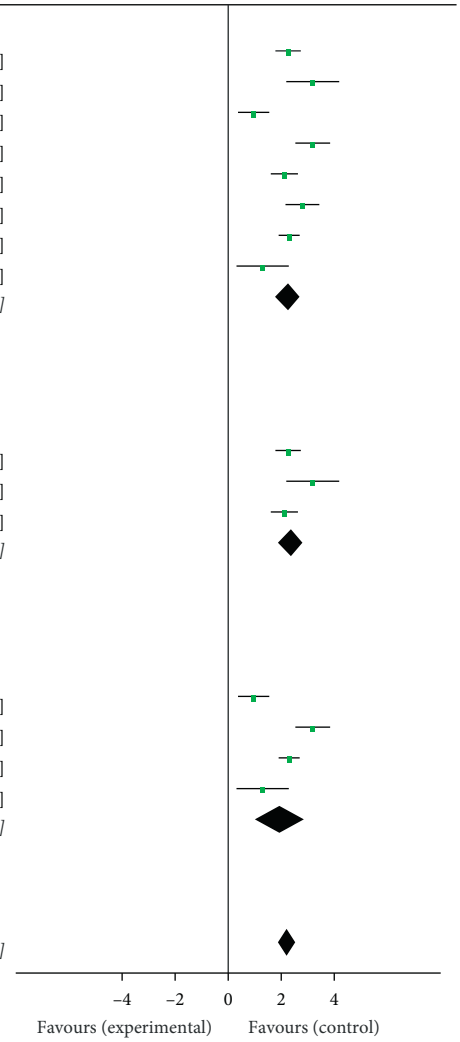

Figure 7: Forest plot of the VFSS effective rate.

efficacy of acupuncture, such as age, comorbidity, gender, disease severity, stimulation of acupuncture, expectations of patients, and doctor-patient interaction, which may be sources of heterogeneity. However, due to the inability to obtain more relevant data, we cannot analyze based on relevant influencing factors. It was necessary to use strict evaluation standards and high-quality RCT designs to explore acupuncture for dysphagia on poststroke.

Electroacupuncture is a technique of acupuncture based on a traditional acupuncture method combined with modern electrotherapy. Six of the 35 studies included in the meta-analysis used electroacupuncture. The results of subgroup analysis showed that both electroacupuncture and simple acupuncture could improve patients' swallowing function, but the effect was not significantly different between the two, which may be related to the small sample size, the diversity of acupuncture treatment options, and the different evaluation criteria for the efficacy of swallowing disorders. There is a need for more high-quality trials with large sample sizes to investigate electroacupuncture.

In this systematic review, the acupoints used in these 35 RCTs were different. Many studies employed individualized acupoints, but there were 5 points that were most commonly used. In this study, the acupoints of the nape were selected according to the adjacent therapeutic effects of the acupoints (Figure 9). Among them, Fengchi (GB 20), an important point for wind, can be used to suppress yang, extinguish wind, dissolve phlegm and benefit the throat, and clear away heat from the head [38]. Lianquan (RN 23) is an important acupoint mainly for aphasia and deglutition disorder, and it can be used to benefit the pharynx [28]. Jinjin (EX-HN12) and Yuye (EX-HN13) are acupoints for dredging meridians, activating collaterals, and regulating and smoothening qi and blood [55]. Yifeng (SJ17) can be used to open depression winds and benefit pharynges [32]. Hence, the above 5 acupoints could nourish yin, activate the collaterals, wake up

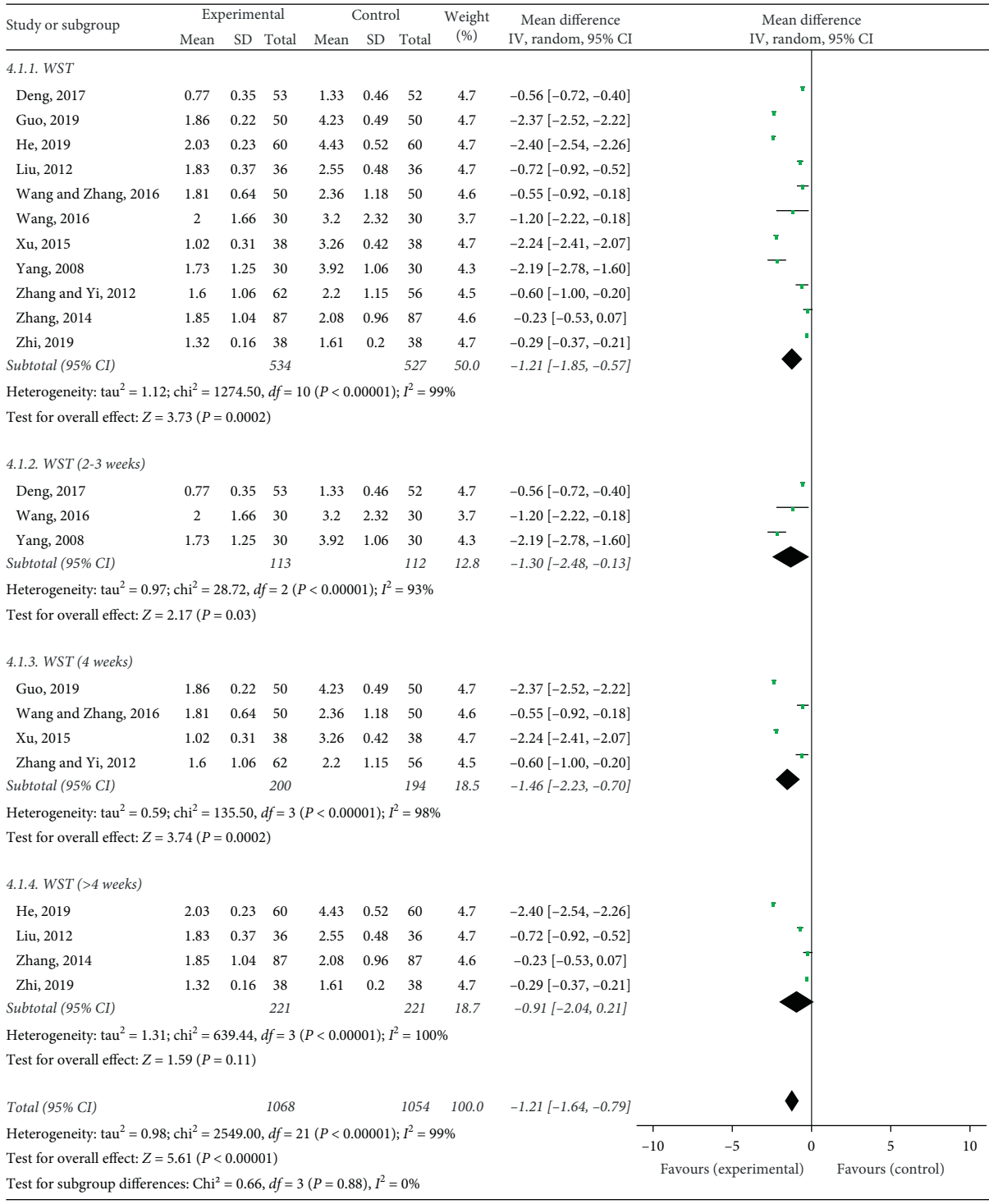

Figure 8: Forest plot of the WST effective rate.

the brain, open the aperture, and remove obstruction, thus benefiting dysphagia patients.

In this systematic review, only three studies [28, 32, 49] reported adverse events, including bleeding, pain, and discomfort, and the reactions were tolerable and not serious. The remaining RCTs did not mention any adverse events or side effects. Therefore, acupuncture is safe for dysphagia.

The results of this systematic review show that acupuncture may offer some benefits to patients with dysphagia. However, this review has several limitations. First, we searched only Chinese and English databases, which may cause publication bias. Second, most clinical evaluation scales included in this study were subjective clinical evaluation tools based on the observation of the evaluator, which

(a) (b)

Figure 9: Acupoints in the neck: (a) bilateral Fengchi (GB20), bilateral Wangu (GB12), bilateral Yifeng (SJ17), Fengfu (DU16), and Yamen (DU15); (b) Lianquan (RN23) and bilateral Jialianquan (extra).

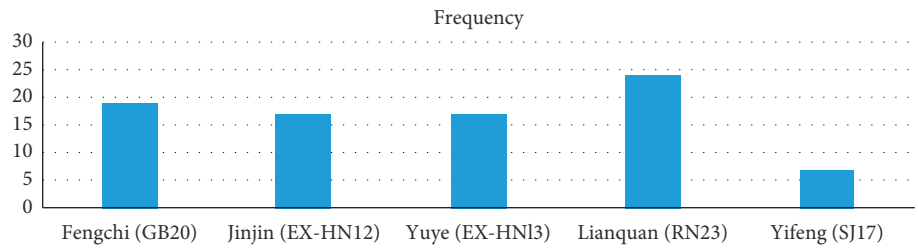

Figure 10: The most frequently used acupoints in these studies.

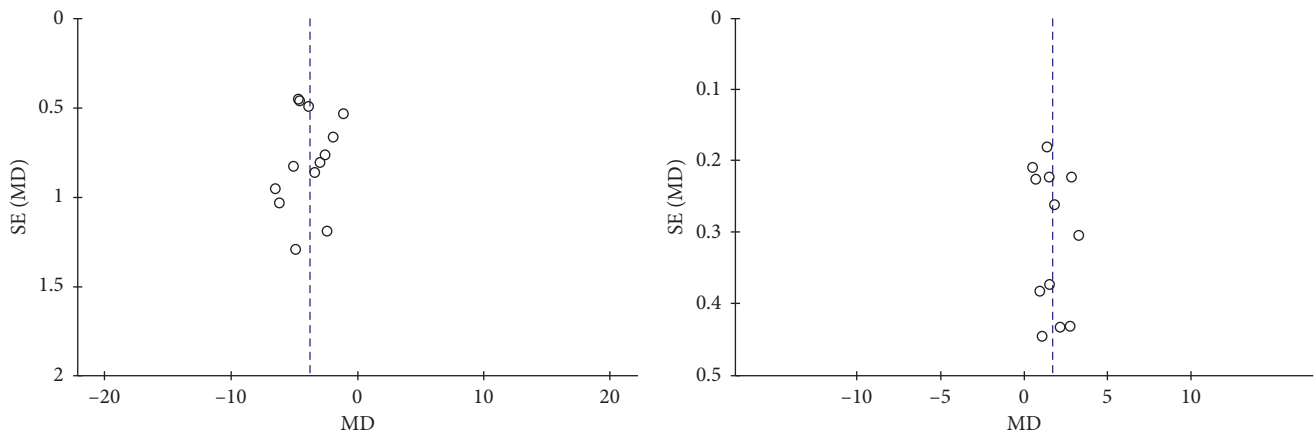

(a) (b)

Figure 11: Continued.

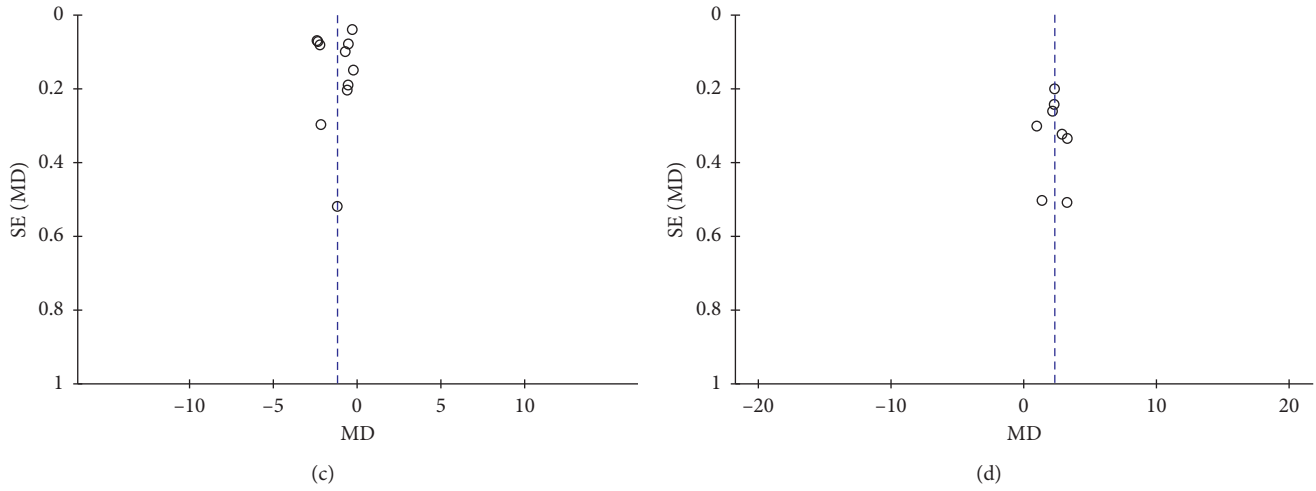

Figure 11: Funnel plot of the publication bias of acupuncture in the (a) SSA, (b) IFRS, (c) VFSS, and (d) WST.

may lead to an inaccurate evaluation of the treatment effect. Third, in the therapeutic schedule of acupuncture, acupoint selection, stimulation method, needle holding time, and treatment durations in the included studies were not identical, which may affect the outcomes. Fourth, in this systematic review, two studies [28, 51] reported a three-month follow-up, and the remaining RCTs reported only the short-term treatment, so the treatment duration and follow-up time were insufficient to draw conclusions. Fifth, the challenge of blinding arises from the unique nature of acupuncture treatment. Acupuncture treatment involves not only a device but also the acupuncture process and its techniques, such as needle insertion and needle manipulations. It was difficult to achieve true double blinding, which may cause a potential performance bias [67]. In the future, to minimize the ascertainment bias of subjects, implementation of the intervention should be carefully designed to achieve effective blinding of the subjects. The outcome assessor should be blinded to the treatment assignment to reduce detection bias in the study, and the statistician involved in data analysis is usually blinded to group assignments so that the data can be analyzed and interpreted appropriately without bias. These limitations could lead to highly heterogeneous results that prevent us from making a definitive conclusion.

5. Conclusion

In conclusion, acupuncture for dysphagia after stroke has therapeutic efficacy and safety. More strict evaluation standards and high-quality RCT designs are necessary for further exploring acupuncture for the treatment of dysphagia after stroke.

Conflicts of Interest

The authors declare that there are no conflicts of interest regarding the publication of this paper.

Authors' Contributions

All authors contributed to the writing and redrafting of the manuscript. Pu Wang had the original idea. Huiyu Liu and Xiao Bao provided support and advice. Lida Zhong, Jing Wang, and Fang Li performed literature search, assessed study quality, and undertook data collection. Results were analyzed by Lida Zhong. Results were interpreted and discussed by Lida Zhong and Jin Wang.

Acknowledgments

The authors thank Yuebei people's hospital and Sun Yat-sen University for providing the literature resources.

References

[1] L. Rofes, N. Vilardell, and P. Clavé, "Post-stroke dysphagia: progress at last," *Neurogastroenterology & Motility*, vol. 25, no. 4, pp. 278–282, 2013.

[2] P. Clavé, L. Rofes, S. Carrión et al., "Pathophysiology, relevance and natural history of oropharyngeal dysphagia among older people," *Stepping Stones to Living Well with Dysphagia*, vol. 72, pp. 57–66, 2012.

[3] M. Arnold, K. Liesirova, A. Broeg-Morvay et al., "Dysphagia in acute stroke: incidence, burden and impact on clinical outcome," *PLoS One*, vol. 11, no. 2, Article ID e0148424, 2016.

[4] C. Geeganage, J. Beavan, S. Ellender et al., "Interventions for dysphagia and nutritional support in acute and subacute stroke," *Cochrane Database of Systematic Reviews*, vol. 10, Article ID CD000323, 2012.

[5] S. M. Lim, J. Yoo, E. Lee et al., "Acupuncture for spasticity after stroke: a systematic review and meta-analysis of randomized controlled trials," *Evidence Based Complementary and Alternative Medicine*, vol. 2015, Article ID 870398, 2015.

[6] Y. Hou, Y. Liu, M. Li et al., "Acupuncture plus rehabilitation for unilateral neglect after stroke: a systematic review and meta-analysis," *Evidence Based Complementary and Alternative Medicine*, vol. 2020, Article ID 5301568, 2020.

[7] S. Kwon, S. Y. Cho, S. U. Park et al., "Study on the evaluation of various types of sham acupuncture treatments in hemiplegic stroke patients: the protocol of a randomized clinical

trial," *Evidence Based Complementary and Alternative Medicine*, vol. 2019, Article ID 7395927, 2019.

[8] L.-X. An, X. Chen, X.-J. Ren, and H.-F. Wu, "Electro-acupuncture decreases postoperative pain and improves recovery in patients undergoing a supratentorial craniotomy," *The American Journal of Chinese Medicine*, vol. 42, no. 5, pp. 1099–1109, 2014.

[9] S. Y. Seo, K.-B. Lee, J.-S. Shin et al., "Effectiveness of acupuncture and electroacupuncture for chronic neck pain: a systematic review and meta-analysis," *The American Journal of Chinese Medicine*, vol. 45, no. 8, pp. 1573–1595, 2017.

[10] Y. T. Chan, H. W. Zhang, W. Z. Sun et al., "Acupuncture for poststroke dysphagia: a pilot, nonrandomized, self-controlled trial," *Evidence Based Complementary and Alternative Medicine*, vol. 2020, Article ID 4689296, 2020.

[11] L. Chen, J. Fang, R. Ma et al., "Acupuncture for acute stroke: study protocol for a multicenter, randomized, controlled trial," *Trials*, vol. 15, no. 1, p. 214, 2014.

[12] P. M. Bath, H. S. Lee, and L. F. Everton, "Swallowing therapy for dysphagia in acute and subacute stroke," *Cochrane Database of Systematic Reviews*, vol. 10, no. 10, Article ID CD000323, 2018.

[13] D. Moher, A. Liberati, J. Tetzlaff, and D. G. Altman, "Preferred reporting items for systematic reviews and meta-analyses: the PRISMA statement," *International Journal of Surgery*, vol. 8, no. 5, pp. 336–341, 2010.

[14] D. M. Suiter and S. B. Leder, "Clinical utility of the 3-ounce water swallow test," *Dysphagia*, vol. 23, no. 3, pp. 244–250, 2008.

[15] J. Ellul and D. Barer, "On behalf of ESDB/COSTAR collaborative dysphagia study. Interobserver reliability of a standardised swallowing assessment (SSA)," *Cerebrovascular Diseases*, vol. 6, pp. 152-153, 1996.

[16] L. Perry, "Screening swallowing function of patients with acute stroke. part two: detailed evaluation of the tool used by nurses," *Journal of Clinical Nursing*, vol. 10, no. 4, pp. 474–481, 2001.

[17] L. Perry, "Screening swallowing function of patients with acute stroke. part one: identification, implementation and initial evaluation of a screening tool for use by nurses," *Journal of Clinical Nursing*, vol. 10, no. 4, pp. 463–473, 2001.

[18] J. C. Rosenbek, J. A. Robbins, E. B. Roecker, J. L. Coyle, and J. L. Wood, "A penetration-aspiration scale," *Dysphagia*, vol. 11, no. 2, pp. 93–98, 1996.

[19] M. A. Crary, G. D. C. Mann, and M. E. Groher, "Initial psychometric assessment of a functional oral intake scale for dysphagia in stroke patients," *Archives of Physical Medicine and Rehabilitation*, vol. 86, no. 8, pp. 1516–1520, 2005.

[20] B. Martin-Harris and B. Jones, "The videofluorographic swallowing study," *Physical Medicine and Rehabilitation Clinics of North America*, vol. 19, no. 4, pp. 769–785, 2008.

[21] C.-W. Kuo, C. T. Allen, C.-C. Huang, and C.-J. Lee, "Murray secretion scale and fiberoptic endoscopic evaluation of swallowing in predicting aspiration in dysphagic patients," *European Archives of Oto-Rhino-Laryngology*, vol. 274, no. 6, pp. 2513–2519, 2017.

[22] J. P. Higgins, D. G. Altman, P. C. Gøtzsche et al., "The cochrane collaboration's tool for assessing risk of bias in randomised trials," *BMJ*, vol. 343, Article ID d5928, 2011.

[23] J. P. T. Higgins, S. G. Thompson, J. J. Deeks et al., "Measuring inconsistency in meta-analyses," *BMJ*, vol. 327, no. 7414, pp. 557–560, 2003.

[24] Z. J. Wang, Y. Zhang, J. C. Qing et al., "Clinical study on acupuncture combined with swallowing training in the treatment of dysphagia after stroke," *China Foreign Medical Treatment*, vol. 35, no. 36, pp. 174–176, 2016.

[25] Y. J. Jiang, L. Lin, Y. M. You et al., "Clinical study on the treatment of swallowing dysfunction after stroke with three tongue needles," *Shanghai Journal of Acupuncture and Moxibustion*, vol. 39, no. 5, pp. 530–535, 2020.

[26] W.-b. Wu, D.-f. Fan, C. Zheng et al., "Relieving throat and opening orifice acupuncture therapy for the post-stroke dysphagia," *World Journal of Acupuncture - Moxibustion*, vol. 29, no. 1, pp. 37–41, 2019.

[27] H. T. Wei, T. Peng, D. Yang et al., "Clinical observation of acupuncture combined with rehabilitation training in the treatment of dysphagia after stroke," *Journal of Emergency in Traditional Chinese Medicine*, vol. 24, no. 10, pp. 1808–1810, 2015.

[28] W. G. Xia, C. J. Zheng, J. H. Xia et al., "Treatment of dysphagia after stroke by acupuncture based on syndrome differentiation: a randomized controlled study," *Chinese Acupuncture & Moxibustion*, vol. 36, no. 7, pp. 673–678, 2016.

[29] H. H. Zeng, C. Ma, S. L. Wu et al., "Comparative observation on acupuncture treatment for dysphagia after stroke," *Chinese Journal of Rehabilitation Medicine*, vol. 21, no. 4, pp. 343-344, 2006.

[30] L. Chang, P. L. He, Z. Z. Zhou et al., "Observation on the effect of acupuncture combined with functional electrical stimulation on dysphagia after acute stroke," *Chinese Acupuncture & Moxibustion*, vol. 34, no. 8, pp. 737–740, 2014.

[31] F. Y. Chen, X. P. Liu, Y. H. Bao et al., "Clinical observation on the treatment of pseudobulbar paralysis after stroke by "Xiang Zhen" combined with rehabilitation training," *Shanghai Journal of Acupuncture and Moxibustion*, vol. 37, no. 2, pp. 135–139, 2018.

[32] S. W. Feng, S. H. Cao, S. J. Du et al., "Acupuncture combined with swallowing training in the treatment of dysphagia after stroke: a randomized controlled study," *Chinese Acupuncture & Moxibustion*, vol. 36, no. 4, pp. 347–350, 2016.

[33] T. T. Guo and X. H. Li, "Treatment of dysphagia after ischemic stroke with Xiang Wuzhen," *China Journal of Chinese Medicine*, vol. 34, no. 2, pp. 431–434, 2019.

[34] Q. S. He, L. F. Yang, and W. B. Wang, "Acupuncture treatment of dysphagia caused by ischemic stroke," *China Journal of Chinese Medicine*, vol. 34, no. 7, pp. 1551–1554, 2019.

[35] H. Y. Li and X. Y. Ma, "42 cases of dysphagia after stroke treated with acupuncture," *Henan Traditional Chinese Medicine*, vol. 35, no. 2, pp. 289-290, 2015.

[36] J. Z. Li, J. H. Li, and Z. Y. Si, "Clinical observation of electroacupuncture on dysphagia after stroke," *China's Naturopathy*, vol. 27, no. 24, pp. 9-10, 2019.

[37] X. Z. Li, B. L. Gu, H. Zhou et al., "The effect of nape acupuncture on swallowing function in patients with cerebral infarction," *Medical Journal of Chinese People's Liberation Army*, vol. 44, no. 4, pp. 322–326, 2019.

[38] D.-D. Liu, X. Tong, J.-y. Kou, Y. Wei, T.-S. Yang, and L.-D. Qiao, "Influence of acupuncture on remodeling of swallowing functions for patients with pseudobulbar palsy after cerebral infarction," *Journal of Acupuncture and Tuina Science*, vol. 10, no. 1, pp. 44–48, 2012.

[39] Z. Q. Qiao, F. F. Chen, and Y. H. Luo, "43 cases of dysphagia after stroke treated with acupuncture," *Henan Traditional Chinese Medicine*, vol. 36, no. 8, pp. 1356–1358, 2016.

[40] Q. L. Wang and L. Chen, "Observation on the therapeutic effect of three tongue needles combined with VitalStim electric stimulation on dysphagia after stroke," *Shanghai*

Journal of Acupuncture and Moxibustion, vol. 38, no. 2, pp. 183–187, 2019.

[41] Y. D. Wang, "Clinical observation on acupuncture treatment of dysphagia after stroke," *Chinese Journal of Ethnomedicine and Ethnopharmacy*, vol. 25, no. 23, pp. 89-90, 2016.

[42] B. Xu, "Analysis of therapeutic effect of acupuncture on stroke pseudobulbar palsy," *Shanxi Journal of Traditional Chinese Medicine*, vol. 36, no. 10, pp. 1413-1414, 2015.

[43] X. H. Yang and S. L. Zhang, "30 cases of dysphagia due to pseudobulbar palsy after stroke treated by acupuncture," *Journal of Changchun University of Traditional Chinese Medicine*, vol. 24, no. 6, p. 712, 2008.

[44] Z. H. Yu and J. F. Hu, "Observation on the effect of acupuncture combined with rehabilitation training on dysphagia after stroke," *Shanghai Journal of Acupuncture and Moxibustion*, vol. 31, no. 9, pp. 642–644, 2012.

[45] Y. H. Zhu, "Clinical observation on 50 cases of dysphagia after acute cerebral infarction treated by acupuncture," *Jiangsu Journal of Acupuncture and Moxibustion*, vol. 44, no. 7, pp. 64-65, 2012.

[46] T. X. Zhou, L. J. Li, E. H. Feng et al., "Clinical observation on the treatment of dysphagia after stroke with scalp acupuncture and swallowing speech diagnosis and treatment instrument," *Journal of Guangzhou University of Traditional Chinese Medicine*, vol. 34, no. 6, pp. 859–863, 2017.

[47] K. X. Zhou, H. N. Ou, D. Zheng et al., "Observation on the clinical effect of swallowing training under scalp acupuncture on dysphagia after stroke," *Chinese Journal of Physical Medicine and Rehabilitation*, vol. 37, no. 12, pp. 936–939, 2015.

[48] J. M. Zhi, X. H. Bu, G. Liu et al., "Effect of tongue acupuncture combined with rehabilitation training on swallowing function and limb function of patients with stroke in recovery period," *Journal of Clinical Acupuncture and Moxibustion*, vol. 35, no. 9, pp. 12–16, 2019.

[49] Y. Zhang and J. Li, "Therapeutic effect of acupuncture combined with VitalStim electric stimulation on dysphagia after ischemic stroke," *Chinese Journal of Integrated Traditional and Western Medicine in Intensive and Critical Care*, vol. 24, no. 4, pp. 346–350, 2017.

[50] X. L. Zhang, Z. M. Tang, L. Y. Mao et al., "Effect of acupuncture combined with repetitive transcranial magnetic stimulation on oral dysphagia after stroke," *Chinese Journal of Physical Medicine and Rehabilitation*, vol. 41, no. 4, pp. 257–260, 2019.

[51] S. Zhang and G. M. Zhang, "87 cases of dysphagia after stroke treated by acupuncture combined with swallowing rehabilitation training," *Journal of Anhui University of Traditional Chinese Medicine*, vol. 33, no. 5, pp. 56–59, 2014.

[52] R. Y. Zhang and Y. D. Yin, "Observation on therapeutic effect of kidney tonifying acupuncture on dysphagia after cerebral infarction," *Shanghai Journal of Acupuncture and Moxibustion*, vol. 31, no. 9, pp. 637–639, 2012.

[53] Q. Zhang, H. Y. Fu, H. Liu et al., "Effect of acupuncture combined with neuromuscular electrical stimulation on dysphagia after stroke," *Chinese Journal of Rehabilitation*, vol. 31, no. 1, pp. 39–41, 2016.

[54] Z. L. Yin, Z. X. Meng, Y. J. Xue et al., "Observation on the effect of swallowing training combined with acupuncture and electrical stimulation on moderate and severe dysphagia in the recovery period of stroke," *Chinese Journal of Physical Medicine and Rehabilitation*, vol. 33, no. 12, pp. 916–919, 2011.

[55] J. X. Gao and H. F. Zhou, "Observation on therapeutic effect of nape cluster acupuncture combined with swallowing function training on dysphagia in stroke," *Chinese Acupuncture & Moxibustion*, vol. 40, no. 6, pp. 586–590, 2020.

[56] G. Q. Dong, "Observation on the therapeutic effect of acupuncture on 120 patients with dysphagia after stroke," *The Journal of Medical Theory and Practice*, vol. 31, no. 5, pp. 666-667, 2018.

[57] X. X. Deng and C. Wu, "Clinical study of Xingnaokaiqiao acupuncture combined with VitalStim swallowing therapeutic apparatus in the treatment of dysphagia in stroke," *China Journal of Chinese Medicine*, vol. 32, no. 226, pp. 466–469, 2017.

[58] P. Y. Zhu, D. Wu, D. Chen et al., "Treatment of dysphagia after cerebral hemorrhage with Yu's nape needle," *Journal of Changchun University of Traditional Chinese Medicine*, vol. 34, no. 2, pp. 282–284, 2018.

[59] L. F. Chen, J. Q. Fang, L. N. Chen et al., "The results and Enlightenment of modern acupuncture treatment for stroke based on neuroanatomy," *Acupuncture Research*, vol. 39, no. 2, pp. 164–168, 2014.

[60] Z. Xie, F. Cui, Y. Zou et al., "Acupuncture enhances effective connectivity between cerebellum and primary sensorimotor cortex in patients with stable recovery stroke," *Evidence Based Complementary and Alternative Medicine*, vol. 2014, Article ID 603909, 2014.

[61] N. Zhou and H. F. Zhou, "Clinical research progress of acupuncture in the treatment of dysphagia after stroke," *Journal of Liaoning University of Traditional Chinese Medicine*, vol. 16, no. 8, pp. 250-251, 2014.

[62] S. E. Langmore, "History of fiberoptic endoscopic evaluation of swallowing for evaluation and management of pharyngeal dysphagia: changes over the years," *Dysphagia*, vol. 32, no. 1, pp. 27–38, 2017.

[63] J. Allen, D. Blair, and A. Miles, "Assessment of videofluoroscopic swallow study findings before and after cricopharyngeal myotomy," *Head & Neck*, vol. 39, no. 9, pp. 1869–1875, 2017.

[64] G. X. Shi, X. M. Yang, C. Z. Liu et al., "Factors contributing to therapeutic effects evaluated in acupuncture clinical trials," *Trials*, vol. 21, no. 13, p. 42, 2012.

[65] L. Klaus, N. Karin, A. Schneider et al., "How large are the nonspecific effects of acupuncture? A meta-analysis of randomized controlled trials," *BMC Medicine*, vol. 8, no. 1, p. 75, 2010.

[66] H. Pan, R. Jin, M. Li, Z. Liu, Q. Xie, and P. Wang, "The effectiveness of acupuncture for osteoporosis: a systematic review and meta-analysis," *The American Journal of Chinese Medicine*, vol. 46, no. 3, pp. 489–513, 2018.

[67] H. Chen, M. Yang, Z. Ning et al., "A guideline for randomized controlled trials of acupuncture," *The American Journal of Chinese Medicine*, vol. 47, no. 1, pp. 1–18, 2019.

Hindawi
Evidence-Based Complementary and Alternative Medicine
Volume 2021, Article ID 1207092, 10 pages
https://doi.org/10.1155/2021/1207092

Research Article

Neuroprotective Effects of Early Hypothermia Induced by Phenothiazines and DHC in Ischemic Stroke

Yun Han,[1,2] Xiao-kun Geng,[1,2,3] Hangil Lee,[3] Fengwu Li,[1] and Yuchuan Ding[3,4]

[1]*Luhe Institute of Neuroscience, Capital Medical University, Beijing, China*
[2]*Department of Neurology, Luhe Clinical Institute, Capital Medical University, Beijing, China*
[3]*Department of Neurosurgery, Wayne State University School of Medicine, Detroit, Michigan, USA*
[4]*Department of Research & Development Center, John D. Dingell VA Medical Center, Detroit, Michigan, USA*

Correspondence should be addressed to Xiao-kun Geng; xgeng@ccmu.edu.cn

Received 27 May 2020; Revised 11 December 2020; Accepted 31 December 2020; Published 18 January 2021

Academic Editor: Shao-Hsuan Kao

Background and Purpose. Studies have shown that interischemia hypothermia is able to reduce the size of myocardial infarctions and improve their clinical outcomes. The present study determined whether interischemia hypothermia induced by the pharmacological approach induced stronger neuroprotection in ischemic brains. *Methods*. Adult male Sprague Dawley rats were studied in 4 groups: (1) sham; (2) stroke; (3) stroke treated with pharmacological hypothermia before reperfusion (interischemia hypothermia); and (4) stroke treated with pharmacological hypothermia after reperfusion is initiated (inter-reperfusion hypothermia). The combination of chlorpromazine and promethazine with dihydrocapsaicin (DHC) was used to induce hypothermia. To compare the neuroprotective effects of drug-induced hypothermia between the interischemia and inter-reperfusion groups, brain damage was evaluated using infarct volume and neurological deficits at 24 h reperfusion. In addition, mRNA expressions of NADPH oxidase (NOX) subunits ($gp91^{phox}$, $p67^{phox}$, $p47^{phox}$, and $p22^{phox}$) and glucose transporter subtypes (GLUT1 and GLUT3) were determined by real-time PCR at 6 and 24 h reperfusion. ROS production was measured by flow cytometry assay at the same time points. *Results*. In both hypothermia groups, the cerebral infarct volumes and neurological deficits were reduced in the ischemic rats. At 6 and 24 h reperfusion, ROS production and the expressions of NOX subunits and glucose transporter subtypes were also significantly reduced in both hypothermia groups as compared to the ischemic group. While there were no statistically significant differences between the two hypothermia groups at 6 h reperfusion, brain damage was significantly further decreased by interischemia hypothermia at 24 h. *Conclusion*. Both interischemia and inter-reperfusion pharmacological hypothermia treatments play a role in neuroprotection after stroke. Interischemia hypothermia treatment may be better able to induce stronger neuroprotection after ischemic stroke. This study provides a new avenue and reference for stronger neuroprotective hypothermia before vascular recanalization in stroke patients.

1. Introduction

Stroke is a leading cause of severe disability and a serious threat to human health worldwide. It has caused serious social and economic burdens [1, 2]. Super-early (4.5 hours) rt-PA intravenous thrombolysis is currently the most commonly used method of treatment for acute cerebral infarction. However, because of the narrow "time window," high bleeding risk, inadequate national health consciousness, poor medical resource distribution, and problematic traffic congestion in our country, the actual thrombolysis rate is less than 30% [3]. Because of these limitations, a majority of patients cannot get timely and effective treatment [4]. Intra-arterial contact thrombolysis, mechanical thrombolysis, direct stent implantation, and other technologies have gradually appeared in recent years, hence extending the treatment time window and enabling the recanalization rate of occluded vessels to reach 71% [5–7]. However, the favorable prognosis in patients with recanalization was still less than 46%.

The core principle of acute ischemic cerebral infarction treatment is twofold: to prevent the expansion of irreversible

injury and to save reversible ischemic tissue (also known as ischemic penumbra) [8]. Hypothermia therapy is currently recognized as one of the few effective neuroprotective strategies in the world [9–14]. In fact, due to its positive neuroprotective effects, mild hypothermia has been used worldwide for brain protection after neonatal hypoxic ischemic encephalopathy [15, 16], traumatic brain injury [17, 18], and cardiac resuscitation [19]. Clinically, the major limitations of physical hypothermia are the delays in cooling initiation and onset of target temperature. The late start necessitates prolonged cooling duration, which requires extensive medical and nursing efforts, and causes secondary complications [20]. Considering interischemia hypothermia, its benefits have been shown in cardiac studies, where it has improved the prognosis of patients [21]. However, it is not known whether interischemia hypothermia reduces tissue damage in acute ischemic stroke.

Studies have shown that therapeutic hypothermia can play a neuroprotective role by inhibiting the activity of nicotinamide adenine dinucleotide phosphate (NADPH) oxidase (NOX) and reducing the generation of reactive oxygen species (ROS) [22, 23]. NOX activation is an important mechanism of brain injury, which can be further aggravated by high glucose metabolism after stroke. After the occurrence of ischemic stroke, ATP in the penumbra is rapidly exhausted, and the brain tissue produces a large amount of reduced NADPH through the anoxic metabolic pathway through the hexose phosphate bypass. Under the action of NOX, a large amount of ROS is produced, leading to oxidative stress injury [24–26]. Previous studies have proved that NOX gene knockout mice [27] or NOX inhibitor intervention [28] can successfully inhibit ROS production and thereby reduce the oxidative stress injury after ischemia [29, 30]. In addition, our previous studies have found that drug-induced hypothermia after reperfusion inhibited the activity of NOX, reduced the production of ROS, and reduced the consequent oxidative stress, so as to play a neuroprotective role [31].

In this study, we determined whether interischemia hypothermia induced by the pharmacological approach induced stronger neuroprotection in the brain through inhibiting the activity of NOX and reducing the production of ROS. If successful, this study on the treatment of acute cerebral infarction before recanalization provides a reference for effective treatments and provides a basis for clinical transformation. In this way, stroke patients could receive drug hypothermia treatment with less medical and nursing efforts before vascular recanalization to protect the brain from further injury.

2. Materials and Methods

2.1. Subjects. All experimental protocols were approved by the Animal Care and Use Committee, Capital Medical University, Beijing, China, according to the National Institutes of Health (NIH, Bethesda, MD, USA) Guide for the Care and Use of Laboratory Animals. All adult male Sprague Dawley rats (280–320 g, Vital River Laboratory Animal Technology Co., Ltd., Beijing, China) were randomly divided into 4 groups (Figure 1(a)): (1) sham-operated group without middle cerebral artery occlusion (MCAO); (2) stroke group without pharmacological hypothermia (MCAO 2 h); (3) stroke group treated with pharmacological hypothermia 1 h before reperfusion (interischemia hypothermia) (MCAO 2 h/1 h); and (4) stroke group treated with pharmacological hypothermia after reperfusion is initiated (inter-reperfusion hypothermia) (MCAO 2 h/2 h). Each group was further divided into three subgroups, with 8 rats in each subgroup. The combination of chlorpromazine and promethazine with dihydrocapsaicin (DHC) was used to induce hypothermia. All experimental procedures and data analysis were performed in a randomized and blinded manner. At 24 h reperfusion, neurological deficits and infarct volume were examined in each group, and biochemical assays were performed.

2.2. Focal Cerebral Ischemia. The procedures have been described previously by us [31]. The animals underwent fasting for 12 h before the operation began. Animals were anesthetized in a chamber with 1–3% isoflurane along with a mixture of 70% nitrous oxide and 30% oxygen and maintained with 1% isoflurane. A 2 h right MCAO was induced using an intraluminal filament [32]. During operation, body temperature (rectal temperature), blood pH, pCO_2 and pO_2, and mean arterial pressure (MAP) were all monitored. Laser Doppler was used to monitor blood flow in the MCA-supplied region to ensure the success of the model.

2.3. Pharmacological Hypothermia. In all ischemia models with 2 h MCAO following reperfusion, a 1 : 1 ratio of chlorpromazine and promethazine (C + P) at 4 mg/kg in 3 ml of saline combined with dihydrocapsaicin (DHC) at doses of 0.5 mg/kg [33] was injected intraperitoneally, as described by us previously [31] at 1 or 2 h after the onset of ischemia. In order to maintain and enhance the efficacy of the drugs, a second injection with 1/3 of the initial dose was delivered in 2 h.

2.4. Body Temperature Monitoring. Rectal temperature (body temperature) was monitored in 30-minute or 1 h increments from before hypothermia until it returned to the initial levels.

2.5. Cerebral Infarct Volume. The rats were anesthetized with 1% chloral hydrate, and the brain tissue of the ischemic rats was removed and immediately sliced into seven coronal sections (2 mm thick), as described previously by us [34]. The sections were stained with 2,3,5-triphenyltetrazolium chloride (TTC, Sigma, USA) at 37°C. ImageJ image analysis software was used to measure cerebral infarction volume. In order to reduce the error caused by cerebral edema, the cerebral infarction volume was measured indirectly using the indirect calculation method, relative to the noninfarcted hemisphere.

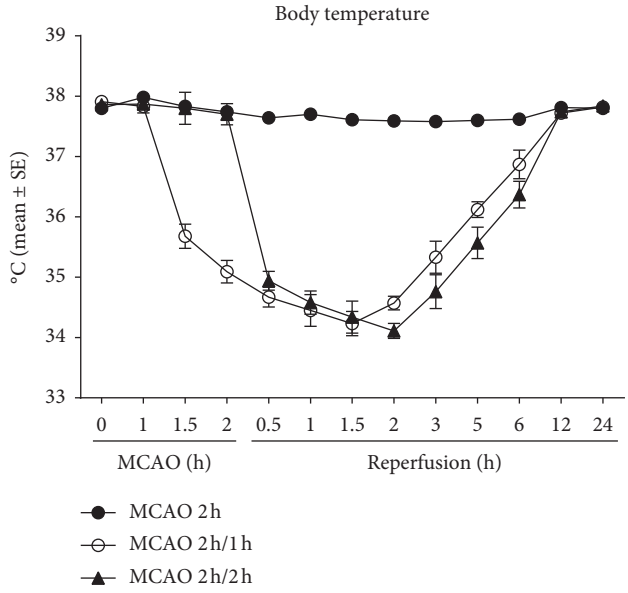

Figure 1: Body temperatures of 2 h MCAO rats with or without hypothermia at different time points.

2.6. Neurological Deficits. The neurological function deficits were determined by the 5-scoring system [32] before surgery, 2 h after stroke, and 24 h after reperfusion. The higher scores indicate more serious neurological defects.

2.7. ROS Production Measurement by Flow Cytometry Assay. As described previously by us [35], the adult brain dissociation kit (130-107-677, Miltenyi Biotec, Bergisch Gladbach, Germany) was used for brain cell isolation. Rats were sacrificed at 6 and 24 h after reperfusion, and the right hemispheres were cut into small pieces, ground, and filtered through a 70 μm cell strainer (Miltenyi Biotec, Bergisch Gladbach, Germany) to obtain single-cell suspensions. Fluorescent-labeled antibodies were added to the cells and incubated at 37°C for 60 minutes according to the instructions. Cells were then washed and analyzed on a FACSCalibur flow cytometer with CellQuest software (BD, San Jose, CA, USA). Results were expressed by the fluorescence value.

2.8. Expression of NOX Subunits and Glucose Transporter Subtypes. After homogenization of the isolated cerebral microvessels, TRIzol reagent (Invitrogen, Carlsbad, CA) was used to extract mRNA according to the instructions. Total RNA was then converted into cDNA by a High-Capacity cDNA Reverse Transcription Kit (Applied Biosystems, Foster City, CA). Using cDNA, gene expression was quantified by Prism 7500 real-time PCR (Applied Biosystems, CA, USA). All reactions were performed under the following conditions: 95°C for 15 minutes, 40 cycles of 95°C for 10 seconds, and 60°C for 30 seconds. The sequences for the primers of rat NOX subunits (gp91^{phox}, p67^{phox}, p47^{phox}, and p22^{phox}), glucose transporter subtypes (GLUT1 and GLUT3), and GADPH are shown in Table 1. GADPH was used as the control gene to determine the relative expression of mRNA.

2.9. Statistical Analyses. All data are expressed as mean ± SE. All of the analyses were performed using GraphPad Prism v7.0 (GraphPad Software, San Diego, CA). The differences between the groups were assessed using one-way analysis of variance (ANOVA) with the significance level set at $P < 0.05$. Post hoc comparisons between groups were further performed using the least significant difference method.

3. Results

3.1. Physiological Parameters. There were no significant differences in blood pH, pO_2, and pCO_2 between the groups (data not shown).

3.2. Body Temperature. In the interischemia hypothermia group, a 2.23°C drop was seen in the temperature within 30 minutes of drug administration at 1 h after stroke (1 h before reperfusion) and continued to fall to the lowest of 3.68°C below the initial temperature at 1.5 h reperfusion (Figure 1). Meanwhile, in the inter-reperfusion hypothermia group, a 2.92°C drop was seen within 30 minutes of pharmacological hypothermia induction at 30 min reperfusion and continued to fall to the lowest of 3.75°C under the initial temperature at 2 h reperfusion. For both groups, the body temperatures remained under the initial measurements for up to 12 h reperfusion. Notably, hypothermia was achieved 1 h earlier in the interischemia group compared to the inter-reperfusion hypothermia group.

3.3. Cerebral Infarct Volume and Neurological Deficits. As compared to the stroke group without hypothermia, with the largest cerebral infarct volume at 24 h reperfusion (48.5%) (Figures 2(a) and 2(b)), both hypothermia groups had significantly decreased infarct volumes. The interischemia hypothermia group had a greater decrease in infarct volume of 25.2% ($^{###}p < 0.001$) vs. 32.1% ($^{##}p < 0.01$) in the inter-reperfusion hypothermia group. As compared to the stroke group at 24 h reperfusion (3.0) (Figure 2(c)), again, both interischemia hypothermia group ($^{##}p < 0.01$) and inter-reperfusion hypothermia group ($^{#}p < 0.05$) had reduced neurological deficit scores, with interischemia hypothermia being more neuroprotective.

3.4. Expression of NOX Subunits and Glucose Transporter Subtypes. The stroke group without hypothermia had a significant increase in the mRNA expression of NOX subunits (gp91^{phox}, p67^{phox}, p47^{phox}, and p22^{phox}) at 6 and 24 h reperfusion (Figure 3). Compared to this group, both hypothermia groups observed significantly reduced mRNA expressions of NOX subunits at 6 and 24 h reperfusion. At 24 h reperfusion (Figures 3(b), 3(d), 3(f), and 3(h)), the interischemia hypothermia group had a significant additional reduction in NOX subunit mRNA expression.

Table 1: Primers for real-time polymerase chain reaction (PCR) analysis.

Genes	Forward primer (5'-3')	Reverse primer (5'-3')
gp91^{phox}	TGACTCGGTTGGCTGGCATC	CGCAAAGGTACAGGAACATGGG
p67^{phox}	AGCAGAAGAGCAGTTAGCATTGG	TGCTTTCCATGGCCTTGTC
p47^{phox}	TCACCGAGATCTACGAGTTC	ATCCCATGAGGCTGTTGAAGT
p22^{phox}	TGTTGCAGGAGTGCTCATCTGTCT	AGGACAGCCCGGACGTAGTAATTT
GLUT1	CAGAGCGACAAGACACCTGA	ACTGAAGAAAGGTGCCCAGG
GLUT3	GTGGAGCGGTGAAGATCAGATA	GGCAACAGTAACAGCGAACA
GADPH	CAAGAAGGTGGTGAAGCAG	AAAGGTGGAAGAATGGGAG

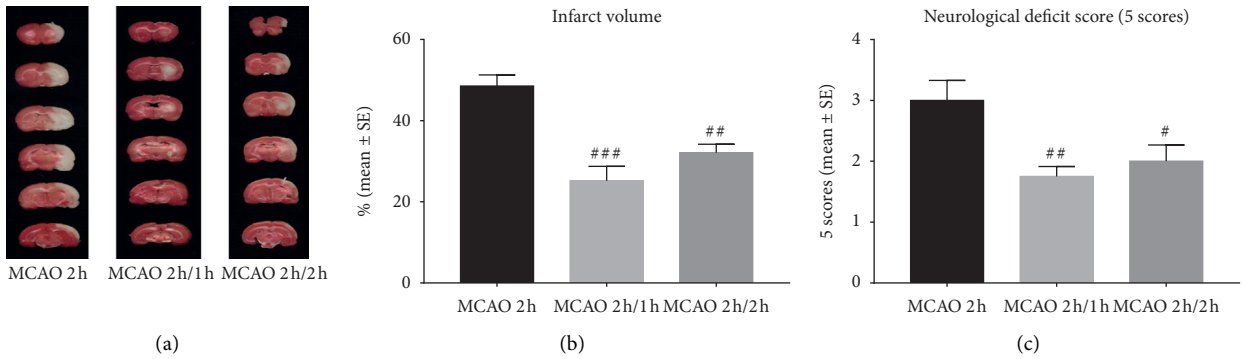

Figure 2: TTC histology demonstrated cerebral infarct volume after stroke with or without hypothermia (a, b). Neurological deficits after stroke and pharmacological hypothermia, using the 5-score system (c). $^{\#}p < 0.05$, $^{\#\#}p < 0.01$, and $^{\#\#\#}p < 0.001$ as compared to the MCAO 2 h group ($n = 8$).

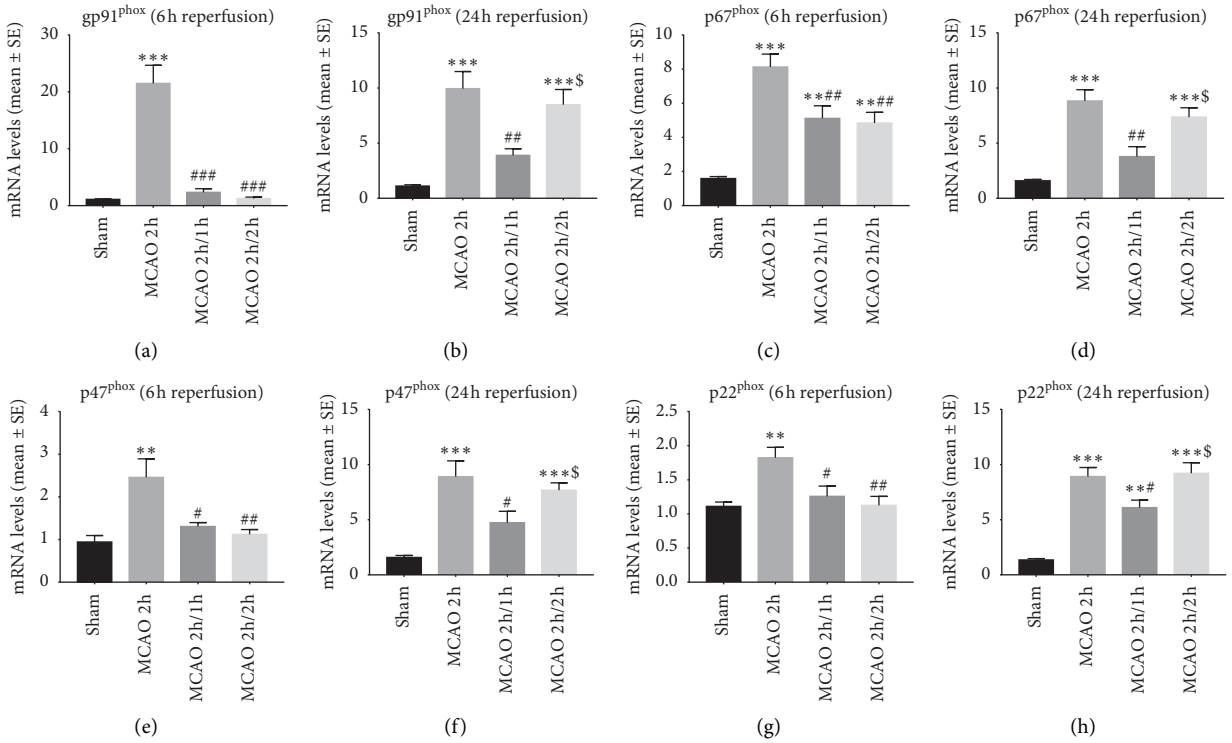

Figure 3: The mRNA expressions of NOX subunits (gp91^{phox}, p67^{phox}, p47^{phox}, and p22^{phox}) determined by real-time PCR at 6 and 24 h reperfusion. $^{*}P < 0.05$, $^{**}P < 0.01$, and $^{***}P < 0.001$ as compared to the sham group; $^{\#}p < 0.05$, $^{\#\#}p < 0.01$, and $^{\#\#\#}p < 0.001$ as compared to the MCAO 2 h group; $^{\$}P < 0.05$ as compared to the MCAO 2 h/1 h group ($n = 8$).

A significant increase in the mRNA expression of glucose transporter subtypes (GLUT1 and GLUT3) was seen in ischemic rats with 6 and 24 h reperfusion (Figure 4). Both hypothermia groups observed significantly reduced mRNA expressions. Although there was no difference between interischemia and inter-reperfusion in the reduction of glucose transporter subtype mRNA at 6 h reperfusion (Figures 4(a) and 4(c)), at 24 h reperfusion (Figures 4(b) and 4(d)), interischemia hypothermia induced a significantly greater reduction of mRNA expression.

3.5. ROS Production. Stroke induced a significant increase in ROS production at 6 and 24 h reperfusion ($^{**}P < 0.01$) (Figure 5). The two hypothermia protocols significantly decreased the ROS production at 6 h reperfusion (Figures 5(a) and 5(c)) ($^{\#\#}p < 0.01$), while the interischemia hypothermia group enhanced the ROS reduction ($P\$ < 0.05$) at 24 h reperfusion (Figures 5(b) and 5(d)).

4. Discussion

In this study, we reported that hypothermia conducted interischemia or inter-reperfusion reduced cerebral infarction volume, neurological deficits, ROS production, and mRNA expression of NOX subunits as well as glucose transporter subtypes. In addition, we found that interischemia hypothermia had further reduced the indications for brain damage compared to inter-reperfusion hypothermia at 24 h after stroke. These findings support our hypothesis that interischemia hypothermia induced by the pharmacological approach provided stronger neuroprotection of the ischemic brain.

Hypothermia therapy depends largely on several factors, such as the time of initiation, the duration, and the depth of hypothermia [11, 36]. Studies have shown that hypothermia should be initiated as soon as possible, target temperature reached quickly, and the lower temperature maintained for a considerable period for better neuroprotective effect [20]. Some earlier studies have shown that reducing the body temperature by only a few degrees, if it is induced in the early ischemic period, can have significant neuroprotective effects [37–39].

The benefits of interischemia hypothermia have been shown in cardiac studies [40, 41]. Studies have reported that hypothermia before reperfusion can reduce the size of myocardial infarction, save more dying myocardial cells, and improve the outcome of myocardial infarction. Many studies of animal models and human trials have shown that interischemia hypothermia is not only safe and feasible but also has good protective effects on ischemic myocardium [42–45]. Compared to postreperfusion hypothermia, interischemia hypothermia has been shown to be more beneficial to cardiomyocytes, which may be related to decreased core infarction volume, oxidative damage, and cell damage after reperfusion. To further illustrate, a previous study showed that the induction of hypothermia 25 minutes after ischemia onset with 40 minutes total ischemia time resulted in a 39% reduction in myocardial infarction area in pigs, whereas hypothermia after reperfusion did not reduce myocardial infarct volume [43]. Furthermore, reaching target temperature before reperfusion is of crucial importance in reducing the infarct size in the treatment of ST-segment elevation myocardial infarction (STEMI) patients [46].

In cerebral ischemia, some evidence supports that early prophylactic mild-to-moderate hypothermia induced shortly after injury in patients with severe traumatic brain injury could decrease mortality and improve neurologic recovery [47]. Ding et al. showed that local cerebral hypothermia induced by infusion of cold saline prior to reperfusion that is maintained for 10 minutes and followed by complete reperfusion can reduce brain injury, improve neurological function, and maintain long-term functional recovery [48]. The advantage of interischemia hypothermia is that the target temperature is reached prior to reperfusion, which not only reduces ischemia injury but also reperfusion injury. Therefore, it is more beneficial to start hypothermia treatment as soon as possible after brain injury.

At present, hypothermia therapy in clinical practice is mainly systemic physical cooling or endovascular intracarotid infusion of cold saline [49–52]. It is difficult to establish, slow in cooling, cannot reach the target temperature quickly, and can easily lead to serious complications such as arrhythmias and pulmonary infections [53–55]. Therefore, current clinical application of hypothermia is limited. In contrast, drug hypothermia is more convenient and can achieve the target temperature before vascular recanalization without extensive medical and nursing efforts. This may have a certain clinical application prospect, where it could become a better choice for hypothermia induction before vascular recanalization [11]. However, drug hypothermia also has some limitations. The efficiency of single-drug application is low with many complications. When drugs are combined in low doses, they can build a synergistic effect, improving the efficiency of low temperature, reducing the side effects of any single drug, and minimizing complications. Our previous study demonstrated that chlorpromazine and promethazine (C + P) significantly reduced the volume of cerebral infarction in rats and attenuated neurological deficit [31, 56]. Dihydrocapsaicin (DHC), a potential capsaicin channel transient receptor agonist (TRPV1), is also currently being investigated as a promising drug cryogenic inducer [57, 58]. Studies have shown that DHC in high doses can independently achieve effective hypothermia therapy, although its applications alone are limited due to the significant toxicity and complications [11, 33]. However, combined with low doses of C + P, it might play a synergistic effect, improve the efficiency of hypothermia, reduce the side effects of the single drug, and reduce the complications [59]. Therefore, in this study, we chose C + P combined with DHC to induce pharmacological hypothermia.

The full mechanism of hypothermia's neuroprotective effects is still being explored and described. A review has shown that hypothermia may act on several pathways in the ischemic cascade and have different effects on the inflammatory response at different time points [60]. ROS

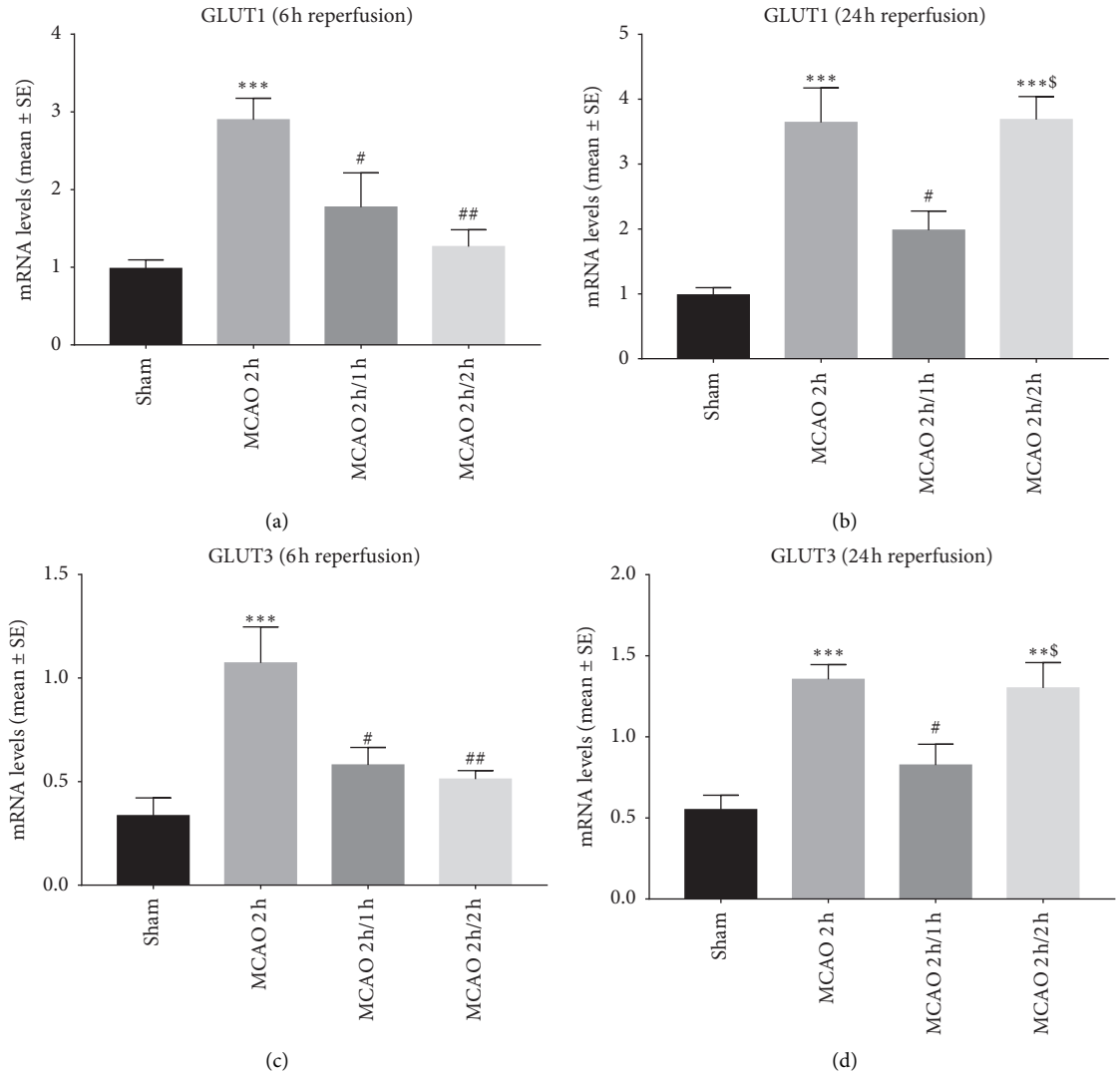

Figure 4: The mRNA expressions of glucose transporter subtypes (GLUT1 and GLUT3) determined by real-time PCR at 6 and 24 h reperfusion. $^{**}P < 0.01$ and $^{***}P < 0.001$ as compared to the sham group; $^{\#}p < 0.05$ and $^{\#\#}p < 0.01$ as compared to the MCAO 2 h group; $^{\$}P < 0.05$ as compared to the MCAO 2 h/1 h group ($n = 8$).

plays an important role in the pathophysiological process of ischemic neuron injury [23]. NADPH oxidase complex produces superoxide (O_2) and is involved in ROS production during ischemia and reperfusion [61]. Explosive ROS production has been shown to occur mainly in the first 10–15 minutes of reperfusion in the MCAO rat model [22]. In this model, our study shows that interischemia hypothermia and inter-reperfusion hypothermia induced by both low doses of phenothiazine drugs and DHC reduced ischemia-reperfusion injury, protected brain tissue, and induced neuroprotection compared to stroke without treatment. Interischemia hypothermia treatment may be better able to induce stronger neuroprotection after stroke.

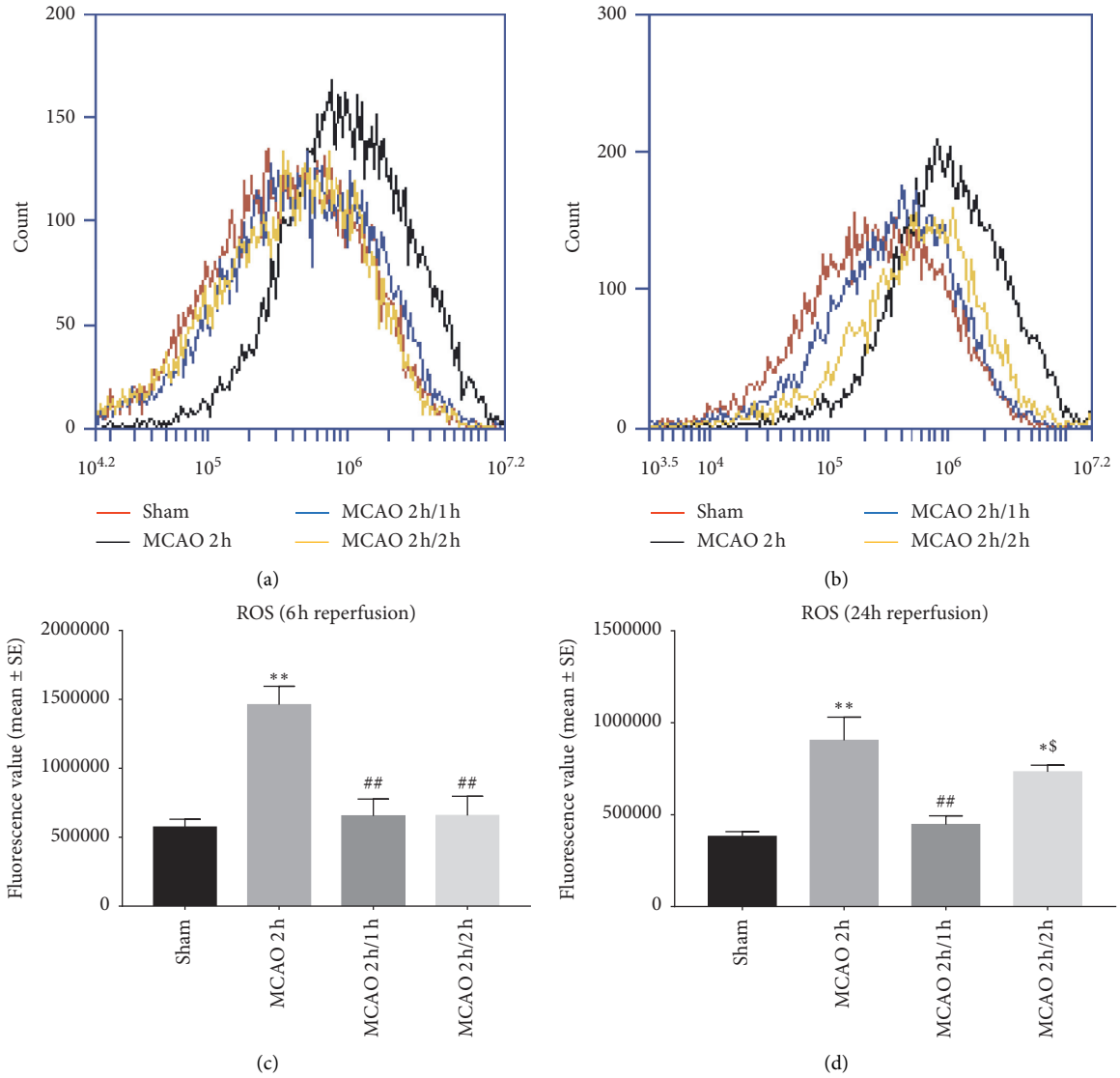

FIGURE 5: ROS production by flow cytometry assay. $^{*}P < 0.05$ and $^{**}P < 0.01$ as compared to the sham group; $^{\#}p < 0.05$ and $^{\#\#}p < 0.01$ as compared to the MCAO 2 h group; $^{\$}P < 0.05$ as compared to the MCAO 2 h/1 h group ($n = 8$). The x-axis is the fluorescence value. Red: sham; black: MCAO 2 h; blue: MCAO 2 h/1 h; yellow: MCAO 2 h/2 h.

5. Conclusion

In conclusion, both interischemia and inter-reperfusion pharmacological hypothermia treatments play a role in neuroprotection after stroke. Interischemia hypothermia treatment may be better able to induce stronger neuroprotection after ischemic stroke. In the current clinical environment, delaying reperfusion therapy to wait for hypothermia induction is not feasible. Fortunately, pharmacological hypothermia with low dose is quick and easy to use and has few side effects when used in combination. Patients could be cooled upon arrival to the emergency room or even prior to, perhaps in the ambulance by Emergency Medical Services (EMS), en route to the primary or advanced stroke unit, before thrombolysis or thrombectomy. This study provides a referential and effective treatment strategy for cerebral protection before vascular recanalization in acute ischemic stroke, as well as the basis for the realization of clinical transformation.

Data Availability

The original data used to support the findings of this study are included within the article.

Disclosure

Part of this study was presented as a poster in Medical Student Research Symposium at Wayne State University, School of Medicine.

Conflicts of Interest

The authors declare no conflicts of interest.

Authors' Contributions

Yun Han designed the study, performed the research, analyzed the data, and wrote the paper. Hangil Lee edited the paper and polished the language. Fengwu Li conceived the study, analyzed the data, and edited the paper. Xiaokun Geng conceived and designed the study and reviewed the paper. Yuchuan Ding designed the study and reviewed the paper. All authors read and approved the final manuscript.

Acknowledgments

This work was partially supported by the National Nature Science Foundation of China (nos. 81871838 and 81802231), Beijing Tongzhou District Financial Fund, and the Science and Technology Plan of Beijing Tongzhou District (KJ2018CX006).

References

[1] J. Minnerup, B. A. Sutherland, A. M. Buchan, and C. Kleinschnitz, "Neuroprotection for stroke: current status and future perspectives," *International Journal of Molecular Sciences*, vol. 13, no. 9, pp. 11753–11772, 2012.

[2] S. Wu, B. Wu, M. Liu et al., "Stroke in China: advances and challenges in epidemiology, prevention, and management," *The Lancet Neurology*, vol. 18, no. 4, pp. 394–405, 2007.

[3] T. Knecht, C. Borlongan, and I. Dela Pena, "Combination therapy for ischemic stroke: novel approaches to lengthen therapeutic window of tissue plasminogen activator," *Brain Circulation*, vol. 4, no. 3, pp. 99–108, 2018.

[4] R. Kollmar and S. Schwab, "Hypothermia and ischemic stroke," *Current Treatment Options in Neurology*, vol. 14, no. 2, pp. 188–196, 2012.

[5] M. Goyal, B. K. Menon, W. H. van Zwam et al., "Endovascular thrombectomy after large-vessel ischaemic stroke: a meta-analysis of individual patient data from five randomised trials," *The Lancet*, vol. 387, no. 10029, pp. 1723–1731, 2016.

[6] R. G. Nogueira, A. P. Jadhav, D. C. Haussen et al., "Thrombectomy 6 to 24 hours after stroke with a mismatch between deficit and infarct," *New England Journal of Medicine*, vol. 378, no. 1, pp. 11–21, 2018.

[7] G. W. Albers, M. P. Marks, S. Kemp et al., "Thrombectomy for stroke at 6 to 16 hours with selection by perfusion imaging," *New England Journal of Medicine*, vol. 378, no. 8, pp. 708–718, 2018.

[8] M. Paciaroni, V. Caso, and G. Agnelli, "The concept of ischemic penumbra in acute stroke and therapeutic opportunities," *European Neurology*, vol. 61, no. 6, pp. 321–330, 2009.

[9] J. H. Choi and J. Pile-Spellman, "Reperfusion changes after stroke and practical approaches for neuroprotection," *Neuroimaging Clinics of North America*, vol. 28, no. 4, pp. 663–682, 2018.

[10] M. A. Yenari and H. S. Han, "Neuroprotective mechanisms of hypothermia in brain ischaemia," *Nature Reviews Neuroscience*, vol. 13, no. 4, pp. 267–278, 2012.

[11] M. Zhang, H. Wang, J. Zhao et al., "Drug-induced hypothermia in stroke models: does it always protect?" *CNS & Neurological Disorders - Drug Targets*, vol. 12, no. 3, pp. 371–380, 2013.

[12] X. Liu, D. Wu, S. Wen et al., "Mild therapeutic hypothermia protects against cerebral ischemia/reperfusion injury by inhibiting miR-15b expression in rats," *Brain Circulation*, vol. 3, no. 4, pp. 219–226, 2017.

[13] L. Liu, X. Liu, R. Wang et al., "Mild focal hypothermia regulates the dynamic polarization of microglia after ischemic stroke in mice," *Neurological Research*, vol. 40, no. 6, pp. 508–515, 2018.

[14] Z. Zhang, L. Zhang, Y. Ding, Z. Han, and X. Ji, "Effects of therapeutic hypothermia combined with other neuroprotective strategies on ischemic stroke: review of evidence," *Aging and Disease*, vol. 9, no. 3, pp. 507–522, 2018.

[15] S. Shankaran, A. Pappas, S. A. McDonald et al., "Childhood outcomes after hypothermia for neonatal encephalopathy," *New England Journal of Medicine*, vol. 366, no. 22, pp. 2085–2092, 2012.

[16] L. A. Papile, "Systemic hypothermia--a "cool" therapy for neonatal hypoxic-ischemic encephalopathy," *New England Journal of Medicine*, vol. 353, no. 15, pp. 1619-1620, 2005.

[17] H. Ma, B. Sinha, R. S. Pandya et al., "Therapeutic hypothermia as a neuroprotective strategy in neonatal hypoxic-ischemic brain injury and traumatic brain injury," *Current Molecular Medicine*, vol. 12, no. 10, pp. 1282–1296, 2012.

[18] W. D. Dietrich and H. M. Bramlett, "Therapeutic hypothermia and targeted temperature management for traumatic brain injury: experimental and clinical experience," *Brain Circulation*, vol. 3, no. 4, pp. 186–198, 2017.

[19] G. Hypothermia, "After cardiac arrest study mild therapeutic hypothermia to improve the neurologic outcome after cardiac arrest," *New England Journal of Medicine*, vol. 346, no. 8, pp. 549–556, 2002.

[20] M. Kohlhauer, A. Berdeaux, B. Ghaleb, and R. Tissier, "Therapeutic hypothermia to protect the heart against acute myocardial infarction," *Archives of Cardiovascular Diseases*, vol. 109, no. 12, pp. 716–722, 2016.

[21] S. A. Bernard, T. W. Gray, M. D. Buist et al., "Treatment of comatose survivors of out-of-hospital cardiac arrest with induced hypothermia," *New England Journal of Medicine*, vol. 346, no. 8, pp. 557–563, 2002.

[22] C. M. Maier, G. H. Sun, D. Cheng, M. A. Yenari, P. H. Chan, and G. K. Steinberg, "Effects of mild hypothermia on superoxide anion production, superoxide dismutase expression, and activity following transient focal cerebral ischemia," *Neurobiol Dis*, vol. 11, no. 1, pp. 28–42, 2002.

[23] T. Horiguchi, K. Shimizu, M. Ogino, S. Suga, J. Inamasu, and T. Kawase, "Postischemic hypothermia inhibits the generation of hydroxyl radical following transient forebrain ischemia in rats," *Journal of Neurotrauma*, vol. 20, no. 5, pp. 511–520, 2003.

[24] A. Y. Abramov, A. Scorziello, and M. R. Duchen, "Three distinct mechanisms generate oxygen free radicals in neurons and contribute to cell death during anoxia and reoxygenation," *Journal of Neuroscience*, vol. 27, no. 5, pp. 1129–1138, 2007.

[25] S. Manzanero, T. Santro, and T. V. Arumugam, "Neuronal oxidative stress in acute ischemic stroke: sources and contribution to cell injury," *Neurochemistry International*, vol. 62, no. 5, pp. 712–718, 2013.

[26] J. Shen, R. Rastogi, L. Guan et al., "Omega-3 fatty acid supplement reduces activation of NADPH oxidase in intracranial atherosclerosis stenosis," *Neurological Research*, vol. 40, no. 6, pp. 499–507, 2018.

[27] H. Chen, Y. S. Song, and P. H. Chan, "Inhibition of NADPH oxidase is neuroprotective after ischemia-reperfusion," *Journal of Cerebral Blood Flow & Metabolism*, vol. 29, no. 7, pp. 1262–1272, 2009.

[28] J. Shen, X. Y. Bai, Y. Qin et al., "Interrupted reperfusion reduces the activation of NADPH oxidase after cerebral I/R injury," *Free Radical Biology and Medicine*, vol. 50, no. 12, pp. 1780–1786, 2011.

[29] T. Kahles and R. P. Brandes, "NADPH oxidases as therapeutic targets in ischemic stroke," *Cellular and Molecular Life Sciences*, vol. 69, no. 14, pp. 2345–2363, 2012.

[30] B. Cairns, J. Y. Kim, X. N. Tang, and M. A. Yenari, "NOX inhibitors as a therapeutic strategy for stroke and neurodegenerative disease," *Current Drug Targets*, vol. 13, no. 2, pp. 199–206, 2012.

[31] X. Geng, F. Li, J. Yip et al., "Neuroprotection by chlorpromazine and promethazine in severe transient and permanent ischemic stroke," *Molecular Neurobiology*, vol. 54, no. 10, pp. 8140–8150, 2017.

[32] E. Z. Longa, P. R. Weinstein, S. Carlson, and R. Cummins, "Reversible middle cerebral artery occlusion without craniectomy in rats," *Stroke*, vol. 20, no. 1, pp. 84–91, 1989.

[33] J. Zhang, K. Liu, O. Elmadhoun et al., "Synergistically induced hypothermia and enhanced neuroprotection by pharmacological and physical approaches in stroke," *Aging and Disease*, vol. 9, no. 4, pp. 578–589, 2018.

[34] X. Geng, O. Elmadhoun, C. Peng et al., "Ethanol and normobaric oxygen: novel approach in modulating pyruvate dehydrogenase complex after severe transient and permanent ischemic stroke," *Stroke*, vol. 46, no. 2, pp. 492–499, 2015.

[35] C. Chen, W. Jiang, Z. Liu et al., "Splenic responses play an important role in remote ischemic preconditioning-mediated neuroprotection against stroke," *Journal of Neuroinflammation*, vol. 15, no. 1, p. 167, 2018.

[36] V. Feigin, N. Anderson, A. Gunn, A. Rodgers, and C. Anderson, "The emerging role of therapeutic hypothermia in acute stroke," *The Lancet Neurology*, vol. 2, no. 9, p. 529, 2003.

[37] R. Busto, W. D. Dietrich, M. Y. Globus, I. Valdes, P. Scheinberg, and M. D. Ginsberg, "Small differences in intraischemic brain temperature critically determine the extent of ischemic neuronal injury," *Journal of Cerebral Blood Flow & Metabolism*, vol. 7, no. 6, pp. 729–738, 1987.

[38] M. D. Ginsberg, L. L. Sternau, M. Y. Globus, W. D. Dietrich, and R. Busto, "Therapeutic modulation of brain temperature: relevance to ischemic brain injury," *Neurobiology of Ischemic Brain Damage,Progress in Brain Research*, vol. 4, no. 3, pp. 189–225, 1993.

[39] T. Miki, G. S. Liu, M. V. Cohen, and J. M. Downey, "Mild hypothermia reduces infarct size in the beating rabbit heart: a practical intervention for acute myocardial infarction?" *Basic Research in Cardiology*, vol. 93, no. 5, pp. 372–383, 1998.

[40] S. R. Dixon, R. J. Whitbourn, M. W. Dae et al., "Induction of mild systemic hypothermia with endovascular cooling during primary percutaneous coronary intervention for acute myocardial infarction," *ACC Current Journal Review*, vol. 40, no. 11, pp. 1928–1934, 2003.

[41] D. Stub, S. Bernard, V. Pellegrino et al., "Refractory cardiac arrest treated with mechanical CPR, hypothermia, ECMO and early reperfusion (the CHEER trial)," *Resuscitation*, vol. 86, pp. 88–94, 2015.

[42] L. Darbera, M. Chenoune, F. Lidouren et al., "Hypothermic liquid ventilation prevents early hemodynamic dysfunction and cardiovascular mortality after coronary artery occlusion complicated by cardiac arrest in rabbits," *Critical Care Medicine*, vol. 41, no. 12, pp. e457–465, 2013.

[43] M. Gotberg, G. K. Olivecrona, H. Engblom et al., "Rapid short-duration hypothermia with cold saline and endovascular cooling before reperfusion reduces microvascular obstruction and myocardial infarct size," *BMC Cardiovascular Disorders*, vol. 8, p. 7, 2008.

[44] M. Gotberg, G. K. Olivecrona, S. Koul et al., "A pilot study of rapid cooling by cold saline and endovascular cooling before reperfusion in patients with ST-elevation myocardial infarction," *Circulation: Cardiovascular Interventions*, vol. 3, no. 5, pp. 400–407, 2010.

[45] H. Hamamoto, H. Sakamoto, B. G. Leshnower et al., "Very mild hypothermia during ischemia and reperfusion improves postinfarction ventricular remodeling," *The Annals of Thoracic Surgery*, vol. 87, no. 1, pp. 172–177, 2009.

[46] D. Erlinge, "A review of mild hypothermia as an adjunctive treatment for ST-elevation myocardial infarction," *Therapeutic Hypothermia and Temperature Management*, vol. 1, no. 3, pp. 129–141, 2011.

[47] J. L. Fox, E. N. Vu, M. Doyle-Waters, J. R. Brubacher, R. Abu-Laban, and Z. Hu, "Prophylactic hypothermia for traumatic brain injury: a quantitative systematic review," *CJEM*, vol. 12, no. 4, pp. 355–364, 2010.

[48] Y. Ding, J. Li, X. Luan et al., "Local saline infusion into ischemic territory induces regional brain cooling and neuroprotection in rats with transient middle cerebral artery occlusion," *Neurosurgery*, vol. 54, no. 4, pp. 956–964, 2004.

[49] J. Caroff, R. M. King, J. E. Mitchell et al., "Focal cooling of brain parenchyma in a transient large vessel occlusion model: proof-of-concept," *Journal of NeuroInterventional Surgery*, vol. 12, 2020.

[50] S. A. Bernard, K. Smith, J. Finn et al., "Induction of therapeutic hypothermia during out-of-hospital cardiac arrest using a rapid infusion of cold saline: the RINSE trial (rapid infusion of cold normal saline)," *Circulation*, vol. 134, no. 11, pp. 797–805, 2016.

[51] D. Erlinge, M. Gotberg, I. Lang et al., "Rapid endovascular catheter core cooling combined with cold saline as an adjunct to percutaneous coronary intervention for the treatment of acute myocardial infarction. The CHILL-MI trial: a randomized controlled study of the use of central venous catheter core cooling combined with cold saline as an adjunct to percutaneous coronary intervention for the treatment of acute myocardial infarction," *Journal of the American College of Cardiology*, vol. 63, no. 18, pp. 1857–1865, 2014.

[52] J. H. Choi, R. S. Marshall, M. A. Neimark et al., "Selective brain cooling with endovascular intracarotid infusion of cold saline: a pilot feasibility study," *American Journal of Neuroradiology*, vol. 31, no. 5, pp. 928–934, 2010.

[53] S. Liu and J. F. Chen, "Strategies for therapeutic hypometabothermia," *Journal of Experimental Stroke & Translational Medicine*, vol. 5, no. 1, pp. 31–42, 2012.

[54] M. Yenari and J. Kim, "Hypothermia for treatment of stroke," *Brain Circulation*, vol. 11 page, 2015.

[55] K. H. Polderman, "Mechanisms of action, physiological effects, and complications of hypothermia," *Critical Care Medicine*, vol. 37, no. 7, pp. S186–S202, 2009.

[56] M. V. Narayanan, W. Zhang, I. G. Stavrovskaya, B. S. Kristal, and R. M. Friedlander, "Promethazine: a novel application as a neuroprotectant that reduces ischemia-mediated injury by inhibiting mitochondrial dysfunction," *Clinical Neurology and Neurosurgery*, vol. 51, pp. 102–107, 2008.

[57] Z. Cao, A. Balasubramanian, and S. P. Marrelli, "Pharmacologically induced hypothermia via TRPV1 channel agonism provides neuroprotection following ischemic stroke when initiated 90 min after reperfusion," *American Journal of*

Physiology-Regulatory, Integrative and Comparative Physiology, vol. 306, no. 2, pp. R149–R156, 2014.

[58] K. Fosgerau, U. J. Weber, J. W. Gotfredsen et al., "Drug-induced mild therapeutic hypothermia obtained by administration of a transient receptor potential vanilloid type 1 agonist," *BMC Cardiovascular Disorders*, vol. 10, p. 51, 2010.

[59] S. Liu, X. Geng, B. Forreider et al., "Enhanced beneficial effects of mild hypothermia by phenothiazine drugs in stroke therapy," *Neurological Research*, vol. 37, no. 5, pp. 454–460, 2015.

[60] H. Zhao, G. K. Steinberg, and R. M. Sapolsky, "General versus specific actions of mild-moderate hypothermia in attenuating cerebral ischemic damage," *Journal of Cerebral Blood Flow & Metabolism*, vol. 27, no. 12, pp. 1879–1894, 2007.

[61] C. E. Walder, S. P. Green, W. C. Darbonne et al., "Ischemic stroke injury is reduced in mice lacking a functional NADPH oxidase," *Stroke*, vol. 28, no. 11, pp. 2252–2258, 1997.

Hindawi
Evidence-Based Complementary and Alternative Medicine
Volume 2020, Article ID 8824530, 8 pages
https://doi.org/10.1155/2020/8824530

Research Article

Human Theta Burst Stimulation Combined with Subsequent Electroacupuncture Increases Corticospinal Excitability

Jiali Li,[1,2] **Meng Ren**,[2] **Wenjing Wang**,[1] **Shutian Xu**,[2,3] **Sicong Zhang**,[1] **Yuanli Li**,[1,2,3] **and Chunlei Shan**[1,2,3]

[1]*Center of Rehabilitation, Yueyang Hospital of Integrated Traditional Chinese and Western Medicine, Shanghai University of Traditional Chinese Medicine, Shanghai, China*
[2]*School of Rehabilitation Science, Shanghai University of Traditional Chinese Medicine, Shanghai, China*
[3]*Engineering Research Center of Traditional Chinese Medicine Intelligent Rehabilitation, Ministry of Education, Shanghai, China*

Correspondence should be addressed to Yuanli Li; liyuan218@126.com and Chunlei Shan; shanclhappy@163.com

Received 25 September 2020; Revised 15 November 2020; Accepted 10 December 2020; Published 23 December 2020

Academic Editor: Feng Zhang

Objective. Intermittent theta burst stimulation (iTBS) is a widely used noninvasive brain stimulation for the facilitation of corticospinal excitability (CSE). Previous studies have shown that acupuncture applied to acupoints associated with motor function in healthy people can reduce the amplitude of the motor-evoked potentials (MEPs), which reflects the inhibition of CSE. In our work, we wanted to test whether the combination of iTBS and electroacupuncture (EA) would have different effects on CSE in humans. *Methods*. A single-blind sham-controlled crossover design study was conducted on 20 healthy subjects. Subjects received 20 minutes' sham or real EA stimulation immediately after sham or real iTBS. MEPs, short-interval intracortical inhibition (SICI), intracortical facilitation (ICF), cortical silent period (CSP), and central motor conduction time (CMCT) were recorded before each trial, and immediately, 20 minutes, and 40 minutes after the end of stimulation. *Results*. In the sham iTBS group, EA produced a reduction in MEPs amplitude, lasting approximately 40 minutes, while in the real iTBS group, EA significantly increased MEPs amplitude beyond 40 minutes after the end of stimulation. In sham EA group, the recorded MEPs amplitude showed no significant trend over time compared to baseline. Among all experiments, there were no significant changes in SICI, ICF, CSP, CMCT, etc. *Conclusion*. These data indicate that immediate application of EA after iTBS significantly increased corticospinal excitability. This trial was registered in the Chinese Clinical Trial Registry (registration no. ChiCTR1900025348).

1. Introduction

In 2005, Huang et al. proposed theta burst stimulation (TBS) as a special paradigm of repetitive transcranial magnetic stimulation (rTMS) which mimics endogenous theta oscillation and is able to modulate human brain excitability beyond the time of stimulation [1]. TBS was originally developed by observing the pattern of neuronal firing that occurred during the exploration of rats and was able to modulate brain activity beyond the time of stimulation in humans [2]. TBS mimics the combination of a 100 Hz gamma frequency and a 5 Hz theta frequency and induces obvious long-term potentiation (LTP) in rat hippocampal slices [3]. This patterned stimulation protocol was adapted in humans using similar frequency parameters to animal models and has been widely used for over a decade. Typically, TBS in humans involves the application of high-frequency bursts (3 pulses at 50 Hz) at low-frequency interval (5 Hz) using a total of 600 pulses at 70~80% of active/resting motor threshold (a/rMT). When applied continuously (cTBS) for 40 s, TBS has shown to change corticospinal excitability (CSE) measured via motor-evoked potentials (MEPs) for up

to at least 20 min. When applied intermittently (iTBS; 2 s on, 8 s off) for 192 s, an opposite effect was observed up to 30 min [1].

Many studies used the amplitude of MEPs recorded from peripheral muscles, which is widely used to evaluate CSE, to assess the effect of iTBS, and have demonstrated that iTBS increases cortical excitability in healthy individuals beyond 20 min after stimuli [4, 5]. This kind of increase is thought to be associated with long-term potentiation (LTP), which plays an important role in learning [6, 7]. In addition to MEPs, various TMS paradigms are also used to evaluate the state of neural circuits, and potentially revealing the underlying mechanism for the interventions and treatments, such as short-interval intracortical inhibition (SICI) and intracortical facilitation (ICF) [8]. MEPs reflects the overall excitability of the cortex, spinal, and corticospinal [9]. SICI refers to the phenomenon that a subthreshold conditioning stimulation (CS) suppresses the MEP induced by subsequent suprathreshold test stimulation (TS) at interstimulus intervals (ISIs) of 1–5 ms. SICI is the most common and well-studied intracortical circuits in the primary motor cortex (M1) [10]. ICF is assessed at an ISI of 10 ms. The CS intensities usually ranged from 75 to 95% AMT in different individuals to produce consistent test MEP facilitation [11].

Acupuncture is an important part of traditional Chinese medicine. Electroacupuncture (EA) combines acupuncture and electrical stimulation, which is widely welcomed worldwide due to its standardization and repeatability. Compared with manual acupuncture, electroacupuncture is more effective because of its more standardized parameters, higher repeatability, wider range of stimulation, and lower demands on acupuncturists [12]. Previous studies have proved that acupuncture suppresses corticomotor excitability of healthy individuals [13–16]. However, the underlying mechanisms and efficacy of acupuncture on brain function remain confused, commonly hindered by low-quality study designs. In this study, four most frequently used acupoints in treatment of dyskinesia after stroke, Quchi (LI11), Hegu (LI4), Zusanli (ST36), and Yanglingquan (GB34), are chosen to be studied [17].

In the present study, we used single TMS to measure resting motor threshold (RMT), active motor threshold (AMT), MEP, CSP, CMCT, and paired pulse TMS to measure SICI and ICF to determine whether combination of iTBS and EA could modulate the neural excitability of the M1 in healthy adults when compared with only iTBS, electroacupuncture, or none. We hypothesized that combination of acupuncture and iTBS could increase motor cortical excitation and reduce motor cortical inhibition.

2. Methods

2.1. Subjects. 22 healthy, right-handed subjects were recruited for participation in the current study via recruitment advertisements. One subject dropped out in the experiment process, while one was excluded because of taking antidepressants. Finally, a total of 20 subjects (22.8 ± 3.09 years, 11 females) were included in the statistical analysis. All subjects were right-handed, as assessed by the Edinburgh Handedness Inventory [18], without taking any regular drugs (recreational or clinically indicated), and no contraindication to TMS, and no history of neurological or psychiatric disorders [19]. All subjects provided written informed consent prior to experimentation. This experimental procedure was approved by the local ethics committee of Yueyang Hospital of Integrated Traditional Chinese and Western Medicine. All experiments conformed to the declaration of Helsinki. This trial was registered in the Chinese Clinical Trial Registry (registration no. ChiCTR1900025348).

2.2. Transcranial Magnetic Stimulation. TMS was delivered by two Magstim 200 stimulators connected via a Bistim module to a figure-of-eight coil (double-circular-70 mm coil) (Magstim 2002, Magstim Co., UK), held with the handle pointing posterolateral. Ag/AgCl surface electrodes in a belly-tendon montage were used to record electromyography (EMG) from the right first dorsal interosseous (FDI) muscle. EMG signals were amplified, digitized, band-pass-filtered (20 Hz-10 KHz), sampled, and saved to a disk for offline analysis (Keypoint, Dantec, Denmark).

The approximate position of the left M1 is C3 point in the international 10/20 EEG positioning system. The "hot spot," i.e., the location on the scalp with the largest and most consistent MEP, was found using manually triggered single-pulse TMS (sp-TMS). Resting motor threshold (RMT) was defined as the lowest stimulus intensity required to evoke MEPs with peak-peak amplitudes of $\geq 50\,\mu$V in the relaxed FDI in 5 out of 10 consecutive trails [20]. When subjects maintained the voluntary contraction of FDI muscle at 20% of the maximum strength, active motor threshold (AMT) was defined as the lowest stimulus intensity required to evoke MEPs with peak-peak amplitudes of $\geq 200\,\mu$V in 5 out of 10 consecutive trials [20]. Use 2 msec interstimulus interval (ISI) to measure SICI, and ISI of 10 msec to measure ICF. The conditioning stimulus was 80% of RMT and the test stimulus was 120% MT1 mV [21]. Both SICI and ICF were calculated by averaging of the peak-peak amplitude for 15 consecutive tests. Cortical silent period (CSP) was measured with single pulses applied at RMT, with subjects pinching their right thumbs and forefingers together at 20% of their maximum voluntary contraction which was visualized by electromyography waveform recorded in real time. In a single trial, CSP was measured as the time from the onset of MEP until the recurrence of voluntary EMG activity. Mean CSP duration was calculated from 15 consecutive trials [20]. CMCT was calculated by subtracting the conduction time in the peripheral nerve obtained by magnetic stimulation of the cervical root (peripheral motor latency) from the MEP cortical latency. A total of 15 pairs of trials each were recorded, and mean CMCT was calculated from them. All experiments were completed in a quiet and well-shielded room, with subjects relaxed and alert.

We used iTBS as introduced by Huang and colleagues [1]. iTBS was performed with the MC-B70 Butterfly "8" shaped coil (MagPro X100, MagVenture, Denmark). The coil was placed tangentially to the subject's scalp so that the

midpoint of the coil is aligned with the "hot spot" position, with an angle of 45° from the midline. Theta burst stimulation (TBS) contains of a burst of 3 stimuli at 50 Hz, which was repeated at intervals of 200 msec. In the iTBS protocol, 2 seconds' TBS trains (30 pulses) were repeated every 10 seconds for 190 s, with a total number of 600 pulses. The stimulus intensity was 80% AMT. We used one of the most reliable methods reported in previous studies to implement the sham stimuli, with the figure of "8" coil placed vertically on the scalp, and the edge of the coil in contact with the "hot spot" position on the scalp [22]. The parameters of sham iTBS were set the same as real iTBS protocol.

2.3. Electroacupuncture. An experienced acupuncturist performs the electroacupuncture intervention. Real EA was applied to right extremities at acupoints of Quchi (LI11), Hegu (LI4), Zusanli (ST36), and Yanglingquan (GB34) using disposable acupuncture needles (0.30 × 40 mm, Hwato, Suzhou, China) and hollow foam pads attached to the skin. Subjects were asked to close their eyes during inserting needles. When subjects had a sense of Deqi, the needles were connected to electroacupuncture apparatus (Hwato, Suzhou, China) with a 5 Hz continuous wave for 20 minutes, while sham EA was delivered using custom blunt needles (0.30 × 25 mm, Hwato, Suzhou, China), which gave the skin a tingling sensation without penetrating into the skin, standing on the acupoints with foam pads. Piercing against the foam pad gave the subjects a sense of acanthesthesia similar to real acupuncture. The electroacupuncture apparatus was modified so that there was no current out and the subjects were told that the apparatus was in low-frequency low-intensity mode.

2.4. Experimental Design. The effect of iTBS in combination with EA on corticospinal excitability was assessed using a randomized, single-blinded, sham-controlled, crossover study design. Subjects attended 4 sessions: (1) sham iTBS + sham EA; (2) sham iTBS + real EA; (3) real iTBS + sham EA; (4) real iTBS + real EA. The order of sessions was counter-balanced across the 4 groups, and the carryover possibility was reduced by separating each session by at least 5 days. Use MATLAB 2013 software to achieve randomization of the intervention sequence. The combination of the four intervention methods has a total of 24 permutations. Use MATLAB to generate two random numbers between 1 and 24, and remove the corresponding permutations from the 24 permutations. The 22 subjects were randomly numbered, the numbers from 1 to 22 were randomly arranged using MATLAB, and the subjects were randomly assigned to the 22 sorting orders according to this set of numbers.

The experimental outline is shown schematically in Figure 1. Outcome indicators such as MEP were measured prior to each trial (baseline), and then real or sham iTBS was delivered, and real or sham EA intervention was applied immediately after iTBS. After the intervention of EA, outcome indicators measurements were performed immediately and every 20 minutes until 40 minutes (T0, T20, and T40).

Studies have shown that the after-effects of iTBS vary significantly among different subjects. The reasons for this variability are varied; there were many physiological factors contributing to this variability in response to iTBS, such as age, gender, handedness, genetics, quality of sleep and arousal, the state of motor system activation, and intake of caffeine, nicotine, alcohol, antidepressants, benzodiazepines, and antiepileptic drugs, and so on [23]. The experimental outline is illustrated in Figure 1. iTBS (real or sham) was delivered first after baseline MEP measurement and EA (real or sham) was delivered immediately after iTBS. Measurements of outcome indicators were performed immediately after EA and every 20 minutes until 40 minutes (T0, T20, and T40).

In this study, the electrophysiological index of right hand FDI ($MEP_{MT1\,mV}$) was used as the main outcome index. When at least 5 MEP peak-peak amplitude of MEP recorded in 10 consecutive single pulse magnetic stimuli is ≥1 mV, the threshold value of stimulate intensity is denoted as MT1 mV. MT1 mV was measured before intervention (baseline). MEP at 4 time points before and after the intervention (baseline, T0, T20, T40) was measured using MT1 mV at baseline ($MEP_{MT1\,mV}$); i.e., MEP at different time points was assessed using a fixed stimulus intensity to evaluate the difference of cortical excitability at each time point. At each time point, 15 MEPs were recorded continuously, and the mean value of peak-to-peak amplitude was calculated during offline processing. SICI, ICF, CMCT, and CSP were secondary outcome indicators.

2.5. Data Analysis and Statistics. In the 15 trials recorded at each time point, peak-to-peak amplitudes or CMCT was measured using a custom-made MATLAB script (MATLAB 2013b, The MathWorks, Inc., Natick, MA, USA). Average MEP amplitude was calculated and converted to logarithmic value (LOG $MEP_{MT1\,mV}$) to make the data follow a normal distribution. Do the same conversion for other indicators such as SICI, etc.

Three-factorial repeated-measures analysis of variance (rm-ANOVA) was used to analyze the changes in outcome indicators, including three factors: iTBS ("real," "sham") and EA ("real," "sham") and time (pre-stimulation, 0, 20, and 40 min after stimulation). Post hoc paired *t*-tests were used to examine differences from baseline and differences between values at every time point (Bonferroni-corrected for multiple comparisons). $P < 0.05$ was considered to be statistically significant. The SPSS 21.0 software was used for statistical analysis.

3. Results

RMT and AMT at baseline of the four conditions are listed in Table 1, and there is no significant difference between the conditions (Bonferroni-corrected pairwise *t*-test). The amplitudes of $MEP_{MT1\,mV}$ of all subjects are plotted in Figure 2. A 2-way ANOVA of LOG $MEP_{MT1\,mV}$ with main factors of

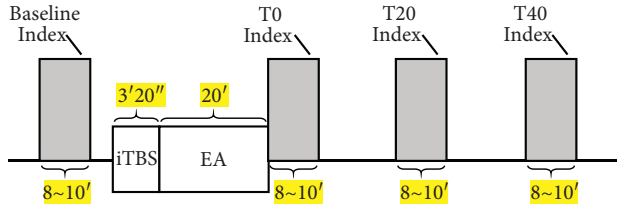

Figure 1: Experimental design. Before intervention (baseline), electrophysiological indexes (RMT, AMT, MT1 mV, $MEP_{MT1\,mV}$, SICI, ICF, CSP, CMCT) were measured and recorded. The stimulation included 192 sec iTBS session (sham or real), followed by 20 min EA session (sham or real). Electrophysiological indexes were recorded immediately after the end of stimulation and 20 and 40 minutes later.

Table 1: Physiological indexes at baseline.

iTBS	EA	RMT (% MSO)	AMT (% MSO)	LOG $MEP_{MT1\,mV}$ (log (uV))
Sham	Sham	37.0 ± 4.28	—	3.05 ± 0.07
	Real	37.1 ± 4.66	—	3.05 ± 0.05
Real	Sham	37.1 ± 4.73	27.3 ± 2.58	3.03 ± 0.05
	Real	37.4 ± 4.92	27.5 ± 2.24	3.05 ± 0.07

MSO, mean stimulator output. Data format is mean ± standard error.

iTBS and EA at baseline showed no difference between the 4 experimental conditions (interaction: F (1, 19) = 0.185, P = 0.672; main effect of iTBS: F (1, 19) = 0.954, P = 0.341; main effect of EA: F (1, 19) = 0.346, P = 0.563). This result indicated that the cortical excitability of the subjects was similar at the start of every session.

As shown in Table 2, a three-way ANOVA with main factors of iTBS, EA, and time showed a strong interaction between three factors (F (3, 57) = 11.019, P < 0.001), indicating that the $MEP_{MT1\,mV}$ amplitude at different time points differs across the conditions. Two-way ANOVAs with main factors of iTBS or time were performed, respectively, in the conditions of real EA and sham EA. The results indicated that, in the real EA condition, there was significant interaction between iTBS and time (F (3, 57) = 23.484, P < 0.001). So, the presence of EA resulted in strong influences of iTBS on the $MEP_{MT1\,mV}$ amplitudes at different time points. The main effect of iTBS was significant (F (3, 57) = 126.851, P < 0.001), corresponding to the distinct difference of the real EA arms in Figure 2. Nonetheless, in the sham EA condition, there was no discerning iTBS × EA interaction (F (2.274, 43.206) = 0.186, P = 0.856) or main effect of iTBS (F (2.274, 43.206) = 0.023, P = 0.881). Thus, with the absence of EA, iTBS did not have distinct influence on the $MEP_{MT1\,mV}$ amplitudes at the time points. As shown in Figure 2, the sham EA arms does not differ significantly. The main effect of time was not significant (F (2.274, 43.206) = 1.199, P = 0.318), so the $MEP_{MT1\,mV}$ amplitude did not vary with time points.

Table 3 shows the Bonferroni-corrected pairwise comparison results of LOG $MEP_{MT1\,mV}$ amplitude at different time points of the sham-iTBS-real-EA arm. $MEP_{MT1\,mV}$ amplitude had a significant reduction at T0 and T20 compared to baseline (T0-baseline = −0.181, P = 0.001; T20-baseline = −0.121, P = 0.006), indicating that the condition of sham iTBS and real EA suppressed the $MEP_{MT1\,mV}$ amplitude significantly. Table 4 shows the Bonferroni-corrected pairwise comparison results of LOG $MEP_{MT1\,mV}$ amplitude

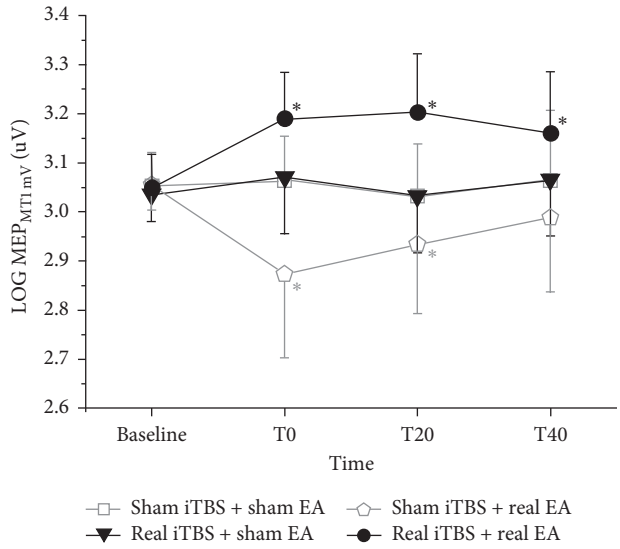

Figure 2: LOG $MEP_{MT1\,mV}$ with different interventions. There was no significant difference between 4 conditions at baseline. And the $MEP_{MT1\,mV}$ amplitude at different time points differs across the conditions. With sham EA, the $MEP_{MT1\,mV}$ amplitude did not vary significantly with time points. The condition of sham iTBS and real EA suppressed the $MEP_{MT1\,mV}$ amplitude significantly, and the condition of sham iTBS and real EA improved the $MEP_{MT1\,mV}$ amplitude significantly. *There is a significant difference from the baseline, P < 0.01.

at different time points of the real-iTBS-real-EA arm. $MEP_{MT1\,mV}$ amplitude had a significant improvement at T0, T20, and T40 compared to baseline (T0-baseline = 0.141, P < 0.001; T20-baseline = 0.155, P = 0.001; T40-baseline = 0.112, P = 0.021), indicating that the condition of sham iTBS and real EA improved the $MEP_{MT1\,mV}$ amplitude significantly.

2-way ANOVAs with main factors of EA and time in the real iTBS and sham iTBS conditions were performed as well.

Table 2: ANOVA results.

ANOVA	Main factors	Degrees of freedom; error	Effects	F	P
3-way	iTBS × EA × Time	3, 57	$I \times E \times T$	11.02	<0.001
			I	62.61	<0.001
			E	0.084	0.774
			T	0.659	0.581
2-way	iTBS × Time				
	Sham EA	2.27, 43.21	$I \times T$	0.186	0.856
			I	0.023	0.881
			T	1.199	0.318
	Real EA	3, 57	$I \times T$	23.48	<0.001
			I	126.9	<0.001
			T	1.019	0.391
2-way	EA × Time				
	Sham iTBS	3, 57	$E \times T$	5.658	0.002
			E	18.00	<0.001
			T	5.669	0.002
	Real iTBS	3, 57	$E \times T$	5.342	0.003
			E	28.24	<0.001
			T	7.573	<0.001

Whether iTBS was sham or real, there was significant interaction between EA and time (sham iTBS: $F(3, 57) = 5.658$, $P = 0.002$, real iTBS: $F(3, 57) = 5.342$, $P = 0.003$).

In all the above experiments, there were no statistically significant differences in SICI, ICF, CMCT, and CSP between groups and between time points.

In summary, with real iTBS and real EA, the $MEP_{MTI\,mV}$ amplitude was significantly improved and lasted for 40 minutes after the intervention. On the contrary, with sham iTBS and real EA, $MEP_{MTI\,mV}$ amplitude was significantly suppressed and gradually returned to the pre-intervention level 40 minutes after the intervention. And when EA was sham, no matter whether iTBS was real or sham, there was no significant impact on $MEP_{MTI\,mV}$. And throughout the experiment, there were no statistically significant differences in SICI, ICF, CMCT, and CSP between groups and between various time points.

Table 3: Pairwise comparison results of the sham-iTBS-real-EA arm.

	LOG $MEP_{MTI\,mV}$	
	Difference	P
T0-baseline	0.141	<0.001
T20-baseline	0.155	0.001
T40-baseline	0.112	0.021
T20-T0	0.014	1.00
T40-T0	−0.029	1.00
T40-T20	−0.043	1.00

Table 4: Pairwise comparison results of the real-iTBS-real-EA arm.

	LOG $MEP_{MTI\,mV}$	
	Difference	P
T0-baseline	−0.181	0.001
T20-baseline	−0.121	0.006
T40-baseline	−0.066	0.283
T20-T0	0.060	0.971
T40-T0	0.115	0.106
T40-T20	0.055	0.895

4. Discussion

In our study, we applied EA immediately after the end of iTBS on Hegu (LI4), Quchi (LI11), Zusanli (ST36), and Yanglingquan (GB34), which are four acupuncture points that are most commonly used in the rehabilitation of stroke exercise in the clinic. The results indicated that iTBS combined with EA can significantly increase the excitability of the motor cortex for 40 minutes after the end of the intervention, while applying EA alone will inhibit the excitability of the motor cortex. When the EA is sham, it does not cause changes in cortical excitability. So, this study demonstrates that the interaction of EA with iTBS increases cortical spinal cord excitability and the effect of this increase is extended.

4.1. The Effect of EA on Cortical Spinal Excitability. In our study, a sham acupuncture that did not invade the body was used as a control. It was found that the EA had an inhibitory effect on MEP amplitude but had no significant effect on SICI, ICF, etc. In former studies of Hegu (LI4) and Tiaokou (ST38) [13, 14], the researchers used real acupuncture at nonacupoint as a control group, and inhibition of motor cortex excitement was observed in experimental group and changes in MEP amplitude were also observed in control group. Zunhammer et al. [15] used the sham acupuncture without skin insertion as a control for the first time and reported that acupuncture at Yanglingquan (GB34) caused RMT elevation in the contralateral hemisphere, but AMT, SICI, and ICF had no significant variations. The results of the above studies are consistent with the results of our study. However, a double-blind, sham-controlled study showed that acupuncture at Hegu (LI4) did not cause changes in excitability of the motor cortex [24]. In general, acupuncture

can cause an inhibition in excitability of the contralateral cerebral cortex, which is consistent with the results of this study. At present, there are relatively little studies with TMS on the mechanism of acupuncture to evaluate the excitability of the motor cortex, and the research qualities are relatively low, which limits the research progress of the acupuncture mechanism to some extent.

4.2. After-Effect of iTBS. There have been a lot of previous studies revealing that iTBS could improve the cortex excitability of healthy subjects, and the effect could last for 20–40 min. ITBS could effectively help the recovery of dyskinesia in stroke patients [1, 25, 26]. In our study, no changes in cortical excitability were observed after real iTBS + sham EA intervention. We speculate that this was because the iTBS intervention was followed immediately by the 20 min sham EA intervention before any MEP measurement. Therefore, no significant after-effect of iTBS was observed after 20 minutes of sham EA. In the real iTBS + real EA condition, the MEP amplitude increased significantly after the intervention, lasting more than 40 minutes, which was never observed in previous studies. Although the mechanisms involved in promoting neural plasticity are currently not fully understood, the well-defined forms of neuroplasticity include long-term potentiation (LTP) and long-term depression (LTD). Noninvasive brain stimulation (NIBS) technology can induce and measure LTP-and-LTD-like changes in the human brain [27], while iTBS improves cortical excitability by inducing LTP-like plasticity. Previous studies have shown that iTBS induces LTP-like plasticity by affecting N-methyl-D-aspartate receptor (NMDA-R [28]) and changing the expression of some proteins including zif268 [29] and calcium-binding protein [30], thereby enhancing the excitability of the motor cortex.

4.3. Possible Mechanism of Real iTBS + Real EA Intervention. Experiments on animals revealed that acupuncture can induce neurogenesis, synaptogenesis, and alterations of synaptic efficiency [31]. But unfortunately, the current number of studies on the effects of acupuncture on brain plasticity in healthy people is very limited, which significantly limited people's understanding of the influence of acupuncture on brain plasticity. After acupuncture needles penetrate the skin, they first activate the afferent fibers of the peripheral nerves, producing a feeling called "Deqi," which is a feeling of numbness, filling, and pain [32, 33]. Through this strong sensory stimulation, acupuncture or electroacupuncture can promote the release of certain neurotransmitters in the central nervous system, such as norepinephrine, glutamic acid, dopamine, etc., thereby activating related receptors and downstream signalling pathways [34]. Therefore, it is speculated that regulation of the neurotransmitter system may be one of the potential mechanisms for acupuncture to regulate neural plasticity.

The results of our study showed that the application of EA immediately after the end of iTBS stimulation can significantly improve the excitability of the motor cortex. In addition to the possibilities mentioned above, the mechanism of this phenomenon may also be related to the priming effect. The priming effect is based on a concept of metaplasticity, the plasticity process of synaptic plasticity, which refers to the change in the threshold required for subsequent synaptic excitability changes due to some previous activity of the brain network [35]. NIBS can have an effect on the metaplasticity of young healthy subjects, and this change in neural plasticity is stronger, longer lasting, and more stable [36]. The change in one type of NIBS effect caused by the priming of another type of NIBS is not only related to the type of stimulation of the NIBS, but also closely related to the time interval between the two NIBS stimulation protocols [37]. However, most of the current studies on meta-plasticity focus on two different NIBS protocols acting on the same cortical region, exploring the priming effect of one NIBS on another. There are few studies [38–40] on the initiation of a single NIBS protocol combined with other interventions. In future research, how to combine NIBS with acupuncture and use meta-plasticity to improve functional recovery of stroke should be paid more attention to.

In summary, the underlying mechanisms of acupuncture and iTBS regulation of motor cortex excitability may have similar neural pathways and molecular biological mechanisms and in some special cases produce a mutually reinforcing effect, thereby inducing stronger, more persistent cortical excitability changes. Unfortunately, there are no relevant animal experiments to show how the two have produced this interaction. Future research should focus more on basic research that can reveal this phenomenon.

5. Limitations

In this study, only SICI of 2 ms interval and ICF of 10 ms interval were selected as indicators to evaluate neural circuits, but the changes of SICI and ICF indicators in other intervals were not tested, which may have missed some potential mechanisms, which will be further supplemented by future studies.

The use of TMS-MEP and pp-TMS to study the central effect of acupuncture is still a small number of reports, and there are no high-quality studies, or large sample clinical trials to verify. This will be the focus of future research.

Data Availability

Data are available on http://www.chictr.org.cn/showproj.aspx?proj=42076.

Conflicts of Interest

The authors declare no conflicts of interest.

Acknowledgments

This work was supported by Shanghai Health Commission which accelerated the development of traditional Chinese medicine three-year action plan project (Grant No. ZY (2018–2020)-CCCX-2001-06/2004-05); Intelligent Medical Program of Shanghai Health Commission (Grant No. 2018ZHYL0216); and Clinical Science and Technology

Innovation Project of Shanghai Shen Kang Hospital Development Center (Grant No. SHDC12018126).

References

[1] Y.-Z. Huang, M. J. Edwards, E. Rounis, K. P. Bhatia, and J. C. Rothwell, "Theta burst stimulation of the human motor cortex," *Neuron*, vol. 45, no. 2, pp. 201–206, 2005.

[2] J. Larson and E. Munkácsy, "Theta-burst LTP," *Brain Research*, vol. 1621, pp. 38–50, 2015.

[3] J. Larson, D. Wong, and G. Lynch, "Patterned stimulation at the theta frequency is optimal for the induction of hippocampal long-term potentiation," *Brain Research*, vol. 368, no. 2, pp. 347–350, 1986.

[4] Y. Shirota, S. Dhaka, W. Paulus, and M. Sommer, "Current direction-dependent modulation of human hand motor function by intermittent theta burst stimulation (iTBS)," *Neuroscience Letters*, vol. 650, pp. 109–113, 2017.

[5] T. Gedankien, P. J. Fried, A. Pascual-Leone, and M. M. Shafi, "Intermittent theta-burst stimulation induces correlated changes in cortical and corticospinal excitability in healthy older subjects," *Clinical Neurophysiology*, vol. 128, no. 12, pp. 2419–2427, 2017.

[6] N. Gutierrez-Castellanos, C. M. Da Silva-Matos, K. Zhou et al., "Motor learning requires purkinje cell synaptic potentiation through activation of AMPA-receptor subunit GluA3," *Neuron*, vol. 93, no. 2, pp. 409–424, 2017.

[7] A. Hernandez, C. Tan, G. Mettlach et al., "Cdk5 modulates long-term synaptic plasticity and motor learning in dorsolateral striatum," *Scientific Reports*, vol. 6, no. 1, Article ID 29812, 2016.

[8] L. Ming-Kuei, C. Jui-Cheng, C. Chun-Ming, J. R. Duann, U. Ziemann, and C. H. Tsai, "Impaired cerebellum to primary motor cortex associative plasticity in Parkinson's disease and spinocerebellar ataxia type 3," *Frontiers in Neurology*, vol. 8, p. 445, 2017.

[9] I. Greenhouse, M. King, S. Noah, R. J. Maddock, and R. B. Ivry, "Individual differences in resting corticospinal excitability are correlated with reaction time and GABA content in motor cortex," *The Journal of Neuroscience*, vol. 37, no. 10, pp. 2686–2696, 2017.

[10] J. F. M. Müller-Dahlhaus, Y. Orekhov, Y. Liu, and U. Ziemann, "Interindividual variability and age-dependency of motor cortical plasticity induced by paired associative stimulation," *Experimental Brain Research*, vol. 187, no. 3, pp. 467–475, 2008.

[11] U. Ziemann, "Pharmaco-transcranial magnetic stimulation studies of motor excitability," *Handbook of Clinical Neurology*, vol. 116C, pp. 387–397, 2013.

[12] N. Vitaly, M. Nikos, L. Jing, N. W. Kettner, K. K. Kwong, and K. K. Hui, "Effects of electroacupuncture versus manual acupuncture on the human brain as measured by fMRI," *Human Brain Mapping*, vol. 24, no. 3, pp. 193–205, 2005.

[13] Y. L. Lo and S. L. Cui, "Acupuncture and the modulation of cortical excitability," *NeuroReport*, vol. 14, no. 9, pp. 1229–1231, 2003.

[14] C. Maioli, L. Falciati, M. Marangon, S. Perini, and A. Losio, "Short-and long-term modulation of upper limb motor-evoked potentials induced by acupuncture," *European Journal of Neuroscience*, vol. 23, no. 7, pp. 1931–1938, 2006.

[15] M. Zunhammer, P. Eichhammer, J. Franz, G. Hajak, and V. Busch, "Effects of acupuncture needle penetration on motor system excitability," *Neurophysiologie Clinique/Clinical Neurophysiology*, vol. 42, no. 4, pp. 225–230, 2012.

[16] Y. Yi, E. Ines, C. Siqi, S. Wang, F. Zhang, and L. Wang, "Neuroplasticity changes on human motor cortex induced by acupuncture therapy: a preliminary study," *Neural Plasticity*, vol. 2017, Article ID 4716792, 8 pages, 2017.

[17] Y. Zhang, Y. Ren, X. Wang et al., "Study on the prescription of acupuncture and moxibustion for hemiplegia in modern acupuncture," *Journal of Liaoning University of Traditional Chinese Medicine*, vol. 2012, no. 9, pp. 61–64, 2012.

[18] R. C. Oldfield, "The assessment and analysis of handedness: the Edinburgh inventory," *Neuropsychologia*, vol. 9, no. 1, p. 113, 1971.

[19] S. Rossi, M. Hallett, P. M. Rossini, and A. Pascual-Leone, "Safety, ethical considerations, and application guidelines for the use of transcranial magnetic stimulation in clinical practice and research," *Clinical Neurophysiology*, vol. 120, no. 12, pp. 2008–2039, 2009.

[20] P. M. Rossini, A. T. Barker, A. Berardelli et al., "Non-invasive electrical and magnetic stimulation of the brain, spinal cord and roots: basic principles and procedures for routine clinical application. report of an IFCN committee," *Electroencephalography and Clinical Neurophysiology*, vol. 91, no. 2, pp. 79–92, 1994.

[21] A. Wagle-Shukla, Z. Ni, C. A. Gunraj, N. Bahl, and R. Chen, "Effects of short interval intracortical inhibition and intracortical facilitation on short interval intracortical facilitation in human primary motor cortex," *The Journal of Physiology*, vol. 587, no. 23, pp. 5665–5678, 2009.

[22] S. H. Lisanby, D. Gutman, B. Luber, C. Schroeder, and H. A. Sackeim, "Sham TMS: intracerebral measurement of the induced electrical field and the induction of motor-evoked potentials," *Biological Psychiatry*, vol. 49, no. 5, pp. 460–463, 2001.

[23] A. Guerra, V. López-Alonso, B. Cheeran, and A. Suppa, "Variability in non-invasive brain stimulation studies: reasons and results," *Neuroscience Letters*, vol. 719, Article ID 133330, 2017.

[24] A. B. Mccambridge, C. Zaslawski, and L. V. Bradnam, "Investigating the mechanisms of acupuncture on neural excitability in healthy adults," *NeuroReport*, vol. 30, no. 2, pp. 71–76, 2019.

[25] M. Simonetta-Moreau, "Non-invasive brain stimulation (NIBS) and motor recovery after stroke," *Annals of Physical and Rehabilitation Medicine*, vol. 57, no. 8, pp. 530–542, 2014.

[26] S. Diekhoff-Krebs, E.-M. Pool, A.-S. Sarfeld et al., "Interindividual differences in motor network connectivity and behavioral response to iTBS in stroke patients," *NeuroImage: Clinical*, vol. 15, pp. 559–571, 2017.

[27] F. Müller-Dahlhaus, U. Ziemann, and J. Classen, "Plasticity resembling spike-timing dependent synaptic plasticity: the evidence in humancortex," *Frontiers in Synaptic Neuroscience*, vol. 2, p. 34, 2010.

[28] Y.-Z. Huang, R.-S. Chen, J. C. Rothwell, and H.-Y. Wen, "The after-effect of human theta burst stimulation is NMDA receptor dependent," *Clinical Neurophysiology*, vol. 118, no. 5, pp. 1028–1032, 2007.

[29] S. Aydin-Abidin, J. Trippe, K. Funke, U. T. Eysel, and A. Benali, "High- and low-frequency repetitive transcranial magnetic stimulation differentially activates c-Fos and zif268 protein expression in the rat brain," *Experimental Brain Research*, vol. 188, no. 2, pp. 249–261, 2008.

[30] A. Mix, A. Benali, U. Eysel, and K. Funke, "The effect of chronic transcranial magnetic theta burst stimulation on an associative tactile learning task in the rat," *Brain Stimulation*, vol. 1, no. 3, p. 282, 2007.

[31] L. Y. Xiao, X. R. Wang, Y. Yang et al., "Applications of acupuncture therapy in modulating plasticity of central nervous system," *Neuromodulation Technology at the Neural Interface*, vol. 21, no. 8, pp. 762–776, 2018.

[32] I. Veith, *The Yellow Emperor's Classic of Internal Medicine*, University of California Press, Berkeley, CA, USA, 2015.

[33] H. Park, J. Park, H. Lee, and H. Lee, "Does Deqi (needle sensation) exist?" *The American Journal of Chinese Medicine*, vol. 30, no. 1, pp. 45–50, 2002.

[34] L. Chavez, S.-S. Huang, I. MacDonald, J.-G. Lin, Y.-C. Lee, and Y.-H. Chen, "Mechanisms of acupuncture therapy in ischemic stroke rehabilitation: a literature review of basic studies," *International Journal of Molecular Sciences*, vol. 18, no. 11, p. 2270, 2017.

[35] S. Sajikumar, *Synaptic Tagging and Capture*, Springer Nature, Cham, Switzerland, 2015.

[36] G. M. Opie, E. Vosnakis, M. C. Ridding, U. Ziemann, and J. G. Semmler, "Priming theta burst stimulation enhances motor cortex plasticity in young but not old adults," *Brain Stimulation*, vol. 10, no. 2, pp. 298–304, 2017.

[37] M. Hassanzahraee, M. Zoghi, and S. Jaberzadeh, "How different priming stimulations affect the corticospinal excitability induced by noninvasive brain stimulation techniques: a systematic review and meta-analysis," *Reviews in the Neurosciences*, vol. 29, no. 8, pp. 883–899, 2018.

[38] L. Zhu, Z. Gong, M. Wang et al., "Effects of acupuncture combined with low frequency repetitive transcranial magnetic stimulation on upper extremity motor dysfunction after stroke," *Journal of Clinical and Pathological Medicine*, vol. 2017, no. 6, 2017.

[39] L. Zhu, Clinical study of acupuncture combined with low frequency repetitive transcranial magnetic stimulation (LF-rTMS) in the treatment of upper limb dysfunction after stroke, 2017.

[40] Y. Lin, X. Huang, W. Zhou et al., "Effects of acupuncture combined with repetitive transcranial magnetic stimulation on limb motor function and quality of life in stroke patients with hemiplegia," *New Journal of Traditional Chinese Medicine*, vol. 51, no. 1, pp. 175–178, 2019.

Hindawi
Evidence-Based Complementary and Alternative Medicine
Volume 2020, Article ID 8850119, 9 pages
https://doi.org/10.1155/2020/8850119

Research Article

Enriched Environment Promotes Cognitive Function Recovery following Cerebral Ischemic Injury via Upregulating GABAergic and Glutamatergic Systems in the Contralateral Hippocampus

Yuyang Wang,[1] Junfa Wu,[1] Hongyu Xie,[1] Liping Wang,[2] Chuanjie Wang,[1] and Yi Wu[1]

[1]*Department of Rehabilitation Medicine, Huashan Hospital, Fudan University, WuLuMuQi Middle Road 12, Shanghai 200040, China*
[2]*Department of Neurology, Renji Hospital, School of Medicine, Shanghai Jiao Tong University, Shanghai 200025, China*

Correspondence should be addressed to Yi Wu; wuyi@fudan.edu.cn

Received 15 September 2020; Revised 23 November 2020; Accepted 4 December 2020; Published 15 December 2020

Academic Editor: Feng Zhang

Poststroke cognitive impairment severely affects the long-term recovery of patients. However, it remains unknown whether an enriched environment can remodel contralateral hippocampal function and promote cognitive function recovery after cerebral ischemic injury. To further explore, 36 C57BL/6 mice that underwent permanent middle cerebral artery occlusion (pMCAO) were randomly assigned to three groups: enriched environment (EE), standard condition (SC), and sham surgery (Sham). After 21 days of intervention, the Morris water maze and step-through test was utilized for testing the cognitive function of the mice, cresyl violet staining for measuring the degree of atrophy in the hippocampal tissues, and western blotting for quantitating the expression levels of GA1B, GAD67, and NR2B, and immunohistochemistry for levels of NR2B in the CA1 region of the contralateral hippocampus. The results showed that cognitive function-related behavioral performance decreased in the SC group, and performance was better in the EE group than that in the SC group ($p < 0.01$); no significant difference in the degree of contralateral cerebral atrophy was observed between the EE and SC groups ($p > 0.05$); levels of GA1B, GAD67, and NR2B in the contralateral hippocampus were significantly higher in the EE group than those in the SC group ($p < 0.01$); and the level of NR2B in the CA1 region of the contralateral hippocampus significantly increased in the EE group compared to the SC group ($p < 0.01$). We believe that contralateral hippocampal function is inhibited after cerebral ischemic injury, further affecting cognitive function. However, enriched environment can upregulate GABAergic and glutamatergic systems in the contralateral hippocampus to promote cognitive function recovery after cerebral ischemic injury.

1. Introduction

Cognitive impairment is one of the most common complications of stroke [1]. The long-term effects of poststroke cognitive impairment is much more severe than those of physical impairment and can cause patients to experience difficulties in connection with the perception and adaptation to the external environment. Simultaneously, the cognitive impairment caused by stroke further aggravates other functional deficits. These impairments will ultimately decrease self-care ability, work ability, social function, and psychological health. These defects could aggravate the burden on patients, families, and society [2]. Unfortunately, the benefits of drug treatment on poststroke cognitive impairment are minimal [2, 3]. Therefore, identifying feasible rehabilitation measures and elucidating their effector mechanisms are imperative.

Enriched environment (EE) refers to an intervention of providing equipment and tissue stimulation environment to promote exercise, cognitive activities, and social activities [4]. EE intervention is a new, simple, and effective treatment that is widely used in medical practice, including

rehabilitation for cognitive impairment. EE not only provides sufficient multisensory stimulation but also includes training and learning opportunities for social interactions, spatial exploration, and spontaneous exercise activity. Through EE, the opportunities for humans and animals to obtain material and social stimulation from the environment significantly increase. Therefore, EE may play an important role in improving brain plasticity and behavior [5].

Currently, the mechanisms by which EE improves cognitive function are still not completely understood. A previous study found that EE's role in the improvement of cognitive impairment may be associated with restoration of hippocampal neuronal regeneration, increasing the length of myelinated nerve fibers in the hippocampus, or promoting cerebral blood vessels and blood flow in areas around ischemic cortical regions. After mice were exposed to EE for a certain period of time, the volume of cortical neuronal cell bodies and the quantity and length of dendrites increased [6]. EE demonstrated some benefits in various animal models of brain diseases, including improving cognition, delaying disease progression, increasing cell plasticity, and expression levels of related proteins [7].

However, most previous studies on the effector mechanisms of EE on poststroke cognitive impairment focused on the site of brain injury and the area surrounding the infarct [7, 8], and studies on the fundamental mechanisms of indirect injury sites are limited. In this study, we selected a suitable mouse model of permanent middle cerebral artery occlusion (pMCAO). We assumed that contralateral hippocampal GABAergic and glutamatergic systems-related proteins GAD67 (glutamic acid decarboxylase-67), GA1B (GABAB receptor 1), and NR2B (N-methyl-D-aspartate receptor 2B) were upregulated by EE to further reveal the effects and mechanisms by which EE can improve cognitive function after cerebral ischemia [9–11].

2. Materials and Methods

2.1. Experimental Animals and Experiment Design. Specific pathogen-free (SPF)-grade, 2 to 3-month-old male C57BL/6 mice weighing 25–27 grams were obtained from Lingchang Biotechnology (Shanghai, China). The mice were reared at the MED-X Research Institute, School of Biomedical Engineering, and Shanghai Jiao Tong University. Before surgery, the mice were distributed to different standard condition cages (5 mice per cage) which were 30 cm long, 20 cm wide, and 15 cm tall. The base of each cage contained 2 cm of bedding material (Figure 1(c)) and given ad libitum access to food and water, daily light cycle of 12 h, and room temperature of $24 \pm 1^{\circ}$C. The mice were fasted for 12 h before surgery but allowed to drink water. The experiment protocol was approved by the Institutional Animal Care and Use Committee of Fudan University (approval no. 20160858A232).

A total of 36 mice were used in the experiment, which included 12 mice that received standard environment intervention after the sham surgery (Sham) group and 24 mice that underwent successful pMCAO model construction and were randomized into the standard condition (SC, $n = 12$) group and enriched environment (EE, $n = 12$) group. Twenty-four hours after surgery, various groups of mice were placed in their corresponding environments for rehabilitation intervention. Figure 1(a) shows the overall study design.

2.2. Enriched Environment Intervention. The EE cage was 90 cm long, 70 cm wide, and 40 cm tall. The base of each cage contained 2 cm of bedding material. Twelve mice were kept in the EE cage. The cage contained abundant material stimuli such as slopes, small wooden ladders, platforms for climbing, tunnels, dark boxes, blocks of different colors and shapes, swings for playing and rolling, and treadmills for autonomous exercise. The position of the objects was changed once every three days, and the object combination was changed once a week to maintain novelty (Figure 1(d)). Mice in the SC and Sham groups were returned to standard condition cages.

2.3. Preparation of Permanent Middle Cerebral Artery Occlusion (pMCAO) in C57BL/6 Mice. Before the mouse model construction, the mice were housed in standard environments for seven days of acclimatization. pMCAO was performed as previously described [12]. Briefly, a 15 mm long 6-0 nylon suture was used to create the occlusion. The thread occlusion end underwent blunt electrocoagulation, and silica gel was applied to it. The silica gel head length was 1.5–2 mm. Before surgery, 5% of isoflurane was used for anesthesia induction. During surgery, 1.8–2.0% of isoflurane was used for anesthesia maintenance in mice. After anesthesia, a laser Doppler flowmetry (Moor Instruments, Devon, UK) probe was placed vertically on the skull surface for 5 seconds for continuous measurement. After the readings had stabilized, the baseline of cerebral blood flow was recorded. Subsequently, the mice were fixed in a supine position on a $37^{\circ}\text{C} \pm 0.5$ heating pad. After the skin on the neck was disinfected, a midline incision was made, and the left common carotid artery (CCA), internal carotid artery (ICA), and external carotid artery (ECA) were separated. The external carotid artery and CCA were ligated. An incision was made at the ligation site on the CCA, and a thread occlusion was finally sent through this incision to the middle cerebral artery. Cerebral blood flow was again measured and ensured it was $20 \pm 3\%$ of the base line. The thread occlusion was advanced 60–65 mm at the junction of the ICA and ECA. In the Sham mice, dissection of the arteries was conducted except for the insertion of sutures.

2.4. Modified Neurological Severity Scores (mNSS). Approximately 24 hours after the pMCAO model was constructed, mNSS were used for preliminary assessment of the degree of injury in the different groups of mice. The mNSS ranged from 0–14 points and was used to assess the motor, sensory, balance, and reflex functions of the mice [13]. In this study, mouse models with mNSS of 7–9 points were used to simulate cerebral ischemic injury (Figure 1(b)).

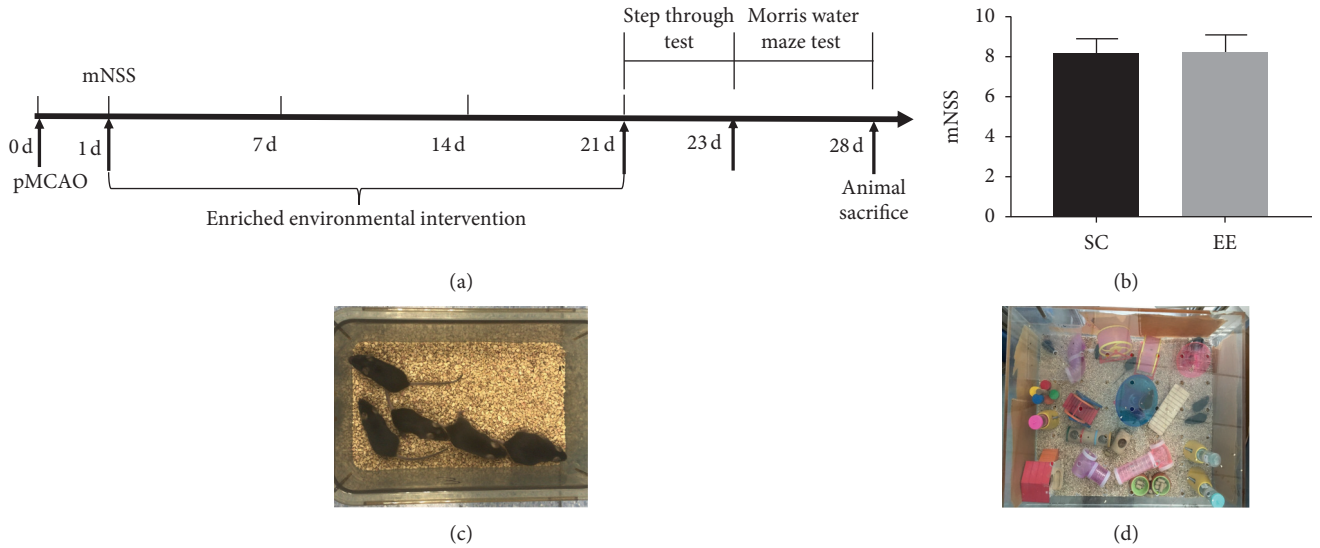

Figure 1: (a) Experiment design. (b) Modified neurological severity scores (mNSS) used at 24 hours after the pMCAO model was constructed. There was no difference between SC and EE groups (p = NS, Student's t-test). Data are shown as mean ± SD, n = 12 per group. (c) Standard condition. (d) Enriched environment. mNSS, modified neurological severity scores; SC, standard condition; EE, enriched environment.

2.5. Step-through Test. The step-through test is used to measure memory function in animals after stroke [14]. The smartcage system (Precisionary, NC, USA) was employed in this experiment. This system includes an infrared detection base, an electrostimulation base, a red dark box, and a transparent casing. The first day of the test is the training day in which animals were placed in the test cage for 3 minutes of acclimatization. The electrostimulation device at the base of the dark box was then turned on. When a mouse enters the dark box, an electrical stimulus was released one second later. The animal will rapidly escape from the dark box to the light box due to pain. The dark box was powered up for five continuous minutes to strengthen memory. The second day is the test day. After 24 hours of training, mice were placed in the light box with their backs facing the dark box, and the electrostimulation device was turned off. The entire process was recorded for 300 seconds. The time taken for the mouse to first enter the dark box was recorded as step-through latency. The escape latency of mice which did not enter the dark box for the entire experiment was recorded as 300 seconds. In addition, the time the mouse remained in the dark box was recorded.

2.6. Morris Water Maze Test (MWM). The MWM is a common cognitive and behavioral science tool that is used to assess spatial learning and memory [15]. This maze consists of a circular pool that is filled with opaque water. Animals are required to swim toward a submerged circular platform and climb to escape the water maze. The diameter of the maze pool was 122 cm. The height of the pool was 51 cm, water temperature was adjusted to 19–22°C, and the diameter of platform was 10 cm. White titanium oxide was added to the water surface to conceal the position of the platform.

In the six-day period of MWM, positioning navigation test was used for the first 5 days. A pool was divided into four quadrants, namely, southwest, northwest, northeast, and southeast. Also, the underwater escape platform was located at the northeast quadrant. For each day, mice were placed into the water by facing the pool wall at four different entry-points away from the platform. For any mice that were unable to find the platform in 60 seconds, they will be manually guided to the platform. Regardless of how the mice reached the platform, they would be allowed to stay on it for 10 seconds to strengthen learning. At Day 6, the spatial exploration test was initiated. The platform was removed, and the animals were only placed into the water at the opposite quadrant of the platform, southwest. The test duration was 60 seconds.

In the positioning navigation test, escape latency (the time cost to find the platform) was recorded for Days 3–5. Also, in the spatial exploration test, time spent in the northeast zone was recorded. These data were used to evaluate the experimental subjects' ability of spatial learning and memory.

2.7. Immunohistofluorescence. After the behavioral science tests, six mice were randomly selected from each group for immunohistochemical staining. Briefly, mice were successively perfused with 0.9% physiological saline and 4% paraformaldehyde (pH 7.4) before entire brain tissues were extracted. A cryomicrotome was used to extract 20 μm-thick coronal cryosections which were then mounted on microscope slides. The sections were fixed in methanol at −20°C for 10 min. Then, diluted donkey serum (Jackson Immuno Research, West Grove, PA) was used for blocking at room temperature for 60 min. The glass slides were incubated with the primary antibody against NR2B (1:200, Proteintech, IL,

USA) at 4°C overnight. The next day, the slides were washed with PBS and then incubated with fluorescent secondary antibodies at room temperature for 1 hour. A fluorescence confocal microscope (Leica, Wetzlar, Germany) was used to image the tissue sections. The same parameters were used for taking microscopic photographs. All photographs were captured under identical conditions.

2.8. Measurement of Cerebral Atrophy Volume. A series of 20 μm-thick coronal sections were made at 200 μm intervals from the anterior commissure to the hippocampus for measurement of cerebral atrophy volume. The sections were stained with cresyl violet. The ImageJ software (National Institutes of Health, MD, USA) was used to plot and calculate the volume of the ipsilateral and contralateral brain slices. Infarct volume was calculated as described previously [16].

2.9. Western Blot Analysis. After the behavior tests, the contralateral hippocampal tissues from the six remaining mice in every group were collected for western blotting. Briefly, the tissues were placed in RIPA lysis buffer containing protease inhibitors and homogenized. After centrifugation, the supernatant was collected. The BSA assay was used to quantitate protein concentration in the supernatant. Protein samples were denatured at 95°C for 10 min. Then, 20 μg were used for SDS-PAGE and transferred onto a nitrocellulose (NC) membrane. The membrane was incubated with blocking solution at room temperature for one hour. Then, the membrane was incubated with primary antibodies at 4°C overnight: GAD76 (1:500, Proteintech, IL, USA), GA1B (1:1000, Abcam, MA, USA), and N-methyl-D-aspartate receptor 2B (NR2B) (1:500, Proteintech, IL, USA). The membrane was then washed and then incubated with horseradish peroxidase-(HRP-)-conjugated secondary antibodies at room temperature for 1 hour. An enhanced chemiluminescence (ECL) reagent kit was used for detection of western blotting results. A western blotting imaging system (Bio-Rad, Hercules, CA) was used to measure the fluorescence intensity of protein bands, and ImageJ was used for quantitation.

2.10. Statistical Analysis. All results were presented as mean ± SD. Data were analyzed using SPSS 22.0 software. Student's *t* test or one or two-way repeated ANOVA with the Student–Newman–Keuls multiple comparison test was used in the research. p values <0.05 were considered to be statistically significant.

3. Results

3.1. mNSS in Mice from the SC and EE Groups before EE Intervention. The mice were randomized into the SC and EE groups one day after the pMCAO models were constructed. mNSS of the two groups of mice were assessed for any differences, and there is no significant difference between the mice from the SC and EE groups (p = NS) (Figure 1(b)). This shows that the nerve damage caused by the pMCAO model was consistent. Therefore, interference on experimental results after grouping was eliminated, and the experimental results could be more accurate.

3.2. Morris Water Maze Performance of Different Groups after EE Intervention. Comparison of the SC and the Sham groups indicated that the former had a longer escape latency in the positioning navigation test at the last three days ($p < 0.01$), and the SC group showed poorer cognitive function. When the EE group was compared to the SC group, the former showed a shorter escape latency only at the last two days ($p < 0.01$) (Figures 2(a) and 2(d)). In the spatial exploration test, the time spent in the quadrant where the platform was located was longer in both EE and Sham groups compared to the SC group (both $p < 0.01$) (Figures 2(b) and 2(e)). This shows that the SC group had poorer cognitive function. From both tests, we can conclude that EE intervention can improve cognitive function after cerebral ischemic injury.

3.3. Step-through Test Performance of Various Groups after EE Intervention. The time spent before entering the dark box was longer in the EE group and Sham group compared to the SC group in the step-through test (both $p < 0.01$) (Figure 2(g)), while the duration in the dark box was shorter in the EE and Sham groups compared to the SC group (both $p < 0.01$) (Figures 2(f) and 2(h)). This again shows that the SC group had poorer cognitive function and EE intervention that can improve cognitive function after cerebral ischemic injury.

3.4. Cresyl Violet Staining and Calculation of Atrophy Volume in Hippocampal Brain Slices. There is no statistical difference in the relative cerebral atrophy volume (% of con.) between the EE and the SC groups (p = NS) (Figure 3). EE cannot reverse the incurred damage to the structure of the hippocampus in the pMCAO model.

3.5. Improvement Status of GABAergic Nervous System in Contralateral Hippocampus of Various Groups after EE Intervention. The expression levels of GAD67 and GA1B proteins that are related to the GABAergic nervous system were higher in the EE and Sham groups compared to the SC group (both $p < 0.01$) (Figures 4(a) and 4(b)). This indicated a deterioration of GABAergic neurological function in the contralateral hippocampus during the chronic phase of cerebral ischemic injury. However, EE intervention can upregulate the expression of GAD67 and GA1B.

3.6. Expression of Glutamatergic Receptors in Contralateral Hippocampi of Various Groups after EE Intervention. Immunofluorescence and western blot analysis demonstrated that the expression of NR2B related to the glutamatergic systems significantly reduced in the SC group

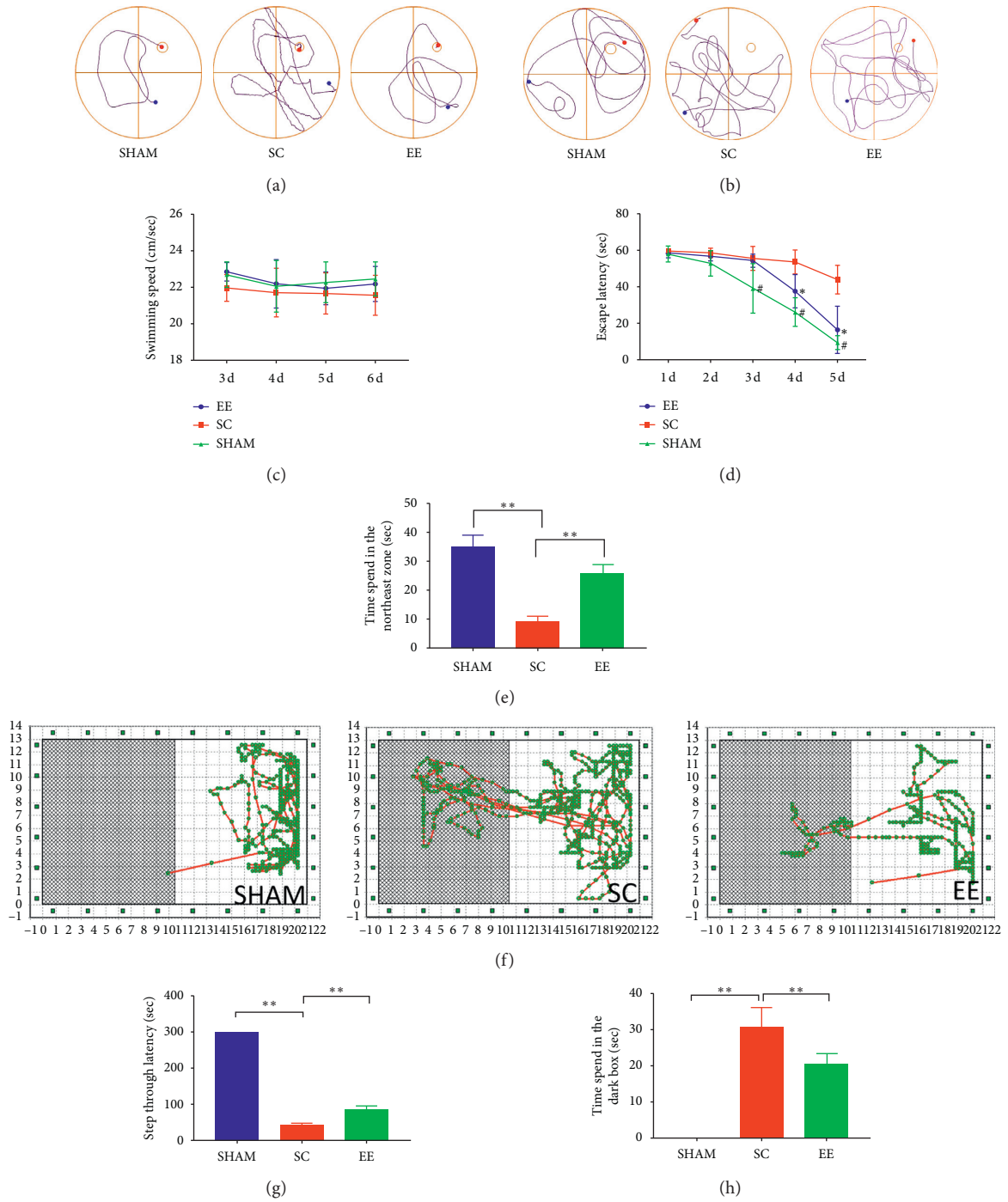

Figure 2: Cognitive function analyses using the Morris water maze and step-through tests. (a) The typical swimming paths of sham, SC, EE groups in positioning navigation test. (b) The typical swimming paths of sham, SC, EE groups in spatial exploration test. (c) The average swimming speed of mice during the last 4 days. No significant difference was shown among these groups (p = NS). (d) Escape latency to find the hidden platform for day 3–5. Comparison of the SC and the Sham groups indicated that the former had a longer escape latency in the tests at the last three days ($\#p < 0.05$), and the EE group was compared to the SC group, the former showed a shorter escape latency only at the last two days ($*p < 0.05$). (e) Spatial exploration test, the time spent in the quadrant where the platform was located was longer in both EE and Sham groups compared to the SC group (both $**p < 0.01$). (f) The typical movement paths of sham, SC, EE groups in step-through test. (g) The step-through latency was longer in the EE and Sham groups compared to the SC group (both $**p < 0.01$). (h) The duration in the dark box was shorter in the EE and Sham group. SC, standard condition; EE, enriched environment.

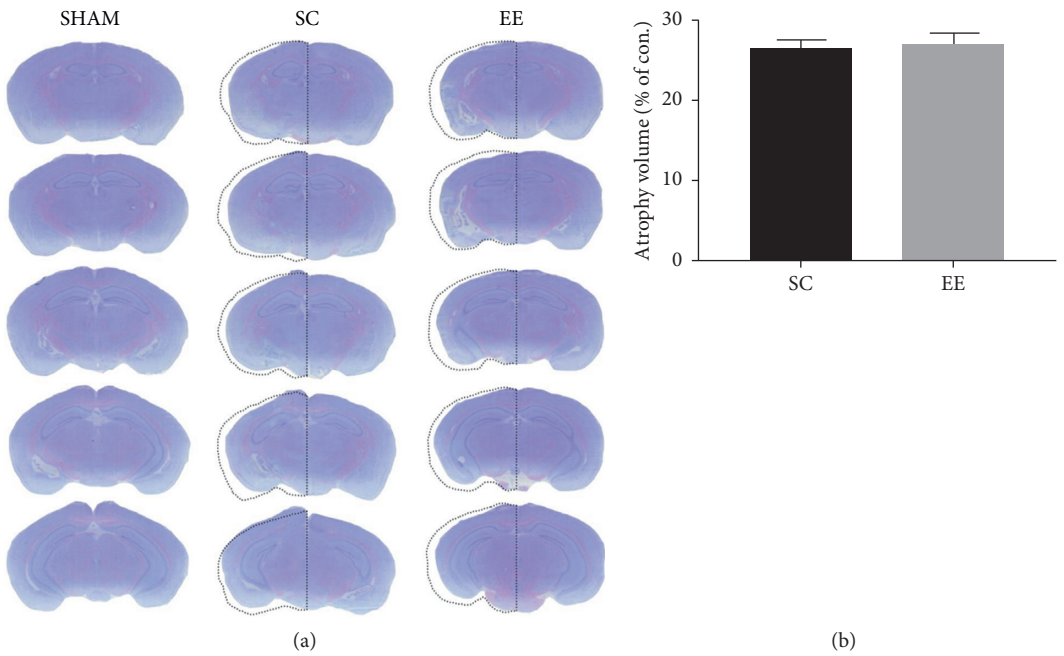

Figure 3: Measurement of cerebral atrophy volume (a) Photographs showed brain coronal sections with cresyl violet staining in the sham, SC and EE groups. (b) No statistical difference in cerebral atrophy volume between the SC and EE groups (p = NS). Data are shown as mean ± SD, $n = 6$ per group. p = NS. SC, standard condition; EE, enriched environment.

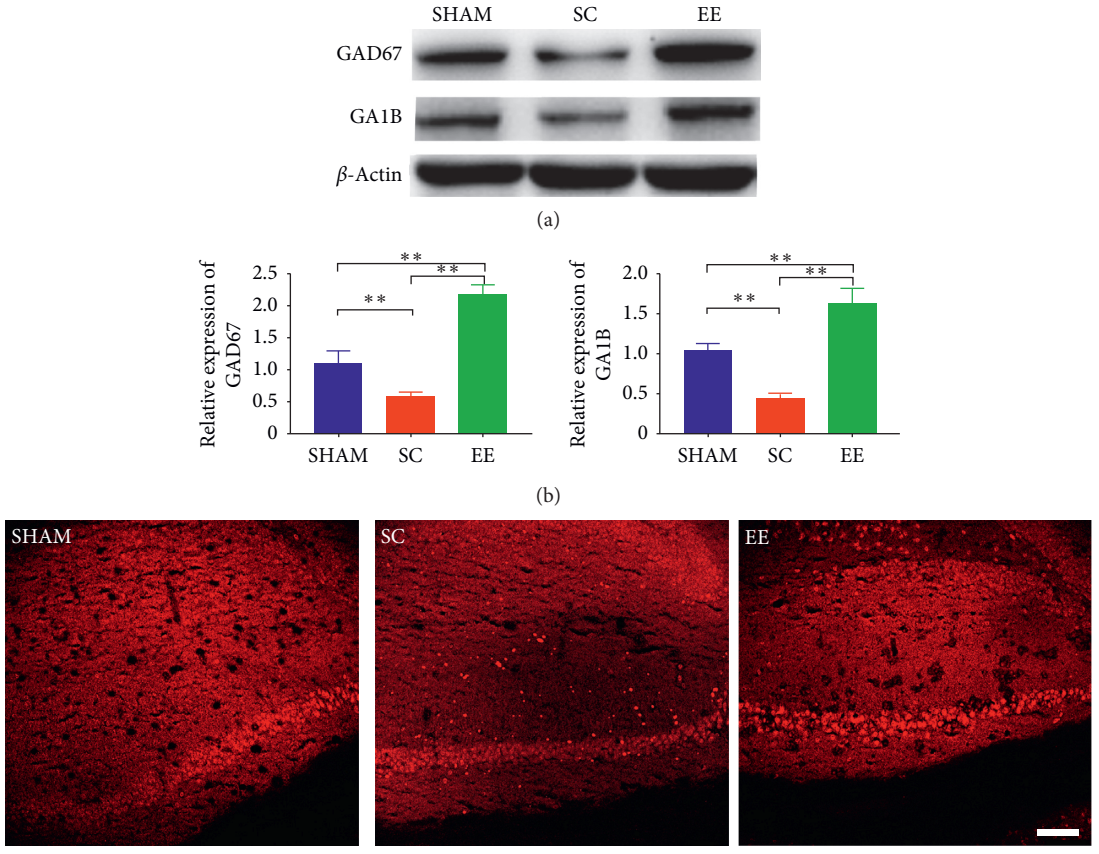

Figure 4: Continued.

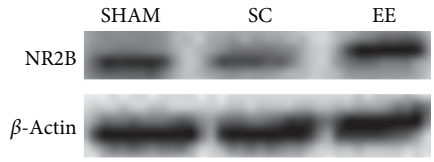

(d)

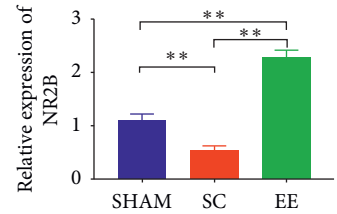

(e)

Figure 4: GABAergic and glutamatergic systems in the contralateral hippocampus of cerebral ischemic injury were inhibited. EE can upregulate the aforementioned systems related protiens. (a) The expression levels of GAD67 and GA1B proteins that are related to the GABAergic nervous system were higher in the EE and Sham groups compared to the SC group (both $**$ $p < 0.01$). (b, c) Immunofluorescence and Western blot analysis demonstrated that the expression of NR2B related to the glutamatergic systems significantly reduced in the SC group compared to the sham or EE groups (both $**$ $p < 0.01$). Scale bar = 100 μm. Data are shown as mean ± SD, $n = 6$ per group. SC, standard condition; EE, enriched environment; GAD76, glutamic acid decarboxylase-67; GA1B, GABAB receptor 1; NR2B, N-methyl-D-aspartate receptor 2B.

compared to the sham groups ($p < 0.01$). EE intervention can reverse this phenomenon (Figures 4(c)–4(e)).

4. Discussion

In this study, we found that the pMCAO model may cause persistent cognitive impairment, and both GABAergic nervous system and glutamatergic receptors in the contralateral hippocampus of cerebral ischemic injury were inhibited. EE promotes recovery of cognitive function after cerebral ischemic injury that may in part be mediated by upregulating GA1B, GAD67, and NR2B which were relevant to the aforementioned systems in the contralateral hippocampus.

The MCAO model is widely used in basic research on stroke, and common models include transient middle cerebral artery occlusion (tMCAO) and pMCAO [17]. The core difference between these two models is whether thread occlusion was moved. In clinical practice, patients with central nervous system damage, particularly those with chronic phase cerebral ischemic injury, mainly undergo neurological rehabilitation. These patients usually miss the opportunity for acute thrombectomy and thrombolysis, resulting in an inability for spontaneous recovery of neurological function for a long period of time [18]. Therefore, we selected the pMCAO model, which is similar to the clinical problems described in this study. In our present study, there is no significant difference in mNSS after pMCAO surgery was observed between the SC and EE groups, which excluded the effects of differences in degree of injury before grouping.

Cresyl violet staining used in the pMCAO model indicated that there was no statistical difference in cerebral atrophy volume between the SC and EE groups. This indicates that when permanent ischemic injury occurs in the middle cerebral arteries, EE cannot reverse the incurred damage to the structure of the hippocampus in the MCAO model. The hippocampus plays an important role in information processing, memory formation, and subsequent behavioral regulation [19]. In the Morris water maze and step-through tests, which are highly correlated with the cognitive function of the hippocampus, mice from the SC group showed a significant decline in cognitive function compared to the Sham group. This shows that cognitive impairment caused by the pMCAO model persists. However, EE intervention could improve cognitive impairment after cerebral ischemic injury. This further suggests that EE may participate in compensatory functions in the contralateral hippocampus.

Excitation/inhibition balance is mainly maintained by the GABAergic nervous system in the central nervous system [20]. In our present study, the experiment results first showed that compared to mice from the Sham group, the expression of GAD67 and GA1B in the contralateral hippocampi of SC mice was downregulated, indicating a decline in the GABAergic nervous system of the contralateral hippocampus during the chronic phase of cerebral ischemic injury. GABA is synthesized by GAD67 and GAD65. In the central nervous system, GAD67 plays an important role in the synthesis and synaptic release of GABA [9]. Further, GABA can activate GABA receptors that are located in various neurons in the brain. In particular, reduction in GABA B receptors during cerebral ischemia has been observed [21]. The activation of GABA B receptors can restore the balance in the cell membrane surface expression of cyclic-nucleotide-gated cation nonselective (HCN)1/HCN2 in the CA1 region in the rat hippocampus, and the HCN1 channel regulates distal synaptic input to integrate dendrites in the pyramidal cells to participate in learning and memory [22]. In addition, a recent study reported that GA1B is an effective factor that improves cognitive impairment caused by chronic insufficient cerebral perfusion [11]. Therefore, during cerebral ischemia injury, the upregulation of the GABAergic nervous system (such as GAD67 and GA1B) in the hippocampus may improve cognitive impairment. Previous study mainly focus on the ipsilateral hippocampus after cerebral ischemia. However, our study suggested EE

upregulated the expression of GAD67 and GA1B in the contralateral hippocampus and could promote recovery of cognitive function.

Ischemic stroke triggers the transient efflux of large levels of glutamate and overactivation of NMDAR, which may lead to neuronal death [23, 24]. The results of this study showed that NR2B expression decreased during the chronic phase in the pMCAO model and showed for the first time that EE increased NR2B expression and enhanced synapse plasticity in the contralateral hippocampus, which may promote recovery of cognitive function. We also found that the protein expression in EE is higher when compared with SHAM. The traditional viewpoint is that NMDAR, particularly NR2B, accelerates neuronal death during cerebral ischemic injury and should be inhibited. However, these studies involved observations during the acute phase of stroke, but few studies have evaluated the chronic phase. Therefore, most clinical trials on NMDA antagonists cannot improve and may even worsen stroke outcomes [10, 25]. A recent study revealed that the persistent decline in NMDAR density after stroke plays an important role in plasticity and memory formation. This shows that NMDAR activity should be promoted instead of inhibited during the nonacute phase of stroke. NMDAR excitation during the poststroke recovery stage may have beneficial effects to the cognitive function, which may be due to enhanced neuroplasticity and not neuroprotective effects [26].

Our prediction is that the ipsilateral hippocampus after permanent cerebral ischemic injury can no longer be responsible for cognitive function. Thus, contralateral hippocampus must be step up and compensate for this cognitive function. This leads to the increase of related protein in the contralateral hippocampus to achieve the desired outcome. In clinical practice, the most common method for direct regulation of brain excitation is repetitive transcranial magnetic stimulation (rTMS). The traditional viewpoint is that excitatory stimulation should be used on the ipsilateral cortex, whereas inhibitory stimulation should be used on the contralateral cortex during poststroke rehabilitation. [27] However, recent studies have shown that excitation of the contralateral cortex can improve motor function in patients when there is severe damage to the ipsilateral cortex after stroke, and motor function shows persistent signs of no recovery [28]. This study may have similar concepts as the aforementioned recent studies.

In summary, contralateral hippocampal function is inhibited after cerebral ischemic injury, further affecting cognitive function for a prolonged period. However, enriched environment can upregulate GABAergic and glutamatergic systems in the contralateral hippocampus to promote cognitive function recovery. However, this speculation needs further investigation and requires further clinical trials for validation.

Data Availability

The data used to support the findings of this study are available from the corresponding author upon request.

Conflicts of Interest

The authors declare that there are no conflicts of interest.

Acknowledgments

This study was supported by the National Natural Science Foundation of China (no. 81672242, 81472150, and 81601960) and the Key Construction Projects of Shanghai Health and Family Planning on Weak Discipline, China (no. 2015ZB0401).

References

[1] D. A. Levine, A. T. Galecki, K. M. Langa et al., "Trajectory of cognitive decline after incident stroke," *JAMA*, vol. 314, no. 1, pp. 41–51, 2015.

[2] M. D. Mijajlovic, A. Pavlovic, M. Brainin et al., "Post-stroke dementia-a comprehensive review," *BMC Medicine*, vol. 15, no. 1, p. 11, 2017.

[3] J.-S. Lim, M. S. Oh, J.-H. Lee et al., "Prediction of post-stroke dementia using NINDS-CSN 5-minute neuropsychology protocol in acute stroke," *International Psychogeriatrics*, vol. 29, no. 5, pp. 777–784, 2017.

[4] J. Nithianantharajah and A. J. Hannan, "Enriched environments, experience-dependent plasticity and disorders of the nervous system," *Nature Reviews Neuroscience*, vol. 7, no. 9, pp. 697–709, 2006.

[5] S. Mering and J. Jolkkonen, "Proper housing conditions in experimental stroke studies-special emphasis on environmental enrichment," *Frontiers in Neuroscience*, vol. 9, p. 106, 2015.

[6] M. C. Diamond, D. Krech, and M. R. Rosenzweig, "The effects of an enriched environment on the histology of the rat cerebral cortex," *The Journal of Comparative Neurology*, vol. 123, no. 1, pp. 111–119, 1964.

[7] T. Y. C. Pang and A. J. Hannan, "Enhancement of cognitive function in models of brain disease through environmental enrichment and physical activity," *Neuropharmacology*, vol. 64, pp. 515–528, 2013.

[8] P. Dahlqvist, A. Ronnback, S.-A. Bergstrom, I. Soderstrom, and T. Olsson, "Environmental enrichment reverses learning impairment in the Morris water maze after focal cerebral ischemia in rats," *European Journal of Neuroscience*, vol. 19, no. 8, pp. 2288–2298, 2004.

[9] H. Asada, Y. Kawamura, K. Maruyama et al., "Cleft palate and decreased brain-aminobutyric acid in mice lacking the 67 kDa isoform of glutamic acid decarboxylase," *Proceedings of the National Academy of Sciences*, vol. 94, no. 12, pp. 6496–6499, 1997.

[10] L. Hoyte, P. Barber, A. Buchan, and M. Hill, "The rise and fall of NMDA antagonists for ischemic stroke," *Current Molecular Medicine*, vol. 4, no. 2, pp. 131–136, 2004.

[11] Y. Lu, C. Li, M. Zhou et al., "Clonidine ameliorates cognitive impairment induced by chronic cerebral hypoperfusion via up-regulation of the GABABR1 and GAD67 in hippocampal CA1 in rats," *Pharmacology Biochemistry and Behavior*, vol. 132, pp. 96–102, 2015.

[12] G. Tang, Y. Liu, Z. Zhang et al., "Mesenchymal stem cells maintain blood-brain barrier integrity by inhibiting aquaporin-4 upregulation after cerebral ischemia," *Stem Cells*, vol. 32, no. 12, pp. 3150–3162, 2014.

[13] J. Chen, P. R. Sanberg, Y. Li et al., "Intravenous administration of human umbilical cord blood reduces behavioral deficits

after stroke in rats," *Stroke*, vol. 32, no. 11, pp. 2682–2688, 2001.

[14] D.-Y. Choi, J. W. Lee, G. Lin et al., "Obovatol attenuates LPS-induced memory impairments in mice via inhibition of NF-κB signaling pathway," *Neurochemistry International*, vol. 60, no. 1, pp. 68–77, 2012.

[15] C. V. Vorhees and M. T. Williams, "Morris water maze: procedures for assessing spatial and related forms of learning and memory," *Nature Protocols*, vol. 1, no. 2, pp. 848–858, 2006.

[16] A. Jaillard, C. Cornu, A. Durieux et al., "Hemorrhagic transformation in acute ischemic stroke," *Stroke*, vol. 30, no. 7, pp. 1326–1332, 1999.

[17] F. Fluri, M. K. Schuhmann, and C. Kleinschnitz, "Animal models of ischemic stroke and their application in clinical research," *Drug Design, Development and Therapy*, vol. 9, pp. 3445–3454, 2015.

[18] S. Wu, B. Wu, M. Liu et al., "Stroke in China: advances and challenges in epidemiology, prevention, and management," *The Lancet Neurology*, vol. 18, no. 4, pp. 394–405, 2019.

[19] M. A. Lynch, "Long-term potentiation and memory," *Physiological Reviews*, vol. 84, no. 1, pp. 87–136, 2004.

[20] R. Gutiérrez, H. Romo-Parra, J. Maqueda et al., "Plasticity of the GABAergic phenotype of the "glutamatergic" granule cells of the rat dentate gyrus," *The Journal of Neuroscience*, vol. 23, no. 13, pp. 5594–5598, 2003.

[21] L. Huang, L. B. Zhao, Z. Y. Yu et al., "Long-term inhibition of Rho-kinase restores the LTP impaired in chronic forebrain ischemia rats by regulating GABAA and GABAB receptors," *Neuroscience*, vol. 277, pp. 383–391, 2014.

[22] M. Nolan, G. Malleret, J. Dudman et al., "A behavioral role for dendritic integration HCN1 channels constrain spatial memory and plasticity at inputs to distal dendrites of CA1 pyramidal neurons," *Cell*, vol. 119, no. 5, pp. 719–732, 2004.

[23] H. Benveniste, J. Drejer, A. Schousboe, and N. H. Diemer, "Elevation of the extracellular concentrations of glutamate and aspartate in rat hippocampus during transient cerebral ischemia monitored by intracerebral microdialysis," *Journal of Neurochemistry*, vol. 43, no. 5, pp. 1369–1374, 1984.

[24] A. Dávalos, J. Castillo, J. Serena, and M. Noya, "Duration of glutamate release after acute ischemic stroke," *Stroke*, vol. 28, no. 4, pp. 708–710, 1997.

[25] R. L. Sacco, J. T. DeRosa, E. C. Haley et al., "Glycine antagonist in neuroprotection for patients with acute stroke," *JAMA*, vol. 285, no. 13, pp. 1719–1728, 2001.

[26] J. Dhawan, H. Benveniste, Z. Luo, M. Nawrocky, S. D. Smith, and A. Biegon, "A new look at glutamate and ischemia: NMDA agonist improves long-term functional outcome in a rat model of stroke," *Future Neurology*, vol. 6, no. 6, pp. 823–834, 2011.

[27] Z. Hao, D. Wang, Y. Zeng, and M. Liu, "Repetitive transcranial magnetic stimulation for improving function after stroke," *Cochrane Database of Systematic Reviews*, vol. 5, Article ID C, 2013.

[28] V. Sankarasubramanian, A. G. Machado, A. B. Conforto et al., "Inhibition versus facilitation of contralesional motor cortices in stroke: deriving a model to tailor brain stimulation," *Clinical Neurophysiology*, vol. 128, no. 6, pp. 892–902, 2017.

Hindawi
Evidence-Based Complementary and Alternative Medicine
Volume 2020, Article ID 8896123, 9 pages
https://doi.org/10.1155/2020/8896123

Research Article

Electroacupuncture at Zusanli (ST36) Repairs Interstitial Cells of Cajal and Upregulates c-Kit Expression in Rats with SCI-Induced Neurogenic Bowel Dysfunction

Yujie Yang,[1] **Jie Cheng**,[2] **Yongni Zhang**,[3] **Jiabao Guo**,[4] **Bin Xie**,[5] **Wenyi Zhang**,[6] **Zhaojin Zhu**,[7] **and Yi Zhu**[8]

[1]*Department of Biomedical Sciences, City University of Hong Kong, Kowloon, Hong Kong*
[2]*The Second Clinical Medical School, Nanjing University of Chinese Medicine, Nanjing, Jiangsu, China*
[3]*Yueyang Hospital of Integrated Traditional Chinese and Western Medicine, Shanghai, China*
[4]*Department of Rehabilitation Medicine, The Second School of Clinical Medicine, Xuzhou Medical University, Xuzhou, Jiangsu, China*
[5]*Jiangyin Orthopedics Hospital of Traditional Chinese Medicine, Wuxi, Jiangsu, China*
[6]*Zhongshan Rehabilitation Branch of Jiangsu Provincial Hospital, Nanjing, Jiangsu, China*
[7]*Department of Rehabilitation, Changzhou Higher Vocational and Technical College of Health, Changzhou, Jiangsu, China*
[8]*Department of Pain and Musculoskeletal Rehabilitation, The Fifth Affiliated Hospital of Zhengzhou University, Zhengzhou, Henan, China*

Correspondence should be addressed to Yi Zhu; zhuyi1010@163.com

Received 23 September 2020; Revised 26 October 2020; Accepted 9 November 2020; Published 27 November 2020

Academic Editor: Feng Zhang

Background. Electroacupuncture (EA) could improve colonic transit activity in rats with neurogenic bowel dysfunction (NBD) caused by spinal cord injury (SCI). The function of interstitial cells of Cajal (ICCs) and c-Kit expression may play essential roles in this process. *Material and Methods*. Thirty-six Sprague Dawley rats were randomized to the sham group, the SCI group, or the SCI + EA group (bilateral Zusanli, 30 min/day, 14 days). Changes in the ultrastructural morphology of ICCs were observed. The c-Kit expression on different levels was analyzed by immunohistochemistry, Western blotting, and RT-qPCR, respectively. *Results*. Abnormal morphology of ICCs and downregulation of the c-Kit expression occurred after SCI. While the number of ICCs was increased, the ultrastructural morphology was improved significantly in EA rats. They also showed better improvement in c-Kit expression at both protein and gene levels. *Conclusion*. Abnormal ICCs in colon tissues and the downregulated expression of c-Kit could be observed after SCI. EA at Zusanli (ST36) could improve the colon function by repairing the morphology and increasing the number of ICCs and upregulating c-Kit expression.

1. Introduction

Neurogenic bowel dysfunction (NBD) is a term that refers to colonic dysfunction caused by the central nervous system (CNS) disease or injury [1]. It occurs in almost all patients with a chronic spinal cord injury (SCI) [2]. They suffer from functional obstruction, constipation, fecal incontinence, abdominal pain, or their combination [3]. More than 40% of SCI patients complained that the NBD seriously affects their quality of life [4, 5] because it not only aggravates the physical condition but also causes the psychological problem by imposing restrictions on their participation in daily life activities and threatening their privacy and dignity [4, 5].

Thus, management of bowel function ranks in the most priorities among SCI patients [1]. Various therapeutic interventions have been applied for NBD management [3], including multiple forms of electrical stimulation [6]. EA, as a convenient, repeatable, and less-lesion intervention, is commonly used to treat in both clinical trials and laboratory experiments [7]. The combination of traditional Chinese

medicine theory and modern neuromodulation theory make EA more acceptable than the traditional acupuncture. Zusanli (ST36) is one of the most frequently used acupoints to prevent and treat gastrointestinal disorders. Although a considerable amount of research has reported the effect and mechanism of EA on gastrointestinal dysfunction [8–12] or other complications of SCI (such as the neurogenic bladder dysfunction) [13–15], the quality and quantity of EA studies on SCI-induced NBD are relatively insufficient. Some research supported the effect of EA on NBD patients or animal models. A clinical trial has proven that EA is effective at managing NBD by decreasing the burden of bowel care and episodes of fecal incontinence in SCI patients [16]. Our previous study has found that EA at ST36 could increase the colonic propulsive movement in SCI rats [17, 18]. However, the mechanism of EA on NBD remains unclear.

The decline in colonic motility and delay in colonic transit are considered as the primary mechanisms of NBD after SCI [19]. Interstitial cells of Cajal (ICCs) have a function in regulating gastrointestinal motility by generating and propagating slow waves as well as transducing signals between the enteric nervous system (ENS) and smooth muscle cells [20]. Studies have shown that a reduction in the ICC population may cause slow-transit constipation [21, 22]. A clinical histology study conducted in the Netherlands confirmed that patients with spina bifida or SCI experienced a loss of ICCs and neurons in the myenteric plexus, compared with control patients without gastrointestinal motility disorders [23]. The proto-oncogene c-kit expressed by ICCs encodes the tyrosine kinase receptor (c-Kit). Generally, the c-Kit is considered as the identification marker of ICCs [24]. Some studies found that c-Kit is closely associated with the development, differentiation, and functional maintenance of ICCs in the intestine [25, 26]. In addition, several gastrointestinal motility disorders have been linked to depletion of c-Kit-positive ICCs [27, 28], and re-expression of c-kit protein may contribute to the functional recovery of ICCs [29]. Studies have reported that EA at Zusanli can promote colonic motility [30, 31] and increase the expression of ICCs in partial intestinal obstruction [32]. However, the underlying mechanism has not yet been investigated. Thus, this study aimed to explore the possible mechanisms of EA therapy on defecation dysfunction after SCI.

2. Material and Methods

2.1. Animals and Grouping. Thirty-six female adult-specific pathogen-free Sprague Dawley rats adopted from the Sino-British Sippr/BK Lab Animal Co. Ltd. (Shanghai, China) were used in this research. All the animals were raised under standardized laboratory conditions with a light-dark cycle (12 : 12). The ambient temperature was kept between 21 and 25°C, and the relative humidity was set to 50–55%. They were fed adaptively for ten days with free access to water and food until reaching a weight of 300 ± 20 g.

Twenty-four rats were selected randomly for the SCI model establishment, and the remaining twelve rats received the sham operation. Only the successful SCI models were included in further experiments and then randomly assigned to either the SCI group or the SCI + EA group. Animals that received sham surgery were included in the sham group as a control.

All the experiments were performed in the Jiangsu Province Key Laboratory of Acupuncture and were approved by the Center for Safety Evaluation of Research in the Nanjing University of Chinese Medicine.

2.2. SCI Modeling and Sham Surgery. The SCI model in rats was established with the weight-drop method. The atropine sulfate (0.05 mg/kg, s.c.) was used to inhibit tracheal secretions. Fifteen minutes later, anesthesia was induced with pentobarbital sodium (50 mg/kg, i.p.). Animals then were mounted on the operating table in a prone position. A middle dorsal incision was performed from T10 to T13 following skin preparation. The vertebral plates and spinous process of T11 and T12 were exposed and then removed by laminectomy to make a window revealing the spinal cord. The spinal cord was contused using the New York University Impactor I, which could provide a drop of 10-gram rob from a height of 60 mm. A subdural hemorrhage followed by twitching of posterior limbs and lashing of tails could be observed immediately after the wound. The operative incisions were sutured after debridement.

For animals that received sham operation, the operative incisions were sutured following the removal of the spinous process and vertebral plates from T11 to T12 without any injury on the spinal cord.

All animals were accessed by the modified Basso–Beattie–Bresnahan locomotor scale (mBBB, Table S2) [33] before and 24 h after the operation for judging and evaluating whether or not the modeling succeeded. Each time the assessment was performed by two assessors independently. All animals got 21 points before any operation was performed. Twenty-four hours after the SCI modeling surgery, rats that got 0 points will be considered as successful models. Animals that received sham surgery were included in the further experiments only if they got 21 points 24 h postoperatively.

2.3. Postoperative Nursing. All the rats received intraperitoneal injections of gentamicin (5000 U/kg) daily from the operating day. The abdomen, perineum, and hind limbs of the SCI rats were cleaned every 12 h after Crede's maneuver that was performed to assist with urination. The passive motion was performed on the hind limbs every day before the intervention.

2.4. Electroacupuncture (EA). EA intervention started from the day after the surgery once the rats were considered as the successful model. Animals in the SCI + EA group were mounted on an operation platform in a supine position on the treatment table. The acupoints selected for intervention are the bilateral Zusanli points (ST36), which are 5 mm below the fibular head and 1 mm lateral to the anterior border of tibia [34]. After local disinfection with iodophor, the acupuncture needles (Hua Tuo, 0.25 ∗ 13 mm; Suzhou

Medical Appliance Factory, Co. Ltd., Jiangsu, China) were perpendicularly inserted to a depth of 5 mm. Then, the needles were connected with a Hua Tuo electroacupuncture apparatus (SDZ-II; Suzhou Medical Appliance Factory, Co. Ltd., Jiangsu, China) with the disperse-dense wave at a current intensity of 1-2 mA and a frequency of 3 Hz/15 Hz. The stimulation strength was limited to a tolerable range within which rats could freely vocalize, and the subtle vibration of the needle could be observed. At the same time, animals of the sham group and the SCI groups were mounted in the same method only without EA. All the interventions started around 11 am and lasted 30 min, once daily, for 14 days.

2.5. Tissue Preparation. After a 2-week intervention, rats fasted for 24 h were sacrificed by cervical dislocation under deep anesthesia. One centimeter sections of the proximal colon (one centimeter below the cecum) were removed from all animals for subsequent examinations. For the ultrastructural morphology, the proximal colon tissues were immersed in 5% glutaraldehyde at 4°C for 2 h after removing the mucosae and then postfixed in 1% osmic acid at 4°C for 2 h before the 2% uranyl acetate staining. After dehydration with a graded series of ethanol at 4°C, the specimens were stained with toluidine blue. Then, they were sliced to semithin sections with a 70–80 nm thickness using an ultramicrotome (Leica RM2145, Germany). For the immunohistochemistry analysis, 5 μm-thick slices of the proximal colon tissues were cut from the 4% paraformaldehyde-fixed, paraffin wax embedded blocks for further processing. For the RT-qPCR analysis and the Western blotting, the proximal colon tissues with dissection of the mucosa were immersed in the liquid nitrogen and then stored at −80°C.

2.6. Ultrastructural Morphology. The transmission electron microscopy (TEM) was applied to observe the ultrastructural changes in colonic ICCs. The tissue specimens were observed under a transmission electron microscope (JEM-1010; JEOL Ltd., Japan) at 4000x and 25000x magnification, respectively. The images of the ultrastructure of ICCs were searched and captured by researchers who were blinded to the grouping.

2.7. Immunohistochemistry (IHC). The IHC was performed to detect the c-Kit-positive ICCs in the proximal colon tissues. The paraffin slices of the proximal colon tissues were placed in a 60°C oven for 2 h. Then, they were dewaxed with xylene and rehydrated through a graded series of ethanol. Antigen was retrieved in the boiled citric acid buffer after the activity of endogenous peroxidase was blocked with 0.30% H_2O_2. Then, the sample slices were blocked with 5% bovine serum albumin for one hour at room temperature. Slices were incubated with rabbit anti-rat c-Kit multiclonal antibody (1 : 100; Santa Cruz Biotechnology, Inc., USA) at 4°C overnight. After they were washed three times in the phosphate-buffered saline (PBS), the sample slices were incubated with the secondary antibody (1 : 500; SABC kit-SA1022; BOSTER Biological Technology Co. Ltd., Wuhan, China) and later with the streptavidin-biotin Complex (SABC) system. Afterward, the sample slices were washed in PBS after being incubated with 3,3-diaminobenzidine (DAB). Finally, the sample slices were counterstained with hematoxylin. Staining specimens were imaged using an optical microscope (Olympus, Japan) at 400 magnification, and the c-Kit-positive ICCs were quantified by detecting ten randomly selected high power fields from each slice. The average optical density (AOD) of positively stained areas, which is used to measure the staining intensity, was analyzed by the JD801 morphological microimage analysis system (Nanjing Jieda Company, Jiangsu, China).

2.8. Western Blotting (WB). The WB was used to analyze the expression level of colonic c-Kit protein. Frozen samples of proximal colon tissues were homogenized in the RIPA lysis buffer (Nanjing Vazyme Biotech Co. Ltd., Jiangsu, China) with a handheld homogenizer. The homogenate was centrifuged at 10000×g at 4°C for 5 min. Only the supernatant was collected for further use. The concentration of protein in the supernatant was quantified by the bicinchoninic acid (BCA) method. Next, the protein samples were boiled in a sodium dodecyl sulfate (SDS) loading buffer for 5 min. Then, the samples were loaded onto an 8% polyacrylamide gel for electrophoresis. After the proteins were separated, they were transferred onto a polyvinylidene fluoride (PVDF) membrane that would be incubated with 5% nonfat milk at room temperature for 2 h to block nonspecific binding sites. Afterward, the membranes were incubated with the anti-c-Kit antibodies (1 : 200; Santa Cruz Biotechnology, Inc., USA) and tubulin (1 : 5000; Nanjing Vazyme Biotech Co. Ltd., Jiangsu, China) at 4°C overnight on a rotating platform. Next, the PVDF membranes were washed with PBS four times before and after the incubation with a secondary antibody (1 : 5000; one hour at room temperature). A chemiluminescence imaging system (ChemiScope3500; ClinX Science Instruments Co. Ltd., Shanghai, China) was used to scan the immunoblots (Figure S1). The gray value of immunoreactive protein bands was normalized to tubulin expression and was analyzed by a chemical analysis system (Gel Analysis V2.02; Table S1).

2.9. RT-qPCR. The RT-qPCR was applied to measure the expression level of colonic c-Kit protein mRNA. The total RNA was isolated from the lysed proximal colon tissues by using an RNA Isolator Total RNA Extraction Reagent (R401-01; Nanjing Vazyme Biotech Co. Ltd., Jiangsu, China). RNA concentration and integrity were analyzed by measuring ultraviolet absorbance ratios at 260 nm/280 nm. The total RNA was reverse-transcribed to cDNA with the HiScriptQ RT SuperMix (R213; Nanjing Vazyme Biotech Co. Ltd., Jiangsu, China). The AceQ® qPCR SYBR Green Master Mix (Nanjing Vazyme Biotech Co. Ltd., Jiangsu, China) was used for the RT-qPCR of cDNA. The c-Kit primers (forward: CCTCGCCTCCAAGAACTGTATT; reverse: GCCGTGCATTTCCTTTTACC) were designed and synthesized by Vazyme Biotech Co. Ltd. (Nanjing, China). Glyceraldehyde-3-phosphate dehydrogenase (GAPDH) was

treated as an internal control (forward: GAGTCCACTGGCGTCTTCA; reverse: GGGGTGCTAAGCAGTTGGT). The StepOne Plus system (Applied Biosystems, USA) was used for the amplification reaction, and the conditions of thermal cycling were 95°C for 5 min in the start cycle, 95°C for 10 s, and 60°C for 30 s in 40 subsequent cycles. Data were analyzed with the $2^{-\Delta\Delta Ct}$ methods.

2.10. Statistical Analysis. SPSS 20.0 (IBM, USA) was used to do all the statistical analysis. Data were reported as means ± standard deviation (s.d.). The one-way ANOVA was performed to analyze the difference among groups. For the pairwise comparisons, the LSD test will be used when the variance is homoscedastic, and the Dunnett T3 test will be applied when the variation is heteroscedastic. Statistical significance (p-value) was set smaller than 0.05.

3. Results

3.1. Establishment of the Rat Model of SCI. According to the mBBB scale, all rats scored 21 points before any surgical procedure. Twenty-four out of 36 rats received the modeling surgery by the modified drop weight method, and two of them died during the modeling operation. The remaining 22 rats, which scored 0 in the BBB scale twenty-four hours postoperatively, were considered as successfully established SCI models and then were randomly assigned either to the SCI + EA group or to the SCI group. Twelve rats received the sham surgery, and 2 of them were excluded because they had a decreased mBBB score, which indicated partial injury of the spinal cord. The fecal characteristics and defecation condition of different groups were described previously [17, 18].

3.2. Morphology of ICCs Repaired by EA. As observed under the transmission electron microscope, the cell body of colonic ICCs was typically fusiform-shaped with an elongated nucleus in the sham group (Figure 1(a), left panel). The condensed chromatin was scattered throughout the nucleus, surrounded by the extended cytoplasm. The cytoplasm contained abundant mitochondria, ribosomes, endoplasmic reticulum, and Golgi apparatus (Figure 1(a), right panel).

The morphological damage of ICCs in the colon occurred after the SCI. The shape of cell bodies and the nucleus were irregular (Figure 1(b), left panel). Vacuoles, organelle decrease, and structural abnormalities were observed inside the cytoplasm. The mitochondria were swollen, dissolved, or even ruptured and vacuolated. Lipid droplets were observed in the dilated and degranulated endoplasmic reticulum (Figure 1(b), right panel).

However, we found that the morphological lesion of colonic ICCs was repaired after the EA treatment. It seems that the shape of colonic ICCs' cell bodies and nucleus were more similar to those in the sham group (Figure 1(c), left panel). Although there were some vacuoles contained in the cytoplasm, the structure of the organelle was relatively complete. The mitochondria swelled slightly, and the endoplasmic reticulum expanded (Figure 1(c), right panel). Overall, the above findings indicate that EA could rescue the morphology of colonic ICCs after SCI.

3.3. c-Kit Immunoreactive ICC Number Increased by EA. As shown in Figure 2(a), there were apparent differences in the density of c-Kit immunoreactive ICCs among three groups. In contrast with the sham group, the mass of c-Kit-positive ICCs decreased significantly after the SCI. While after the EA treatment, the expression of colonic c-Kit rebounded to the same level in the sham group. The quantitative analysis of c-Kit-positive cell number and the AOD further confirmed the above results (Figures 2(b) and 2(c)). The SCI group showed a fewer number of c-Kit immunoreactive cells (100.38 ± 7.75 vs. 182.92 ± 9.74, $p < 0.01$) and a lower AOD (0.20 ± 0.02 vs. 0.24 ± 0.02, $p < 0.01$) than the sham group. However, the EA treatment reversed the decline caused by the SCI. The number of c-Kit immunoreactive cells (187.702 ± 6.76 vs. 100.38 ± 7.75, $p < 0.01$) and the AOD (0.28 ± 0.02 vs.0.20 ± 0.02) were significantly increased in the SCI + EA group.

3.4. c-Kit mRNA and Protein Expression Level Increased by EA. The results of the colonic c-Kit mRNA and protein expression confirmed what we found in the immunohistochemistry. The expression level of c-Kit protein (Figures 3(a) and 3(b)) and mRNA (Figure 3(c)) in colon tissues varied among groups. The mRNA expression and protein levels of c-Kit in the SCI rats were significantly lower than the sham rats (protein: 0.04 ± 0.02 vs. 0.13 ± 0.05, $p < 0.01$; mRNA: 0.006 ± 0.001 vs. 0.010 ± 0.002, $p < 0.01$). After the EA treatment, the mRNA expression and protein levels of c-Kit in the colon tissues increased significantly compared with the SCI rats (protein: 0.25 ± 0.07 vs. 0.04 ± 0.02, $p < 0.01$; mRNA: 0.014 ± 0.002 vs. 0.006 ± 0.001, $p < 0.01$).

4. Discussion

Our previous study found that EA could improve the bowel function in rats with SCI-induced NBD and revealed the partial underlying mechanism behind the intervention [17, 18]. We found that EA could improve the fecal characteristics and shorten the defecating time of SCI rats. The studies also showed that EA could regulate circadian rhythmicity of intestinal motility and downregulate the expression of neuronal nitric oxide synthase in colon tissues. In this research, we explored the potential mechanism of EA from the aspect of its effect on the ICCs. Results revealed that EA could improve the colon function after SCI by repairing morphology and the number of ICCs and upregulating c-Kit expression.

ICCs are one of the various interstitial cell types contained in gastrointestinal smooth muscles. Under physiological conditions, ICCs were rich in mitochondria; the moderately well developed inner membrane system included the Golgi complex and endoplasmic reticulum. ICCs play an essential role in driving and maintaining the normal functions of gastrointestinal smooth muscles, and the loss or remodeling of ICCs could contribute to intestinal motility

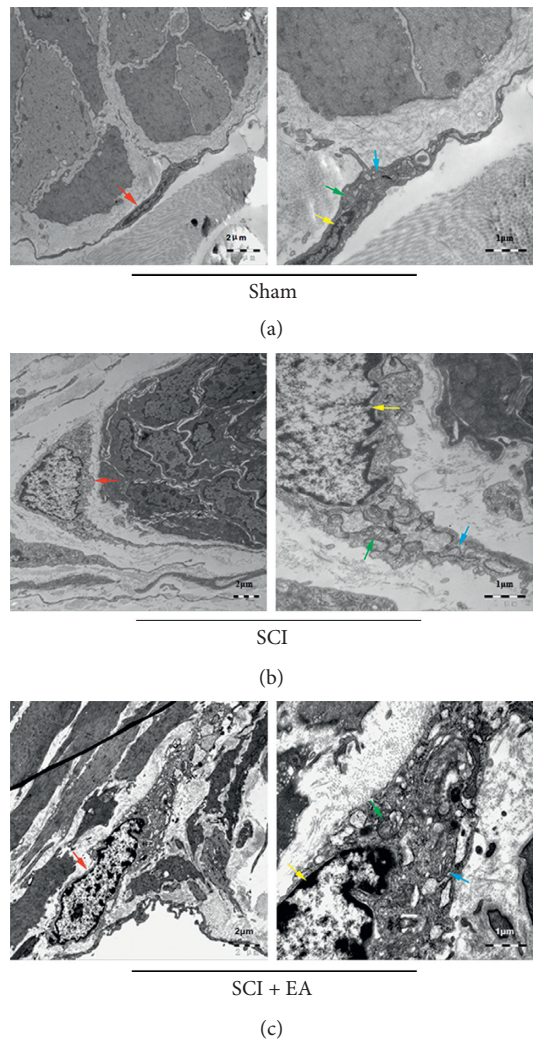

Figure 1: Morphology of ICCs in the colon tissues from rats in different groups. (a) In the sham group ($n = 5$), the typical shape of the cell body and nucleus was observed, and the intracellular organelles were abundant and healthy. (b) In the SCI group ($n = 5$), the structural abnormalities of ICCs and its organelles were observed, and vacuoles and organelle decreasing happened in the cytoplasm. (c) In the SCI + EA group ($n = 5$), the shape of the cell body and intracellular structures were closer to those in the sham group, although the cytoplasm still contained some vacuoles. Red arrow, interstitial cells of Cajal (ICC); yellow arrow, nucleus; green arrow, mitochondria; blue arrow, endoplasmic reticulum. Scale bar, 2 μm in the left panels and 1 μm in the right panels.

dysfunction [35]. As the pacemaker cells, ICCs could generate and conduct slow electrical waves, which are the fundamental of the segmental contraction and peristalsis of the digestive tract [20]. Studies found that slow-wave activity recorded from wild-type and heterozygote mice could not be detected from the W/WV mutated mice that lacked ICCs in the small intestinal muscles [36, 37]. Similar results exist in the Ws/Ws mutated rats. ICCs in the colonic muscles of the Ws/Ws mutated rats were incompletely lost, and the electrical activity shows an irregular pattern and lower frequency than what occurred in the wild-type animals [38]. ICCs offer a pathway for the propagation of slow waves for the smooth muscle cells that could not regenerate the slow waves on their own. Some research found that the slow waves that occurred in the healthy colonic tissue could not propagate to the area in which the ICCs were dysfunctional [39, 40]. As described in our previous studies [17, 18], rats experienced a T11-12 level SCI showed exhibited dry and hard stool, a decrease of fecal weight, and prolonged defecation, which was the result of the colonic transit disorder. The colonic transmission function could be improved by EA treatment later. Our experiments showed that the above changes in colonic function were associated with the ICCs. The ultrastructure injuries in ICCs could be observed in animals with SCI, and later those injuries were repaired after the EA treatment.

Except as an identification marker of ICCs, c-Kit plays an vital role in the ICC function. The importance of c-Kit and its ligand emerged from the mutated animals such as W/WV mice, Ws/Ws rats, and Sl/Sld mice. In those animals, reduction in the ICC population and loss of pacemaker activity were observed [37, 41, 42]. The similar results could be found in the animals treated with c-Kit antibodies [24, 40, 43]. In this study, we also found the downregulation of c-Kit

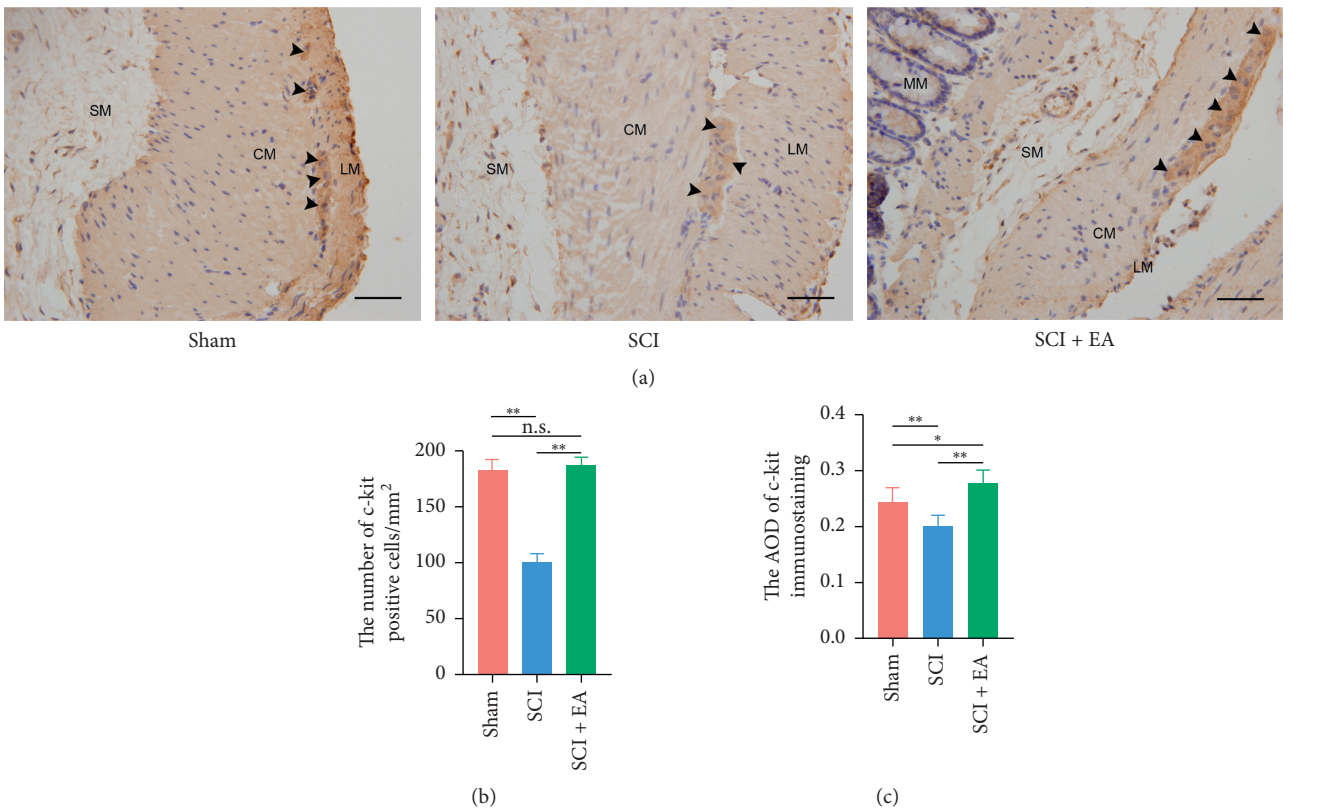

FIGURE 2: Immunochemistry of ICCs in the colon tissues from rats in different groups. (a) Representative images of c-Kit immunoreactive ICCs. The mass of c-Kit-positive ICCs in the SCI group ($n = 5$) was significantly lower than the sham ($n = 5$) and SCI + EA ($n = 5$) groups. Scale bar, 100 μm. (b) The quantitative analysis of c-Kit-positive cell number. (c) The quantitative analysis of the average optical density (AOD). Each bar is shown as mean ± s.d. (n.s., no significance; $^{*}p < 0.05$; $^{**}p < 0.01$).

expression in colon tissues of SCI rats and the rescuing effect of EA.

The intestinal function is double-innervated by the CNS and ENS. Although the ENS could regulate intestinal motility when its connection with the CNS is completely cut off [44], the activity of ENS declined due to loss of modulation from the CNS via sympathetic and parasympathetic nerves [45]. For instance, our previous study showed that the concentration of nitric oxide synthase (nNOS), which could synthesize nitric oxide served as primary neurotransmitters for inhibitory motor neurons, significantly increased in the colon of SCI rats [17]. Substantial evidence suggests enteric motor neurons directly innervate ICCs. The dysfunction of neurotransmitter release could lead to the morphological change and functional disorder of ICCs [45]. ICCs could facilitate communication between enteric motor neurons and smooth muscle cells by transducing the excitatory and inhibitory inputs. Research studies found that the loss of ICCs resulted in the reduction of excitatory and inhibitory potentials in smooth muscles of W/WV mice under circumstances in which the functions of enteric motor neurons and smooth muscle cells themselves are normal [46, 47]. On the other hand, many studies have worked on the mechanism of how EA could regulate gastrointestinal function. Results showed that EA could modulate the excitation and inhibition of the ENS [48], and the high-frequency EA at acupoint ST36 could induce the regeneration of enteric neurons [49]. In our previous study, EA at ST36 could downregulate the nNOS expression in the rats' colon [17]. It was also found that EA is capable of affecting the gastrointestinal motility by regulating the activity of extrinsic autonomic nerves (enhancing vagal activity and suppressing sympathetic activity) [50–52].

Based on these studies so far, there is one probable assumption about the mechanism of SCI-induced NBD and EA treatment. After SCI, the activity of ENS decreased, sending fewer signals to ICCs and then resulting in the ultrastructural damage and dysfunction of ICCs, eventually leading to degradation of the motility of colonic smooth muscles. EA activates the peripheral nerves, transmitting signals to parasympathetic nerves in the sacral segments, facilitating the activity of ENS. The ENS activity contributes to the functional recovery of ICCs innervated by enteric

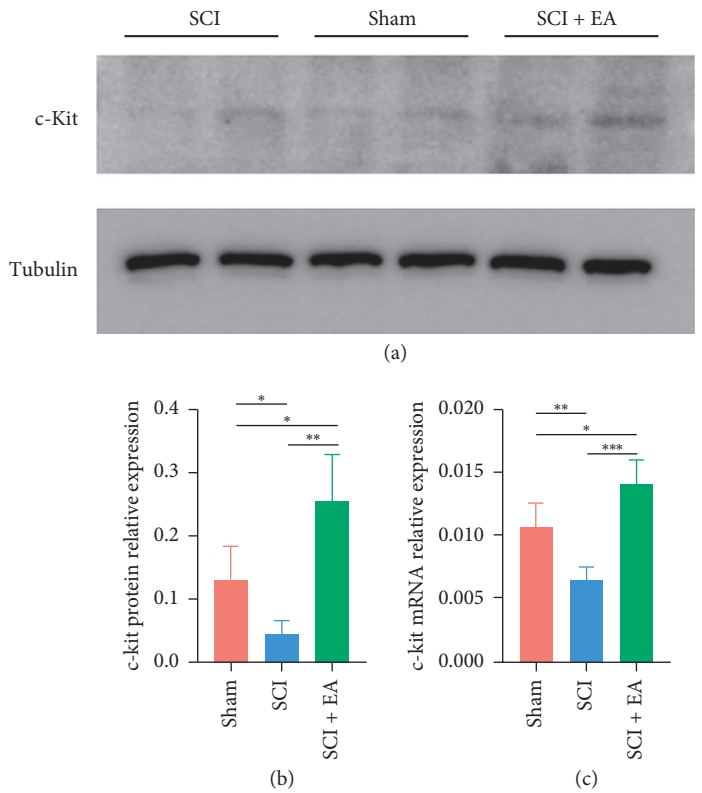

FIGURE 3: The c-Kit mRNA and protein expression in the colon tissues from rats in different groups. (a) Western blotting assays of the c-Kit protein expression from different groups ($n = 4$, each group). (b) The relative expression of the c-Kit protein (normalized with the Tubulin) ($n = 4$, each group). (c) The relative expression of c-Kit mRNA (normalized with the tubulin) ($n = 4$, each group). Each bar is shown as mean ± s.d. ($^{*}p < 0.05$; $^{**}p < 0.01$).

motor neurons, finally causing the retrieval of colonic transit function. More experiments are needed to confirm the proposed mechanism.

5. Conclusion

Abnormal ICCs and the downregulated expression of c-Kit could be observed after SCI, which could be one of the causes of NBD. EA at Zusanli (ST36) could improve the colon function after SCI, and its effect on repairing the morphology and number of ICCs and upregulating c-Kit expression could be one of the potential mechanisms. Further research is necessary to reveal the deep mechanism behind the dysfunction and intervention.

Data Availability

All the data used to support the findings of this study are available from the corresponding author upon request.

Conflicts of Interest

The authors declare that they have no conflicts of interest.

Authors' Contributions

Yujie Yang and Jie Cheng contributed equally to this work.

Acknowledgments

This study was supported by the National Natural Science Foundation of China (Nos. 81860875, 81202735, 81403477, and 20168291) and the Research Innovation Program for College Graduates of Jiangsu Province (Nos. CXZZ13-0617 and SJZZ15-0121).

Supplementary Materials

Original data for the Western blot (Figure S1, Table S1) and the modified Basso–Beattie–Bresnahan locomotor scale (Table S2). (*Supplementary Materials*)

References

[1] A. Krassioukov, J. J. Eng, G. Claxton, B. M. Sakakibara, S. Shum, and The SCIRE Research Team, "Neurogenic bowel management after spinal cord injury: a systematic review of the evidence," *Spinal Cord*, vol. 48, no. 10, pp. 718–733, 2010.

[2] N. Cotterill, H. Madersbacher, J. J. Wyndaele et al., "Neurogenic bowel dysfunction: clinical management recommendations of the neurologic incontinence committee of the Fifth international consultation on incontinence 2013," *Neurourology and Urodynamics*, vol. 37, no. 1, pp. 46–53, 2018.

[3] J. J. Adriaansen, F. W. van Asbeck, D. van Kuppevelt, G. J. Snoek, and M. W. Post, "Outcomes of neurogenic bowel management in individuals living with a spinal cord injury for

at least 10 years," *Archives of Physical Medicine and Rehabilitation*, vol. 96, no. 5, pp. 905–912, 2015.

[4] J. A. Piatt, S. Nagata, M. Zahl, J. Li, and J. P. Rosenbluth, "Problematic secondary health conditions among adults with spinal cord injury and its impact on social participation and daily life," *The Journal of Spinal Cord Medicine*, vol. 39, no. 6, pp. 693–698, 2016.

[5] J. M. Pires, A. M. Ferreira, F. Rocha et al., "Assessment of neurogenic bowel dysfunction impact after spinal cord injury using the International Classification of Functioning, Disability and Health," *European Journal of Physical and Rehabilitation Medicine*, vol. 54, no. 6, pp. 873–879, 2018.

[6] Y. Deng, Y. Dong, Y. Liu et al., "A systematic review of clinical studies on electrical stimulation therapy for patients with neurogenic bowel dysfunction after spinal cord injury," *Medicine (Baltimore)*, vol. 97, no. 41, Article ID e12778, 2018.

[7] J. D. Z. Chen, M. Ni, and J. Yin, "Electroacupuncture treatments for gut motility disorders," *Neurogastroenterology & Motility*, vol. 30, no. 7, Article ID e13393, 2018.

[8] S.-L. Zhou, X.-L. Zhang, and J.-H. Wang, "Comparison of electroacupuncture and medical treatment for functional constipation: a systematic review and meta-analysis," *Acupuncture in Medicine*, vol. 35, no. 5, pp. 324–331, 2017.

[9] Y. Liu, B. H. May, A. L. Zhang et al., "Acupuncture and related therapies for treatment of postoperative ileus in colorectal cancer: a systematic review and meta-analysis of randomized controlled trials," *Evidence-Based Complementary and Alternative Medicine*, vol. 2018, Article ID 3178472, 18 pages, 2018.

[10] J. Fang, J. Fang, X. Shao et al., "Electroacupuncture treatment partly promotes the recovery time of postoperative ileus by activating the vagus nerve but not regulating local inflammation," *Scientific Reports*, vol. 7, Article ID 39801, 2017.

[11] C. Liang, K. Wang, B. Xu, and Z. Yu, "Electroacupuncture at acupoint ST 37 (Shangjuxu) improves function of the enteric nervous system in a novel mouse constipation model," *BMC Complementary and Alternative Medicine*, vol. 16, no. 1, p. 392, 2016.

[12] H. Jin, J. Guo, J. Liu et al., "Anti-inflammatory effects and mechanisms of vagal nerve stimulation combined with electroacupuncture in a rodent model of TNBS-induced colitis," *American Journal of Physiology-Gastrointestinal and Liver Physiology*, vol. 313, no. 3, pp. G192–G202, 2017.

[13] L. P. Xia, F. Fan, A. L. Tang, and W. Q. Ye, "Effects of electroacupuncture combined with bladder training on the bladder function of patients with neurogenic bladder after spinal cord injury," *International Journal of Clinical and Experimental Medicine*, vol. 7, no. 5, pp. 1344–1348, 2014.

[14] Z. Liu, W. Wang, J. Wu, K. Zhou, and B. Liu, "Electroacupuncture improves bladder and bowel function in patients with traumatic spinal cord injury: results from a prospective observational study," *Evidence-Based Complementary and Alternative Medicine*, vol. 2013, Article ID 543174, 9 pages, 2013.

[15] C.-z. Hao, F. Wu, Y. Guo et al., "Acupuncture for neurogenic bladder after spinal cord injury: a systematic review and meta-analysis," *European Journal of Integrative Medicine*, vol. 5, no. 2, pp. 100–108, 2013.

[16] A. M. K. Wong, C.-P. Leong, T.-Y. Su, S.-W. Yu, W.-C. Tsai, and C. P. C. Chen, "Clinical trial of acupuncture for patients with spinal cord injuries," *American Journal of Physical Medicine & Rehabilitation*, vol. 82, no. 1, pp. 21–27, 2003.

[17] J. Guo, Y. Zhu, Y. Yang et al., "Electroacupuncture at Zusanli (ST36) ameliorates colonic neuronal nitric oxide synthase upregulation in rats with neurogenic bowel dysfunction following spinal cord injury," *Spinal Cord*, vol. 54, no. 12, pp. 1139–1144, 2016.

[18] J. Cheng, X. Wang, J. Guo et al., "Effects of electroacupuncture on the daily rhythmicity of intestinal movement and circadian rhythmicity of colonic Per2 expression in rats with spinal cord injury," *BioMed Research International*, vol. 2016, Article ID 9860281, 9 pages, 2016.

[19] A. C. Lynch, A. Antony, B. R. Dobbs, and F. A. Frizelle, "Bowel dysfunction following spinal cord injury," *Spinal Cord*, vol. 39, no. 4, pp. 193–203, 2001.

[20] S. M. Ward and K. M. Sanders, "Physiology and pathophysiology of the interstitial cell of Cajal: from bench to bedside. I. Functional development and plasticity of interstitial cells of Cajal networks," *American Journal of Physiology*, vol. 281, no. 1, pp. G602–G611, 2001.

[21] G. L. Lyford, C. L. He, E. Soffer et al., "Pan-colonic decrease in interstitial cells of Cajal in patients with slow transit constipation," *Gut*, vol. 51, no. 4, pp. 496–501, 2002.

[22] C. L. He, L. Burgart, L. Wang et al., "Decreased interstitial cell of cajal volume in patients with slow-transit constipation," *Gastroenterology*, vol. 118, no. 1, pp. 14–21, 2000.

[23] M. den Braber-Ymker, M. Lammens, M. J. A. M. van Putten, and I. D. Nagtegaal, "The enteric nervous system and the musculature of the colon are altered in patients with spina bifida and spinal cord injury," *Virchows Archiv*, vol. 470, no. 2, pp. 175–184, 2017.

[24] H. Maeda, A. Yamagata, S. Nishikawa et al., "Requirement of c-kit for development of intestinal pacemaker system," *Development (Cambridge, England)*, vol. 116, no. 2, pp. 369–375, 1992.

[25] A. Rich, S. M. Miller, S. J. Gibbons, J. Malysz, J. H. Szurszewski, and G. Farrugia, "Local presentation of Steel factor increases expression of c-kit immunoreactive interstitial cells of Cajal in culture," *American Journal of Physiology-Gastrointestinal and Liver Physiology*, vol. 284, no. 2, pp. G313–G320, 2003.

[26] W. Tong, H. Jia, L. Zhang, C. Li, T. J. Ridolfi, and B. Liu, "Exogenous stem cell factor improves interstitial cells of Cajal restoration after blockade of c-kit signaling pathway," *Scandinavian Journal of Gastroenterology*, vol. 45, no. 7-8, pp. 844–851, 2010.

[27] A. E. Feldstein, S. M. Miller, M. El-Youssef et al., "Chronic intestinal pseudoobstruction associated with altered interstitial cells of cajal networks," *Journal of Pediatric Gastroenterology and Nutrition*, vol. 36, no. 4, pp. 492–497, 2003.

[28] J. Forster, I. Damjanov, Z. Lin, I. Sarosiek, P. Wetzel, and R. McCallum, "Absence of the interstitial cells of Cajal in patients with gastroparesis and correlation with clinical findings," *Journal of Gastrointestinal Surgery*, vol. 9, no. 1, pp. 102–108, 2005.

[29] I. Y. Chang, N. J. Glasgow, I. Takayama, K. Horiguchi, K. M. Sanders, and S. M. Ward, "Loss of interstitial cells of Cajal and development of electrical dysfunction in murine small bowel obstruction," *The Journal of Physiology*, vol. 536, no. 2, pp. 555–568, 2001.

[30] D. Luo, S. Liu, X. Xie, and X. Hou, "Electroacupuncture at acupoint ST-36 promotes contractility of distal colon via a cholinergic pathway in conscious rats," *Digestive Diseases and Sciences*, vol. 53, no. 3, pp. 689–693, 2008.

[31] M. Iwa, M. Matsushima, Y. Nakade, T. N. Pappas, M. Fujimiya, and T. Takahashi, "Electroacupuncture at ST-36 accelerates colonic motility and transit in freely moving conscious rats," *American Journal of Physiology-*

Gastrointestinal and Liver Physiology, vol. 290, no. 2, pp. G285–G292, 2006.

[32] M. Peng, K. Li, X. Zhu et al., "Influence of electroacupuncture in Zusanli (ST36) on number and network of interstitial cells Cajal of small intestine in rats with partial intestinal obstruction," *Journal of Beijing University of Traditional Chinese Medicine*, vol. 8, 2012.

[33] D. M. Basso, M. S. Beattie, and J. C. Bresnahan, "Graded histological and locomotor outcomes after spinal cord contusion using the NYU weight-drop device versus transection," *Experimental Neurology*, vol. 139, no. 2, pp. 244–256, 1996.

[34] Z. R. Li, *Experimental Acupuncture Science*, China Press of Traditional Chinese Medicine, vol. 327, p. 146, Beijing, China, 2003.

[35] K. M. Sanders, S. M. Ward, and S. D. Koh, "Interstitial cells: regulators of smooth muscle function," *Physiological Reviews*, vol. 94, no. 3, pp. 859–907, 2014.

[36] S. M. Ward, A. J. Burns, S. Torihashi, and K. M. Sanders, "Mutation of the proto-oncogene c-kit blocks development of interstitial cells and electrical rhythmicity in murine intestine," *The Journal of Physiology*, vol. 480, no. 1, pp. 91–97, 1994.

[37] J. D. Huizinga, L. Thuneberg, M. Klüppel, J. Malysz, H. B. Mikkelsen, and A. Bernstein, "W/kit gene required for interstitial cells of Cajal and for intestinal pacemaker activity," *Nature*, vol. 373, no. 6512, pp. 347–349, 1995.

[38] E. Albertí, H. B. Mikkelsen, X. Y. Wang et al., "Pacemaker activity and inhibitory neurotransmission in the colon of Ws/Ws mutant rats," *American Journal of Physiology-Gastrointestinal and Liver Physiology*, vol. 292, no. 6, pp. G1499–G1510, 2007.

[39] K. M. Sanders, R. Stevens, E. Burke, and S. W. Ward, "Slow waves actively propagate at submucosal surface of circular layer in canine colon," *American Journal of Physiology-Gastrointestinal and Liver Physiology*, vol. 259, no. 2, pp. G258–G263, 1990.

[40] T. Ördög, S. M. Ward, and K. M. Sanders, "Interstitial cells of Cajal generate electrical slow waves in the murine stomach," *The Journal of Physiology*, vol. 518, no. 1, pp. 257–269, 1999.

[41] R. Mitsui and T. Komuro, "Distribution and ultrastructure of interstitial cells of Cajal in the gastric antrum of wild-type and Ws/Ws rats," *Anatomy and Embryology*, vol. 206, no. 6, pp. 453–460, 2003.

[42] H. B. Mikkelsen, J. Malysz, J. D. Huizinga, and L. Thuneberg, "Action potential generation, Kit receptor immunohistochemistry and morphology of steel dickie (Sl/Sl d) mutant mouse small intestine," *Neurogastroenterology & Motility*, vol. 10, no. 1, pp. 11–26, 1998.

[43] S. Torihashi, S. M. Ward, S.-I. Nishikawa, K. Nishi, S. Kobayashi, and K. M. Sanders, "c-kit-dependent development of interstitial cells and electrical activity in the murine gastrointestinal tract," *Cell and Tissue Research*, vol. 280, no. 1, pp. 97–111, 1995.

[44] M. Camilleri and M. J. Ford, "Review article: colonic sensorimotor physiology in health, and its alteration in constipation and diarrhoeal disorders," *Alimentary Pharmacology & Therapeutics*, vol. 12, no. 4, pp. 287–302, 1998.

[45] M. Radulovic, P. Anand, M. A. Korsten, and B. Gong, "Targeting ion channels: an important therapeutic implication in gastrointestinal dysmotility in patients with spinal cord injury," *Journal of Neurogastroenterology and Motility*, vol. 21, no. 4, p. 494, 2015.

[46] H. Suzuki, S. M. Ward, Y. R. Bayguinov, F. R. Edwards, and G. D. S. Hirst, "Involvement of intramuscular interstitial cells in nitrergic inhibition in the mouse gastric antrum," *The Journal of Physiology*, vol. 546, no. 3, pp. 751–763, 2003.

[47] S. M. Ward, E. A. H. Beckett, X. Wang, F. Baker, M. Khoyi, and K. M. Sanders, "Interstitial cells of Cajal mediate cholinergic neurotransmission from enteric motor neurons," *The Journal of Neuroscience*, vol. 20, no. 4, pp. 1393–1403, 2000.

[48] C. Liang, K. Y. Wang, M. R. Gong, Q. Li, Z. Yu, and B. Xu, "Electro-acupuncture at ST 37 and ST 25 induce different effects on colonic motility via the enteric nervous system by affecting excitatory and inhibitory neurons," *Neurogastroenterology & Motility*, vol. 30, no. 7, Article ID e13318, 2018.

[49] F. Du and S. Liu, "Electroacupuncture with high frequency at acupoint ST-36 induces regeneration of lost enteric neurons in diabetic rats via GDNF and PI3K/AKT signal pathway," *American Journal of Physiology-Regulatory, Integrative and Comparative Physiology*, vol. 309, no. 2, pp. R109–R118, 2015.

[50] K. Imai, H. Ariga, C. Chen, C. Mantyh, T. N. Pappas, and T. Takahashi, "Effects of electroacupuncture on gastric motility and heart rate variability in conscious rats," *Autonomic Neuroscience*, vol. 138, no. 1-2, pp. 91–98, 2008.

[51] S. Liu, S. Peng, X. Hou, M. Ke, and J. D. Z. Chen, "Transcutaneous electroacupuncture improves dyspeptic symptoms and increases high frequency heart rate variability in patients with functional dyspepsia," *Neurogastroenterology & Motility*, vol. 20, no. 11, pp. 1204–1211, 2008.

[52] N. Zhang, Z. Huang, F. Xu et al., "Transcutaneous neuromodulation at posterior tibial nerve and ST36 for chronic constipation," *Evidence-Based Complementary and Alternative Medicine*, vol. 2014, Article ID 560802, 7 pages, 2014.

Hindawi
Evidence-Based Complementary and Alternative Medicine
Volume 2020, Article ID 8839491, 9 pages
https://doi.org/10.1155/2020/8839491

Research Article

The Impact of Electroacupuncture at Hegu, Shousanli, and Quchi Based on the Theory "Treating Flaccid Paralysis by Yangming Alone" on Stroke Patients' EEG: A Pilot Study

Fei Zou,[1] Yi-Fang Lin,[1,2] Shu-Geng Chen,[1] Lei Cao,[3] Hao-ran Wang,[4] Bin Ye,[5] Qiang Wang,[2] He Jie-Ying,[1] and Jie Jia[1]

[1]*Department of Rehabilitation Medicine, Huashan Hospital, Fudan University, Shanghai, China*
[2]*Department of Rehabilitation Medicine, Shanghai Jing'an District Central Hospital, Shanghai, China*
[3]*Department of Electronic Engineering, Shanghai Maritime University, Shanghai, China*
[4]*Department of Computer Science and Technology, College of Electronic and Information Engineering, Tongji University, Shanghai, China*
[5]*Department of Rehabilitation Medicine, The Shanghai Third Rehabilitation Hospital, Shanghai, China*

Correspondence should be addressed to Jie Jia; shannonjj@126.com

Received 24 September 2020; Revised 28 October 2020; Accepted 30 October 2020; Published 24 November 2020

Academic Editor: Feng Zhang

Background. In China, electroacupuncture based on meridians theory "treating flaccid paralysis by *Yangming* alone" has been widely used for stroke rehabilitation in clinical practice. The aim of this study was to explore the electroencephalography change of electroacupuncture intervention on strokes patients with flaccid paralysis. *Methods*. Twenty-three stroke patients with flaccid paralysis and six stroke patients with spasticity accepted electroacupuncture with the acupoints Hegu [LI4], Shousanli [LI10], and Quchi [LI11] for 20 minutes and their EEG data were recorded before, during, and after the electroacupuncture intervention. *Results*. Compared with the baseline EEG signals before electroacupuncture, the ipsilesional and contralesional beta-band average power of patients with flaccid paralysis and spasticity were significantly increased during the needles retention stage and decreased slightly after removing the needles. The significant decrease of the ipsilesional and contralesional delta band average power in patients with flaccid paralysis occurred during the electroacupuncture stimulation, and they increased after the removal of the needles. The ipsilesional delta band average power of patients with spasticity significantly decreased during the electroacupuncture stimulation. *Conclusion*. From this pilot electrophysiological study, we provided a possible electrophysiological mechanism of the curative effect of electroacupuncture for stroke rehabilitation.

1. Introduction

Motor impairment of the upper extremity caused by a cerebral vascular accident is quite difficult to recover from [1]. To improve performance in the functional movement of the upper extremity, we have done a lot of work on scientific research and clinical applications such as mirror therapy, motor imagery, brain-computer interface, and other rehabilitation techniques [2–5]. Electroacupuncture (EA) treatment, an effective alternative approach for improving motor impairment of the upper extremity in stroke patients, is becoming an interesting research point, especially for the management of poststroke flaccid paralysis in clinical practice [6–8]. EA based on the meridians theory of Traditional Chinese Medicine (TCM) "treating flaccid paralysis by *Yangming* alone" was one of the most common rehabilitative approaches for apoplexy and it is still applied in clinical treatment nowadays [9]. This classical theory means the acupoints of Large Inte Stine could be used for treating flaccidity syndrome. From the TCM perspective, there is no distinction between flaccid paralysis and spasticity in stroke patients. It thinks that flaccid paralysis and spasticity are the

two kinds of different performances of "liver qi" catharsis too much, and the acupoints of the Large Inte Stine and Stomach could be used for rebalancing the "liver qi" [10]. Some literature has demonstrated that the acupoints of Large Inte Stine could enhance handgrip strength and pinch strength, thus improving motor impairment, in stroke patients [11, 12]. Previous studies have shown that Hegu [LI4], Shousanli [LI10], and Quchi [LI11] of Large Inte Stine are frequently used acupoints for the upper extremity motor impairment in stroke patients [8, 13].

With the deepening understanding of stroke rehabilitation and the traditional Chinese medicine theory, the mechanism of EA on stroke patients needs to be discovered. How EA combined with modern rehabilitation can play a better role in clinical practice is a question worthy of thinking about. In this study, we intend to explore the change of brain activity in stroke patients during EA treatment.

Electroencephalography (EEG), with an advantage of high time resolution, can detect real-time cortical electrical activity in the cortex [14]. EEG is widely used in the research of brain-computer interface training, the analysis of functional connectivity and brain network in different crowds, the investigation of brain spectral power as a biomarker on disease or injury, and so on [15, 16]. The different frequency of brain wave oscillations had been regarded as biomarkers of injury or recovery after stroke [17, 18]. Beta-band (13–30 Hz) oscillations are reported to traditionally link to motor functions [19]. Additionally, it also played an essential role in the interactions between the motor cortex and the other cortex, such as auditory and sensorimotor brain areas [20]. Recently, some research pointed out that low-frequency oscillations in the delta band (1–3 Hz) related to the motor recovery of stroke. Cassidy et al. reported that delta band power is associated with greater injury and better motor status in the chronic phase [21]. Bönstrup et al. provided evidence for a link between low-frequency oscillations and functional recovery after stroke [22]. Linear models implied a strong relationship between beta-band activity in frontal, central, and parietal regions with upper extremity motor recovery and suggested that delta band power in the primary motor cortex related to better motor status in the chronic stage [21, 23].

To explore the changes of brain wave oscillation of stroke patients with EA treatment based on the theory "treating flaccid paralysis by *Yangming* alone", in this study, we propose inserting needles at the Hegu [LI4], Shousanli [LI10], and Quchi [LI11] in the hemiplegic upper extremity of stroke patients with flaccid paralysis and observing brain wave power change with spectrum analysis. Besides, we also recruited 6 stroke patients with spasticity as a control group. We assumed that EA treatment would influence EEG activity, especially the beta rhythm and delta rhythm, which might provide the electrophysiological mechanism of the curative effect of EA for stroke rehabilitation.

2. Methods

2.1. Study Design and Participants. We recruited inpatients with stroke admitted to the Department of Rehabilitation Medicine, Huashan Hospital, and Shanghai Third Rehabilitation Hospital from April 2020 to August 2020. All patients received the rehabilitation assessments, including the Fugl-Meyer assessment Upper Limb subscale (FMA-UL), Barthel index (BI), and National Institute of Health stroke scale (NIHSS). The inclusion criteria were (1) age between 18 and 80 years; (2) diagnosed with ischemic or hemorrhagic (unilateral subcortical) stroke by computed tomography or magnetic resonance imaging; and (3) the first onset of stroke. The exclusion criteria were (1) severe osteoarthrosis comorbidities; (2) allergy to EEG electrode cream; (3) severe cognitive impairment and mental illness; and (4) pregnancy. A total of 29 patients met these criteria and were enrolled in this study. All patients were informed about the electroacupuncture stimulation as follows: "three acupuncture pins will be inserted into the muscle at three different acupoints of the affected upper extremity" and signed the informed consent forms prior to the participation according to the Declaration of Helsinki. Figure 1 displayed the flow chart of the study subjects. Demographic and clinical characteristics of participants were shown in Table 1. This study was approved by the Medical Ethics Committee of Jing'an District Central Hospital of Shanghai (Ethics reference number: 2020–29), and the trial was registered on the Chinese clinical trial registry (ChiCTR2000036959).

2.2. Electroacupuncture Stimulation. An acupuncturist with more than 5 years of clinical experience inserted the sterile disposable acupuncture needles (Jiajian, 0.30×40 mm; Wuxi Jiajian Medical Instruments, Wuxi, China) in three acupoints of Large Inte Stine on the hemiplegia side (Hegu [LI4], Shousanli [LI10], and Quchi [LI11]), as shown in Figure 2. These acupoints will be needled perpendicularly, with a depth of 10–15 mm approximately. Following insertion, electrical stimulation was applied to the needles with the intermittent wave, the frequency of 2 Hz, and the current intensity adjusted according to the patients' tolerance [24, 25]. After the 20-minute retention of electroacupuncture, the needles were removed.

2.3. EEG Recording. All patients' brain activities were measured by EEG in a sitting position with eyes opened before, during, and after EA treatment. A 32-channel EEG based on the international 10–20 system was placed on the patients' scalp and recorded in a quiet room using BrainCap (Brain Products, Gilching, Germany) with a sampling rate of 1000 Hz. The ground electrode and reference electrode were placed in front and behind the Fz electrode, respectively. The electrode impedances were set to <5 kΩ. The brain wave data were continuously recorded for 30 minutes, including the 5-minute baseline EEG recording before EA treatment, the 20-minute EEG recording during the EA period, and the 5-minute EEG recording after removal of needles.

2.4. EEG Processing. The spectrum analysis was used for revealing brain waves activities of 32 channels (FP1, FP2, F3, F4, C3, C4, P3, P4, O1, O2, F7, F8, T7, T8, P7, P8, Fz, Cz, Pz, IO, FC1, FC2, CP1, CP2, FC5, FC6, CP5, CP6, FT9, FT10, TP9, and TP10). Firstly, raw data were band-pass filtered

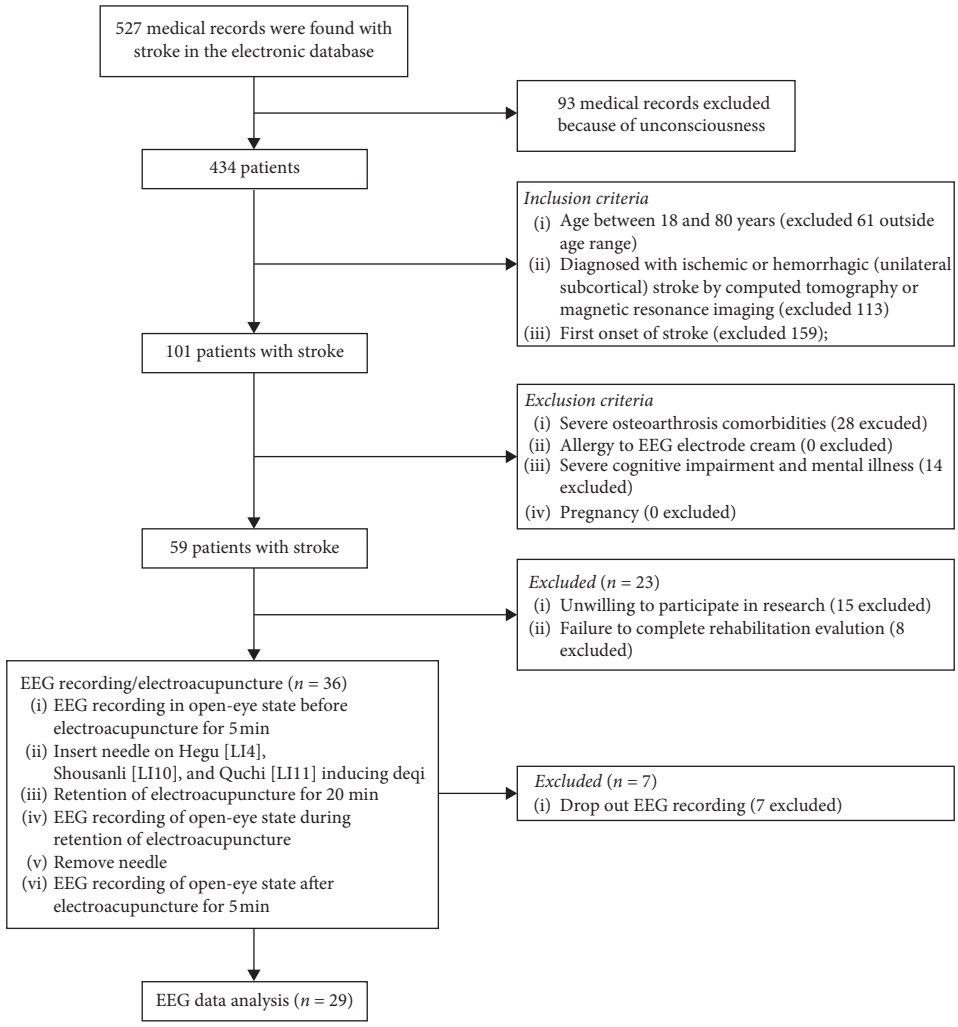

Figure 1: Flow chart of the study participant.

Table 1: Demographic and clinical characteristics of participants.

Characteristics	Flaccid paralysis group ($n = 23$)	Spasticity group ($n = 6$)
Age, years, mean (SD)	60.22 (8.974)	62.62 (12.86)
Days after stroke onset [M (QL, QU)]	22 (15, 60)	77.5 (31, 378.5)
NIHSS	7.13 (4.104)	10.50 (9.63)
Gender, *N*		
Male	13	3
Female	10	3
Side of paralysis		
Left	11	4
Right	12	2
Type of stroke		
Ischemic	18	2
Hemorrhagic	5	4
Handedness		
Left	2	0
Right	21	6

from 0 to 35 Hz. Then, ECG artifacts were removed by using EEGLAB software. After preprocessing, EEGs are divided into the following bands: δ (0.5–4 HZ), θ (4–8 HZ), α (8–13 HZ), and β (13–30 HZ). These features were commonly used for evaluating changes in mental activities [25]. Particularly, the signals were divided into 4 pieces averagely

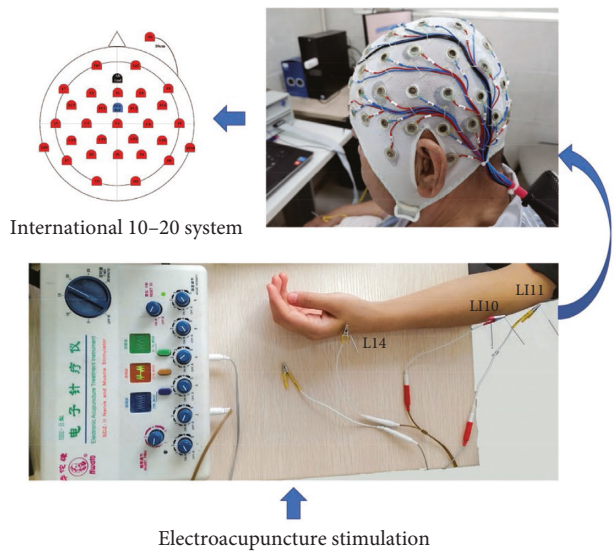

Figure 2: The selected acupoints of the experiment.

for detailed analysis during the electroacupuncture stimulation period. Data for patients with infarct in the damage (right/left) hemisphere was flipped along the midsagittal plane so that the contralesional (left/right) hemisphere corresponded to the ipsilesional hemisphere for all patients. Data for patients with the contralesional hemisphere were also flipped along the midsagittal plane for all patients. We adopted several channels that are associated with motor function for further analysis. They are FC1, FC5, C3, CP1, and CP5 in the left hemisphere and FC2, FC6, C4, CP2, and CP6 in the right hemisphere.

2.5. Statistics. The statistical analyses were conducted using SPSS version 25.0 (IBM Inc., Chicago, IL, USA).

The average power of 5 minutes before the EA treatment was regarded as the baseline, "a". During the EA state, the average power was divided into four phases to calculate, of which "b" is the average power between 5 and 10 minutes, "c" between 10 and 15 minutes, "d" between 15 and 20 minutes, and "e" between 20 and 25 minutes. The average power of 5 minutes after removing needles was named "f" (see Figure 3). One-sample Kolmogorov-Smirnov-tests were firstly used to verify whether the variables followed a normal. After this test indicated non-formal distribution. All data are presented with average (mean) ± standard deviation (SD) (see Tables 2 and 3 for details) and was calculated through Generalized estimating equations (GEEs) to study the statistical differences. GEEs, as a statistical analysis approach used for abnormal distributed repeated measures data, was first proposed by Zeger and Liang in 1986 [27]. In this study, the parameter of GEEs is an unstructured correlation structure with robust variance estimation for CIs and p values.

3. Results

The statistical analysis suggested that the performances of channels FC1, FC5, CP1, and CP5 were similar to channel C3. Channels FC2, FC6, CP2, and CP6 were similar to channel C4. In this study, channels C3 and C4 are representative of motor areas.

Figure 4 shows the average power of β during the electroacupuncture process of flaccid paralysis subjects. Compared with baseline, the average power of β in ipsilesional C3 rose at 5–10 minutes ($p = 0.021$), 10–15 minutes ($p = 0.07$), 15–20 minutes ($p = 0.001$), and 20–25 minutes ($p = 0.04$), as well as at the ipsilesional C4. Upon removing the needles, the power decreased, and no significant differences are noted. As for the contralesional C3, the average power of β rose at 5–10 minutes ($p = 0.001$), 10–15 minutes ($p = 0.05$), 15–20 minutes ($p < 0.001$), and 20–25 minutes ($p = 0.02$), as well as contralesional C4. Upon removing the needles, no significant difference is noted.

Figure 5 shows the average power of β during the electroacupuncture process in spasticity subjects. Compared with baseline, the average power of β in ipsilesional C3 rose at 10–15 minutes ($p = 0.032$), 15–20 minutes ($p = 0.005$), and 20–25 minutes ($p = 0.016$), as well as ipsilesional C4. After removing the needles, the average power decreased and the significant differences are noted compared with those at 10–15 minutes ($p = 0.045$), 15–20 minutes ($p = 0.011$), and 20–25 minutes ($p = 0.027$). As for the contralesional C3, the average power of β rose at 10–15 minutes ($p = 0.009$), 1520 minutes ($p = 0.002$), and 20–25 minutes ($p = 0.008$) was compared with baseline, as well as contralesional C4. After removing the needles, the average power abated and significant differences are noted at 10–15 minutes ($p = 0.011$), 15–20 minutes ($p = 0.002$), and 20–25 minutes ($p = 0.010$).

Figure 6 shows the average power of δ during the electroacupuncture process of flaccid paralysis subjects. Compared with baseline, the average power of δ ipsilesional C3 fell at 5–10 minutes ($p = 0.026$), 10–15 minutes ($p = 0.010$), 15–20 minutes ($p = 0.018$), and 20–25 minutes ($p = 0.017$), as well as at ipsilesional C4. After removing the needles, the average power rose, and the significant differences are noted at 5–10 minutes ($p = 0.017$), 10–15 minutes

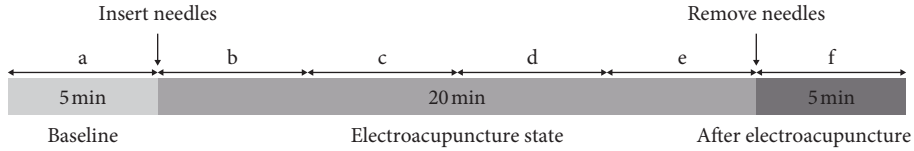

Figure 3: Experimental process of electroacupuncture. (a) The baseline with rest state before electroacupuncture; (b)-(e) During the electroacupuncture with the open-eye state. (f) The rest state after electroacupuncture. (a) Power average of 1–5 minutes. (b)-(e) Power average of every five minutes. (f) Power average of 5 minutes after removing needles.

Table 2: The brain wave power of EEG in the flaccid paralysis group.

	Flaccid paralysis group					
	a	b	c	d	e	f
C3 ipsilesional						
β	0.29 (0.31)	0.50 (0.32)*	0.53 (0.30)*	0.58 (0.34)*	0.54 (0.30)*	0.37 (0.47)
δ	2.02 (2.93)	0.76 (0.70)$^{*\#}$	0.45 (0.34)$^{*\#}$	0.56 (0.45)$^{*\#}$	0.59 (0.54)$^{*\#}$	2.03 (2.72)
C4 ipsilesional						
β	0.29 (0.31)	0.50 (0.32)*	0.53 (0.30)*	0.58 (0.34)*	0.54 (0.30)*	0.37 (0.47)
δ	2.02 (2.93)	0.76 (0.70)$^{*\#}$	0.45 (0.34)$^{*\#}$	0.56 (0.45)$^{*\#}$	0.59 (0.54)$^{*\#}$	2.03 (2.72)
C3 contralesional						
β	0.24 (0.29)	0.62 (0.43)*	0.52 (0.37)*	0.61 (0.41)*	0.63 (0.52)*	0.35 (0.49)
δ	2.06 (2.92)	0.53 (0.46)$^{*\#}$	0.34 (0.23)$^{*\#}$	0.43 (0.38)$^{*\#}$	0.38 (0.35)$^{*\#}$	2.26 (2.90)
C4 contralesional						
β	0.24 (0.29)	0.62 (0.43)*	0.52 (0.37)*	0.61 (0.41)*	0.63 (0.52)*	0.35 (0.49)
δ	2.06 (2.92)	0.53 (0.46)$^{*\#}$	0.34 (0.23)$^{*\#}$	0.43 (0.38)$^{*\#}$	0.38 (0.35)$^{*\#}$	2.26 (2.90)

Mean (SD), *significant difference from a, $^{\#}$significant difference from f ($p < 0.05$).

Table 3: The brain wave power of EEG in the spasticity group.

	Spasticity group					
	a	b	c	d	e	f
C3 ipsilesional						
β	0.18 (0.28)	1.20 (1.53)	0.64 (0.44)$^{*\#}$	0.55 (0.27)$^{*\#}$	0.58 (0.36)$^{*\#}$	0.19 (0.30)
δ	2.88 (2.32)	1.35 (2.17)	0.47 (0.32)$^{*\#}$	0.63 (0.63)*	0.47 (0.41)$^{*\#}$	3.04 (2.91)
C4 ipsilesional						
β	0.18 (0.28)	1.20 (1.53)	0.64 (0.44)$^{*\#}$	0.55 (0.27)$^{*\#}$	0.58 (0.36)$^{*\#}$	0.19 (0.30)
δ	2.88 (2.32)	1.35 (2.17)	0.47 (0.32)$^{*\#}$	0.63 (0.63)*	0.47 (0.41)$^{*\#}$	3.04 (2.91)
C3 contralesional						
β	0.12 (0.18)	1.25 (1.94)	0.51 (0.29)$^{*\#}$	0.44 (0.19)$^{*\#}$	0.48 (0.25)$^{*\#}$	0.12 (0.19)
δ	1.56 (2.08)	1.17 (2.10)	0.33 (0.13)	0.28 (0.05)	0.31 (0.07)	2.40 (3.10)
C4 contralesional						
β	0.12 (0.18)	1.25 (1.94)	0.51 (0.29)$^{*\#}$	0.44 (0.19)$^{*\#}$	0.48 (0.25)$^{*\#}$	0.12 (0.19)
δ	1.56 (2.08)	1.17 (2.10)	0.33 (0.13)	0.28 (0.05)	0.31 (0.07)	2.40 (3.10)

Mean (SD), *significant difference from a, $^{\#}$significant difference from f ($p < 0.05$).

($p = 0.006$), 15–20 minutes ($p = 0.010$), and 20–25 minutes ($p = 0.008$). Also, contralesional C3 fell at 5–10 minutes ($p = 0.007$), 10–15 minutes ($p = 0.003$), 15–20 minutes ($p = 0.005$), and 20–25 minutes ($p = 0.003$), as well as contralesional C4. After removing the needles, the average power rose, and significant differences are noted at 5–10 minutes ($p = 0.003$), 10–15 minutes ($p = 0.001$), 15–20 minutes ($p = 0.002$), and 20–25 minutes ($p = 0.001$).

Figure 7 shows the average power of δ during the electroacupuncture process of spasticity subjects. Compared with baseline, the average power of δ in ipsilesional C3 fell at 10–15 minutes ($p = 0.010$), 15–20 minutes ($p = 0.034$), and 20–25 minutes ($p = 0.013$), as well as ipsilesional C4. After removing the needles, the average power rose, and the significant differences are noted at 10–15 minutes ($p = 0.023$) and 20–25 minutes ($p = 0.027$). Although contralesional C3 and C4 fell at each stage during the electroacupuncture process, no significant difference is noted.

4. Discussion

This is a pilot electrophysiological study of electroacupuncture therapy in patients with cerebral vascular accidents. We explored the cortical effects of EA treatment based on the acupuncture theory "treating flaccid paralysis

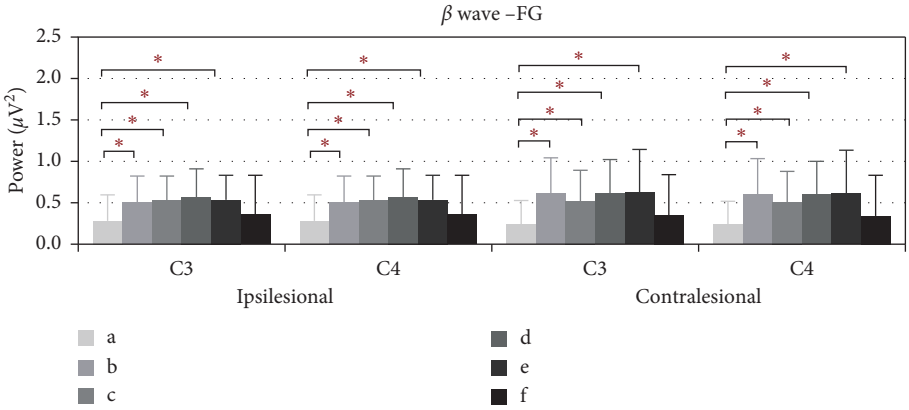

Figure 4: The β wave average power of FG of C3 and C4, $^*p < 0.05$. (a) Power average of 1–5 minutes. (b)–(e) Power average of every five minutes. (f) Power average of 5 minutes after removing needles.

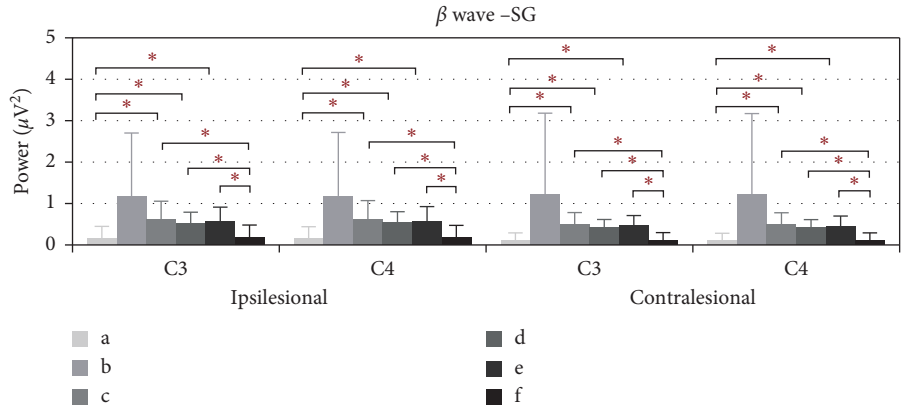

Figure 5: The β wave average power of SG of C3 and C4, $^*p < 0.05$. (a) Power average of 1–5 minutes. (b)–(e) Power average of every five minutes. (f) Power average of 5 minutes after removing needles.

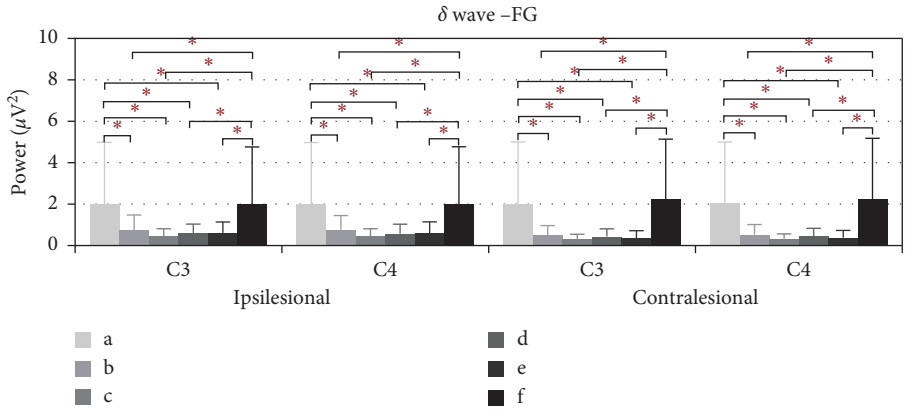

Figure 6: The δ wave average power of FG of C3 and C4, $^*p < 0.05$. (a) Power average of 1–5 minutes. (b)–(e) Power average of every five minutes. (f) Power average of 5 minutes after removing needles.

by *Yangming* alone" on beta and delta band oscillations before, during, and after the EA intervention in stroke patients.

In the current study, EA treatment was found to induce modulation of beta and delta band power from the ipsilesional and contralesional primary motor cortex of stroke patients while, in our previous study, we found that Jin's three-needle acupuncture therapy (an empiric treatment) could induce alpha rhythm oscillations from the occipital and parietal areas [28]. As we know, beta-band

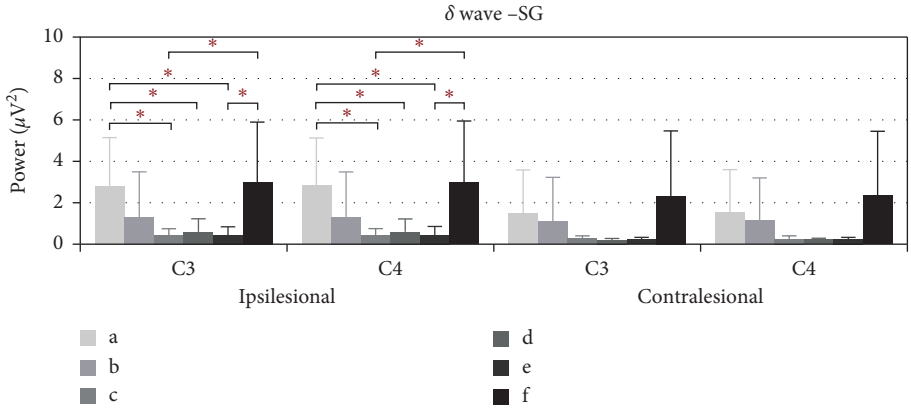

Figure 7: The δ wave average power of SG of C3 and C4, $^{*}p < 0.05$. (a) Power average of 1–5 minutes. (b)–(e) Power average of every five minutes. (f) Power average of 5 minutes after removing needles.

power oscillations within the primary motor cortex (M1) were reported to be linked to upper limb motor recovery in many studies [19, 29, 30]. Previous research also suggested delta band power in M1 was related to a better motor status [21, 31]. For this reason, we measured C3 and C4 electrodes and analyzed the changes in beta and delta band power.

In Tables 2 and 3, the brain wave average power before the needles are inserted shows that the average power of the delta wave was higher than beta waves. This result is consistent with the conclusion of Rabiller et al., who reported that the lower frequencies (delta and theta) increased and faster frequencies (alpha and beta) decreased after the stroke onset [17]. In another study with healthy subjects, they pointed out that the powers of α and β waves were stronger than δ and θ waves [32]. Therefore, compared to healthy individuals, beta oscillations decreased and delta oscillations increased in stroke patients.

In Figures 4 and 6, the ipsilesional and contralesional beta waves average power of stroke patients with flaccid paralysis increased and delta waves average power decreased during the electroacupuncture period. Three possible explanations for this phenomenon are detailed as follows. Firstly, electroacupuncture according to the classic theory adjusted the beta and delta band oscillations from the ipsilesional hemisphere in the direction of a healthy state. Rabiller et al. reported that delta band power increased and beta-band power decreased after stroke onset [17]. Secondly, electroacupuncture also activates the contralesional motor cortex. Park et al. have identified that the beta-band power in the contralesional motor cortex significantly correlated with the motor recovery rates [33]. Thirdly, the brain activities between the hemispheres are interconnecting [34]. The beta and delta band oscillations induced by electroacupuncture stimulation are not limited to the ipsilesional brain. Hence, further exploration is needed for brain network analysis.

In Figures 5 and 7, the performance of the ipsilesional and contralesional beta and delta waves average power of stroke patients with spasticity is similar to the patients with flaccid paralysis. The possible explanation is the readjustment of brain wave activities induced by EA for patients with spasticity. However, Kaiser et al. found that stronger ERD was associated with higher spasticity, and overdrive of the motor system might exist in patients with spasticity [35]. Thus, the beta-band power should be decreased during the electroacupuncture period, while our findings suggested otherwise. Small sample size on spasticity may be the reason for such results.

Our study suggested that electroacupuncture based on "treating flaccid paralysis by *Yangming* alone" induced an increase of beta-band power and a decrease of delta band power in the ipsilesional and contralesional hemispheres during the electroacupuncture needle retention stage. However, as a cross-sectional study, we cannot ensure that the patients will have a similar performance to beta and delta band power oscillation after a period of electroacupuncture treatment. Results from this research could not explain the question of how EA treatment could affect the brain network in the poststroke brain.

The limitations of our study included a small sample size on stroke patients with spasticity and no EEG data collected from healthy individuals and the sham EA group. This may limit the further exploration of brain wave changes in those groups of patients. Based on this pilot study, a further study with a larger sample size could be performed to contribute a clearer result.

5. Conclusions

This study demonstrated that the beta-band power increased and delta band power decreased in the bilateral motor cortex during the electroacupuncture treatment. We speculate that increased beta wave and decreased delta wave by electroacupuncture based on the classic theory provides a possible electrophysiological mechanism of the curative effect of electroacupuncture for stroke rehabilitation.

Data Availability

The data used to support the findings of this research are available from the corresponding author.

Disclosure

Yi-Fang Lin is the co-first author.

Conflicts of Interest

The authors declare that they have no conflicts of interest.

Authors' Contributions

Jie Jia conceived the study design. Fei Zou and Yi-Fang Lin conducted the experiments, collected and analyzed the data, and wrote the manuscript. Shu-Geng Chen, Lei Cao, and Hao-ran Wang made the EEG data processing. Shu-Geng Chen, Bin Ye, Qiang Wang, and Jie-Ying He reviewed and edited the manuscript. All the authors have reviewed the manuscript and agreed to its submission. All authors read and approved the final manuscript.

Acknowledgments

The authors would like to thank all volunteers for their participation in the study. This study was supported by the National Key Research and Development Program of Ministry of Science and Technology of the People's Republic of China under Grant nos. 2018YFC2002300 and 2018YFC2002301.

References

[1] G. Kwakkel, B. J. Kollen, J. van der Grond, and A. J. H. Prevo, "Probability of regaining dexterity in the flaccid upper limb," *Stroke*, vol. 34, no. 9, pp. 2181–2186, 2003.

[2] S. Chen, L. Cao, X. Shu et al., "Longitudinal electroencephalography analysis in Subacute stroke patients during intervention of brain–computer interface with exoskeleton feedback," *Frontiers in Neuroscience*, vol. 14, 2020.

[3] D. Li, W. Xu, C. Shugeng et al., "Camera-based mirror visual input for priming promotes motor recovery, daily function, and brain network segregation in Subacute stroke patients," *Neurorehabilitation and Neural Repair*, vol. 33, no. 4, pp. 307–318, 2019.

[4] W. Hewei, X. Guojun, W. Xu et al., "The reorganization of resting-state brain networks associated with motor imagery training in chronic stroke patients," *IEEE Trans Neural Systems Rehabilitation Engineering*, vol. 27, no. 10, pp. 2237–2245, 2019.

[5] S. Nuerjiayi, Z. Bin, J. Jie, and Z. Dingguo, "Using tdcs as an add-on treatment prior to fes therapy in improving upper limb function in severe chronic stroke patients: a randomized controlled study," *Frontiers in Human Neuroscience*, vol. 12, p. 233, 2018.

[6] H. Wang, C. Bao, H. Li, H. Qi, Z. Jiao, and G. Dong, "Impacts on fine movement of upper extremity with flaccid paralysis in stroke treated with acupuncture combined with motor imagery," *Zhongguo Zhen Jiu*, vol. 35, no. 6, pp. 534–538, 2015.

[7] Y. Chen, H. Zhou, T. Jin, T. Ye, and W. Xie, "Clinical observation of the phased acupuncture for ischemic stroke hemiplegia," *Zhongguo Zhenjiu*, vol. 38, pp. 1027–10, 2018.

[8] J.-S. Yang, X. Gao, R. Sun et al., "[Effect of electroacupuncture intervention on rehabilitation of upper limb motor function in patients with ischemic stroke]," *Zhen Ci Yan Jiu*, vol. 40, no. 6, pp. 489–492, 2015.

[9] S. Ju and L. Zong, "Discussion on acupuncture for flaccid paralysis from treating flaccid paralysis by yangming alone," *Zhōngguó Zhēnjiǔ*, vol. 35, no. 9, p. 956, 2015.

[10] F. Feiyu and C. Wang, "The relationship between muscle tension and yangming," *Clinical Journal of Chinese Medicine*, vol. 7, no. 31, pp. 40-41, 2015.

[11] G. N. Belskaya, S. B. Stepanova, L. D. Makarova, D. A. Sergienko, L. G. Krylova, and K. V. Antimonova, "Acupuncture in the prevention and treatment of stroke: a review of foreign studies," *Voprosy Kurortologii, Fizioterapii I Lechebnoi Fizicheskoi Kul'tury*, vol. 97, no. 2, pp. 68–77, 2020.

[12] S. S. Y. Au-Yeung and C. W. Y. Hui-Chan, "Electrical acupoint stimulation of the affected arm in acute stroke: a placebo-controlled randomized clinical trial," *Clinical Rehabilitation*, vol. 28, no. 2, pp. 149–158, 2014.

[13] Y. Xing, M. Zhang, W.-B. Li, F. Dong, and F. Zhang, "Mechanisms involved in the neuroprotection of electroacupuncture therapy for ischemic stroke," *Frontiers in Neuroscience*, vol. 12, no. 929, 2018.

[14] S. Comani, L. Velluto, L. Schinaia et al., "Monitoring neuromotor recovery from stroke with high-resolution eeg, robotics and virtual reality: a proof of concept," *IEEE Transactions on Neural Systems and Rehabilitation Engineering*, vol. 23, no. 6, pp. 1106–1116, 2015.

[15] S. Xiaokang, C. Shugeng, M. Jianjun et al., "Tactile stimulation improves sensorimotor rhythm-based bci performance in stroke patients," *IEEE Transactions Bio-Medical Engineering*, vol. 66, no. 7, pp. 1987–1995, 2018.

[16] C. Babiloni, R. J. Barry, E. Başar et al., "International Federation of Clinical Neurophysiology (IFCN) - EEG research workgroup: recommendations on frequency and topographic analysis of resting state EEG rhythms. Part 1: applications in clinical research studies," *ClinicaL Neurophysiology*, vol. 131, no. 1, pp. 285–307, 2020.

[17] G. Rabiller, J.-W. He, Y. Nishijima, A. Wong, and J. Liu, "Perturbation of brain oscillations after ischemic stroke: a potential biomarker for post-stroke function and therapy," *International Journal of Molecular Sciences*, vol. 16, no. 10, pp. 25605–25640, 2015.

[18] L. A. Boyd, K. S. Hayward, N. S. Ward et al., "Biomarkers of stroke recovery: consensus-based core recommendations from the stroke recovery and rehabilitation roundtable," *Neurorehabilitation and Neural Repair*, vol. 31, pp. 10-11, 2017.

[19] A. K. Engel and P. Fries, "Beta-band oscillations-signalling the status quo?" *Current Opinion in Neurobiology*, vol. 20, no. 2, pp. 156–165, 2010.

[20] L. H. Arnal and A.-L. Giraud, "Cortical oscillations and sensory predictions," *Trends in Cognitive Sciences*, vol. 16, no. 7, pp. 390–398, 2012.

[21] J. M. Cassidy, A. Wodeyar, J. Wu et al., "Low-frequency oscillations are a biomarker of injury and recovery after stroke," *Stroke*, vol. 51, no. 5, pp. 1442–1450, 2020.

[22] M. Bönstrup, L. Krawinkel, R. Schulz et al., "Low-frequency brain oscillations track motor recovery in human stroke," *Annals of Neurology*, vol. 86, no. 6, pp. 853–865, 2019.

[23] R. I. Carino-Escobar, P. Carrillo-Mora, R. Valdes-Cristerna et al., "Longitudinal analysis of stroke patients' brain rhythms during an intervention with a brain-computer interface," *Neural Plasticity*, vol. 2019, Article ID 7084618, 11 pages, 2019.

[24] J. Zhan, R. Pan, M. Zhou et al., "Electroacupuncture as an adjunctive therapy for motor dysfunction in acute stroke survivors: a systematic review and meta-analyses," *BMJ Open*, vol. 8, no. 1, Article ID e17153, 2018.

[25] Y. S. Kim, J. W. Hong, B. J. Na et al., "The effect of low versus high frequency electrical acupoint stimulation on motor recovery after ischemic stroke by motor evoked potentials study," *The American Journal of Chinese Medicine*, vol. 36, no. 1, pp. 45–54, 2008.

[26] L. Cao, J. Li, Y. Xu, H. Zhu, and C. Jiang, "A hybrid vigilance monitoring study for mental fatigue and its neural activities," *Cognitive Computation*, vol. 8, no. 2, pp. 228–236, 2016.

[27] S. L. Zeger and K.-Y. Liang, "Longitudinal data analysis for discrete and continuous outcomes," *Biometrics*, vol. 42, no. 1, pp. 121–130, 1986.

[28] Y. Xuejie, Y. Haibo, Z. Tao et al., "The effects of Jin's three-needle acupuncture therapy on eeg alpha rhythm of stroke patients," *Topics in Stroke Rehabilitation*, vol. 25, no. 7, pp. 535–539, 2019.

[29] C.-W. Tang, F.-J. Hsiao, P.-L. Lee et al., "β-Oscillations reflect recovery of the paretic upper limb in Subacute stroke," *Neurorehabilitation and Neural Repair*, vol. 34, no. 5, pp. 450–462, 2020.

[30] J. Wagner, S. Makeig, M. Gola, C. Neuper, and G. Müller-Putz, "Distinct β band oscillatory networks subserving motor and cognitive control during gait adaptation," *The Journal of Neuroscience*, vol. 36, no. 7, pp. 2212–2226, 2016.

[31] J. Wu, R. Srinivasan, A. Kaur, and S. C. Cramer, "Resting-state cortical connectivity predicts motor skill acquisition," *Neuroimage*, vol. 91, pp. 84–90, 2014.

[32] S.-F. Hsu, C.-Y. Chen, M.-D. Ke, C.-H. Huang, Y.-T. Sun, and J.-G. Lin, "Variations of brain activities of acupuncture to Te5 of left hand in normal subjects," *The American Journal of Chinese Medicine*, vol. 39, no. 4, pp. 673–686, 2012.

[33] W. Park, Y.-H. Kim, S.-P. Kim, and L. Kim, "EEG Patterns of Subacute Stroke Patients Performing Motor Tasks Correlate with Motor Functional Outcome: Preliminary Results," in *Proceedings of the 38th Annual International Conference of the IEEE Engineering in Medicine and Biology Society*, Chicago, IL;USA, August 2016.

[34] A. Baldassarre, L. Ramsey, J. Rengachary et al., "Dissociated functional connectivity profiles for motor and attention deficits in acute right-hemisphere stroke," *Brain*, vol. 139, no. 7, pp. 2024–2038, 2016.

[35] V. Kaiser, I. Daly, F. Pichiorri, D. Mattia, G. R. Müller-Putz, and C. Neuper, "Relationship between electrical brain responses to motor imagery and motor impairment in stroke," *Stroke*, vol. 43, no. 10, pp. 2735–2740, 2012.

Hindawi
Evidence-Based Complementary and Alternative Medicine
Volume 2020, Article ID 6980398, 14 pages
https://doi.org/10.1155/2020/6980398

Research Article

A20-Binding Inhibitor of NF-κB 1 Ameliorates Neuroinflammation and Mediates Antineuroinflammatory Effect of Electroacupuncture in Cerebral Ischemia/Reperfusion Rats

Xueling Zhou,[1,2] Wenhao Lu,[1,2] You Wang,[3] Jiani Li,[3] and Yong Luo [1]

[1]*Department of Neurology, The First Affiliated Hospital of Chongqing Medical University, Chongqing 400016, China*
[2]*Laboratory Research Center, The First Affiliated Hospital of Chongqing Medical University, Chongqing 400016, China*
[3]*Department of Neurology, The Second Affiliated Hospital of Chongqing Medical University, Chongqing 400010, China*

Correspondence should be addressed to Yong Luo; luoyong1998@163.com

Received 31 July 2020; Revised 22 September 2020; Accepted 25 September 2020; Published 14 October 2020

Academic Editor: Feng Zhang

A20-binding inhibitor of NF-κB 1 (ABIN1) is an inhibitor of NF-κB and exerts anti-inflammatory effect. Electroacupuncture (EA) is considered as a neuroprotective strategy by inhibiting neuroinflammatory damage after cerebral ischemia. This study was performed to explore the role of ABIN1 and investigate whether the ABIN1 is involved in the mechanism of EA in cerebral ischemia/reperfusion (I/R) rats. Male Sprague-Dawley (SD) rats were subjected to middle cerebral artery occlusion/reperfusion (MCAO/R) and received EA after reperfusion once a day. Lentivirus-mediated ABIN1 gene knockdown was used to detect the role of ABIN1 in neuroinflammation after I/R. ABIN1 expression, proinflammatory cytokine levels, microglial activation, neurological function, infarct volumes, and NF-κB activation were assessed. ABIN1 expression was elevated in the peri-infarct cortex and was further upregulated by EA. ABIN1 knockdown increased the levels of proinflammatory cytokines and activation of microglia, worsened neurological deficits, and enlarged the infarct volume. Moreover, ABIN1 was blocked to partially reverse the neuroprotective effect of EA, and this treatment weakened the ability of EA to suppress NF-κB activity. Based on these findings, ABIN1 is a potential suppressor of neuroinflammation and ABIN1 mediates the antineuroinflammatory effect of EA in cerebral I/R rats.

1. Introduction

Ischemic stroke accounts for 84.4% of all strokes, resulting in a high global burden [1]. With the development of endovascular therapy, the treatment of acute ischemic stroke has entered a new stage [2]. However, recanalization can lead to cerebral ischemia/reperfusion damage. Thus, neuroprotection combined with reperfusion therapy is an important next step in the development of ischemic stroke treatment [3, 4]. The pathological mechanism of cerebral ischemia/reperfusion (I/R) is complex. Excessive neuroinflammation after cerebral I/R is one of the main culprits for aggravating brain damage [5–7], which has been considered as a potential therapeutic target [4, 8]. NF-κB acts as a "molecular switch" in ischemic stroke, promoting the initiation and amplification of the inflammatory cascade [9]. The most common dimeric form of NF-κB is p65/p50, and the dimer binds to inhibitor of kappa B (IκB) and is localized in the cytoplasm in the resting state. Upon stimulation by cerebral ischemia, IκB proteins are phosphorylated by the inhibitor of kappa B kinase (IKK) and degraded, allowing NF-κB to enter the nucleus and promote the expression of a series of proinflammatory cytokines [9–11].

A20-binding inhibitor of NF-κB 1 (ABIN1) is a physiological inhibitor of NF-κB that binds the Lys63 and Met-1 polyubiquitin chains with high affinity [12, 13]. As an adaptor protein of A20, ABIN1 promotes the deubiquitination of molecules upstream of NF-κB and inhibits NF-κB

activation [14, 15]. ABIN1-deficient mice die during embryogenesis and the mice that survive exhibit immune cell activation and develop a progressive, lupus-like inflammatory disease [16, 17]. Notably, ABIN1 acts as an inhibitor of inflammation in various inflammatory diseases, such as hepatic I/R, asthma, systemic lupus erythematosus, psoriasis, and osteoarthritis [18–22]. However, the role of ABIN1 in neuroinflammatory damage after cerebral I/R has not been reported.

Electroacupuncture (EA) is a product of modern technology that adds electrical stimulation to acupuncture, which is characterized by a low cost, few side effects, and controllable parameters. EA regulates the immune response and restores homeostasis, which may underlie its use as a treatment for various inflammation-related diseases [23–25]. Furthermore, EA is a widely used treatment for ischemic stroke and has achieved good results [26–28]. The neuroprotective effect of EA is closely related to the inhibition of NF-κB [29–31]; however, the specific regulatory mechanism of EA has not been completely clarified. As shown in our previous studies, EA inhibits IκBα phosphorylation and prevents the nuclear translocation of NF-κB p65 by upregulating the neuronal deubiquitinating enzyme A20 to ultimately improve the neurological deficits in middle cerebral artery occlusion/reperfusion (MCAO/R) rats [32]. Interestingly, ABIN1 is an important member of the A20 complex and may also be regulated by EA. Considering the fact that ABIN1 plays a crucial role in inhibiting NF-κB-related inflammatory responses, EA may inhibit NF-κB activation and exert neuroprotective effect via upregulating ABIN1 expression in cerebral I/R rats. Therefore, in the present study, we initially explored the effect of ABIN1 on neuroinflammatory damage in a MCAO/R rat. Then, the possible mechanism by which EA regulates the expression of ABIN1 to inhibit NF-κB activation was investigated.

2. Methods

2.1. Animals. Healthy Sprague-Dawley (SD) rats weighing 280–300 g were purchased from Experimental Animal Center of Chongqing Medical University (Chongqing, China). Animals were maintained in a specific pathogen-free (SPF) room (12 h light/dark cycle, $22 \pm 2^{\circ}$C, 60–70% humidity). Rats were allowed for free access to food and water. Rats were kept for a week to acclimatize before the experiment. All animal experimental procedures were approved by the Ethics Committee for Animal Experimentation of Chongqing Medical University (number SYXK(Yu) 2018-0003) and were performed in accordance with National Institutes of Health Guide for the Care and Use of Laboratory Animals.

In the first study, rats were randomly divided into 4 groups: sham group, MCAO/R group, MCAO/R + EA group, and MCAO/R + sham EA group to investigate the expression of ABIN1 in the peri-infarct cortex.

The second study elucidated the effect of ABIN1 on neuroinflammatory damage after I/R using sham group, MCAO/R group, MCAO/R + LV-Scramble group, and MCAO/R + LV-shABIN1 group.

The third study explored whether ABIN1 was involved in the antineuroinflammatory mechanism of EA using MCAO/R group, MCAO/R + EA group, MCAO/R + EA + LV-Scramble group, and MCAO/R + EA + LV-shABIN1 group.

2.2. Establishment of the MCAO/R Model. A total of 208 rats were used in this experiment, including 17 rats that were excluded due to death ($n = 14$) or unsuccessful induction of ischemia ($n = 3$). SD rats underwent MCAO/R as previously described [33]. Briefly, rats were anesthetized with sodium pentobarbital (60 mg/kg, i.p.). A nylon monofilament with a silicon-coated rounded tip was inserted to block the right middle cerebral artery. After 2 h of ischemia, the nylon monofilament was removed to induce reperfusion. Rats were detected by a laser Doppler flowmetry (PeriFlux 5000, Perimed AB, Sweden), and regional cerebral blood flow decreased to 20% and recovered to >80% of baseline, indicating the successful establishment of the MCAO/R model. The rats in the sham group underwent the same operation, except that the monofilament was not inserted to block the middle cerebral artery. Rat rectal temperature was maintained at $37 \pm 0.5^{\circ}$C with an electrothermal pad.

2.3. Intracerebral Lentivirus Injection. Lentiviruses containing the ABIN1 shRNA (LV-shABIN1) for ABIN1 knockdown and control shRNA (LV-Scramble) were supplied by Genechem (Shanghai, China). Two weeks prior to the establishment of the MCAO/R model, the right cortex of rat was injected with the lentiviruses. The injection sites were as follows: site 1, A-P 1.0 mm; M-L −2.0 mm; D-V −1.2 mm, and site 2, A-P −3.0 mm; M-L −1.5 mm; D-V −1.2 mm [34]. A total of 2.5 μl of LV-shABIN1 or LV-Scramble were injected into each site.

2.4. EA Treatment. Immediately after reperfusion, the rat was treated with EA once a day until sacrifice. EA was performed as described previously [32] and acupuncture needles were inserted at Baihui (GV 20), Hegu (LI 4), and Taichong (LR 3) (Figure 1) and connected with EA instrument (Model no. SDZ-III, Hwato, China). To construct a circuit, two electrodes were connected, respectively, to the needle at GV 20 and the left ear (nonacupoint). Another two electrodes were connected, respectively, to the needle at LI 4 and LR 3. The stimulation parameters were intensity of 1 mA and a frequency of 20 Hz for 5 min followed by 2 Hz for 30 min. In the sham EA group, needles were affixed to the acupoints without skin penetration, and the animals did not receive electrical stimulation [35].

2.5. Evaluation of the Neurological Function. At 72 h before and 24, 48, and 72 h after cerebral I/R, each rat was assessed with the Modified Neurological Severity Score (mNSS) and Modified Sticky-Tape Test (MST) by an observer who was blinded to the experiments. The mNSS is a comprehensive scoring system that includes motor, balance, sensory, and reflex tests and is graded on a scale of 0 (normal) to 18 (maximal deficit) points [36]. The Modified Sticky-Tape Test

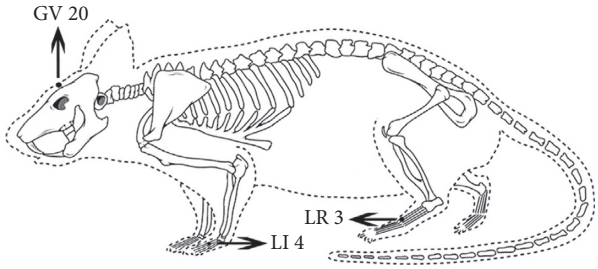

Figure 1: Schematic diagram of GV20, LI 4, and LR 3 acupoints of rat.

was used to evaluate somatosensory dysfunction. The sticky paper tape (3 cm long and 1 cm wide) was placed around the paw of the rat, and the time for the rat to tear the tape within 30 seconds was recorded. Per limbs was tested 5 times a day, and Modified Sticky-Tape Test performance was presented as a ratio of left/right [37].

2.6. Measurement of the Cerebral Infarct Volume. Rats were euthanized with an overdose of sodium pentobarbital (150 mg/kg, i.p.). After sacrifice, brains were cut into 2 mm thick serial coronal slices and immersed in 2,3,5-triphenyltetrazolium chloride (TTC) at 37°C for 15 min in the dark. Images were acquired with a camera and analyzed with ImageJ software. The infarct volume was presented as a percentage of the intact hemisphere.

2.7. Real-Time Quantitative PCR (RT-qPCR). As shown in Figure 2(a), the pale area was considered to be the infarct core. Strips of tissue (2 mm thick) surrounding the infarct core were considered as the peri-infarct tissue and dissected for RT-PCR and western blot analysis [38]. Total RNA was extracted from the peri-infarct cortex using Trizol (TaKaRa, Japan). Then, cDNAs were synthesized using a PrimeScript RT reagent kit with gDNA Eraser (TaKaRa) and were used as a template for RT-qPCR, which was conducted in a CFX96 Real-Time PCR Detection System (Bio-Rad Co., USA) with SYBR Green. The following primer sequences were used (5′ to 3′): GAPDH: forward: AAGTTCAACGGCACAGTCAAGG and reverse: ACGCCAGTAGACTCCACGACAT, and ABIN1: forward: TCGGCTGAAGGGAAAAATACA and reverse: CAAAGGAGACCAAGGAGGGAG. The results were normalized to the levels of the housekeeping gene GAPDH.

2.8. Western Blot Analysis. Proteins were extracted from the peri-infarct cortex using RIPA buffer (Beyotime, China). A cytoplasmic/nuclear protein extraction kit (Beyotime) was used to extract cytoplasmic and nuclear proteins. Western blot was performed as described previously [39]. Briefly, proteins were separated on 10% gels and transferred to PVDF membranes. After blocking with 5% skim milk, membranes were incubated with the primary antibodies at 4°C overnight. The following primary antibodies against specific proteins were used: ABIN1 (#4664, Cell Signaling Technology, USA, 1 : 1000), A20 (#5630, Cell Signaling Technology, USA, 1 : 1000), NF-κB p65 (#8242, Cell Signaling Technology, 1 : 1000), IκBα (18220-1-AP, Proteintech, USA, 1 : 000), phospho-IκBα (Ser32) (#2859, Cell Signaling Technology, 1 : 1000), GAPDH (10494-1-AP, Proteintech, USA, 1 : 1000), and histone H3 (#3638, Cell Signaling Technology, 1 : 1000). Membranes were washed with TBST and immersed in the secondary antibodies at 37°C for 1 h. After washes with TBST, immunoreactive bands were detected using WesternBright ECL (Advansta, USA). Membranes were scanned and analyzed using a Fusion FX5 analysis system (Vilber Lourmat Fusion FX 7 Spectra, France).

2.9. ELISA. The peri-infarct cortex was collected 24 h after reperfusion, and the concentrations of TNF-α, MCP-1, and IL-1β were assayed using ELISA kits (nos. EK0526, EK0902, and EK0393, respectively, BOSTER, China).

2.10. Immunofluorescence Staining. Brain tissues were fixed, dehydrated, and then cut into coronal sections at a thickness of 10 μm. Sections were permeabilized with 0.3% Triton X-100. Then, brain slices were blocked with 5% donkey or goat serum for 1 h and incubated overnight at 4°C with primary antibodies: ABIN1 (bs-9568R, Bioss, China, 1 : 50), NeuN (MAB377, Millipore, Germany, 1 : 200), A20 (3A11G6, Proteintech, USA, 1 : 100), Iba-1 (NB100-1028, Novus, USA, 1 : 50), and GFAP (BM0055, Boster, China, 1 : 100). Then, the following fluorescently labeled secondary antibodies were incubated with the sections at 37°C for 1 h in the dark: CoraLite594-goat anti-rabbit (SA00013-4, Proteintech, 1 : 200), CoraLite488-goat anti-mouse (SA00013-1, Proteintech, 1 : 200), CoraLite594-donkey anti-rabbit (SA00013-8, Proteintech, 1 : 200), FITC-donkey anti-goat (SA00003-3, Proteintech, 1 : 200), and Cell nuclei were stained with DAPI. Brain slices were observed under a laser confocal microscope (LSM-800, Carl Zeiss Micro-Imaging Co., Germany).

2.11. Coimmunoprecipitation. The peri-infarct cortex was homogenized in IP lysis buffer (Beyotime, China) to extract the proteins. One microgram of anti-ABIN1 antibody (#4664, Cell Signaling Technology), anti-A20 antibody (#5630, Cell Signaling Technology), or normal rat IgG was added to each milligram of total protein in the supernatants, and the samples were rotated at 4°C overnight. Forty microliters of protein A/G agarose beads was mixed with the supernatants and rotated at 4°C for 2 h. The beads were washed with lysis buffer and then eluted with 40 μl of SDS loading buffer. The supernatants were collected for western blot.

2.12. Statistical Analyses. All data were analyzed using SPSS 21.0 and graphed using GraphPad Prism 8.0 and expressed as the means ± SEMs. The differences of cellular localization of ABIN1 were assessed using the unpaired *t*-test. All other quantitative data were analyzed using one-way ANOVA. $P < 0.05$ was considered statistically significant.

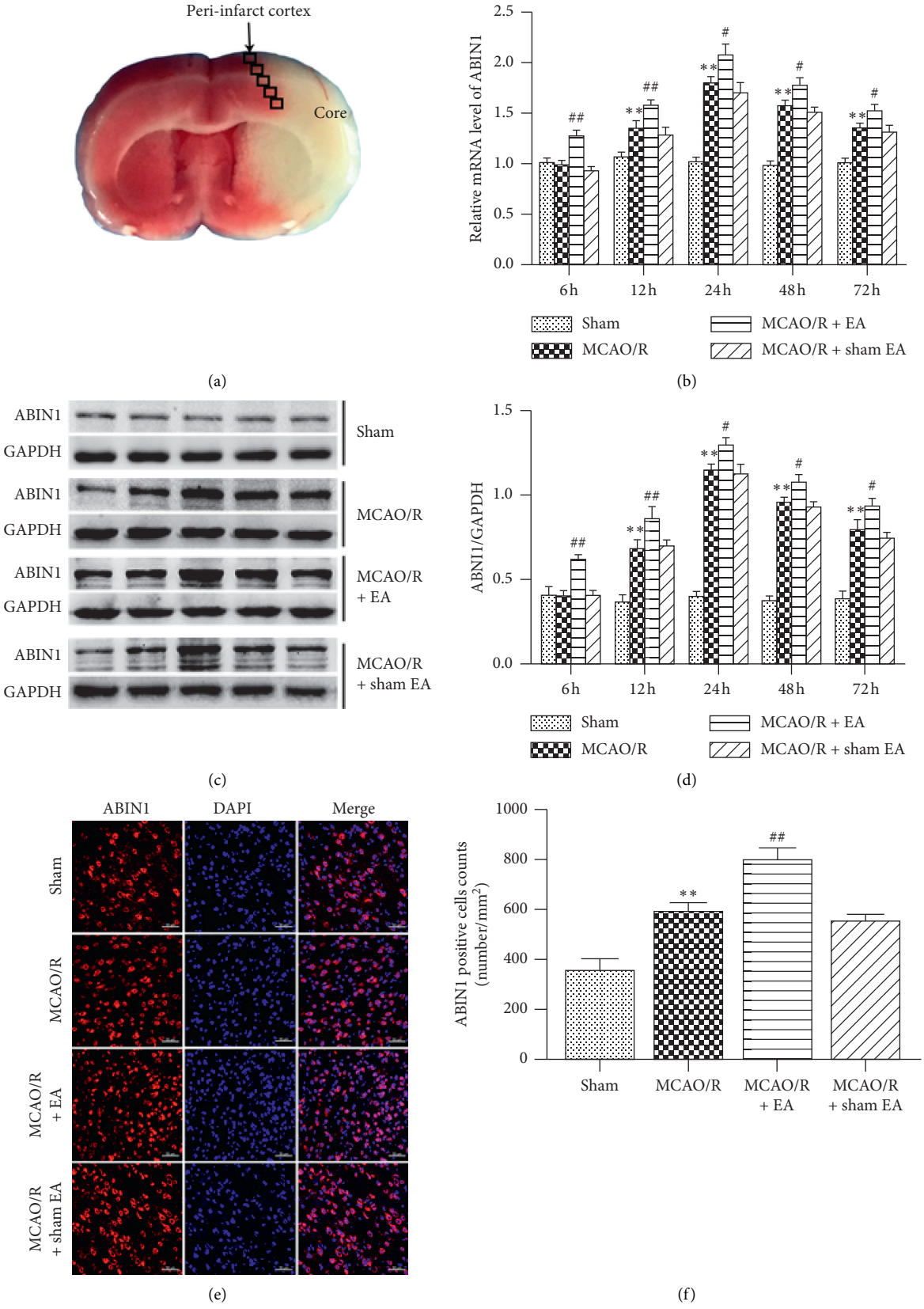

Figure 2: ABIN1 expression in the peri-infarct area at different time points. (a) The core and peri-infarct areas of a MCAO/R rat. (b–d) RT-qPCR and western blot were used to, respectively, detect the levels of the ABIN1 mRNA and protein in the peri-infarct cortex at 6 h, 12 h, 24 h, 48 h, and 72 h after reperfusion ($n = 5$ rats per group). The expression of ABIN1 was normalized to GAPDH. (e) ABIN1 (red) and DAPI (blue) immunofluorescence staining present the distribution of ABIN1 at 24 h after reperfusion ($n = 3$ rats per group). Scale bar = 50 μm. (f) Column chart presenting the ABIN1$^+$ cell counts in the four groups ($^*P < 0.05$ and $^{**}P < 0.01$ compared to the sham group; $^{\#}P < 0.05$ and $^{\#\#}P < 0.01$ compared to the MCAO/R group).

3. Results

3.1. ABIN1 Expression Is Induced in MCAO/R Rats. We measured the levels of the ABIN1 mRNA and protein in the peri-infarct cortex at 6 h, 12 h, 24 h, 48 h, and 72 h after reperfusion. The expression of the ABIN1 mRNA and protein peaked in the MCAO/R group at 24 h after reperfusion and then gradually decreased (Figures 2(b)–2(d)). The ABIN1 mRNA and protein were expressed at higher levels in the MCAO/R group than in the sham group from 12 h to 72 h (Figures 2(b)–2(d)). Moreover, compared with the MCAO/R group, EA further increased the expression of the ABIN1 from 6 h to 72 h (Figures 2(b)–2(d)). In addition, ABIN1 was detected using immunofluorescence staining at 24 h after reperfusion (Figures 2(e) and 2(f)). Compared to the sham group, the number of $ABIN1^+$ cells in the peri-infarct cortex was significantly increased in the MCAO/R group (Figures 2(e) and 2(f)). Moreover, the number of $ABIN1^+$ cells was further increased in rats receiving EA (Figures 2(e) and 2(f)). A significant difference in ABIN1 expression was not observed between the MCAO/R group and MCAO/R + sham EA group (Figures 2(b)–2(f)).

3.2. The Distribution of ABIN1 in the Peri-Infarct Cortex. ABIN1 has been described as an NF-κB suppressor through interacting with A20 [12]; to further verify the interaction between A20 and ABIN1 in the peri-infarct cortex, the immunofluorescence staining and coimmunoprecipitation were performed. The immunofluorescence staining revealed numerous $ABIN1^+$ and $A20^+$ cells in the peri-infarct cortex 24 h after reperfusion, and A20 and ABIN1 were colocalized in the cytoplasm (Figure 3(a)). The coimmunoprecipitation results further suggested that ABIN1 and A20 bind to each other in the peri-infarct cortex at 24 h after reperfusion (Figure 3(b)).

Next, the cellular localization of ABIN1 in the peri-infarct cortex 24 h after reperfusion was evaluated using double immunofluorescence labeling. ABIN1 was colocalized with NeuN (a neuron marker) and Iba-1 (a microglia marker) but not with GFAP (an astrocyte marker) (Figure 3(c)). Moreover, $ABIN1^+NeuN^+$ cells accounted for $70.22 \pm 1.71\%$ of $ABIN1^+$ cells, and $ABIN1^+Iba\text{-}1^+$ cells accounted for 26.83 ± 2.75 % of $ABIN1^+$ cells in the peri-infarct cortex (Figures 3(c) and 3(d)). These results indicated that neurons and microglia were the cellular source of ABIN1 in the peri-infarct cortex.

3.3. ABIN1 Knockdown Increases Proinflammatory Cytokines Production and Microglial Activation. ABIN1 was silenced by a cortical injection of LV-shABIN1 to further explore the role of ABIN1 in neuroinflammation after I/R. First, the levels of the ABIN1 mRNA and protein were measured at 24 h after reperfusion to ensure the effectiveness of ABIN1 knockdown. The expression of ABIN1 was significantly reduced in the MCAO/R + LV-shABIN1 group (Figures 4(a) and 4(b)), indicating that ABIN1 was successfully silenced.

Then, we examined the production of proinflammatory factors and microglial activation using ELISA and immunofluorescence staining, respectively. Typical proinflammatory factors TNF-α, IL-1β, and MCP-1 were produced at higher levels in the MCAO/R group than in the sham group (Figure 4(c)). Higher levels of these cytokines were detected in the MCAO/R + LV-shABIN1 group than in the MCAO/R group (Figure 4(c)). The levels of these proinflammatory factors were not significantly different between the MCAO/R + LV-scramble group and the MCAO/R group (Figure 4(c)).

The morphology of microglia is closely related to their biological functions. Resting microglia are hyperramified. Activated microglia are characterized by enlarged cell bodies with short and thick processes and round and rod-like cell bodies, and some even exhibit an amoeba-like cell bodies [40]. We evaluated the activation of microglia by quantifying the number of endpoints per cell and the length of cell processes, which may serve as indicators of neuroinflammation [41, 42]. Immunofluorescence staining for Iba-1 was used to detect microglia in the peri-infarct cortex at 24 h after I/R. The microglia in the sham group exhibited the resting state phenotype (hyperramification) (Figure 4(d)). As shown in Figures 4(d)–4(f), the number of endpoints per cell and the length of cell process were decreased in the MCAO/R group compared with the sham group, indicating that more activated microglia were present in the MCAO/R rats. Moreover, the number of endpoints per cell and the length of cell process were reduced in the MCAO/R + LV-shABIN1 group compared with the MCAO/R group, suggesting that blockade of ABIN1 expression enhanced microglial activation (Figures 4(d)–4(f)). Significant differences were not observed between the MCAO/R + LV-scramble group and the MCAO/R group (Figures 4(d)–4(f)).

3.4. ABIN1 Knockdown Exacerbates the Neurological Deficits and Enlarges the Infarct Volume. The mNSS and MST were used to assess the neurological function of rats 72 h before and 24, 48, and 72 h after cerebral I/R. At 72 h before reperfusion, the neurological function of rats was normal and no significant differences were observed among the groups (Figures 5(a) and 5(b)). The mNSS and MST ratio of the MCAO/R group were worse than the sham group at 24, 48, and 72 h after I/R (Figures 5(a) and 5(b)). Compared with the MCAO/R group, the neurological deficits of the MCAO/R + LV-shABIN1 group were increased significantly at 72 h but not at 48 h or 24 h (Figures 5(a) and 5(b)). The neurological deficits of the MCAO/R + LV-scramble group was not different from the MCAO/R group at 24, 48, and 72 h after I/R (Figures 5(a) and 5(b)). The infarct volume was assessed using TTC staining at 72 h after reperfusion. The cerebral infarct volume did not differ significantly between the MCAO/R + LV-scramble group and the MCAO/R group but was expanded in the MCAO/R + LV-shABIN1 group (Figures 5(c) and 5(d)).

3.5. ABIN1 Knockdown Weakens the Antineuroinflammatory Effect of EA to Some Extent. The concentrations of TNF-α, IL-1β, and MCP-1 in the peri-infarct cortex were detected at

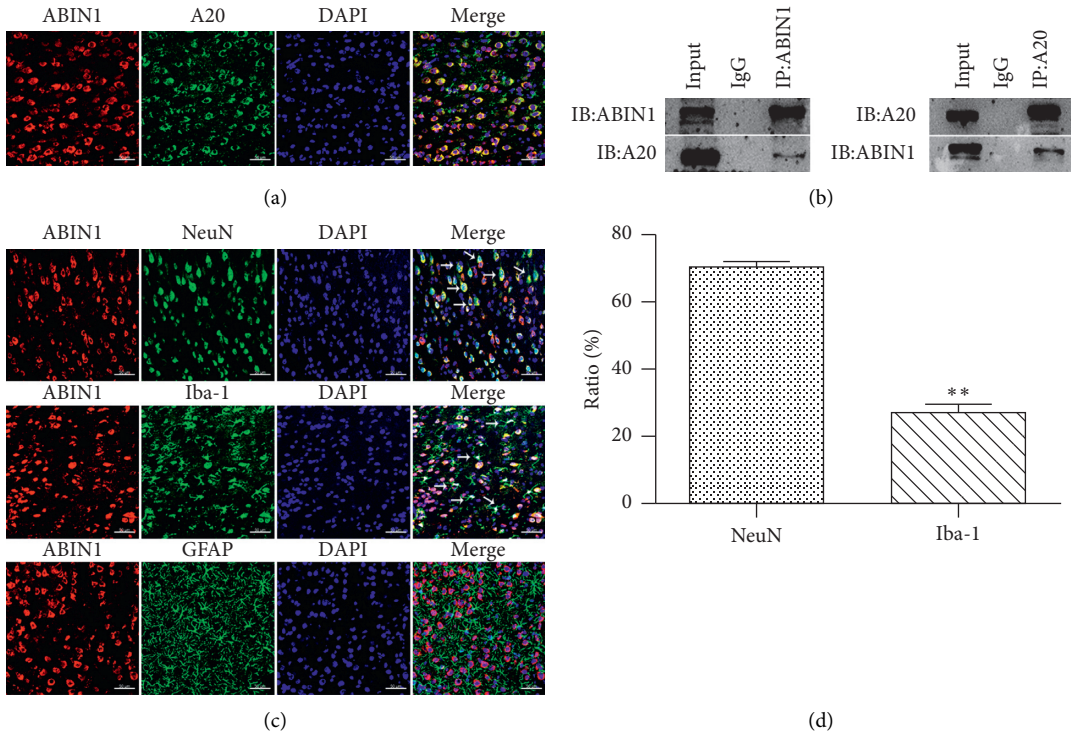

Figure 3: ABIN1 is colocated with A20 and NeuN and Iba-1, respectively, in the peri-infarct cortex. (a) Double immunofluorescence staining for ABIN1 and A20 in the peri-infarct cortex at 24 h after reperfusion ($n = 3$ rats per group). Scale bar = 50 μm. (b) Coimmunoprecipitation of ABIN1 and A20 in the peri-infarct cortex at 24 h after reperfusion ($n = 3$ rats per group). (c) Double immunofluorescence labeling of ABIN1 (red) and NeuN (green, neurons), Iba-1 (green, microglia), and GFAP (green, astrocytes), respectively ($n = 3$ rats per group). White arrows show that ABIN1 is colocalized with NeuN and Iba-1, respectively. Scale bar = 50 μm. (d) Comparisons of the percentage of ABIN1$^+$ NeuN$^+$ cells among ABIN1$^+$ cells and ABIN1$^+$ Iba-1$^+$ cells among ABIN1$^+$ cells in the peri-infarct cortex. $^{**}P < 0.01$ compared to ABIN1$^+$ NeuN$^+$/ABIN1$^+$.

24 h after reperfusion using ELISA to determine the effect of ABIN1 knockdown on the antineuroinflammatory effect of EA. The levels of these proinflammatory cytokines were significantly decreased in the MCAO/R + EA group compared with the MCAO/R group (Figure 6(a)). In addition, ABIN1 knockdown impaired the antineuroinflammatory effect of EA, since higher levels of TNF-α, IL-1β, and MCP-1 were detected in the MCAO/R + EA + LV-shABIN1 group than in the MCAO/R + EA group (Figure 6(a)). The MCAO/R + EA + LV-scramble and MCAO/R + EA groups displayed similar levels of these cytokines (Figure 6(a)). Furthermore, the results of Iba-1 immunofluorescence staining in the peri-infarct cortex at 24 h after reperfusion indicated that the MCAO/R + EA group had more endpoints per cell and longer cell processes than the MCAO/R group; however, ABIN1 knockdown in the MCAO/R + EA + LV-shABIN1 group promoted microglial activation (Figures 6(b)–6(d)). Microglia activation was not significantly different between the MCAO/R + EA + LV-scramble group and MCAO/R + EA group (Figures 6(b)–6(d)).

3.6. ABIN1 Knockdown Partially Inhibits the Neuroprotective Effect of EA. The mNSS and MST of rats in the four groups were assessed at 72 h before and 24, 48, and 72 h after reperfusion. At 72 h before reperfusion, the neurological function of rats was normal and no significant differences were observed among groups. The neurological impairments observed in rats in the MCAO/R + EA group were significantly improved at 72 h but not 24 and 48 h after reperfusion compared with rats in the MCAO/R group (Figures 7(a) and 7(b)). Rats in the MCAO/R + EA + LV-shABIN1 group exhibited worse neurological deficits than rats in the MCAO/R + EA group at 72 h after reperfusion (Figures 7(a) and 7(b)). The mNSS and MST of rats in the MCAO/R + EA group were similar to rats in the MCAO/R + EA + LV-scramble group (Figures 7(a) and 7(b)). TTC staining at 72 h after reperfusion revealed a smaller infarct volume in the MCAO/R + EA group than in the MCAO/R group (Figures 7(c) and 7(d)). However, in the MCAO/R + EA + LV-shABIN1 group, ABIN1 knockdown increased the infarct volume compared with the MCAO/R + EA group (Figures 7(c) and 7(d)). The infarct volume did not significantly differ between the MCAO/R + EA + LV-Scramble group and the MCAO/R + EA group (Figures 7(c) and 7(d)). Based on these results, EA exerted a protective effect on the brain after I/R, but ABIN1 knockdown weakened the effect of EA.

3.7. EA Inhibits NF-κB Activation by Upregulating ABIN1. As mentioned above, NF-κB plays a key role in focal cerebral I/R-induced neuroinflammation. To further explore whether ABIN1 mediated EA induced inhibition of NF-κB

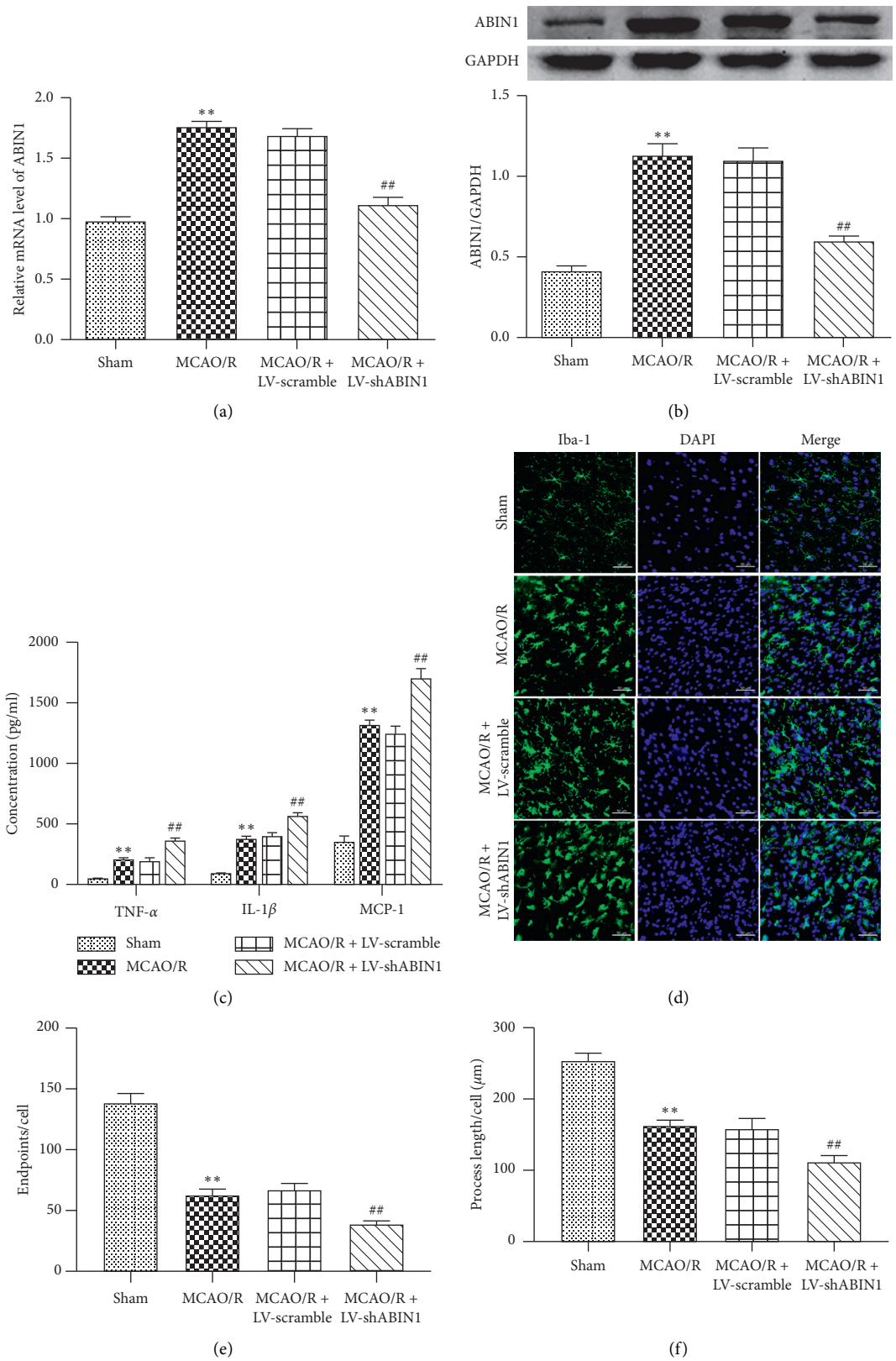

FIGURE 4: ABIN1 knockdown increases proinflammatory cytokine production and microglial activation. (a-b) Levels of the ABIN1 mRNA and protein were detected 24 h after reperfusion using RT-qPCR and western blot, respectively, to confirm the efficiency of ABIN1 gene knockdown ($n = 5$ rats per group). (c) ELISA was used to detect the concentrations of TNF-α, IL-1β and MCP-1 in the peri-infarct cortex at 24 h after reperfusion ($n = 5$ rats per group). (d) Microglial morphology was observed using immunofluorescence staining for Iba-1 (green) in the peri-infarct cortex at 24 h after reperfusion ($n = 3$ rats per group). Scale bar = 50 μm. (e and f) Quantification of microglia process endpoints and cell and process lengths/cell ($^{**}P < 0.01$ compared to the sham group; $^{\#\#}P < 0.01$ compared to the MCAO/R group).

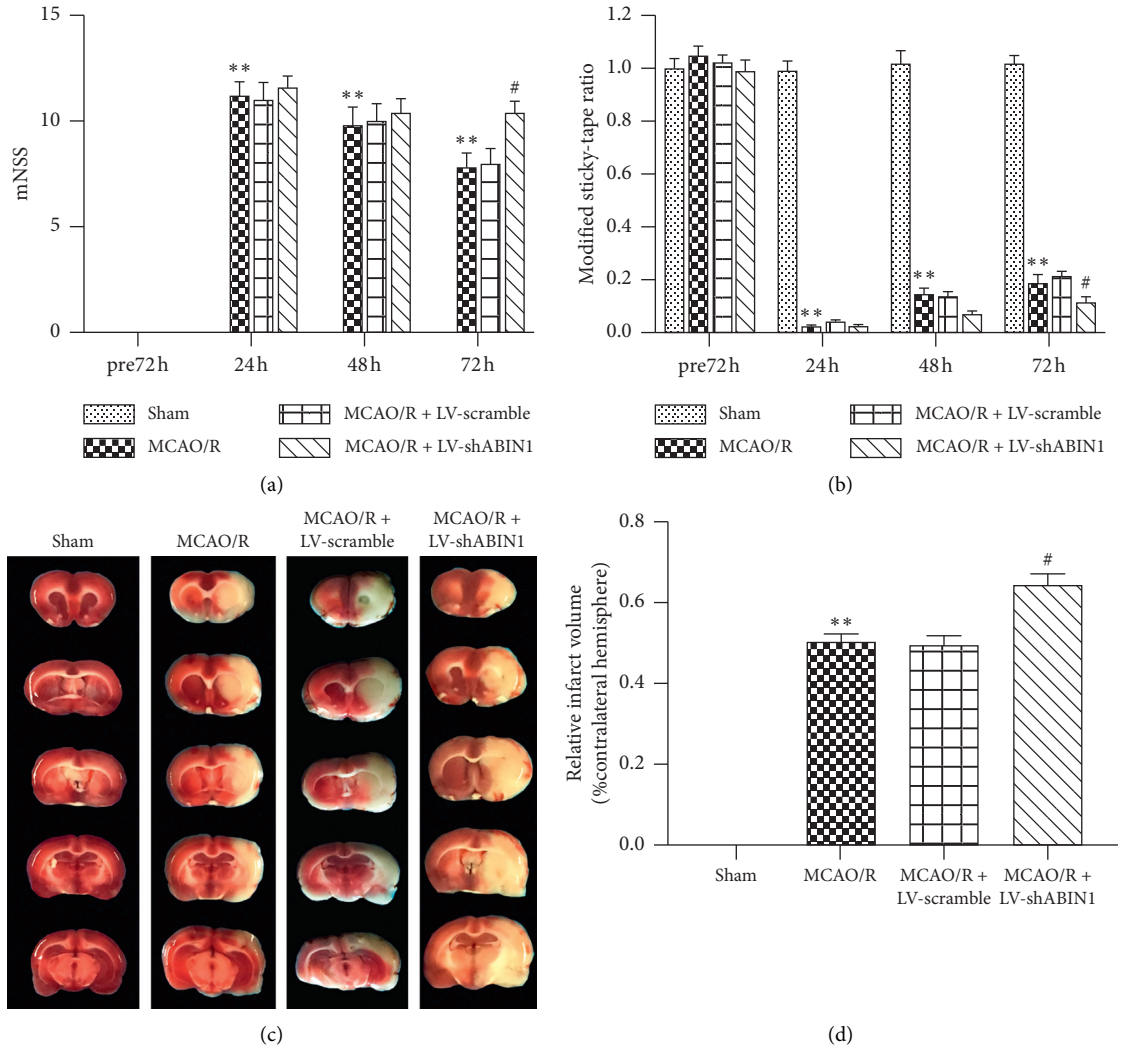

Figure 5: ABIN1 knockdown exacerbates the neurological deficits and enlarges the infarct volume. (a and b) The mNSS and MST were, respectively, analyzed at 72 h before and 24, 48, and 72 h after reperfusion ($n = 5$ rats per group). (c) Brain tissue sections were stained with TTC at 72 h after reperfusion ($n = 5$ rats per group). (d) The infarct volume is presented as a percentage of the intact hemisphere ($^{**}P < 0.01$ compared to the sham group; $^{\#}P < 0.05$ compared to the MCAO/R group).

activation, levels of the ABIN1, p-IκBα, IκBα, and nuclear/cytoplasmic NF-κB p65 proteins were measured in the peri-infarct cortex at 24 h after reperfusion using western blot and the nuclear translocation of NF-κB p65 was observed using immunofluorescence staining. EA significantly increased the level of the ABIN1 protein and decreased the p-IκBα/IκBα ratio and NF-κB p65 nuclear translocation compared with the MCAO/R group (Figures 8(a)–8(d)). However, ABIN1 knockdown diminished the anti-inflammatory effect of EA as observed that p-IκBα/IκBα ratio was increased and NF-κB p65 nuclear translocation was enhanced in the MCAO/R + EA + LV-shABIN1 group compared with the MCAO/R + EA group (Figures 8(a)–8(d)). The levels of these proteins were not significantly different between the MCAO/R + EA + LV-scramble group and the MCAO/R + EA group (Figures 8(a)–8(d)). Hence, EA may inhibit NF-κB activation by upregulating ABIN1 expression.

4. Discussion

EA plays a beneficial role in ischemic stroke, but the mechanism of EA needs further research [43]. In the present study, we showed for the first time that ABIN1 was induced in MCAO/R rats. ABIN1 knockdown aggravated cerebral I/R injury by promoting activation of microglia and releasing proinflammatory factors (TNF-α, IL-1β, and MCP-1). Moreover, upregulation of ABIN1 expression was essential for EA to inhibit NF-κB related neuroinflammatory damage after cerebral I/R.

ABIN1 mRNA is highly expressed in human peripheral lymphocytes, skeletal muscle, and spleen, and its polymorphisms are associated with autoimmune diseases [15]. We assessed the expression of ABIN1 in the early phase of cerebral I/R. The ABIN1 mRNA and protein were expressed in the cerebral cortex of the sham group, indicating that ABIN1 is constitutively expressed in the cerebral

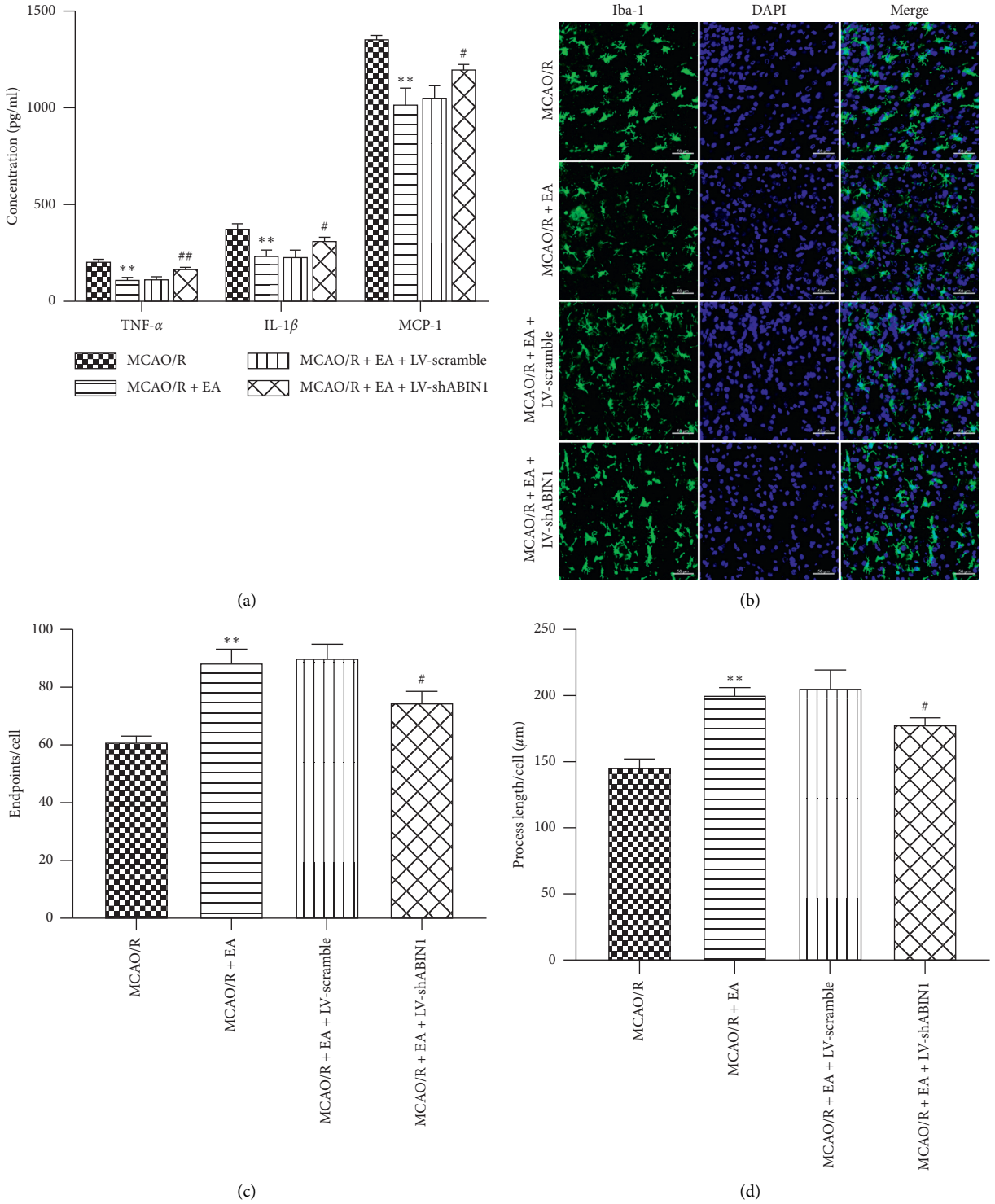

Figure 6: ABIN1 knockdown impairs the antineuroinflammatory effect of EA. (a) The concentrations of TNF-α, IL-1β, and MCP-1 in the peri-infarct cortex were detected using ELISAs at 24 h after reperfusion ($n = 5$ rats per group). (b) Microglial morphology was observed by conducting immunofluorescence staining for Iba-1 (green) in the peri-infarct cortex at 24 h after reperfusion ($n = 3$ rats per group). Scale bar = 50 μm. (c and d) Quantification of microglial endpoints/cell and process length/cell ($^{**}P < 0.01$ compared to the MCAO/R group; $^{\#}P < 0.05$ and $^{\#\#}P < 0.01$ compared to the MCAO/R + EA group).

cortex under normal conditions. In addition, ABIN1 expression was induced in the peri-infarct cortex, peaking at 24 h and then gradually decreasing. NF-κB is strongly activated during cerebral ischemia in cells such as neurons, microglia, astrocytes, and endothelial cells [11, 44]. The expression of some negative regulators of NF-κB is regulated

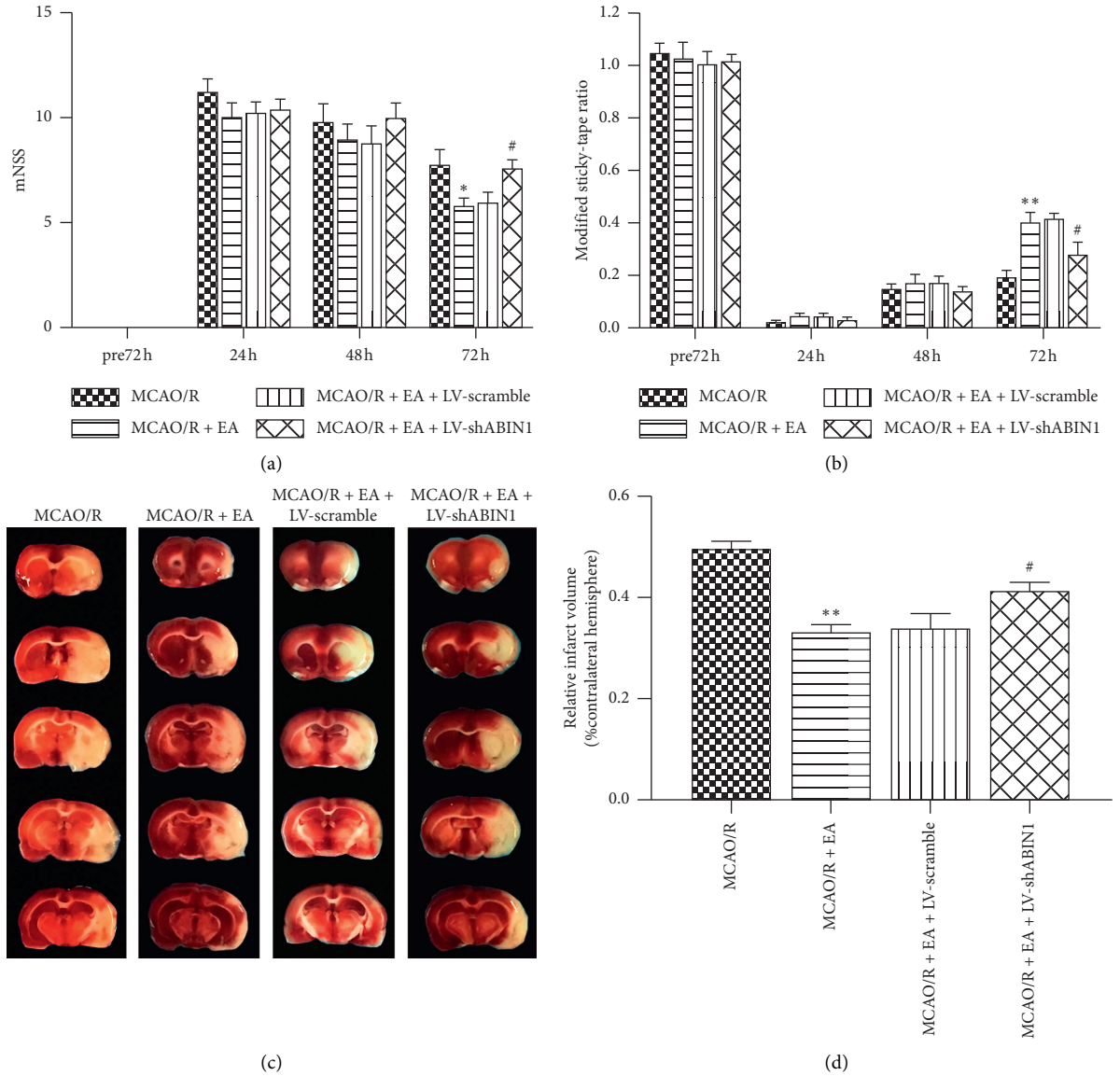

Figure 7: ABIN1 knockdown inhibits the neuroprotective effect of EA. (a-b) The mNSS and MST were recorded at 72 h before and 24, 48, and 72 h after reperfusion ($n = 5$ rats per group). (c) Brain tissue sections were stained with TTC at 72 h after reperfusion ($n = 5$ rats per group). (d) The infarct volume is presented as a percentage of the intact hemisphere ($^{*}P < 0.05$ and $^{**}P < 0.01$ compared to the MCAO/R group; $^{\#}P < 0.05$ compared to the MCAO/R + EA group).

by NF-κB to prevent its continuous activation [13, 45]. A20 is one of these negative regulators. A20 is expressed at low levels in most cells under physiological conditions, but its expression is rapidly induced upon the activation of NF-κB [46]. Similarly, ABIN1 expression is also regulated by NF-κB. The human ABIN1 gene promoter contains an NF-κB response element, and its promoter activity is regulated by NF-κB [47]. The expression of the ABIN1 mRNA is upregulated in various cell types with NF-κB activation [15]. Thus, the increase in ABIN1 expression observed in the early stage of focal cerebral I/R may be attributed to the activation of NF-κB, thus forming a negative feedback loop.

The A20 complex is expressed at higher levels in neurons than in glial cells [45, 48]. Similarly, as shown in our previous study, A20 is mainly expressed in neurons in the cortex of MCAO/R rats [32]. In the current study, we found that ABIN1 and A20 colocalized in the cytoplasm and interacted with each other in the peri-infarct cortex at 24 h. Besides, we determined the spatial distribution of ABIN1 in the peri-infarct cortex in MCAO/R rats for the first time. ABIN1 was prominently localized in neurons, followed by microglia, and no expression was observed in astrocytes at 24 h after I/R. The mechanism underlying the predominant expression of ABIN1 in neurons is unclear, but this differential distribution may be a protective strategy for neurons due to their high sensitivity to ischemia and hypoxia and limited tolerance to excessive activation of NF-κB and neuroinflammation after I/R [49].

In the early phase of cerebral I/R, damaged neurons release cytokines, chemokines and damage-associated

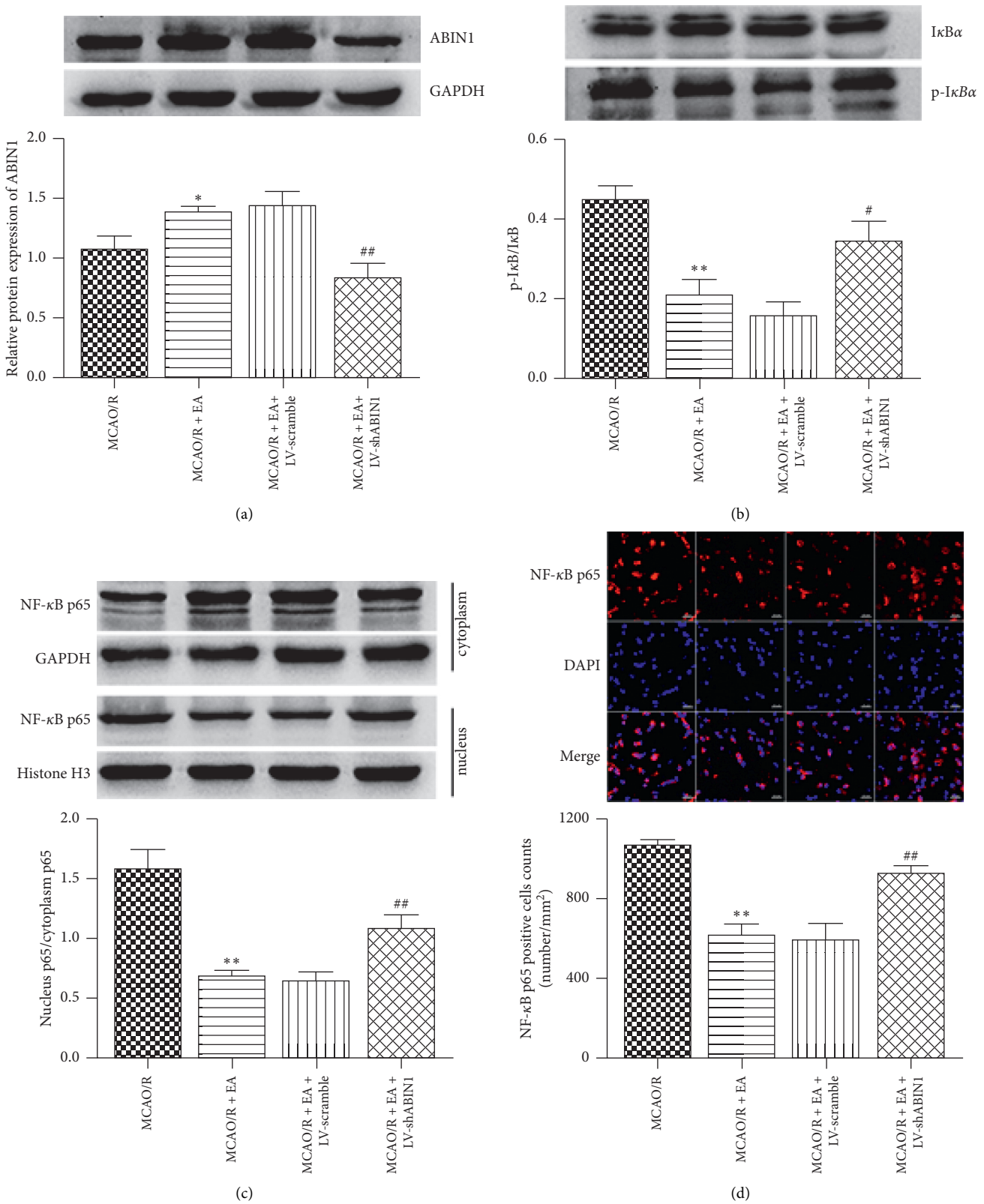

Figure 8: EA prevents NF-κB activation by upregulating ABIN1 expression. (a-c) The levels of ABIN1, p-IκBα, IκBα, nuclear NF-κB p65, and cytoplasmic NF-κB p65 proteins in the peri-infarct cortex at 24 h after reperfusion were detected using western blot. GAPDH served as the internal reference for total and cytoplasmic proteins, and histone H3 served as the internal reference for nuclear proteins ($n = 5$ rats per group). (d) The nuclear translocation of NF-κB p65 was observed with immunofluorescence staining in the peri-infarct area at 24 h after reperfusion ($n = 3$ rats per group). Scale bar = 20 μm. Column chart presenting the NF-κB p65$^+$ cell counts in the four groups ($^*P < 0.05$ and $^{**}P < 0.01$ compared to the MCAO/R group; $^{\#}P < 0.05$ and $^{\#\#}P < 0.01$ compared to the MCAO/R + EA group).

molecular patterns; microglia, the first line of defense in the brain, are activated within minutes after receiving signals from neurons [50, 51]. In the penumbra, proinflammatory microglia gradually dominate the response, resulting in an imbalance between proinflammatory and anti-inflammatory effects [52, 53]. Excessive proinflammatory factors such as TNF-α, IL-1β, and MCP-1 contribute to neuron death and the aggravation of brain damage [6, 54]. ABIN1 knockdown used lentivirus-mediated delivery of shABIN1 to investigate the effect of ABIN1 on focal cerebral I/R-induced neuroinflammation. ABIN1 knockdown increased microglial activation and proinflammatory factor production (TNF-α, IL-1β, and MCP-1), worsened neurological function, and enlarged the infarct volume. Thus, ABIN1 may confer neuroprotection by reducing inflammatory damage during cerebral I/R. However, in the MCAO/R group, the upregulation of endogenous ABIN1 expression by focal cerebral I/R is insufficient to resist strong neuroinflammation; thus, the increase in ABIN1 expression may represent a promising therapeutic strategy to alleviate neuroinflammation after cerebral I/R.

EA is a supplemental and alternative treatment for ischemic stroke that is recommended by the World Health Organization [26]. EA therapy requires a combination of specific acupoints and electrical stimulation. Acupoints GV 20, LI 4, and LR 3 exert the effects of tranquilization and resuscitation and are selected for treating ischemic stroke in traditional Chinese medicine [55, 56]. Our previous study showed that EA treatment at acupoints GV 20, LI 4, and LR 3 played a neuroprotective role in MCAO/R rats by suppressing NF-κB activation [31]. Subsequently, it was shown that deubiquitinating enzyme A20 was upregulated by EA to inhibit IκBα phosphorylation and prevent NF-κB p65 nuclear translocation [32]. As an adaptor protein of A20, ABIN1 has similar biological functions to A20. For example, A20- and ABIN1-deficient mice showed premature death and severe inflammation, and the SNPs of A20 and ABIN1 genes were closely related to autoimmune diseases [12, 13]. Thus, whether ABIN1 is involved in the mechanism of EA is of great interest to us. The current study revealed that EA treatment at acupoints GV 20, LI 4, and LR 3 increased the expression of ABIN1 in the peri-infarct cortex. Since sham EA is biologically inactive because of the absence of important EA elements, such as the insertion of needles into acupoints and electrical stimulation [57–60], the expression of ABIN1 in peri-infarct cortex was not altered by sham EA. Besides, we showed that EA inhibited IκBα phosphorylation, prevented NF-κB p65 nuclear translocation, suppressed neuroinflammation, and improved neurological deficits. However, the neuroprotective effect of EA was partially reversed by ABIN1 knockdown. Based on these results, it was suggested that ABIN1 was involved in the mechanism of EA in alleviating cerebral I/R inflammatory damage. As mentioned above, ABIN1 was predominantly localized in neurons in the peri-infarct cortex; thus EA may inhibit neuronal NF-κB activation by upregulating ABIN1 expression and eventually indirectly inhibit microglia aggregation and activation. Since some ABIN are also expressed in microglia, EA may reduce the production of proinflammatory factors by directly inhibiting NF-κB activation in microglia. Further research will address these hypotheses in vitro to determine the effect of ABIN1 expression levels on NF-κB activation in neurons and microglia, respectively.

5. Conclusion

In conclusion, ABIN1, which is induced in cerebral I/R, plays a neuroprotective role as an inflammatory suppressor. Furthermore, this study indicated that the EA-induced upregulation of ABIN1 expression may be an important mechanism by which EA blocks NF-κB activation to alleviate neuroinflammation after cerebral I/R.

Data Availability

The data used to support the findings of this study are available from the corresponding author upon request.

Disclosure

These funding bodies were not involved in the design of the study or collection, analysis, interpretation of data, or writing of the manuscript.

Conflicts of Interest

The authors declare that they have no conflicts of interest.

Acknowledgments

This work was supported by the National Natural Science Foundation of China (Grant no. 30470606), the National Natural Science Foundation of China Youth Fund Project (Grant no. 81403243), and the Chinese Medicine Science and Technology Project of Chongqing Municipal Health Bureau (Grant 2012-2-128).

References

[1] C. O. Johnson, M. Nguyen, G. A. Roth et al., "Global, regional, and national burden of stroke, 1990–2016: a systematic analysis for the global burden of disease study 2016," *The Lancet. Neurology*, vol. 18, no. 5, pp. 439–458, 2019.

[2] M. Goyal, B. K. Menon, W. H. van Zwam et al., "Endovascular thrombectomy after large-vessel ischaemic stroke: a meta-analysis of individual patient data from five randomised trials," *The Lancet*, vol. 387, no. 10029, pp. 1723–1731, 2016.

[3] S. I. Savitz, J.-C. Baron, M. A. Yenari, N. Sanossian, and M. Fisher, "Reconsidering neuroprotection in the reperfusion era," *Stroke*, vol. 48, no. 12, pp. 3413–3419, 2017.

[4] Á. Chamorro, U. Dirnagl, X. Urra, and A. M. Planas, "Neuroprotection in acute stroke: targeting excitotoxicity, oxidative and nitrosative stress, and inflammation," *The Lancet Neurology*, vol. 15, no. 8, pp. 869–881, 2016.

[5] H. A. Seifert and K. R. Pennypacker, "Molecular and cellular immune responses to ischemic brain injury," *Translational Stroke Research*, vol. 5, no. 5, pp. 543–553, 2014.

[6] M. Fricker, A. M. Tolkovsky, V. Borutaite, M. Coleman, and G. C. Brown, "Neuronal cell death," *Physiological Reviews*, vol. 98, no. 2, pp. 813–880, 2018.

[7] K. Shi, D.-C. Tian, Z.-G. Li, A. F. Ducruet, M. T. Lawton, and F.-D. Shi, "Global brain inflammation in stroke," *The Lancet Neurology*, vol. 18, no. 11, pp. 1058–1066, 2019.

[8] L. Wu, X. Xiong, X. Wu et al., "Targeting oxidative stress and inflammation to prevent ischemia-reperfusion injury," *Frontiers in Molecular Neuroscience*, vol. 13, 2020.

[9] O. A. Harari and J. K. Liao, "NF-κB and innate immunity in ischemic stroke," *Annals of the New York Academy of Sciences*, vol. 1207, no. 1, pp. 32–40, 2010.

[10] S. Miyamoto, "Nuclear initiated NF-κB signaling: NEMO and ATM take center stage," *Cell Research*, vol. 21, no. 1, pp. 116–130, 2011.

[11] D. A. Ridder and M. Schwaninger, "NF-κB signaling in cerebral ischemia," *Neuroscience*, vol. 158, no. 3, pp. 995–1006, 2009.

[12] R. T. G'Sell, P. M. Gaffney, and D. W. Powell, "Review: A20-binding inhibitor of NF-κB activation 1 is a physiologic inhibitor of NF-κB: a molecular switch for inflammation and autoimmunity," *Arthritis & Rheumatology*, vol. 67, no. 9, pp. 2292–2302, 2015.

[13] A. Ma and B. A. Malynn, "A20: linking a complex regulator of ubiquitylation to immunity and human disease," *Nature Reviews Immunology*, vol. 12, no. 11, pp. 774–785, 2012.

[14] C. Mauro, F. Pacifico, A. Lavorgna et al., "ABIN-1 binds to NEMO/IKKγ and Co-operates with A20 in inhibiting NF-κB," *Journal of Biological Chemistry*, vol. 281, no. 27, pp. 18482–18488, 2006.

[15] L. Verstrepen, I. Carpentier, K. Verhelst, and R. Beyaert, "ABINs: A20 binding inhibitors of NF-κB and apoptosis signaling," *Biochemical Pharmacology*, vol. 78, no. 2, pp. 105–114, 2009.

[16] J. Zhou, R. Wu, A. A. High et al., "A20-binding inhibitor of NF-κB (ABIN1) controls toll-like receptor-mediated CCAAT/enhancer-binding protein beta activation and protects from inflammatory disease," *Proceedings of the National Academy of Sciences*, vol. 108, no. 44, pp. E998–E1006, 2011.

[17] S. Oshima, E. E. Turer, J. A. Callahan et al., "ABIN-1 is a ubiquitin sensor that restricts cell death and sustains embryonic development," *Nature*, vol. 457, no. 7231, pp. 906–909, 2009.

[18] Y. Zhang, X. Lei, W. Li et al., "TNIP1 alleviates hepatic ischemia/reperfusion injury via the TLR2-Myd88 pathway," *Biochemical and Biophysical Research Communications*, vol. 501, no. 1, pp. 186–192, 2018.

[19] K. El Bakkouri, A. Wullaert, M. Haegman, K. Heyninck, and R. Beyaert, "Adenoviral gene transfer of the NF-κB inhibitory protein ABIN-1 decreases allergic airway inflammation in a murine asthma model," *Journal of Biological Chemistry*, vol. 280, no. 18, pp. 17938–17944, 2005.

[20] E. A. Korte, D. J. Caster, M. T. Barati et al., "ABIN1 determines severity of glomerulonephritis via activation of intrinsic glomerular inflammation," *The American Journal of Pathology*, vol. 187, no. 12, pp. 2799–2810, 2017.

[21] J. A. Callahan, G. E. Hammer, A. Agelides et al., "Cutting edge: ABIN-1 protects against psoriasis by restricting MyD88 signals in dendritic cells," *The Journal of Immunology*, vol. 191, no. 2, pp. 535–539, 2013.

[22] K. Peng, Y. Li, C. Lu, and S. Hu, "ABIN-1 protects chondrocytes from lipopolysaccharide-induced inflammatory injury through the inactivation of NF-κB signalling," *Clinical and Experimental Pharmacology and Physiology*, vol. 47, no. 7, pp. 1212–1220, 2020.

[23] Y. Xing, M. Zhang, W. B. Li, F. Dong, and F. Zhang, "Mechanisms involved in the neuroprotection of electroacupuncture therapy for ischemic stroke," *Front Neurosci*, vol. 12, p. 929, 2018.

[24] L. Ulloa, S. Quiroz-Gonzalez, and R. Torres-Rosas, "Nerve stimulation: immunomodulation and control of inflammation," *Trends in Molecular Medicine*, vol. 23, no. 12, pp. 1103–1120, 2017.

[25] J.-Y. Park and U. Namgung, "Electroacupuncture therapy in inflammation regulation: current perspectives," *Journal of Inflammation Research*, vol. 11, pp. 227–237, 2018.

[26] L. M. Chavez, S. S. Huang, I. MacDonald, J. G. Lin, Y. C. Lee, and Y. H. Chen, "Mechanisms of acupuncture therapy in ischemic stroke rehabilitation: a literature review of basic studies," *International Journal of Molecular Sciences*, vol. 18, no. 11, Article ID E2270, 2017.

[27] L. Chi, K. Du, D. Liu, Y. Bo, and W. Li, "Electroacupuncture brain protection during ischemic stroke: a role for the parasympathetic nervous system," *Journal of Cerebral Blood Flow & Metabolism*, vol. 38, no. 3, pp. 479–491, 2017.

[28] M. H. Shen, C. B. Zhang, J. H. Zhang, and P. F. Li, "Electroacupuncture attenuates cerebral ischemia and reperfusion injury in middle cerebral artery occlusion of rat via modulation of apoptosis, inflammation, oxidative stress, and excitotoxicity," *Evidence-Based Complementary and Alternative Medicine*, vol. 2016, Article ID 9438650, 15 pages, 2016.

[29] Z. Jin, J. Liang, J. Wang, and P. E. Kolattukudy, "Delayed brain ischemia tolerance induced by electroacupuncture pretreatment is mediated via MCP-induced protein 1," *Journal of Neuroinflammation*, vol. 10, no. 63, Article ID 845, 2013.

[30] L. Lan, J. Tao, A. Chen et al., "Electroacupuncture exerts anti-inflammatory effects in cerebral ischemia-reperfusion injured rats via suppression of the TLR4/NF-κB pathway," *International Journal of Molecular Medicine*, vol. 31, no. 1, pp. 75–80, 2013.

[31] W. Y. Qin, Y. Luo, L. Chen et al., "Electroacupuncture could regulate the NF-κB signaling pathway to ameliorate the inflammatory injury in focal cerebral ischemia/reperfusion model rats," *Evidence-Based Complementary and Alternative Medicine*, vol. 2013, Article ID 924541, 15 pages, 2013.

[32] J. Zhan, W. Qin, Y. Zhang et al., "Upregulation of neuronal zinc finger protein A20 expression is required for electroacupuncture to attenuate the cerebral inflammatory injury mediated by the nuclear factor-kB signaling pathway in cerebral ischemia/reperfusion rats," *Journal of Neuroinflammation*, vol. 13, no. 1, p. 258, 2016.

[33] J. Jiang, Y. Luo, W. Qin et al., "Electroacupuncture suppresses the NF-κB signaling pathway by upregulating cylindromatosis to alleviate inflammatory injury in cerebral ischemia/reperfusion rats," *Frontiers in Molecular Neuroscience*, vol. 10, p. 363, 2017.

[34] K. Zhang, Q. Zhang, J. Deng et al., "ALK5 signaling pathway mediates neurogenesis and functional recovery after cerebral ischemia/reperfusion in rats via Gadd45b," *Cell Death & Disease*, vol. 10, no. 5, p. 360, 2019.

[35] X. Han, H. Wu, P. Yin et al., "Electroacupuncture restores hippocampal synaptic plasticity via modulation of 5-HT receptors in a rat model of depression," *Brain Research Bulletin*, vol. 139, pp. 256–262, 2018.

[36] J. Chen, P. R. Sanberg, Y. Li et al., "Intravenous administration of human umbilical cord blood reduces behavioral deficits after stroke in rats," *Stroke*, vol. 32, no. 11, pp. 2682–2688, 2001.

[37] R. J. Komotar, G. H. Kim, M. E. Sughrue et al., "Neurologic assessment of somatosensory dysfunction following an

experimental rodent model of cerebral ischemia," *Nature Protocols*, vol. 2, no. 10, pp. 2345–2347, 2007.

[38] J. Agulla, D. Brea, F. Campos et al., "In vivo theranostics at the peri-infarct region in cerebral ischemia," *Theranostics*, vol. 4, no. 1, pp. 90–105, 2013.

[39] H. Xu, W. Qin, X. Hu et al., "Lentivirus-mediated overexpression of OTULIN ameliorates microglia activation and neuroinflammation by depressing the activation of the NF-κB signaling pathway in cerebral ischemia/reperfusion rats," *Journal of Neuroinflammation*, vol. 15, no. 1, p. 83, 2018.

[40] S. E. Taylor, C. Morganti-Kossmann, J. Lifshitz et al., "Rod microglia: a morphological definition," *PLoS One*, vol. 9, no. 5, Article ID e97096, 2014.

[41] H. W. Morrison and J. A. Filosa, "A quantitative spatiotemporal analysis of microglia morphology during ischemic stroke and reperfusion," *Journal of Neuroinflammation*, vol. 10, p. 4, 2013.

[42] K. Young and H. Morrison, "Quantifying microglia morphology from photomicrographs of immunohistochemistry prepared tissue using ImageJ," *Journal of Visualized Experiments: JoVE*, vol. 136, Article ID e57648, 2018.

[43] W. Zhu, Y. Ye, Y. Liu et al., "Mechanisms of acupuncture therapy for cerebral ischemia: an evidence-based review of clinical and animal studies on cerebral ischemia," *Journal of Neuroimmune Pharmacology*, vol. 12, no. 4, pp. 575–592, 2017.

[44] F.-P. Huang, Z.-Q. Wang, D.-C. Wu, G. P. Schielke, Y. Sun, and G.-Y. Yang, "Early NFκB activation is inhibited during focal cerebral ischemia in interleukin-1β-converting enzyme deficient mice," *Journal of Neuroscience Research*, vol. 73, no. 5, pp. 698–707, 2003.

[45] E. L. Pranski, N. V. Dalal, J. H. Herskowitz et al., "Neuronal RING finger protein 11 (RNF11) regulates canonical NF-κB signaling," *Journal of Neuroinflammation*, vol. 9, p. 247, 2012.

[46] L. Catrysse, L. Vereecke, R. Beyaert, and G. van Loo, "A20 in inflammation and autoimmunity," *Trends in Immunology*, vol. 35, no. 1, pp. 22–31, 2014.

[47] I. Gurevich, C. Zhang, P. C. Encarnacao, C. P. Struzynski, S. E. Livings, and B. J. Aneskievich, "PPARγ and NF-κB regulate the gene promoter activity of their shared repressor, TNIP1," *Biochim Biophys Acta*, vol. 1819, no. 1, pp. 1–15, 2012.

[48] E. L. Pranski, C. D. Van Sanford, N. V. Dalal et al., "Comparative distribution of protein components of the A20 ubiquitin-editing complex in normal human brain," *Neuroscience Letters*, vol. 520, no. 1, pp. 104–109, 2012.

[49] B. Puig, S. Brenna, and T. Magnus, "Molecular communication of a dying neuron in stroke," *International Journal of Molecular Sciences*, vol. 19, no. 9, Article ID 2834, 2018.

[50] Y. Fu, Q. Liu, J. Anrather, and F.-D. Shi, "Immune interventions in stroke," *Nature Reviews Neurology*, vol. 11, no. 9, pp. 524–535, 2015.

[51] S. P. Gadani, J. T. Walsh, J. R. Lukens, and J. Kipnis, "Dealing with danger in the CNS: the response of the immune system to injury," *Neuron*, vol. 87, no. 1, pp. 47–62, 2015.

[52] L.-y. Ao, Y.-Y. Yan, L. Zhou et al., "Immune cells after ischemic stroke onset: roles, migration, and target intervention," *Journal of Molecular Neuroscience*, vol. 66, no. 3, pp. 342–355, 2018.

[53] X. Hu, P. Li, Y. Guo et al., "Microglia/macrophage polarization dynamics reveal novel mechanism of injury expansion after focal cerebral ischemia," *Stroke*, vol. 43, no. 11, pp. 3063–3070, 2012.

[54] D. Amantea, G. Nappi, G. Bernardi, G. Bagetta, and M. T. Corasaniti, "Post-ischemic brain damage: pathophysiology and role of inflammatory mediators," *FEBS Journal*, vol. 276, no. 1, pp. 13–26, 2009.

[55] F. Wan, X. Niu, Y.-L. Song, and Y.-C. Si, "The role of Chinese herbs and acupuncture on the inflammation reaction after cerebral ischemia," *Current Pharmaceutical Design*, vol. 22, no. 6, pp. 709–719, 2016.

[56] R. Ma, B. Yuan, J. Du et al., "Electroacupuncture alleviates nerve injury after cerebra ischemia in rats through inhibiting cell apoptosis and changing the balance of MMP-9/TIMP-1 expression," *Neuroscience Letters*, vol. 633, pp. 158–164, 2016.

[57] Z. X. Chen, Y. Li, X. G. Zhang et al., "Sham electroacupuncture methods in randomized controlled trials," *Scientific Reports*, vol. 7, Article ID 40837, 2017.

[58] R. Sha, B. Zhang, X. Han et al., "Electroacupuncture alleviates ischemic brain injury by inhibiting the miR-223/NLRP3 pathway," *Medical Science Monitor*, vol. 25, pp. 4723–4733, 2019.

[59] J. Huang, X. You, W. Liu et al., "Electroacupuncture ameliorating post-stroke cognitive impairments via inhibition of peri-infarct astroglial and microglial/macrophage P2 purinoceptors-mediated neuroinflammation and hyperplasia," *BMC Complementary and Alternative Medicine*, vol. 17, no. 1, 2017.

[60] Y. Wang, Y. Shen, H. P. Lin, Z. Li, Y. Y. Chen, and S. Wang, "Large-conductance Ca(2+)-activated K(+) channel involvement in suppression of cerebral ischemia/reperfusion injury after electroacupuncture at Shuigou (GV26) acupoint in rats," *Neural Regeneration Research*, vol. 11, no. 6, pp. 957–962, 2016.

Hindawi
Evidence-Based Complementary and Alternative Medicine
Volume 2020, Article ID 6415083, 9 pages
https://doi.org/10.1155/2020/6415083

Research Article

The Therapeutic Effect of Electroacupuncture Therapy for Ischemic Stroke

Bao-Hai Yu,[1] Ying Xing,[2] and Feng Zhang [2,3]

[1]*Department of Radiology, The Third Hospital of Hebei Medical University, Shijiazhuang 050051, China*
[2]*Department of Rehabilitation Medicine, The Third Hospital of Hebei Medical University, Shijiazhuang 050051, China*
[3]*Hebei Provincial Orthopedic Biomechanics Key Laboratory, The Third Hospital of Hebei Medical University, Shijiazhuang 050051, China*

Correspondence should be addressed to Feng Zhang; ydsyzf@hebmu.edu.cn

Received 5 July 2020; Revised 9 September 2020; Accepted 18 September 2020; Published 29 September 2020

Academic Editor: Mark Moss

Electroacupuncture (EA) stimulation is a supplementary therapy and commonly applied in treatment of ischemic stroke in clinic. Stroke is an important cause of long-term disability in individuals in both developing and developed countries. In our review, we show the application of EA stimulation for apoplectic pain, limbs spasticity, blood flow interruption, depression, swallowing dysfunction, aphasia, urinary incontinence, cognition and memory impairment, and constipation following stroke in patients and the related mechanisms in animals. The effectiveness of EA involves with acupoints, intensity, intervals, and duration of intervention for treatment of stroke. The combination of EA and common rehabilitation treatment may exert better effect compared with EA alone. In summary, EA might provide a potential treatment strategy for treating apoplectic patients in clinic.

1. Introduction

Ischemic stroke is a usual cerebrovascular illness and a leading cause of disabilities and death worldwide, accounting for approximately 87% of all stroke patients. Also known as brain attack, patients may suddenly suffer from incoherent speech, paralysis, or loss of vision owing to interrupting blood flow (ischemia) resulted from embolism or thrombosis [1]. Ischemic stroke induces a decrease in cerebral blood flow, which is enough to impair normal cellular function [2, 3]. Fast reperfusion is a crucial therapy method for patients with acute ischemic stroke but usually results in cerebral ischemia/reperfusion injury [4]. Therefore, a feasible therapeutic method that attenuates the poststroke neural deficits still is essential in the clinical setting. Acupuncture has been used in treating cerebral diseases and mental disorders for a long time [5, 6]. Electroacupuncture (EA) is another type of acupuncture, originating from the combination of acupuncture and electrical stimulation. As a relatively feasible, simple, and cheap therapy, it is commonly accepted by stroke patients in clinic [7]. The clinical effectiveness of EA in stroke rehabilitation has been demonstrated in numerous studies [8–10].

2. The Therapeutic Effect of EA for Ischemic Stroke in Experimental Animals

2.1. The Effect of EA on Neurocytes in Animals. EA may prompt neuronal regeneration, migration of newborn neuron, and their maturation in the ischemic brain striatum of rats [11]. EA stimulation at Dazhui (GV 14) and Baihui (GV 20) four-day postischemia (subacute stage) can enhance astrogliosis and neurogenesis, which likely contributed to long-term functional recovery after focal cerebral ischemia [12]. Deng et al. show that EA stimulation may increase new projections and axon regeneration from the corticospinal tract at 28 d following ischemic stroke in rats [13]. The vagus dorsal motor nucleus, as the largest origin of parasympathetic preganglionic neurons, may be activated by EA in the lower brainstem, and parasympathetic dysfunction may inhibit these abovementioned alterations, indicating that EA may be an alternative therapy to activate the

parasympathetic nervous system after stroke [14]. Han et al. indicate that EA may be involved in activation of astrocytes in peri-ischemic brain, promotion of the recovery of behavioral deficits, and prevention of excess reactive gliosis after ischemic stroke [15]. EA stimulation at Renzhong may exert benefits in improvement of motor function and the motor cortical excitability following ischemic stroke [16]. Si et al. show that EA may prompt somatosensory evoked potential of rats following ischemic stroke [17]. EA treatment at points of Quchi and Zusanli can increase the functional connectivity between the ipsilateral motor cortex and the motor function-related brain regions, consisting of the motor cortex, striatum, and sensory cortex in focal ischemic rats [18].

2.2. The Effect of EA on Cerebral Angiogenesis and Blood Flow in Animals. Du et al. suggest that EA might play a crucial role on promotion of angiogenesis in cerebral ischemic rats [19]. Shi et al. also show that EA at Shuigou (GV26) enhances angiogenesis and establishment of collateral circulation and prompts neurological function [20]. Increased expression of apelin-APJ protein and mRNA induced by EA (15 Hz, 2 mA) applied at Shuigou (GV 26) exerted a crucial role in cerebral ischemic rats which maybe involved in facilitated collateral circulation and blood vessel regeneration [21]. EA at Yin meridian acupoints can significantly facilitate neurobehavioural functional recovery, which is associated with increased vascular density and enhanced vascular endothelial growth factor (VEGF) expression and protein kinase B/endothelial nitric oxide synthase (Akt/eNOS) phosphorylation in the peri-ischemia cortex of rats [22]. Liu et al. show that EA can balance miRNA levels, such as mir-328 and mir-126, so as to promote angiogenesis in ischemic cortex via regulating expression of VEGF family genes and proteins [23]. Furthermore, Hsieh et al. show that EA with a frequency of 2 and 15 Hz at Zusanli acupoints in both two legs may lead to the enhancement of cerebral blood flow in normal or ischemic stroke rat [24]. Zhou et al. demonstrate that EA intervention may exert brain protection via rapidly upregulating blood flow of the infarction region [25].

2.3. The Effect of EA on Improving Motor Dysfunction of Animals. EA with low frequency at Shuigou acupoint may exert obvious effect to prompt motor functional recovery in rats following ischemic stroke [26]. Liu and Lai demonstrate that EA plays a critical role in treatment of ischemic brain injury in the early stage of stroke and may effectively alleviate ischemic pathological damage, infarct volume, and neurologic deficit [27]. Liu et al. also suggest that EA at the points of ST36 and LI11 may reduce the infarct volumes, alleviate neurological deficit, and improve motor dysfunction [28]. It should be noted that many clinical research has identified that there can be no direct evidence/relationship between the infarct volume change/difference and the functional recovery. Therefore, rationale of reduction in the infarct volume by electroacupuncture therapy is not clear.

2.4. The Effect of EA on Autophagy and Apoptosis in Animals. EA treatment at points of Quchi and Zusanli can exert protective effects in rats with cerebral ischemia/reperfusion injury, associating with the inhibition of neuronal autophagy and apoptosis through activating the PI3K/AKT/mTOR pathway [29]. EA may also effectively alleviate central poststroke pain and suppress autophagy in the hippocampus through reducing β-catenin/COX-2 protein levels [30]. Xing et al. show that the neuroprotective effect induced by EA treatment against cell apoptosis in ischemic brain might associated with upregulation of midkine and regulation of ERK/JNK/$p38$ signal pathway [31].

2.5. The Effect of EA on Cerebral Edema and Blood-Brain Barrier (BBB) in Animals. Jung et al. show that EA pretreatment alleviates cerebral edema and blood-brain barrier (BBB) destruction, which may improve neural function. The BBB recovery by EA pretreatment might be associated with reduction of NOX4 expression and ROS generation [32]. Zhang et al. show that EA may improve brain edema in rats with ischemic stroke [33]. The inhibition of cerebral edema and BBB permeability induced by EA pretreatment was correlated with inhibition of p-caveolin-1 expression and alleviation of tight junction protein degradation and in the endothelial cells [34].

2.6. The Effect of EA on Other Aspects in Animals. Acupuncture treatment is a crucial part of Chinese traditional medicine and its feasible analgesic effect is widely accepted worldwide [35]. Lin et al. show that EA at Shenting and Baihui acupoints exerts a beneficial effect in promoting the cognitive function recovery after cerebral ischemic stroke [36]. EA may decrease the episodes of spreading depression after cerebral ischemic stroke, which may involve in the reduction of infarct volume of ischemic brain [36]. EA at Shuigou (GV26) significantly improved the neurological deficit symptoms in rats with ischemic stroke, which may be involved in upregulating Wnt7a and LEF1 proteins and mRNAs levels and decreasing GSK-3β and DKK1 proteins and mRNAs levels [37]. Jiang et al. showed a novel anti-inflammatory mechanism induced by EA via α7nAChR-mediated inhibition of NLRP3 inflammasome in rats after cerebral ischemic injury [38].

3. The Therapeutic Effect of EA for Ischemic Stroke in Clinic

3.1. The Effect of EA on Central Nervous System in Stroke Patients. EA at head acupoints in stroke patients may contribute to the stimulation of nerve tissue involved with motion via activating the bilateral cerebral motor areas. Furthermore, in six right-handed stroke patients, EA stimulation at Baihui (GV 20) and right Qubin for twenty minutes may also activate other neural regions, suggesting that injured motor functional reorganization is a neural network behavior, and EA may affect several aspects of neural network so as to further promote motor function recovery [39]. Both exercise and EA may promptly improve

somatosensory evoked potential of stroke patients in the recovery stage, and the Bobath therapy in combination with EA stimulation was proved to improve cerebral function in stroke patients [40]. Si et al. suggest that EA may improve the neurological function in patients with acute ischemic stroke [17]. Ho et al. demonstrate that EA exerts beneficial effects in stroke, and it might be a suitable nondrug therapy for mobilization of stem cells in CNS [41]. Ouyang et al. suggest that EA of 2/15 Hz and 100 Hz exerts better benefits in improving brain cell functions and local cerebral blood perfusion than that of EA of 2 Hz according to the results of single photon emission computed tomography (SPECT) [42].

3.2. The Effect of EA on Poststroke Psychological Illness following Stroke. Man et al. suggest that the dense cranial EA intervention combined with body acupuncture with 2 Hz at 9 volts for 30 minutes at Baihui (GV 20), Yintang (EX-HN 3), Hegu (LI 4), and Quchi (LI 11) might be a feasible therapy for poststroke neuropsychiatric sequelae [43]. Wu and Liu demonstrate that acupuncture at Taichong (LR 3), Shenting (GV 24), GV20, EX-HN 3, GV26, and LI 4, as an effective and crucial therapy, may effectively improve the symptom of poststroke anxiety neurosis (PSAN). The total effective rate of acupuncture stimulation was 82.35% [44]. Tang et al. suggest that the low-frequency EA treatment at the aupoints of Dazhui (GV 14) and Shenshu (BL 23) exerts similar effect for poststroke insomnia to oral medication of estazolam as a secure and effective therapy [45].

Poststroke depression (PSD) is characterized by anxiety, disordered sleep, hopelessness, and lowered responsiveness and is a common stroke complication [46]. Cai et al. show that EA stimulation might be safe and effective for treating poststroke depression (PSD) in clinic [8]. Acupuncture plus auricular point sticking are effective and safe for poststroke depression (PSD). During course of treatment, acupuncture was applied at Baihui (GV 20), Shenting (GV 24), Sishencong (EX-HN 1), Yintang (GV 29), Neiguan (PC 6), Shenmen (HT 7), Taichong (LR 3), Zusanli (ST 36), Hegu (LI 4), Fenglong (ST 40), and Sanyinjiao (SP 6). This combination treatment may improve the clinical symptoms as evidenced by lowered scores, including the sleep disturbance factor, anxiety/somatization factor, and hopelessness factor [47]. EA plus body acupuncture has positive effect on alleviating PSD and cognitive deterioration after stroke, particularly with electrical stimulation on forehead acupoints [48]. Wrist-ankle acupuncture plus fluoxetine can mitigate the depression symptoms after stroke. Moreover, wrist-ankle acupuncture stimulation can increase the antidepressant effect of fluoxetine [49].

3.3. The Effect of EA on Improving Spasticity following Stroke. Spasm is the commonest poststroke complication, and its occurrence rate is 20–40 percent in stroke survivors [50]. Moon et al. demonstrate that EA at Shousanli (LI 10), Waiguan (TE 5), LI 11, and LI 4 may transiently alleviate spasticity following stroke, and repeated EA stimulation may sustain the effect of mediating spasticity [51]. Wu indicates that EA treatment at the nerve trunk may significantly facilitate the limbs functional recovery and reduce the rate of disability at the spastic phase of poststroke hemiplegic patients [52]. In addition, the combined application of EA and acupuncture produced a better effect in improving hand spasm, alleviating hand dysfunction and upregulating the quality of life for patients with stroke compared with simple acupuncture [10]. Furthermore, the combination of EA and rehabilitation therapy plays a critical role in regulating lower limbs spasticity in poststroke patients [53]. Wang et al. show that 6-week EA at Zeqian (EX-UE, A32), Shounizhu (EX-UE), Shaohai (HT3), and Neiguan (PC6) in affected side, combined with standard rehabilitation treatment, may decrease the elbow spasticity of chronic stroke survivors [54]. EA at LI 4, Houxi (SI 3), TE 5, LI 11, LI 10, and Jianyu (LI 15), in combination with muscle strengthening training for 6 weeks, may obviously alleviate spasticity of the wrist joint in chronic stroke patients [55]. Liu et al. show that EA plus strength training may promote motor function recovery and alleviate muscle spasticity for moderate or severe muscle spasticity in chronic stroke patients [56].

3.4. The Effect of EA on Improving Limbs Function following Stroke. According to enhancement of the upper limbs function, traditional Chinese acupuncture may be beneficial for improving chronic stroke symptoms in patients [57]. Zhao et al. also show that Jingjin acupuncture at GV 26, GV 20, and PC 6 may effectively enhance daily-life ability via improving subtle activity of hemiplegic hand in the phase of poststroke recovery [58]. However, Yang et al. demonstrated that EA therapy may exert beneficial effect in the upper-extremity function following ischemic stroke and provide a better effect than simple manual acupuncture [59]. Hsieh et al. indicate that EA at GV 20, Fengchi (GB 20), LI 15, LI 11, LI 4, Fengshi (GB 31), Yanglingquan (GB 34), and ST 36 on the affected side, may effectively promote motor function recovery, particularly in upper extremity motor function and in patients with the primary ischemic stroke [60]. EA at LI 15, LI 4, TE 5, and LI 10, combined with exercise training, may improve arms and legs function in poststroke hemiplegia patients [61]. Moreover, Liu and Xiao show that EA at Juci and Tanci may improve nail-bed microcirculation in hemiplegic side of poststroke patients, and the effect of Juci stimulation is better Tanci stimulation [62]. Wang suggests that EA at acupoints of different channels exerts benefits on poststroke hemiplegia patients at different stages of stroke [63].

Chen et al. suggest that EA as a supplemental therapy may exert benefits in apoplexy patients with shoulder subluxation [64]. EA treatment at Jianwaishu (SI 14), Jianzhen (SI 9), Naoshu (SI 10), Binao (LI 14), and Bingfeng (SI 12) with intermittent wave and common rehabilitation therapy exerts a better effect compared to continuous and disperse-dense wave for the treatment of shoulder subluxation, and the combination treatment may effectively prompt shoulder functional recovery and improve subluxation [65]. The combination of EA at LI 15, Jianliao (TE 14), and SI 9 and rehabilitation techniques also may exert

benefits in regulating the muscular tension of shoulder joint and the muscles around the scapula and muscle strength and improving the shoulder subluxation [66].

In addition, acupuncture intervention at lateral side of BL 10 associated with scalp points, including Zhenxiapangxian (MS 14) and Dingnieqianxiexian (MS 6), plays a critical role in walking ability and standing balance ability after stroke [67]. EA at bilateral MS 6 plays important role in recovery of nerve defects in the hemiplegic patients following acute ischemic brain injury, enhancing limb motor function and the daily-life activity ability [68]. EA (20 Hz, 2 mA) at GV 20, EX-HN 3, GV 26, LI 4, ST 36, SP 6, and Taichong(LR 3), with cupping at the lumboback, exerts a better effect than medication in relief of fatigue in poststroke patients [69]. Liu et al. indicated that EA at Pishu (BL 20), Shenshu (BL 23), Dachangshu (BL 25), and Qihaishu (BL 24) may elevate the single-foot supporting phase rate in stroke patients [70].

3.5. The Effect of EA on Improving Swallowing after Stroke. EA stimulation as a feasible and effective therapy may alleviate swallowing dysfunction following stroke at Chonggu acupoints with deep insertion [71]. EA treatment integrated with swallowing functional training may promote the recovery of swallowing ability in poststroke patients with dysphagia [9]. However, Huang et al. show that either electric stimulation or acupuncture at GB 20, LI 18, three-needles on the forehead, etc. combined with rehabilitation training exerts a better effect compared with simple rehabilitation training. The effect of acupuncture in dysphagia is equal to that of electric stimulation [72]. EA at eight-neck-occiput acupoints exerts a better effect on improving swallowing of medulla oblongata palsy following brainstem infarction compared with the routine acupoints [73]. In addition, Su et al. show that EA at Yamen (GV 15), bilateral GB 20, bilateral Renying (ST 9), bilateral Sanyinjiao (SP 6), bilateral LI 4, and bilateral Fenglong (ST 40), may effectively enhance the spleen, clear phlegm, dredge the channels, clean dampness, bring out resuscitation, increase cerebral blood flow, alleviate brain edema, reduce cerebrovascular spasm, promote anoxic tolerance of neuronal cells, and regulate internal organs functions in patients with poststroke dysphagia [74].

3.6. The Effect of EA on Speech Apraxia after Stroke. Speech rehabilitation training associated with the scalp electric acupuncture (2 mA, 50 Hz) in Broca's area under anatomic orientation for four weeks may obviously relieve the speech disorder in with poststroke speech apraxia patients (18 cases with cerebral hemorrhage (lesion of 15 cases in the left basal ganglia, lesion of 1 case in the left frontal temporal and parietal, lesion of 2 cases in the left side of the basal ganglia and thalamus) and 42 cases with cerebral infarction (lesion of 11 cases in left bottom of the base section, 12 cases in left frontotemporal top, 11 cases in left insula temporal lobe, 5 cases in left insula and left ventricle narrator, and 3 cases in left frontal lobe and insular lobe) [75]. Chang et al. demonstrate that the stimulation of Xuanzhong and Tongli acupoints provides a therapeutic effect on the aphasia recovery after stroke via activating several brain regions related to language in poststroke aphasic patients [76]. In comparison with the routine acupoints, EA at eight-neck-occiput points plays a better role on speech disability of medulla oblongata palsy following brainstem infarction [73].

3.7. The Effect of EA on Improving Cognition and Memory after Stroke. Chou et al. show that EA at PC6 and Shenmen (HT7) for twenty minutes twice a week for eight weeks may improve the recovery of cognition function and life quality in poststroke patients [77]. Based on the rehabilitation training and conventional medication, EA stimulation at Dingniehouxiexian (MS 7), bilateral Ezhongxian (MS 1), Xuanzhong (GB 39), Dingzhongxian (MS 5), LI 4, Taichong (LR 3), ST 36, Taixi (KI 3), and GB 20 five times per week for eight weeks may promote recovery of memory function and the metabolism of cerebral tissue in the poststroke patients (infarct regions: 19 cases of basal ganglia, 9 cases of lateral ventricle, 1 case of thalamus, and 1 case of brainstem), and it has a better effect compared to medication associated with rehabilitation training [78]. Zeng et al. also show that acupuncture at GV 20, EX-HN 1, GV 24, GV 29, LI 4, LR 3, EX-HN 1, GV 24, and GV 29, five times per week for eight weeks can prompt the recovery of cognitive function and improve daily-life ability in subacute stroke patients with mild cognitive dysfunction on the basis of the traditional therapy and the cognitive rehabilitation training [79].

3.8. The Effect of EA on Easing Pain after Stroke. EA exerts effective benefits in well-being and pain control via activating antinociceptive pathway in the brain of patients with a history of ischemia in the left temporoparietal region [80]. EA at LI15 and LI 4, plus either penetration needling or routine acupuncture, may exert benefits in improvement of motion function and alleviation of edema and pain for patients with poststroke shoulder-hand syndrome [81]. Chau et al. show that EA treatment may be effective for patients with poststroke shoulder pain to ease the pain, promote upper limbs function, and improve physical function [82]. EA stimulation at Huatuojiaji points may obviously improve postapoplectic thalamic spontaneous pain [83]. Li et al. indicate that EA at Chize (LU 5), LI 15, TE 14, Quze (PC 3), Jianjing (GB 21), and Shaohai (HT 3), in association with Tuina exerts a better effect on poststroke shoulder pain than comprehensive rehabilitation treatment such as the electrostimulation in patients [84].

3.9. The Effect of EA on Improving Urinary Function after Stroke. In comparison with indwelling catheter therapy, EA stimulation at Qugu (CV 2), Zhongji (CV 3), Shuidao (ST 28), Qihai (CV 6), and Guanyuan (CV 4) has a better effect in promoting bladder capacity and attenuating apoplectic urinary incontinence in poststroke patients with urinary incontinence [85]. EA treatment (1 Hz, 15 min) at Sanyinjiao (SP6), Ciliao (BL32), and Pangguangshu (BL28) might be a

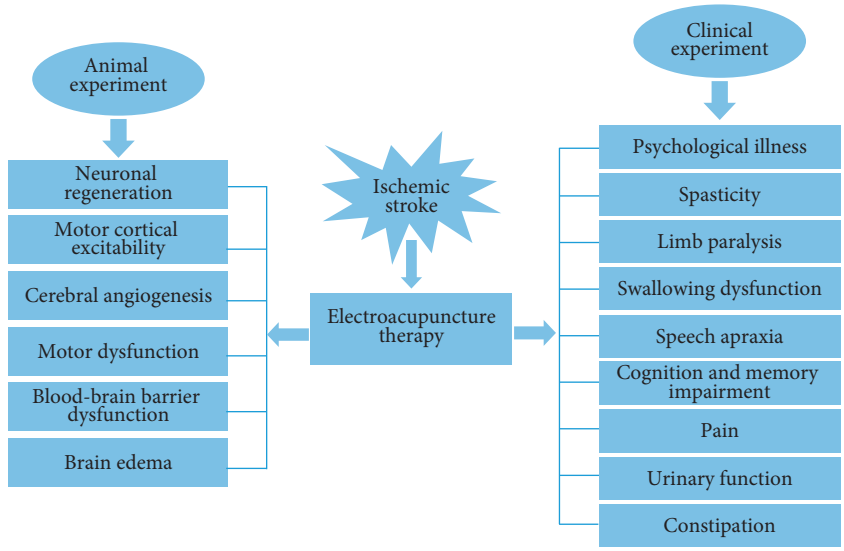

Figure 1: Electroacupuncture could promote neuronal regeneration, increase motor cortical excitability, improve cerebral angiogenesis, reduce motor dysfunction, decrease brain edema, and alleviate the impairment of blood-brain barrier according to the results of animal experiments. Meanwhile, electroacupuncture could improve a series of dysfunctions following stroke, including constipation, urinary function, pain, cognition and memory impairment, speech apraxia, swallowing disability, limb paralysis, spasticity, and psychological illness according to the results of clinical trial.

safe therapy for improvement of urinary function because of the effective effects induced by EA on stroke patients with incomplete bladder emptying [86]. EA at Jianyu (LI 15), Xuehai (SP 10), Shenshu (BL 23), Huiyang (BL 35) may also improve micturition clinical symptom and attenuate urinary incontinence severity in stroke patients [87]. Liu et al. indicate that EA intervention at Huiyang and Baliao provides a beneficial effect in alleviating detrusor overactivity after stroke by markedly mitigating symptoms of lower urinary tract, improving bladder compliance and cystometric capacity, reducing upper urinary tract injury risk, and alleviating pressure of detrusor leak point [88].

3.10. The Effect of EA on Improving Constipation after Stroke. Abdominal EA treatment at Daheng (SP 15), Fujie (SP 14), Tianshu (ST 25), Shuidao (ST 28), etc. may effectively improve poststroke constipation and accelerate gastrointestinal movement in patients with stroke [89]. Wang et al. show that basic comprehensive treatment in combination with EA at the point of Zusanli (ST 36) and Tian-shui (ST 25) plays a key role in prevention and treatment of constipation symptom in the acute phase of ischemic stroke [90].

3.11. The Effect of EA on Other Aspects after Stroke. Fu et al. show that EA at Jianyu (LI 15), Biguan (ST 31), Hegu (LI 4), Taichong (LR 3), Quchi (LI 11), Yanglingquan (GB 34), and Shenshu (BL 23), combined with dissolve-stasis herbs, rehabilitation training, and active-blood herbs, may be effective for treating ischemic stroke in clinic [91]. Electrospoon needles or electrofiliform needle may effectively promote motor dysfunction and daily-life ability in ischemic stroke patients [92]. Qian et al. show that acupuncture intervention at Jiquan (HT 1), Quchi (LI 11), Hegu (LI 4), Huantiao (GB 30), etc., twice per day in convalescence of cerebral infarction may exert more benefits than once per day in patients [93]. Li shows that EA at acupoints of either Yin Meridians or Yang Meridians may induce protection in poststroke patients [94]. Wong et al. suggest that EA via adhesive surface electrodes combined with appropriate rehabilitation therapy is an effective and convenient treatment for stroke patients [95]. EA and acupoint injection may significantly elevate daily-life ability and improve the neural function for the ischemic stroke patients, exerting a better effect than that EA alone [96]. Li et al. indicate that the combination therapy of EA at GV 20, Shenzhu (GV 12), Tianding (LI 17), LI 10, Biguan (ST 31), and Fenglong (ST40) and intracarotid drug injection may increase the cerebral blood vessels elasticity, promote vasodilation, and elevate the cerebral blood flow, contributing to sufficient supply of blood and oxygen and recovery of ischemic brain function following cerebral infarction [97].

Pei et al show that EA stimulation plays an important role in improving life quality and in health care, social services, and daily living ability of patients in acute stage EA stimulation at LI 4, LI 10, LI11, LI15, SP 6, Fenglong (ST 40), ST 36, and DU20 may prompt motor function recovery and then improve the living activities in the early stage of stroke [98]. Wang et al. suggest that EA treatment is important in improving the nervous dysfunction deficits following four-week intervention and enhancing the daily-life activity level following six-month follow-up visit, and systematic acupuncture treatment may alleviate the occurrence rate of secondary apoplexy in patients [99].

4. Conclusion

In summary, as demonstrated in Figure 1, EA treatment or preconditioning may play an important role in alleviating edema, easing pain, enhancing cerebral blood flow and

daily-life ability, improving cognition and memory function, speech function, swallowing function, motor function, as well as nerve, intestinal, and urinary system. In addition, EA stimulation combined with other common rehabilitation treatment might exert better effect for treatment of stroke than EA alone. EA with high frequency or long duration may elicit effective improvement in apoplectic patients. The effect of EA stimulation also involves acupoints, intensity, and interval of stimulation. All of those mentioned above provide a potential treatment strategy for treating apoplectic patients in clinic.

Data Availability

This is a review article with no underlying data.

Conflicts of Interest

The authors declare that there are no conflicts of interest.

References

[1] M. A. Moskowitz, E. H. Lo, and C. Iadecola, "The science of stroke: mechanisms in search of treatments," *Neuron*, vol. 67, no. 2, pp. 181–198, 2010.

[2] M. Wang, Y.-J. Li, Y. Ding et al., "Silibinin prevents autophagic cell death upon oxidative stress in cortical neurons and cerebral ischemia-reperfusion injury," *Molecular Neurobiology*, vol. 53, no. 2, pp. 932–943, 2016.

[3] P. Wicha, J. Tocharus, A. Janyou et al., "Hexahydrocurcumin protects against cerebral ischemia/reperfusion injury, attenuates inflammation, and improves antioxidant defenses in a rat stroke model," *PLoS One*, vol. 12, no. 12, Article ID e0189211, 2017.

[4] J. F. Wang, Z. G. Mei, Y. Fu et al., "Puerarin protects rat brain against ischemia/reperfusion injury by suppressing autophagy via the AMPK-mTOR-ULK1 signaling pathway," *Neural Regeneration Research*, vol. 13, no. 6, pp. 989–998, 2018.

[5] G. X. Ni and Y. Y. Song, "Exploration of xingnao tiaochang acupuncture therapy in treatment of Parkinson's disease on the base of brain-gut axis theory," *Zhongguo Zhen Jiu*, vol. 40, no. 3, pp. 315–317, 2020.

[6] B. R. Stacey, R. E. Williams, R. G. Buckner, and J. A. Hair, "Changes in weight and blood composition of hereford and brahman steers in drylot and infested with adult gulf coast ticks12," *Journal of Economic Entomology*, vol. 71, no. 6, pp. 967–970, 1978.

[7] J. Zhan, R. Pan, M. Zhou et al., "Electroacupuncture as an adjunctive therapy for motor dysfunction in acute stroke survivors: a systematic review and meta-analyses," *BMJ Open*, vol. 8, no. 1, Article ID e017153, 2018.

[8] W. Cai, W. Ma, G. T. Wang, and W. D. Shen, "Efficacy and safety of electroacupuncture for post stroke depression: study protocol for a randomized controlled trial," *Trials*, vol. 19, no. 1, p. 152, 2018.

[9] S. Y. Zhang, S. B. Liu, W. Wu et al., "Clinical trials for treatment of stroke patients with dysphagia by vitalstim electroacupuncture combined with swallowing rehabilitation training," *Zhen Ci Yan Jiu*, vol. 42, no. 2, pp. 168–172, 2017.

[10] M. Tian, T. Lou, and J. Leng, "Clinical observation of acupuncture plus electroacupuncture for hand spasm in stroke patients," *Zhongguo Zhen Jiu*, vol. 37, no. 9, pp. 932–935, 2017.

[11] Z. J. Yang, D. H. Shen, X. Guo, and F. Y. Sun, "Electroacupuncture enhances striatal neurogenesis in adult rat brains after a transient cerebral middle artery occlusion," *Acupuncture & Electro-Therapeutics Research*, vol. 30, no. 3-4, pp. 185–199, 2005.

[12] P. Young-Wook, H. Gi Yoon, K. Min Jae, L. Seo-Yeon, C. Byung Tae, and S. Hwa Kyoung, "Subacute electroacupuncture at baihui (GV 20) and dazhui (GV 14) promotes post-stroke functional recovery via neurogenesis and astrogliosis in a photothrombotic stroke mouse model," *Journal of Traditional Chinese Medicine*, vol. 39, no. 6, pp. 833–841, 2019.

[13] B. Deng, F. Bai, H. Zhou et al., "Electroacupuncture enhances rehabilitation through miR-181b targeting PirB after ischemic stroke," *Scientific Reports*, vol. 6, p. 38997, 2016.

[14] L. Chi, K. Du, D. Liu, Y. Bo, and W. Li, "Electroacupuncture brain protection during ischemic stroke: a role for the parasympathetic nervous system," *Journal of Cerebral Blood Flow & Metabolism*, vol. 38, no. 3, pp. 479–491, 2018.

[15] X. Han, X. Huang, Y. Wang, and H. Chen, "A study of astrocyte activation in the periinfarct region after cerebral ischemia with electroacupuncture," *Brain Injury*, vol. 24, no. 5, pp. 773–779, 2010.

[16] H. Lin, W. Shu, M. Jinquan, Y. Wenping, S. Yan, and S. Xuemin, "The effects of electro-acupuncturing DU26 (renzhong) on motor cortical excitability and neurofunction after focal cerebral ischemia injury in rats," *Acupuncture & Electro-Therapeutics Research*, vol. 35, no. 1-2, pp. 29–44, 2010.

[17] Q.-M. Si, G.-C. Wu, and X.-D. Cao, "Effects of electroacupuncture on acute cerebral infarction," *Acupuncture & Electro-Therapeutics Research*, vol. 23, no. 2, pp. 117–124, 1998.

[18] Z. Li, M. Yang, Y. Lin et al., "Electroacupuncture promotes motor function and functional connectivity in rats with ischemic stroke: an animal resting-state functional magnetic resonance imaging study," *Acupuncture in Medicine*, Article ID 964528420920297, 2020.

[19] Y. Du, L. Shi, J. Li, J. Xiong, B. Li, and X. Fan, "Angiogenesis and improved cerebral blood flow in the ischemic boundary area were detected after electroacupuncture treatment to rats with ischemic stroke," *Neurological Research*, vol. 33, no. 1, pp. 101–107, 2011.

[20] L. Shi, H. M. Cao, Y. Li et al., "Electroacupuncture improves neurovascular unit reconstruction by promoting collateral circulation and angiogenesis," *Neural Regeneration Research*, vol. 12, no. 12, pp. 2000–2006, 2017.

[21] L. H. Yang, Y. H. Du, and J. Li, "Effect of electroacupuncture on expression of apelin-APJ system of cerebral vascular endothelial cell in rats with cerebral infarction," *Zhen Ci Yan Jiu*, vol. 42, no. 1, pp. 9–13, 2017.

[22] L. Liu, Q. Zhang, H.-Y. Xie et al., "Differences in post-ischemic motor recovery and angiogenesis of MCAO rats following electroacupuncture at different acupoints," *Current Neurovascular Research*, vol. 17, no. 1, pp. 71–78, 2020.

[23] L. Liu, N. H. Wang, Q. Zhang, S. Y. Li, W. J. Gu, and Y. Wu, "Micro-ribonucleic acids participate in electroacupuncture intervention-induced improvement of ischemic stroke," *Zhen Ci Yan Jiu*, vol. 44, no. 9, pp. 686–692, 2019.

[24] C.-L. Hsieh, Q.-Y. Chang, I.-H. Lin et al., "The study of electroacupuncture on cerebral blood flow in rats with and without cerebral ischemia," *The American Journal of Chinese Medicine*, vol. 34, no. 02, pp. 351–361, 2006.

[25] F. Zhou, J. Guo, J. Cheng, G. Wu, and Y. Xia, "Electroacupuncture increased cerebral blood flow and reduced

ischemic brain injury: dependence on stimulation intensity and frequency," *Journal of Applied Physiology*, vol. 111, no. 6, pp. 1877–1887, 2011.

[26] W.-P. Yao, S. Wang, L. Han, J.-Q. Ma, and Y. Shen, "Effects of different frequencies of electro-acupuncture at shuigou (GV 26) on recovery of motor function in rats with focal cerebral ischemic injury," *Journal of Traditional Chinese Medicine*, vol. 32, no. 1, pp. 99–104, 2012.

[27] Z. Liu and X. S. Lai, "Effects of electroacupuncture on neurological deficit and pathomorphologic lesion in the rat of focal cerebral ischemia," *Zhongguo Zhen Jiu*, vol. 25, no. 12, pp. 879–884, 2005.

[28] W. Liu, G. Shang, S. Yang et al., "Electroacupuncture protects against ischemic stroke by reducing autophagosome formation and inhibiting autophagy through the mTORC1-ULK1 complex-beclin1 pathway," *International Journal of Molecular Medicine*, vol. 37, no. 2, pp. 309–318, 2016.

[29] M. M. Wang, M. Zhang, Y. S. Feng et al., "Electroacupuncture inhibits neuronal autophagy and apoptosis via the PI3K/AKT pathway following ischemic stroke," *Front Cell Neurosci*, vol. 14, p. 134, 2020.

[30] L. Zheng, X.-Y. Li, F.-Z. Huang et al., "Effect of electroacupuncture on relieving central post-stroke pain by inhibiting autophagy in the hippocampus," *Brain Research*, vol. 1733, Article ID 146680, 2020.

[31] Y. Xing, S.-D. Yang, M.-M. Wang, F. Dong, Y.-S. Feng, and F. Zhang, "Electroacupuncture alleviated neuronal apoptosis following ischemic stroke in rats via midkine and ERK/JNK/p38 signaling pathway," *Journal of Molecular Neuroscience*, vol. 66, no. 1, pp. 26–36, 2018.

[32] Y. S. Jung, S. W. Lee, J. H. Park, H. B. Seo, B. T. Choi, and H. K. Shin, "Electroacupuncture preconditioning reduces ROS generation with NOX4 down-regulation and ameliorates blood-brain barrier disruption after ischemic stroke," *Journal of Biomedical Science*, vol. 23, p. 32, 2016.

[33] F. Zhang, Y. Wu, and J. Jia, "Electro-acupuncture can alleviate the cerebral oedema of rat after ischemia," *Brain Injury*, vol. 25, no. 9, pp. 895–900, 2011.

[34] R. Zou, Z. Wu, and S. Cui, "Electroacupuncture pretreatment attenuates blood-brain barrier disruption following cerebral ischemia/reperfusion," *Molecular Medicine Reports*, vol. 12, no. 2, pp. 2027–2034, 2015.

[35] G. H. Tian, S. S. Tao, M. T. Chen et al., "Electroacupuncture treatment alleviates central poststroke pain by inhibiting brain neuronal apoptosis and aberrant astrocyte activation," *Neural Plasticity*, vol. 2016, no. 1, 14 pages, Article ID 1437148, 2016.

[36] R. Lin, Y. Wu, J. Tao et al., "Electroacupuncture improves cognitive function through rho GTPases and enhances dendritic spine plasticity in rats with cerebral ischemia-reperfusion," *Molecular Medicine Reports*, vol. 13, no. 3, pp. 2655–2660, 2016.

[37] J. J. Zhang, Y. H. Du, J. Li, L. H. Yang, L. L. Chen, and Q. P. Zha, "Effect of electroacupuncture on neurological function and Wnt signaling pathway in ischemic brain tissue of cerebral infarction rats," *Zhen Ci Yan Jiu*, vol. 45, no. 3, pp. 202–208, 2020.

[38] T. Jiang, M. Wu, Z. Zhang et al., "Electroacupuncture attenuated cerebral ischemic injury and neuroinflammation through alpha7nAChR-mediated inhibition of NLRP3 inflammasome in stroke rats," *Molecular Medicine*, vol. 25, no. 1, p. 22, 2019.

[39] Z. Fang, J. Ning, C. Xiong, and Y. Shulin, "Effects of electroacupuncture at head points on the function of cerebral motor areas in stroke patients: a pet study," *Evidence-Based Complementary and Alternative Medicine*, vol. 2012, Article ID 902413, , 2012.

[40] D. E. Huang, Q. Wu, Z. R. Lin, D. Lin, F. F. Shen, and J. Z. Liu, "Effects of different interference orders of acupuncture and exercise therapy on the amplitude of somatosensory evoked potential (SEP) in the patient of hemiplegia after stroke," *Zhongguo Zhen Jiu*, vol. 26, no. 12, pp. 869–872, 2006.

[41] T. J. Ho, T. M. Chan, L. I. Ho et al., "The possible role of stem cells in acupuncture treatment for neurodegenerative diseases: a literature review of basic studies," *Cell Transplantation*, vol. 23, no. 4-5, pp. 559–566, 2014.

[42] G. Ouyang, S. W. Jia, F. Wang, Y. Shi, and Z. Gao, "Effects of electroacupuncture of different frequencies on cerebral blood perfusion and cerebral function in the patient of stroke," *Zhongguo Zhen Jiu*, vol. 25, no. 11, pp. 776–778, 2005.

[43] S. C. Man, B. H. Hung, R. M. Ng et al., "A pilot controlled trial of a combination of dense cranial electroacupuncture stimulation and body acupuncture for post-stroke depression," *BMC Complementary Medicine and Therapies*, vol. 14, p. 255, 2014.

[44] P. Wu and S. Liu, "Clinical observation on post-stroke anxiety neurosis treated by acupuncture," *Journal of Traditional Chinese Medicine = Chung I Tsa Chih Ying Wen pan*, vol. 28, no. 3, pp. 186–188, 2008.

[45] L. Tang, C. Ma, F. You, and L. Ding, "Impacts of the low-frequency electric stimulation at the acupoints on the content of plasma 5-HT and NE in the patients with post-stroke insomnia," *Zhongguo Zhen Jiu*, vol. 35, no. 8, pp. 763–767, 2015.

[46] G. C. Medeiros, D. Roy, N. Kontos, and S. R. Beach, "Post-stroke depression: a 2020 updated review," *General Hospital Psychiatry*, vol. 66, pp. 70–80, 2020.

[47] L. Zhang, Y. Zhong, S. Quan et al., "Acupuncture combined with auricular point sticking therapy for post stroke depression:a randomized controlled trial," *Zhongguo Zhen Jiu*, vol. 37, no. 6, pp. 581–585, 2017.

[48] Z. J. Zhang, H. Zhao, G. X. Jin et al., "Assessor-and participant-blinded, randomized controlled trial of dense cranial electroacupuncture stimulation plus body acupuncture for neuropsychiatric sequelae of stroke," *Psychiatry and Clinical Neurosciences*, vol. 74, no. 3, pp. 183–190, 2020.

[49] Y. You, T. Zhang, S. Shu, X. Qian, S. Zhou, and F. Yao, "Wrist-ankle acupuncture and fluoxetine in the treatment of post-stroke depression: a randomized controlled clinical trial," *Journal of Traditional Chinese Medicine = Chung I Tsa Chih Ying Wen pan*, vol. 40, no. 3, pp. 455–460, 2020.

[50] S. M. Lim, J. Yoo, E. Lee et al., "Acupuncture for spasticity after stroke: a systematic review and meta-analysis of randomized controlled trials," *Evidence-Based Complementary and Alternative Medicine*, vol. 2015, Article ID 870398, , 2015.

[51] S.-K. Moon, Y.-K. Whang, S.-U. Park et al., "Antispastic effect of electroacupuncture and moxibustion in stroke patients," *The American Journal of Chinese Medicine*, vol. 31, no. 03, pp. 467–474, 2003.

[52] Y. Wu, "Effects of electroacupuncture at the nerve trunk for treatment of apoplectic hemiplegia at the spastic stage," *Journal of Traditional Chinese Medicine = Chung I Tsa Chih Ying Wen pan*, vol. 28, no. 3, pp. 183–185, 2008.

[53] X. B. Wang, J. Chen, T. J. Li et al., "Effect of electroacupuncture in different frequencies on electromyography and ambulation in stroke patients with lower-extremity spasticity: a randomized controlled study," *Zhongguo Zhen Jiu*, vol. 31, no. 7, pp. 580–584, 2011.

[54] B. H. Wang, C. L. Lin, T. M. Li, S. D. Lin, J. G. Lin, and L. W. Chou, "Selection of acupoints for managing upper-extremity spasticity in chronic stroke patients," *Clinical Interventions in Aging*, vol. 9, pp. 147–156, 2014.

[55] M. Mukherjee, L. K. McPeak, J. B. Redford, C. Sun, and W. Liu, "The effect of electro-acupuncture on spasticity of the wrist joint in chronic stroke survivors," *Archives of Physical Medicine and Rehabilitation*, vol. 88, no. 2, pp. 159–166, 2007.

[56] W. Liu, M. Mukherjee, C. Sun, H. Liu, and L. K. McPeak, "Electroacupuncture may help motor recovery in chronic stroke survivors: a pilot study," *The Journal of Rehabilitation Research and Development*, vol. 45, no. 4, pp. 587–596, 2008.

[57] P. M. Wayne, D. E. Krebs, E. A. Macklin et al., "Acupuncture for upper-extremity rehabilitation in chronic stroke: a randomized sham-controlled study," *Archives of Physical Medicine and Rehabilitation*, vol. 86, no. 12, pp. 2248–2255, 2005.

[58] Y. L. Zhao, W. C. Li, J. Huang et al., "Effects of jingjin acupuncture on fine activity of hemiplegic hand in recovery period of stroke," *Zhongguo Zhen Jiu*, vol. 34, no. 2, pp. 120–124, 2014.

[59] J. S. Yang, X. Gao, R. Sun et al., "Effect of electroacupuncture intervention on rehabilitation of upper limb motor function in patients with ischemic stroke," *Zhen Ci Yan Jiu*, vol. 40, no. 6, pp. 489–492, 2015.

[60] R. Hsieh, L. Wang, and W. Lee, "Additional therapeutic effects of electroacupuncture in conjunction with conventional rehabilitation for patients with first-ever ischaemic stroke," *Journal of Rehabilitation Medicine*, vol. 39, no. 3, pp. 205–211, 2007.

[61] F. F. Shen, Q. Wu, Z. R. Lin et al., "Effects of different interference orders of electroacupuncture and exercise therapy on the therapeutic effect of hemiplegia after stroke," *Zhongguo Zhen Jiu*, vol. 28, no. 10, pp. 711–713, 2008.

[62] G. Liu and Y. Xiao, "The influence of electric needling "juci" on nail-bed microcirculation of apoplectic patients," *Zhen Ci Yan Jiu*, vol. 15, no. 1, pp. 40–43, 1990.

[63] Q. Y. Wang, "Observation on therapeutic effect of electroacupuncture at points of different channels at different stages on hemiplagia after apoplexy," *Zhongguo Zhen Jiu*, vol. 26, no. 1, pp. 33–35, 2006.

[64] C. H. Chen, T. W. Chen, M. C. Weng, W. T. Wang, Y. L. Wang, and M. H. Huang, "The effect of electroacupuncture on shoulder subluxation for stroke patients," *The Kaohsiung Journal of Medical Sciences*, vol. 16, no. 10, pp. 525–532, 2000.

[65] B. T. Wu and Z. H. Zhao, "Efficacy control observation on electroacupuncture with different waveforms combined with rehabilitation therapy for post-stroke shoulder subluxation," *Zhongguo Zhen Jiu*, vol. 33, no. 10, pp. 901–904, 2013.

[66] J. Lu, L. X. Zhang, K. J. Liu et al., "Clinical observation on electroacupuncture combined with rehabilitation techniques for treatment of shoulder subluxation after stroke," *Zhongguo Zhen Jiu*, vol. 30, no. 1, pp. 31–34, 2010.

[67] J. M. Chu, Y. H. Bao, and M. Zhu, "Effects of acupuncture intervention combined with rehabilitation on standing-balance-walking ability in stroke patients," *Zhen Ci Yan Jiu*, vol. 40, no. 6, pp. 474–478, 2015.

[68] L. Tian, X. Du, J. Wang et al., "Comparative study on the effects between manual acupuncture and electroacupuncture for hemiplegia after acute ischemic stroke," *Zhongguo Zhen Jiu*, vol. 36, no. 11, pp. 1121–1125, 2016.

[69] Y. Zhou, G. Y. Zhou, S. K. Li, and J. H. Jin, "Clinical observation on the therapeutic effect of electroacupuncture combined with cupping on post-stroke fatigue," *Zhen Ci Yan Jiu*, vol. 35, no. 5, pp. 380–383, 2010.

[70] G. Liu, C. S. Lu, and L. X. Yuan, "Study on electroacupuncture improving the single-foot supporting phase rate of stroke patients," *Zhongguo Zhen Jiu*, vol. 30, no. 6, pp. 446–448, 2010.

[71] Z. L. Zhang, S. H. Zhao, G. H. Chen et al., "Randomized controlled study on dysphagia after stroke treated with deep insertion of chonggu (EX-HN 27) by electroacupuncture," *Zhongguo Zhen Jiu*, vol. 31, no. 5, pp. 385–390, 2011.

[72] Z. Huang, F. Huang, H. X. Yan et al., "Dysphagia after stroke treated with acupuncture or electric stimulation: a randomized controlled trial," *Zhongguo Zhen Jiu*, vol. 30, no. 12, pp. 969–973, 2010.

[73] R. P. She and C. H. Ge, "Clinical observation on medulla oblongata palsy after brainstem infarction treated with electroacupuncture at eight-neck-occiput points," *Zhongguo Zhen Jiu*, vol. 34, no. 6, pp. 539–542, 2014.

[74] Y. Su, P. Li, and G. Zhao, "Electroacupuncture treatment for 45 cases of postapoplectic dysphagia," *Journal of Traditional Chinese Medicine = Chung I Tsa Chih Ying Wen pan*, vol. 24, no. 2, pp. 129-130, 2004.

[75] Y. Jiang, Y. Yang, R. Xiang et al., "Clinical study of post-stroke speech apraxia treated with scalp electric acupuncture under anatomic orientation and rehabilitation training," *Zhongguo Zhen Jiu*, vol. 35, no. 7, pp. 661–664, 2015.

[76] J. Chang, H. Zhang, Z. Tan, J. Xiao, S. Li, and Y. Gao, "Effect of electroacupuncture in patients with post-stroke motor aphasia:neurolinguistic and neuroimaging characteristics," *Wien Klin Wochenschr*, vol. 129, no. 3-4, pp. 102–109, 2017.

[77] P. Chou, H. Chu, and J. G. Lin, "Effects of electroacupuncture treatment on impaired cognition and quality of life in Taiwanese stroke patients," *Journal of Alternative and Complementary Medicine*, vol. 15, no. 10, pp. 1067–1073, 2009.

[78] J. Zhang and Y. Shen, "Magnetic resonance spectroscopic study of memory impairment after cerebral infarction treated with electroacupuncture," *Zhongguo Zhen Jiu*, vol. 35, no. 7, pp. 657–660, 2015.

[79] Y. Zeng, Y. Bao, M. Zhu, S. Chen, and J. Fang, "Mild cognitive impairment of stroke at subacute stage treated with acupuncture: a randomized controlled trial," *Zhongguo Zhen Jiu*, vol. 35, no. 10, pp. 979–982, 2015.

[80] A. B. O. Santos and J. L. Gozzani, "Acupuncture as adjuvant therapy in thalamic syndrome: case report," *Brazilian Journal of Anesthesiology*, vol. 61, no. 1, pp. 88–94, 2011.

[81] L. W. Xue, Q. Li, and J. Q. Sun, "Clinical observation on penetration needling combined with electroacupuncture for treatment of post-stroke shoulder-hand syndrome," *Zhongguo Zhen Jiu*, vol. 27, no. 7, pp. 491–493, 2007.

[82] J. P. C. Chau, S. H. S. Lo, X. Yu et al., "Effects of acupuncture on the recovery outcomes of stroke survivors with shoulder pain: a systematic review," *Frontiers in Neurology*, vol. 9, p. 30, 2018.

[83] Z. Jiang, C. Li, and Y. Li, "Treatment of postapoplectic thalamic spontaneous pain by electroacupuncture at huatuojiaji points," *Journal of Traditional Chinese Medicine*, vol. 19, no. 3, pp. 195–199, 1999.

[84] N. Li, F. W. Tian, C. W. Wang et al., "Double-center randomized controlled trial on post-stroke shoulder pain treated by electroacupuncture combined with tuina," *Zhongguo Zhen Jiu*, vol. 32, no. 2, pp. 101–105, 2012.

[85] F. J. Song, S. H. Jiang, S. L. Zheng et al., "Electroacupuncture for post-stroke urinary incontinence: a multi-center randomized controlled study," *Zhongguo Zhen Jiu*, vol. 33, no. 9, pp. 769–773, 2013.

[86] K. W. Yu, C. L. Lin, C. C. Hung et al., "Effects of electroacupuncture on recent stroke inpatients with incomplete bladder emptying: a preliminary study," *Clinical Interventions in Aging*, vol. 7, pp. 469–474, 2012.

[87] J. M. Chu, Y. H. Bao, C. Zou, H. L. Zhao, Y. Gong, and C. M. Wang, "Randomized controlled clinical trials for electroacupuncture treatment of urinary incontinence in stroke patients," *Zhen Ci Yan Jiu*, vol. 36, no. 6, pp. 428–432, 2011.

[88] Y. Liu, L. Liu, and X. Wang, "Electroacupuncture at points baliao and huiyang (BL35) for post-stroke detrusor overactivity," *Neural Regeneration Research*, vol. 8, no. 18, pp. 1663–1672, 2013.

[89] D. S. Wang, S. Wang, L. L. Kong, W. Y. Wang, and X. M. Cui, "Clinical observation on abdominal electroacupuncture for treatment of poststroke constipation," *Zhongguo Zhen Jiu*, vol. 28, no. 1, pp. 7–9, 2008.

[90] C. Wang, M. Liu, Q. Wen, and N. Li, "Clinical observation of preventing and treating constipation by electroacupuncture intervention in ischemic stroke patients at acute stage," *Zhongguo Zhen Jiu*, vol. 35, no. 5, pp. 430–434, 2015.

[91] W. B. Fu, Y. Guo, X. K. Chen et al., "Comprehensive therapeutic protocol of electroacupuncture combined with Chinese herbs and rehabilitation training for treatment of cerebral infarction: a multi-center randomized controlled trial," *Zhongguo Zhen Jiu*, vol. 30, no. 1, pp. 6–9, 2010.

[92] Q. Tang, L. Zhang, T. H. Wei, Y. Wang, J. Bai, and H. T. Li, "Randomized controlled clinical trials for electro-spoon-needles treatment of motor dysfunction in cerebral infarction patients," *Zhen Ci Yan Jiu*, vol. 34, no. 3, pp. 193–197, 2009.

[93] X. P. Qian, F. Xu, J. L. Song, and J. H. Zhao, "Influence of different frequencies of acupuncture on therapeutic effect in patients with cerebral infarction at convalescence," *Zhongguo Zhen Jiu*, vol. 29, no. 1, pp. 7–9, 2009.

[94] J. Li, "Forty-five cases of apoplexy treated by electroacupuncture at the points of yin meridians," *Journal of Traditional Chinese Medicine*, vol. 21, no. 1, pp. 20–22, 2001.

[95] A. M. K. Wong, T.-Y. Su, F.-T. Tang, P.-T. Cheng, and M.-Y. Liaw, "Clinical trial of electrical acupuncture on hemiplegic stroke Patients1," *American Journal of Physical Medicine & Rehabilitation*, vol. 78, no. 2, pp. 117–122, 1999.

[96] X. Wang, L. Yang, and Y. Liu, "Clinical observation on treatment of ischemic apoplexy by electroacupuncture plus acupoint-injection," *Journal of Traditional Chinese Medicine = Chung I Tsa Chih Ying Wen pan*, vol. 27, no. 3, pp. 175–177, 2007.

[97] J. Li, Y. Hu, L. Tong, D. Wang, and D. Zhang, "Effects of electroacupuncture plus intra-carotid drug injection on rheoencephalogram in patients with cerebral infarction," *Journal of Traditional Chinese Medicine = Chung I Tsa Chih Ying Wen pan*, vol. 24, no. 1, pp. 28-29, 2004.

[98] J. Pei, L. Sun, R. Chen, T. Zhu, Y. Qian, and D. Yuan, "The effect of electro-acupuncture on motor function recovery in patients with acute cerebral infarction: a randomly controlled trial," *Journal of Traditional Chinese Medicine = Chung I Tsa Chih Ying Wen pan*, vol. 21, no. 4, pp. 270–272, 2001.

[99] C. Wang, Z. Wu, N. Li et al., "Clinical curative effect of electric acupuncture on acute cerebral infarction: a randomized controlled multicenter trial," *Journal of Traditional Chinese Medicine*, vol. 34, no. 6, pp. 635–640, 2014.

Hindawi
Evidence-Based Complementary and Alternative Medicine
Volume 2020, Article ID 1560978, 9 pages
https://doi.org/10.1155/2020/1560978

Research Article

Clinical Effects and Safety of Electroacupuncture for the Treatment of Poststroke Dysphagia: A Comprehensive Systematic Review and Meta-Analysis

Jinke Huang,[1] **Yao Shi**,[2] **Xiaohui Qin**,[2] **Min Shen**,[1] **Manli Wu**,[1] **and Yong Huang**[3]

[1]*The Second Clinical Medical College, Guangzhou University of Chinese Medicine, Guangzhou, Guangdong 510120, China*
[2]*Department of Neurology, Guangdong Provincial Hospital of Chinese Medicine, Guangzhou, Guangdong 510120, China*
[3]*School of Traditional Chinese Medicine, Southern Medical University, Guangzhou, Guangdong 510515, China*

Correspondence should be addressed to Yong Huang; nanfanglihuang@163.com

Received 8 July 2020; Revised 26 August 2020; Accepted 15 September 2020; Published 26 September 2020

Academic Editor: Feng Zhang

Objectives. Electroacupuncture (EA), an extension of acupuncture, which is based on traditional acupuncture combined with modern electrotherapy, is commonly used for poststroke dysphagia (PSD) in clinical treatment and research. However, there is still a lack of sufficient evidence to recommend the routine use of EA for PSD. The aim of this study was to assess the efficacy and safety of EA in the treatment of PSD. *Methods*. Randomized controlled trials (RCTs) evaluating the effects of EA on PSD were identified through a comprehensive literature search of the PubMed, Embase, Cochrane Library, Web of Science, Chinese National Knowledge Infrastructure, Chinese Biomedical Database, and VIP databases from their inception to July 2020. The quality assessment of the included trials was performed based on the guidance of the Cochrane Reviewers' Handbook, and meta-analysis (MA) was performed by using the RevMan 5.3 software. *Results*. Sixteen trials were identified, and these included 1,216 patients with PSD. The results demonstrated that EA in combination with swallowing rehabilitation training (SRT) was significantly superior to SRT alone with regard to effective rate (OR 5.40, 95% CI [3.78, 7.72], $P < 0.00001$, water swallow test (WST) (MD −0.78, 95% CI [−1.07, −0.50], $P < 0.00001$), the video fluoroscopic swallowing study (VFSS) (MD 1.47, 95% CI [1.11, 1.84], $P < 0.00001$), the Ichiro Fujishima Rating Scale (IFRS) (MD 1.94, 95% CI [1.67, 2.22], $P < 0.00001$), and the incidence of aspiration pneumonia (IAP) (OR 0.20, 95% CI [0.06, 0.61], $P = 0.005$). *Conclusions*. The results showed that EA was better than the control treatment in terms of the effective rate, WST, VFSS, IFRS, and IAP of dysphagia after stroke. Strict evaluation standards and high-quality RCT designs are necessary for further exploration.

1. Introduction

Dysphagia is a common disorder that occurs in approximately 34.7%–44% of stroke cases [1]. Poststroke dysphagia (PSD), characterized by swallowing difficulty in the oropharyngeal phase, can lead to many complications, such as dehydration, malnutrition, aspiration, and aspiration pneumonia [2]. It has been reported that patients with PSD have a 3-fold higher risk of aspiration pneumonia and a 5.4-fold higher mortality rate than patients without dysphagia [2]. For patients who experience PSD, the dysfunction can seriously affect their quality of life (QOL) by leading to social anxiety, withdrawal, and depression [3]. Thus, PSD creates a large financial burden on the families of stroke patients. Clinically, PSD treatment is mainly based on nondrug therapies, such as swallowing rehabilitation training (SRT), compensation therapy, physiotherapy, and alternative therapy [4]. However, most treatments only have a temporary and relatively limited effectiveness, and patients experiencing dysphagia after a stroke may seek other approaches.

Among the complementary and alternative therapies, electroacupuncture (EA) is an extension technique of acupuncture based on traditional acupuncture combined with modern electrotherapy, and it has been regarded as a promising method to treat PSD. A literature search yielded

Table 1: Search strategy for the PubMed database.

Query	Search term
#1	Cerebrovascular disorders [Mesh] OR stroke [Mesh] OR brain infarction [Mesh] OR cerebral hemorrhage [Mesh]
#2	Cerebrovascular disorder ∗ [Title/Abstract] OR stroke ∗ [Title/Abstract] OR brain infarction ∗ [Title/Abstract] OR cerebral hemorrhage ∗ [Title/Abstract] OR intracranial vascular disease ∗ [Title/Abstract] OR cerebrovascular disease ∗ [Title/Abstract] OR brain vascular disorder ∗ [Title/Abstract] OR cerebrovascular occlusion ∗ [Title/Abstract] OR cerebrovascular insufficiency ∗ [Title/Abstract] OR cerebrovascular accident ∗ [Title/Abstract] OR cerebrovascular apoplexy [Title/Abstract] OR brain vascular accident ∗ [Title/Abstract] OR apoplexy [Title/Abstract] OR anterior cerebral circulation infarction [Title/Abstract] OR cerebrum hemorrhage ∗ [Title/Abstract] OR intracerebral hemorrhage ∗ [Title/Abstract] OR brain hemorrhage [Title/Abstract]
#3	#1 OR #2
#4	Deglutition disorders [Mesh]
#5	Deglutition disorder ∗ [Title/Abstract] OR swallowing disorder ∗ [Title/Abstract] OR dysphagia [Title/Abstract] OR oropharyngeal dysphagia [Title/Abstract] OR esophageal dysphagia [Title/Abstract]
#6	#4 OR #5
#7	Acupuncture [Mesh]
#8	Acupuncture [Title/Abstract] OR acupuncture therapy [Title/Abstract] OR electroacupuncture [Title/Abstract] OR electro acupuncture [Title/Abstract] OR electric acupuncture [Title/Abstract] OR electrical acupuncture [Title/Abstract] OR electrical stimulation therapy [Title/Abstract]
#9	#7 OR #8
#10	Randomized controlled trials as topic [Mesh]
#11	Randomized controlled trials [Title/Abstract] OR random ∗ [Title/Abstract] OR controlled clinical trial [Title/Abstract] OR rct [Title/Abstract]
#12	#10 OR #11
#13	#3 AND #6 AND #9 AND #12

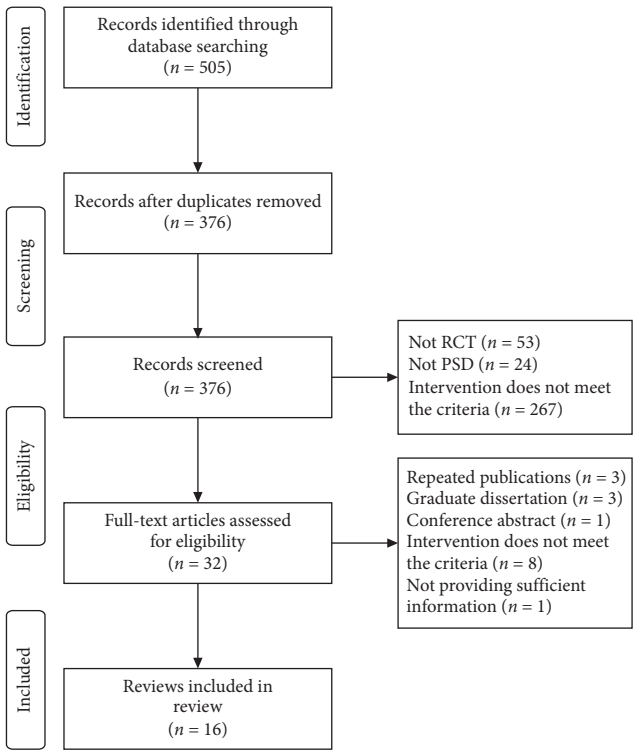

Figure 1: Flow chart of the literature selection process.

many published, clinical randomized controlled trials (RCTs) of EA for PSD. Evidence is the core of evidence-based medicine, and systematic reviews (SRs)/meta-analyses (MAs) based on RCTs are currently recognized as the highest level of evidence [5]. SRs/MAs are considered the gold standard for assessing the effects of health care interventions. The efficacy of acupuncture alone for PSD has been established using SRs/MAs [6]; however, the evidence of EA for PSD has not been assessed. Thus, we aimed to perform an SR/MA to investigate the efficacy and safety of EA for treating dysphagia in patients with stroke.

2. Materials and Methods

This SR/MA adheres to the guidelines for SRs/MAs according to the Cochrane Handbook [7] and the Preferred Reporting Items for Systematic Reviews and Meta-Analyses (PRISMA) guidelines [8]. The literature search, literature selection, data extraction, and quality evaluation were performed by both reviewers independently, and any inconsistencies were resolved through consensus or by consulting an experienced third reviewer.

2.1. Inclusion and Exclusion Criteria. The inclusion criteria were as follows: (a) study design: the trials had to be RCTs that aimed to compare combination therapy with swallowing training alone; (b) participants: participants had PSD diagnosed according to WHO criteria using appropriate radiological methods, not limited by gender, and age; (c) intervention: EA combined with SRT versus SRT alone; (d) outcomes: the primary outcome was an effective rate and swallowing function, as assessed by the water swallowing test (WST), video fluoroscopic swallowing study (VFSS), standardized swallowing assessment (SSA), and the Ichiro Fujishima rating scale (IFRS); the incidence of aspiration pneumonia (IAP) and adverse events were considered secondary outcomes. The exclusion criteria were as follows: (a) nonoriginal research articles; (b) studies in which the required data were unavailable.

Table 2: Characteristics of the included studies.

First author; year	No. of patients		Age		Time after onset		Therapy duration	Outcomes	Intervention	
	I	*C*	*I*	*C*	*I*	*C*			*I*	*C*
Wu et al. [9] 2019	63	65	44.0 ± 2.9	44.3 ± 2.6	3.9 ± 0.1 w	3.7 ± 0.4 w	3 w	IFRS	EA + SRT	SRT
Li et al. [10] 2019	50	50	42.5 ± 2.3	42.5 ± 2.2	26.9 ± 1.6 d	25.7 ± 1.5 d	20 d	IFRS, WST, ER	EA + SRT	SRT
Qin et al. [11] 2019	52	52	53.4 ± 10.7	53.8 ± 11.4	6.2 ± 1.5 m	6.4 ± 1.4 m	4 w	SSA, WST, ER, AE	EA + SRT	SRT
He et al. [12] 2018	35	35	64 ± 6	69 ± 7	32 ± 15 d	27 ± 15 d	4 w	ER, AE	EA + SRT	SRT
Xu et al. [13] 2017	40	40	53.98 ± 5.44	55.43 ± 5.67	9.96 ± 1.47 d	10.34 ± 1.54 d	1 m	ER	EA + SRT	SRT
Zhang et al. [14] 2017	40	40	51~75	53~76	6~28 d	7~27 d	4 w	VFSS,WST, ER	EA + SRT	SRT
Zhang et al. [15] 2016	45	45	62.4 ± 9.6	61.2 ± 10.1	12.8 ± 4.6 d	11.6 ± 4.4 d	4 w	VFSS, ER, IAP	EA + SRT	SRT
Huang and Yang [16] 2015	20	20	50~70	50~70	<72 h	<72 h	2 w	ER	EA + SRT	SRT
Zhang [17] 2014	30	30	54.2 ± 4.3	53.7 ± 2.9	3.9 ± 0.5 m	3.5 ± 0.9 m	2 w	WST, VFSS	EA + SRT	SRT
Wang et al. [18] 2012	32	34	63.8 ± 9.3	68.1 ± 10.3	4d~7 m	3d~6 m	30 d	WST, ER	EA + SRT	SRT
Wang et al. [19] 2011	30	30	36~79	39~73	14~78 d	14~78 d	4 w	ER	EA + SRT	SRT
Yang et al. [20] 2011	35	35	67.9 ± 10.6	67.4 ± 9.8	8.3 ± 11.3 d	9.6 ± 15 d	3 w	SSA	EA + SRT	SRT
Wang and Cheng [21] 2010	40	40	67.4 ± 7.8	68.3 ± 9.3	Unclear	Unclear	30 d	IAP	EA + SRT	SRT
Lv et al. [22] 2009	35	35	52~75	52~75	0.2~10 m	0.2~10 m	2 w	ER, WST	EA + SRT	SRT
Deng and Wang [23] 2009	46	42	42~79	45~76	<10 d	<10 d	30 d	ER	EA + SRT	SRT
Cao [24] 2008	60	60	47~70	51~68	Unclear	Unclear	4 w	ER	EA + SRT	SRT

C: control group; I: intervention group; EA: electroacupuncture; SRT: swallowing rehabilitation training; WST: water swallow test; ER: effective rate; SSA: standardized swallowing assessment; AE: adverse events; VFSS: video fluoroscopic swallowing study; IAP: incidence of aspiration pneumonia; IFRS: Ichiro Fujishima Rating Scale.

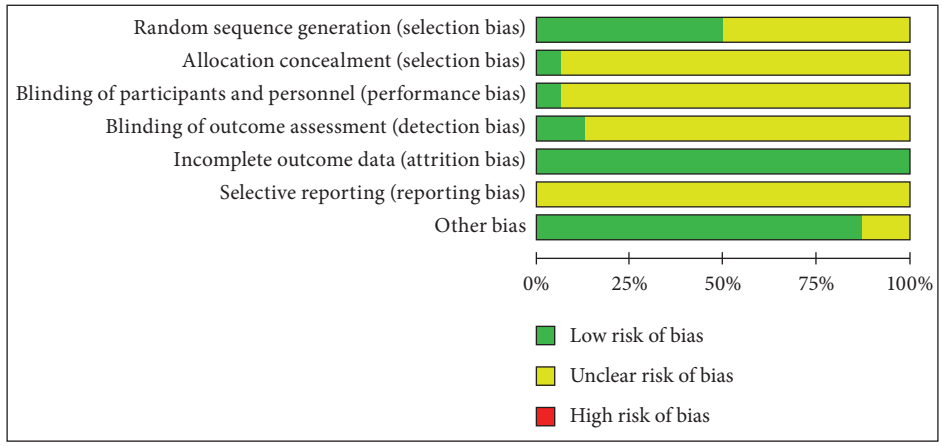

Figure 2: Risk of bias graph.

2.2. Search Strategy. We searched the PubMed, Embase, Cochrane Library, Web of Science, the Chinese National Knowledge Infrastructure, Chinese Biomedical Database, and VIP databases from their inception to July 2020. The following keywords were used: dyssomnia, insomnia, auricular acupuncture, systematic review, and meta-analysis. The search strategy for the PubMed database is presented in Table 1, and it was be adjusted for each database.

2.3. Eligibility Assessment and Data Extraction. The titles and abstracts of all articles were screened first, and potentially eligible articles were retrieved for full-text reviews. The following data were collected from each RCT: first author; publication year; number of eligible cases; age; time after onset; intervention; and data related to effective rate, swallowing function assessment, adverse events, and QOL.

2.4. Quality Assessment. The methodological quality of the extracted trials was independently assessed by the two reviewers using the Cochrane risk of bias tool [6]. The methodological quality was assessed based on the following aspects: (1) random sequence generation; (2) allocation concealment; (3) blinding of participants and personnel; (4) blinding of outcome assessment; (5) incomplete outcome data; (6) selective reporting; and (7) other bias. Each domain includes one entry assigned a judgment of "Low risk," "High risk," or "Unclear risk" of bias.

2.5. Statistical Analyses. Review Manager Software 5.3.0 was used to perform MA of the included RCTs. Data were categorized as continuous and dichotomous variables. Continuous variables were analyzed using mean differences (MD) with 95% confidence intervals (CIs) or standardized mean differences (SMDs) if different measurement scales were used. Dichotomous variables were analyzed using odds ratios (ORs) with 95% CIs. Heterogeneity across studies was tested by the I^2 statistic. The fixed effects model was used to analyze pooled data if heterogeneity was low ($I^2 < 50\%$); otherwise, the random effects model was used to analyze pooled data ($I^2 \geq 50\%$). A funnel plot was used to examine the publication bias if 10 or more studies were pooled.

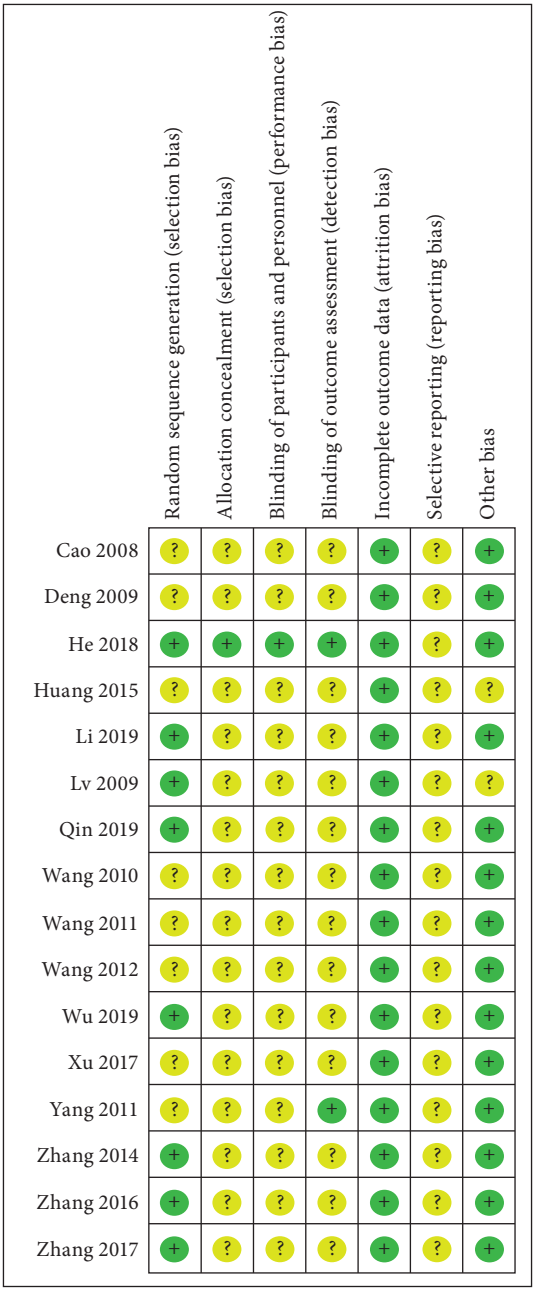

Figure 3: Risk of bias summary.

3. Results

3.1. Results on Literature Search and Selection. The search yielded 505 potential articles for review, 344 of which were excluded for reasons of irrelevance (Figure 1). Thirty-two clinical trials assessing the application of EA for PSD were retrieved for further assessment. Among these 32 trials, 16 were excluded because the intervention did not meet the inclusion criteria; they did not provide sufficient information; or they were duplicate publications, graduate dissertations, or conference abstracts. After excluding these 16 trials, the remaining 16 trials [9–24] were included in our review

3.2. Characteristic Summary of the Included Studies. In total, 16 RCTs involving 1,216 patients with PSD were included in this

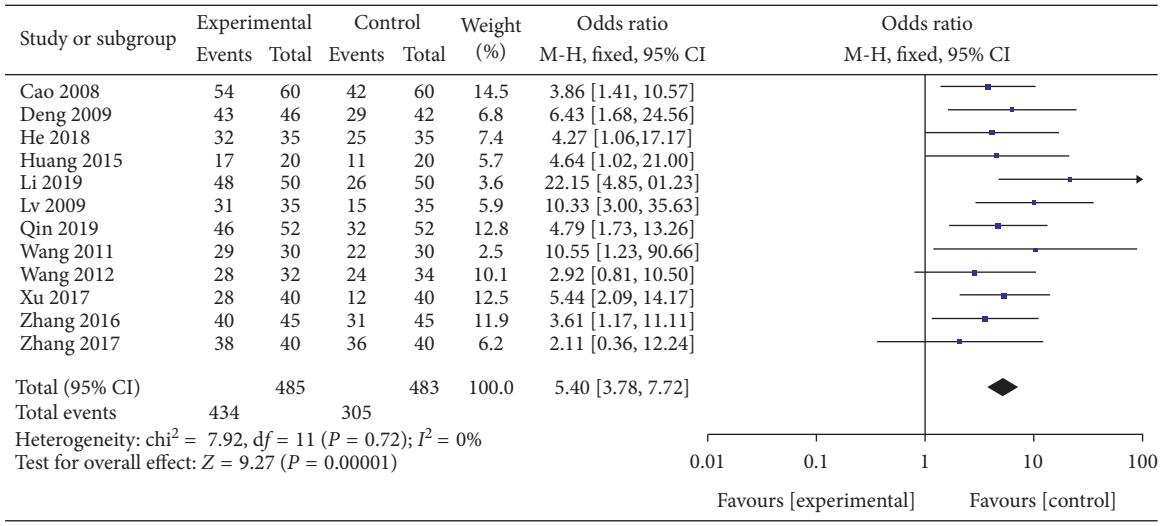

Figure 4: A forest plot for effective rate from 12 RCTs.

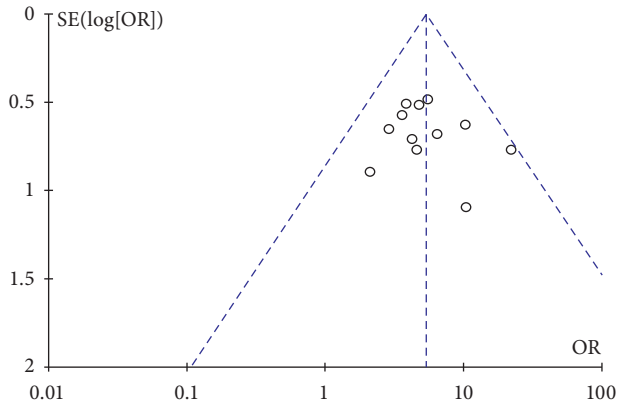

Figure 5: The funnel plot of the clinical efficacy rate.

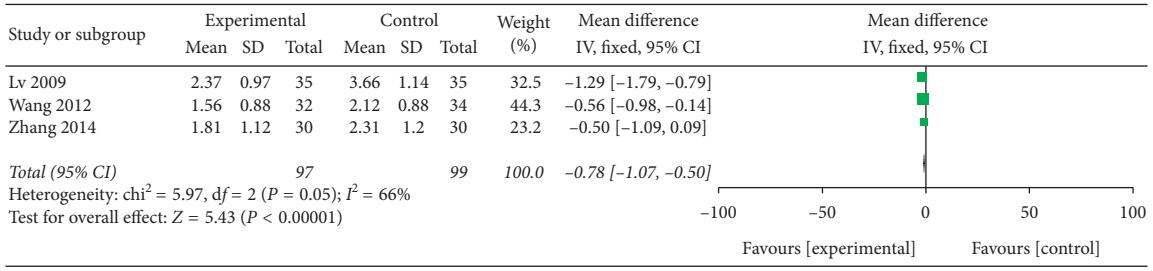

Figure 6: A forest plot for WST from 3 RCTs.

current review. The trials included were published between 2008 and 2019, the sample size ranged from 40 to 128, the ages of patients ranged from 36 to 79 years, and the duration of the treatment course ranged from 2 weeks to 1 month. All studies compared EA plus SRT with SRT alone. The outcome measures included both patient-centered outcomes and other routine test results. Two trials reported the incidence of aspiration pneumonia, and two trials reported adverse events. The detailed characteristics of the included studies are shown in Table 2.

3.3. Risk of Bias in Included Studies. We assessed the risk of bias in all the included trials. Randomization was mentioned in all the trials, but only half of the studies described a specific method of randomization. Allocation concealment was inadequate in most trials ($n = 15$, 92.75%). Only one trial ($n = 1$, 6.25%) blinded their participants or personnel. Also, only one trial ($n = 1$, 6.25%) masked their outcome assessors to the treatment allocation, whereas a risk of selective reporting bias was not reported in all

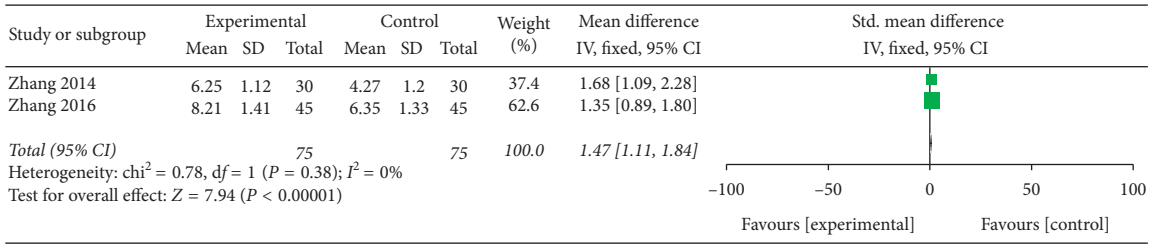

Figure 7: A forest plot for VFSS from 2 RCTs.

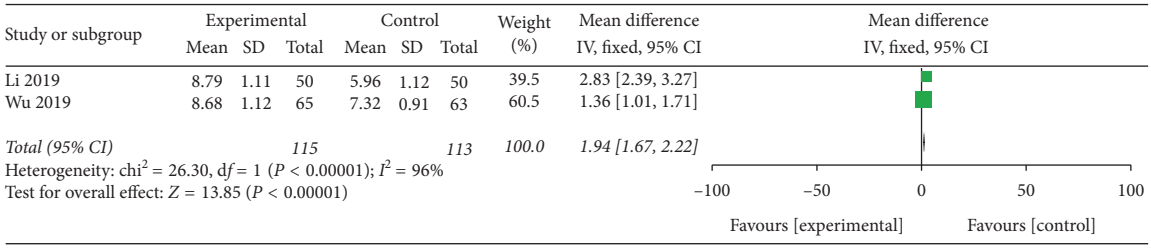

Figure 8: A forest plot for IFRS from 2 RCTs.

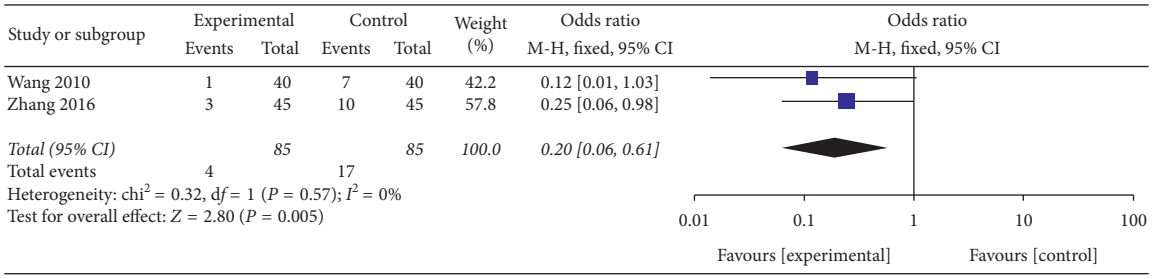

Figure 9: A forest plot for IAP from 2 RCTs.

trials ($n = 11$, 100%). More details are shown in Figures 2 and 3.

3.4. Primary Outcome Measures

3.4.1. Effective Rate. The effective rate was reported by 12 trials, with 485 participants in the investigational group and 483 in the control group. All 12 RCTs were included in this meta-analysis to investigate the efficacy of EA for treating dysphagia in stroke patients. The meta-analysis was conducted using a random effects model. As shown in Figure 4, our meta-analysis revealed that patients who received EA combined with SRT for PSD had significantly greater benefits than SRT alone in terms of the effective rate (OR 5.40, 95% CI [3.78, 7.72], $P < 0.00001$, $I^2 = 0\%$ (Figure 4). Furthermore, there was no publication bias in the funnel plot (Figure 5).

3.5. Second Outcome Measures

3.5.1. Water Swallowing Test (WST). The WST was used in 6 trials; 3 of them used continuous data and were included in this meta-analysis. The meta-analysis was conducted using a random effect model, and the results showed that patients who received EA combined with SRT for PSD showed significantly greater benefits on the WST than those who received SRT alone (MD −0.78, 95% CI [−1.07, −0.50], $P < 0.00001$ (Figure 6)). There was substantial heterogeneity ($P = 0.05$ ($I^2 = 66\%$)); after removing one trial [22], the heterogeneity decreased from 66% to 0%. The sensitivity analysis indicated that the source of the heterogeneity might be the post-onset time of this trial, which was longer than that of other trials.

3.5.2. Video Fluoroscopic Swallowing Study (VFSS). The VFSS was used in 3 trials; 2 of them were included in this

meta-analysis. The meta-analysis was conducted using a random effects model, and the results showed that patients who received EA combined with SRT for PSD showed significantly greater benefits on the VFSS than those who received SRT alone (MD 1.47, 95% CI [1.11, 1.84], $P < 0.00001$, $I^2 = 0\%$ (Figure 7)).

3.5.3. Ichiro Fujishima Rating Scale (IFRS). The IFRS was used in 2 trials, and both of them were included in this meta-analysis. The meta-analysis was conducted using a random effects model, and the results showed that patients who received EA combined with SRT for PSD showed significantly greater benefits on the IFRS than those who received SRT alone (MD 1.94, 95% CI [1.67, 2.22], $P < 0.00001$, $I^2 = 96\%$ (Figure 8)).

3.5.4. Incidence of Aspiration Pneumonia (IAP). The IAP was reported in 2 trials, and both of them were included in this meta-analysis. The meta-analysis was conducted using a random effect model, and the results showed that patients who received EA combined with SRT for PSD showed significantly greater benefits on the IAP than those who received SRT alone (OR 0.20, 95% CI [0.06, 0.61], $P = 0.005$, $I^2 = 0\%$ (Figure 9)).

3.5.5. Adverse Events. Adverse events were mentioned in 2 trials [11, 12] and were reported by a total of 16 patients. Of these patients, 10 had adverse events related to acupuncture, such as pain and hematoma, but they were not severe. The remaining 6 patients developed irritating cough during eating, and they were all in the control group and received only SRT.

4. Discussion

EA and SRT are routine therapies based on traditional Chinese medicine or modern Western medicine and are commonly used to treat PSD. SRT or other therapies combined with EA have been used to treat PSD by physicians aiming to increase the therapeutic effectiveness and reduce the side effects. However, whether combination therapy has a more positive impact on PSD than conventional SRT alone is unclear. Therefore, the current MA was conducted to quantitatively evaluate the existing evidence on the efficacy and safety of the combination of EA and SRT for the treatment of PSD. A previous SR published in Chinese compared EA with acupuncture/SRT and EA plus SRT with SRT/medicine [25]. Our study differed in that we focused more specifically on EA in combination with SRT to explore the effect of this combination.

4.1. Summary of the Main Findings. First, this SR/MA of clinical RCTs published in the past 12 years was conducted to assess the benefits of EA among patients with PSD. Overall, our meta-analysis suggested that EA combined with SRT was significantly superior to SRT alone with regard to the effective rate, WST, VFSS, IFRS, and IAP. EA treatment was not associated with an increased risk of adverse events. However, the credibility of the results is limited due to the generally poor methodological quality of the included trials. Insufficient or inexact reports on allocation concealment, blinding of performance, and assessment were found in most of the included studies. In addition, the sample size of the included RCTs was generally small, and no trial used statistical methods to calculate the sample size before the trial; therefore, it is difficult for this MA to draw robust conclusions. Second, the assessment of the swallowing ability mainly included bedside and instrumental evaluation, and the VFSS is regarded as the "gold standard" for the diagnosis of dysphagia after stroke. However, other scales and questionnaires are more widely used in clinical practice to evaluate dysphagia after stroke due to the potential risks of aspiration, inconvenience of operation, and consideration of cost-effectiveness, while the diagnostic accuracy varies owing to the sensitivity and the specificity of the bedside assessment tools, and the subjective skills of the assessors. The scales of measurement that were used in the enrolled RCTs in our MA included the WST, IFRS, and VFSS, and all of them are subjective clinical assessment tools based on the observation of the assessors. Furthermore, the scale used to determine the clinical effective rate, which was classified as cured, markedly effective, effective, and ineffective, is not internationally recognized; hence, it may not be accurate for the assessment of the effect of treatment. The statistical analysis also demonstrated that the nonquantitative and symptom-descriptive measurements were the main sources of heterogeneity in this MA. This prevented us from drawing robust conclusions from the MA. Third, the long-term effects of this therapy could not be evaluated. The included studies only evaluated the use of EA for 2–4 weeks, and the outcomes were assessed before and immediately after treatment; thus, the long-term effects of EA on dysphagia after stroke could not be revealed. In addition, the protocols of EA are also diverse, including differences in acupoints, stimulation methods, needle retention time, and number of treatments, leading to sources of heterogeneity in this MA. Finally, there may be language bias, as all the included trials were conducted and published by Chinese investigators, which limits the general applicability of the study's conclusions outside of China.

4.2. Potential Mechanism of Action. PSD is a neuropathic swallowing disorder closely related to neuromuscular movement, and stroke leads to neuromuscular blockage involved in swallowing activities, which causes abnormalities in swallowing function. Our findings suggest that EA is beneficial to dysphagia after stroke. Modern studies have demonstrated the basic principle of EA in the treatment of PSD, and it is believed that the central nervous system has plasticity and reorganization ability, both structurally and functionally [2]. As an extension technique of acupuncture based on traditional acupuncture combined with modern electrotherapy, EA not only adheres to the theory of traditional Chinese medicine but also combines the physiotherapy mechanism of electrical stimulation. EA can directly

act on the meridians and acupoints of the human body, promote the coordinated movement of multiple groups of muscle groups in the pharynx, and restore the muscle strength of damaged muscle groups [14]. Changes in EA current waveforms can present rhythmic contraction of muscles near the throat and prevent muscle waste atrophy after stroke [18]. Mechanical stimulation of EA at the lesion site can improve nerve excitability, reconstruct the damaged reflex arc, repair the injured nerve function, and then achieve a therapeutic effect [26]. Furthermore, EA increases blood perfusion in the medulla oblongata and some higher centers, which in turn improves pathological conditions, such as cerebral ischemia and hypoxia, and awakens inhibited nerve cells [12]. Thus, EA has been regarded as a promising method to treat PSD.

4.3. Strength and Limitations. To the best of our knowledge, this current study is the first SR/MA to explore the evidence of EA in combination with SRT for PSD. Based on the current results, it may have a certain reference value for the clinical practice and research of EA in the treatment of PSD. Of the 16 included trials, 75% used the effective rate to assess the effectiveness of EA for PSD, and the definition of the effective rate was as follows: effective rate = ("total number of patients" – "number of patients with no response")/total number of patients, and "no response" meant no significant change in any aspect of the swallowing function or regression of one aspect of the swallowing function after treatment. However, most of these trials did not use consistent measurement tools to assess the changes in the swallowing function before and after the treatment to reflect the effective rate; therefore, the credibility of the effective rate is limited. Hence, the swallowing function assessed by the gold standard of VFSS should be considered as the primary outcome for future research.

5. Conclusion

The findings of this quantitative MA showed that EA combined with SRT treatment for patients with PSD resulted in an additional benefit on the effective rate. Given the low quality of the included trials, these results are not conclusive, and further high-quality and large-scale RCTs are required to verify the therapeutic effects of EA on PSD.

Abbreviations

EA: Electroacupuncture
PSD: Poststroke dysphagia
RCT: Randomized controlled trial
MA: Meta-analysis
SRT: Swallowing rehabilitation training
WST: Water swallowing test
ER: Effective rate
SSA: Standardized swallowing assessment
AE: Adverse events
VFSS: Video fluoroscopic swallowing study
IAP: Incidence of aspiration pneumonia
IFRS: Ichiro Fujishima Rating Scale
QOL: Quality of life
SR: Systematic review
PRISMA: Preferred Reporting Items for Systematic Reviews and Meta-Analyses
MD: Mean differences
CI: Confidence intervals
SMD: Standardized mean difference
OR: Odds ratio.

Data Availability

The data used to support the findings of this study are available from the corresponding author upon request.

Disclosure

Jinke Huang and Yao Shi are co-first authors.

Conflicts of Interest

The authors declare that there are no conflicts of interest.

Authors' Contributions

Jinke Huang and Yao Shi planned and designed the study, and they contributed equally. Min Shen, Manli Wu, and Xiaohui Qin screened potential studies and extracted data from the included studies. Min Shen, Xiaohui Qin, and Yanjuan Xu assessed the reviews; Yong Huang provided guidance on the overview methodology; and Jinke Huang drafted the manuscript. All authors read, critically reviewed, and approved the final manuscript as submitted.

Acknowledgments

The authors thank all investigators and supporters involved in this study. The study was supported by the Scientific Research Project of Guangdong Provincial Bureau of Traditional Chinese Medicine (no. 20201165).

References

[1] C. R. Camara-Lemarroy, B. E. Ibarra-Yruegas, and F. Gongora-Rivera, "Gastrointestinal complications after ischemic stroke," *Journal of the Neurological Sciences*, vol. 346, no. 1-2, pp. 20–25, 2014.

[2] B. Paitoon, K. Hitoshi, I. Yoko et al., "The effect of reclining position on swallowing function in stroke patients with dysphagia," *Journal of Oral Rehabilitation*, vol. 47, 2020.

[3] G. D. Eslick and N. J. Talley, "Dysphagia: epidemiology, risk factors and impact on quality of life - a population-based study," *Alimentary Pharmacology & Therapeutics*, vol. 27, no. 10, pp. 971–979, 2008.

[4] W. X. Qin, Z. J. Wang, Y. Zhong et al., "Comparative efficacy of nonpharmaceutical therapy in the treatment of dysphagia after stroke: a protocol for systematic review," *Medicine (Baltimore)*, vol. 99, 2020.

[5] Li Jing and Y. Li, "Improving and devoloping Cochrane systematic review," *Chinese Journal of Evidence-Based Medicine*, vol. 9, pp. 742-743, 2008.

[6] Z.-Y. Tian, L. Xing, Y. Gao et al., "An overview of systematic reviews and meta- analyses on acupuncture for post-acute stroke dysphagia," *Geriatrics (Basel)*, vol. 4, 2019.

[7] P. H. Julian, G. A. Douglas, and A. S. Jonathan, "Assessing risk of bias in included studies," in *Cochrane Handbook of Systematic Reviews of Interventions Version 5.1.0*, P. H. Julian and G. Sally, Eds., The Cochrane Collaboration, London, UK, 2011.

[8] D. Moher, A. Liberati, J. Tetzlaff, and D. G. Altman, "Preferred reporting items for systematic reviews and meta-analyses: the PRISMA statement," *BMJ*, vol. 339, p. b2535, 2009.

[9] W.-b. Wu, D.-f. Fan, C. Zheng et al., "Relieving throat and opening orifice acupuncture therapy for the post-stroke dysphagia," *World Journal of Acupuncture-Moxibustion*, vol. 29, no. 1, pp. 37–41, 2019.

[10] J. Z. Li, J. H. Li, and Z. Y. Si, "Clinical observation of electroacupuncture on post-stroke dysphagia," *China's Naturopathy*, vol. 27, no. 24, pp. 9-10, 2019.

[11] L. Qin, X. P. Zhang, X. C. Yang et al., "Deep acupuncture of Lianquan (CV23) and Yifeng (TE17) in combination with conventional acupuncture of other acupoints is superior to swallowing rehabilitation training in improving post-stroke dysphagia in apoplexy patients," *Acupuncture Research*, vol. 44, no. 2, pp. 144–147, 2019.

[12] H. He, W. Zhang, J. P. Zhu et al., "Therapeutic observation of electroacupuncture at cervical jiaji points (EX-B2) as the main treatment for deglutition disorders after cerebral stroke," *Shanghai Journal of Acupuncture and Moxibustion*, vol. 37, no. 8, pp. 852–855, 2018.

[13] H. M. Xu, Y. Cui, and Y. T. Xie, "Effect of electroacupuncture combined with rehabilitation training on dysphagia after stroke," *The World Clinical Medicine*, vol. 11, no. 6, pp. 146–148, 2017.

[14] S. Y. Zhang, S. B. Liu, W. Wu et al., "Clinical trials for treatment of stroke patients with dysphagia by vitalstim electroacupuncture combined with swallowing rehabilitation training," *Acupuncture Research*, vol. 42, no. 2, pp. 168–172, 2017.

[15] D. B. Zhang, Z. A. Liang, and Y. W. Zhong, "Therapeutic effects of Vitalstim electroacupuncture combined with deglutition training on dysphagia after stroke," *Chinese Journal of Cardiovascular Rehabilitation Medicine*, vol. 25, no. 3, pp. 335–338, 2016.

[16] K. Y. Huang and L. Yang, "Analysis of the clinical effects of electrical stimulation for dysphagia in acute stroke," *Ke Xue Zi Xun.*no. 21, pp. 61-62, 2015.

[17] J. J. Zhang, "Treatment of 60 cases of dysphagia after stroke by electroacupuncture combined with swallowing rehabilitation training," *Yunnan Journal of Traditional Chinese Medicine and Materia Medica*, vol. 35, no. 6, pp. 57–59, 2014.

[18] J. Q. Wang, Y. J. Sun, Y. X. Zhu et al., "Effect of electroacupuncture combined with rehabilitation training on dysphagia after stroke," *Journal of Emergency in Traditional Chinese Medicine*, vol. 21, no. 10, pp. 1701-1702, 2012.

[19] H. Q. Wang, X. Y. Gao, and Y. L. Zhou, "Clinical research on electroacupuncture of renying for the treatment of dysphagia due to stroke," *Journal of Chinese Medicine*, vol. 26, no. 4, pp. 501-502, 2011.

[20] H. F. Yang, J. W. Gong, T. Wang et al., "Clinical study of electroacupuncture combined with rehabilitation training for treatment of dysphagia patients after stroke," *Journal of New Chinese Medicine*, vol. 43, no. 3, pp. 92–94, 2011.

[21] B. Y. Wang and H. D. Cheng, "Clinical research of low frequency electroacupuncture matching rehabilitation training in post-stroke deglutition disorders," *Chinese Archives of Traditional Chinese Medicine*, vol. 28, no. 10, pp. 2224–2226, 2010.

[22] H. Lv, H. Liu, and J. N. Ni, "Electroacupuncture for dysphagia after stroke: a randomized controlled trial," *Journal of China-Japan Friendship Hospital*, no. 4, pp. 228-229, 2009.

[23] X. H. Deng and Y. L. Wang, "Clinical observation of electroacupuncture combined with early rehabilitation training on dysphagia after stroke," *Journal of Military Surgeon in Southwest China*, vol. 11, no. 4, pp. 623-624, 2009.

[24] Q. Cao, "Treatment of 60 cases of dysphagia after stroke by head electroacupuncture combined with swallowing function training," *Journal of Clinical Acupuncture and Moxibustion*, vol. 24, no. 11, pp. 12-13, 2008.

[25] Y. Zhang, X. H. Zhang, Y. L. Xiong et al., "Meta-analysis of randomized controlled trials on electro-acupuncture in the treatment of dysphagia after stroke," *Journal of Clinical Acupuncture and Moxibustion*, vol. 33, no. 8, pp. 75–79, 2017.

[26] M. A. Crary, G. D. Carnaby-Mann, and A. Faunce, "Electrical stimulation therapy for dysphagia: descriptive results of two surveys," *Dysphagia*, vol. 22, no. 3, pp. 165–173, 2007.

Hindawi
Evidence-Based Complementary and Alternative Medicine
Volume 2020, Article ID 8372647, 10 pages
https://doi.org/10.1155/2020/8372647

Review Article

Detrimental and Beneficial Effect of Autophagy and a Potential Therapeutic Target after Ischemic Stroke

Meng Wang,[1,2] Hangil Lee,[3] Kenneth Elkin,[3] Redina Bardhi,[3] Longfei Guan,[1,3,4] Ankush Chandra,[3] Xiaokun Geng,[1,2,3] and Yuchuan Ding[3,4]

[1]*China-America Institute of Neuroscience, Beijing Luhe Hospital, Capital Medical University, Beijing, China*
[2]*Department of Neurology, Beijing Luhe Hospital, Capital Medical University, Beijing, China*
[3]*Department of Neurosurgery, Wayne State University School of Medicine, Detroit, MI, USA*
[4]*Department of Research & Development Center, John D. Dingell VA Medical Center, Detroit, MI, USA*

Correspondence should be addressed to Xiaokun Geng; xgeng@ccmu.edu.cn

Received 28 May 2020; Revised 14 August 2020; Accepted 8 September 2020; Published 23 September 2020

Academic Editor: Shuang En Chuang

Autophagy, a physiologic mechanism that promotes energy recycling and orderly degradation through self-regulated disassembly of cellular components, helps maintain homeostasis. A series of evidences suggest that autophagy is activated as a response to ischemia and has been well-characterized as a therapeutic target. However, the role of autophagy after ischemia remains controversial. Activated-autophagy can remove necrotic substances against ischemic injury to promote cell survival. On the contrary, activation of autophagy may further aggravate ischemic injury, causing cell death. Therefore, the present review will examine the current understanding of the precise mechanism and role of autophagy in ischemia and recent neuroprotective therapies on autophagy, drug therapies, and nondrug therapies, including electroacupuncture (EA).

1. Introduction

Globally, stroke is the leading cause of disability and presents a great financial burden due to its "3H" effects: high disability, high morbidity, and high mortality [1, 2]. Acute ischemic stroke dominates among the spectrum of stroke disorders and leads to rapid neuronal necrosis due to occlusion of cerebral arteries [3, 4]. Subsequently, several cellular signaling cascades in cerebral tissue are altered in the ischemic state, which result in significant aggravation of brain damage in many cases. Due to the inability of neurons to regenerate, neuronal necrosis often produces many permanent neurological sequelae including paralysis, aphasia, coma, and death. Despite biological and technological advances in the field of cerebrovascular research, the recombinant tissue plasminogen activator (rtPA) remains the most effective FDA-approved treatment. Fibrinolytic therapy is administered intravenously within 4.5 hours of symptom onset and is intended to precipitate intravascular clot-retrieval and occluded vessel reperfusion [2, 5, 6]. Though rtPA is effective, many patients are still subject to significant injury as a result of the narrow therapeutic time window, rehemorrhagic complications, and reperfusion injury [7, 8]. Recent advances in endovascular therapy with new generation stent-retrievers and expanded intervention time windows have achieved higher rates of revascularization for patients with large vessel occlusion acute ischemic stroke [9, 10]. However, only 46% of patients treated with endovascular therapy for anterior circulation large vessel occlusion (LVO) achieve functional independence at 90 days with a 15.3% mortality rate [9, 11]. Thus, neuroprotective agents with broad therapeutic windows are urgently needed. A heightened focus on neuroprotection following reperfusion is warranted to reduce disability, morbidity, and mortality following ischemic brain injury.

Autophagy is a highly conserved lysosome-dependent process that maintains cellular homeostasis. It sequesters aging proteins and misfolded molecules for degradation either nonspecifically or by targeting specific protein aggregates. Based on the method and size of cargo delivery to

the lysosome, autophagy can be divided into three types: macroautophagy, microautophagy, and chaperone-mediated autophagy (CMA) [12]. In this review, our emphasis will be on macroautophagy. Macroautophagy uses a double membrane-bound vesicle to deliver cytoplasmic cargo to the lysosome, to which it subsequently fuses with to form an autolysosome, leading to digestion [13, 14]. In contrast, microautophagy occurs when intracellular contents are taken up directly by the lysosome, while CMA employs targeted proteins, which are taken up by transmembrane complexes in the lysosome. The process of macroautophagy consists of five stages. Induction is the first stage and is triggered by cellular stress such as endoplasmic reticulum (ER) stress and hypoxia/anoxia. In mammalian systems, autophagy is thought to originate in omegasomes, a monolayer membrane. The omegasome expands and bends into a double-membrane structure called the phagophore, which then engulfs cellular macromolecules and organelles. The double-membraned structure first surrounds intracellular contents to form the autophagosome and then fuses with a lysosome to form the autolysosome in a process called phagophore nucleation. In the next two stages, phagophore expansion and phagophore elongation, the phagophore expands and elongates, respectively. Subsequently, maturation of the phagosome occurs via the acquisition of proteins that are trafficked to the lysosome. The nonessential or damaged constituent contents are then digested by the lysosome and recycled to produce substrates for the maintenance of cytoplasmic balance [14–16]. The process is regulated by a group of autophagy-related genes (ATG) that activate an adaptive response to cellular stressors for the purpose of maintaining cellular energetic homeostasis.

An increasing amount of studies suggest that autophagy activity changes under cerebral ischemia/reperfusion (I/R), while the effect of autophagy on stroke is disputable. The activation of autophagy during ischemia has been demonstrated with electron microscopy and Western blot [17]. Immunofluorescence analysis of the microtubule-associated protein 1A/1B-light chain 3 (LC3), an autophagy-associated protein, also has confirmed the activation of autophagy in ischemic rats [18]. A study by Wen et al. found that autophagy inhibitors, 3-methyladenine (3-MA) and bafilomycin (BFA), reduced infarct volume and motor defects when administered before the onset of ischemia. The study also suggested that excessive autophagy after ischemia lead to cell death, possibly encouraging apoptosis by downregulating B cell lymphoma-2 (Bcl-2) [17]. Interestingly, there are reports that autophagy activation through different signaling pathways could alleviate the infarction outcome [1, 19]. Although there have been conflicting findings regarding the effect of autophagy in ischemia, current studies show that many interventions can improve ischemic injury by regulating autophagy. The present review aims to discuss the recent progress of studies on the molecular mechanisms of autophagy after stroke and the potentials of how autophagy serves as a novel target for neuroprotection to mitigate poststroke cerebral injury.

2. Signaling Pathways of Autophagy in Stroke

Postischemic disturbances in the internal environment lead to changes in autophagy activity via the regulation of certain signaling pathways. Ischemia in brain tissue leads to decreased ATP production, oxidative stress, endoplasmic reticulum stress, and calcium overload. Factors regulate autophagy through different pathways [20] and will be discussed as follows. Figure 1 briefly describes the signaling pathway of autophagy after ischemic stroke.

2.1. Mammalian Target of Rapamycin (mTOR) Pathway. mTOR, a protein with serine/threonine kinase activity, coordinates anabolic and catabolic processes to maintain essential homeostasis. It consists of two complexes, mTORC1 and mTORC2, which regulate different aspects of cellular homeostasis [21]. mTORC1 is highly sensitive to rapamycin (specific mTOR inhibitor), promotes anabolic metabolism, and inhibits catabolic processes by inhibiting autophagy. mTORC2 is involved in other distinct signaling complexes and has demonstrated Akt expression promotion [22].

mTOR regulates autophagy activity in ischemia and reperfusion via two major pathways: the Akt-mTOR pathway and the AMPK-mTOR pathway. The Akt-mTOR pathway is modulated by mammalian phosphatidyl-inositol 3-kinase (PI3K) enzymes, which consist of three groups: class I, class II, and class III. Class I PI3Ks are specifically involved in the activation of Akt [23]. Various intracellular and extracellular stimuli activate PI3K, initiating a series of downstream cascades. One of these cascades leads to phosphatidylinositol-3,4,5-trisphosphate (PIP_3) production, which forms a docking site containing proteins PDK1 and Akt [24]. Akt becomes fully activated after it is phosphorylated by PDK1 and mTORC2 at two amino acid residues (Thr308 and Ser473), respectively. Akt activation then inhibits TSC2 (tuberin), inducing its dissociation from TSC1 (hamartin). When in a complex, TSC1/2 convert GTP-Rheb into GDP-Rheb. Thus, the dissociation of TSC1 and TSC2 improves GTP-Rheb activity and subsequently increases the activity of mTORC1 [5, 22, 24, 25]. Following activation, mTORC1 phosphorylates downstream effector proteins and inhibits formation of the ULK1/2 complex, which is necessary in the early steps of autophagy to generate the autophagosome [20, 26]. Taken together, downregulation of the Akt-mTOR pathway may induce autophagy.

On the contrary, elevations of the AMP/ATP ratio and increased calcium influx as a result of ischemic stress enhance AMPK activity [27, 28]. Once activated, AMPK modulates energy balance by stimulating metabolic pro-

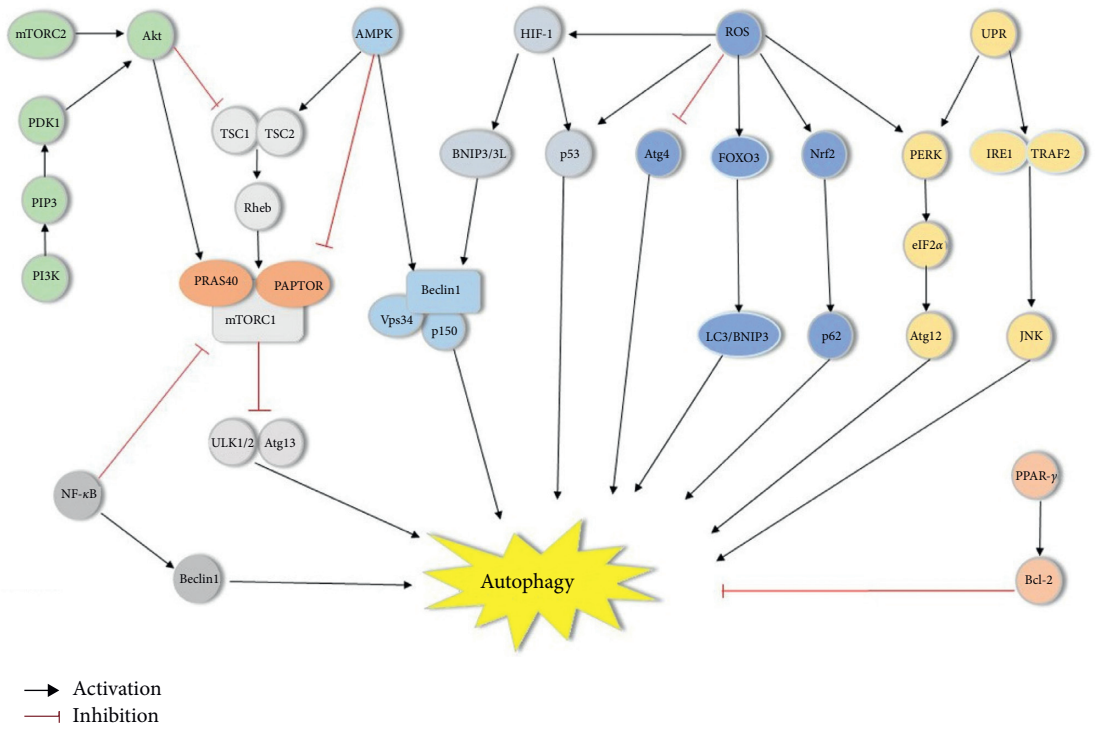

Figure 1: Signaling pathways of autophagy. PI3K produces PIP3 after stimulation. PIP3 forms a docking site containing proteins PDK1 and Akt. When Akt is activated, TSC2 dissociates from TSC1, which improves GTP-Rheb activity and subsequently increases mTORC1 activity. Akt also activates mTORC1 by regulating PRAS40 activity. mTORC1 inhibits ULK1/2 complex activation, causing a decrease in autophagosomes. AMPK regulates the TSC2/TSC1 complex, activating autophagy in contrast to Akt. AMPK also phosphorylates RAPTOR to inhibit mTORC1 activity. AMPK is involved in the regulation of class III PI3K complexes. It modifies VPS34 affinity and phosphorylates Beclin 1 to promote autophagosome formation. HIF-1 can mediate BNIP3/BNIP3L to promote the separation of Beclin 1 from Bcl-2, thus allowing Beclin 1 to participate in autophagosome formation. HIF-1 is involved in the regulation of autophagy through ROS activation. In contrast, PPAR-γ enhances Bcl-2 overexpression and inhibits autophagy occurrences. In addition, HIF-1 and ROS can also activate autophagy by regulating the expression of tumor protein p53. NF-κB activates autophagy by inhibiting mTOR activity and promoting Beclin 1 expression. UPR initiated by endoplasmic reticulum stress can mediate autophagy through the PERK/eIF2α and Ire1/TRAF2/JNK signaling pathways. ROS can also regulate autophagy through the ER stress-mediated PERK pathway. Furthermore, accumulated ROS can induce Nrf2 and FOXO3 expression, subsequently activating p62 and LC3/BNIP3, respectively. Atg4 is regulated by ROS to promote autophagosome formation.

cesses and inhibiting synthetic processes [29]. It stimulates autophagy through the phosphorylation of specific autophagy-initiating protein complexes and is considered an upstream mediator, though its regulation is complicated and cross-reactive [30]. AMPK phosphorylates TSC2 at Thr1227 and Ser1345 residues, which activates TSC2, and inhibits the separation of the TSC1/TSC2 complex. mTORC1 activity is reduced as a result. Furthermore, AMPK inactivates mTORC1 by phosphorylating RAPTOR, a unique complex found in mTORC1 but not in mTORC2, at Ser722 and Ser792 residues. Since mTORC1 inactivates autophagy-inducing proteins ULK1/2 and ATG13, a decrease in mTORC1 activity may augment ULK1 activation and thus promote autophagy flux [31, 32]. In addition to regulating autophagy through mTOR, AMPK is involved in the regulation of class III PI3K complexes. Another complex, consisting of PIK3C3/VPS34, PIK3R4/p150, and Beclin 1, is encouraged by AMPK in its induction of autophagy formation. AMPK, for example, may modify VPS34's affinity for the other components of the complex to regulate the activity of autophagy. Furthermore, AMPK phosphorylation of Beclin 1 at diverse sites (Thr388, Ser91, and Ser94) can promote autophagosome formation under nutrient-deficiency conditions [33, 34].

2.2. Hypoxia-Inducible Factor-1 (HIF-1) Pathway. HIF-1 is a transcription factor that regulates adaptive responses to hypoxic environments, which consists of two subunits: HIF-1α and HIF-1β. It has become a major focus of neuroscience research since it regulates postischemic pathological processes such as apoptosis, energy metabolism, and gene transcription. Additionally, recent literature indicates that HIF-1 is involved in the regulation of autophagy after stroke [35]. Adenovirus (E1B) 19KD-interacting protein 3(BINP3)/BNIP3-like (BNIP3L), a target gene of HIF-1, is an autophagy inducer. Activated HIF-1 promotes the expression of BINP3 under ischemic conditions. BNIP3/BNIP3L competes with Beclin 1 and dissociates it from the Beclin 1/Bcl-2 complex, stimulating Beclin 1 to participate in the formation of the autophagosome [36]. Lu et al. demonstrated that hypoxic preconditioning (HPC) activated autophagy

through the HIF-1/BNIP3/Beclin 1 signaling pathway in SH-SY5Y cells after oxygen and glucose deprivation/reoxygenation (OGD/R). This phenomenon could be reversed by the application of YC-1, a HIF-1 inhibitor. This suggests that HIF is involved in autophagy activation and is a potential therapeutic target for autophagy [37]. Furthermore, BNIP3 can also inhibit Rheb, an upstream activator of mTOR, to promote autophagy. HIF-1 expression is also involved in upregulating mitochondrial autophagy by inhibiting the mTOR signaling pathway, although whether this effect is regulated by BNIP3 needs further verification [38]. Moreover, HIF-1 may activate autophagy by regulating the expression of tumor protein p53 [20].

2.3. Unfolded Protein Response (UPR) Signaling Pathways. The endoplasmic reticulum (ER) plays an important role in maintaining intracellular Ca^{2+} balance and synthesizing proteins. During ischemic conditions, misfolded proteins accumulate and Ca^{2+} balance is disrupted, leading to ER stress and initiation of a self-protecting event called the unfolded protein response (UPR) [14]. Autophagy is activated by UPR through the PERK/eIF2α and Ire1/TRAF2/JNK signaling pathways [39]. UPR upregulates protein kinase RNA-like ER kinase (PERK) and inositol requiring kinase 1(Ire1) [40]. PERK promotes the expression of Atg12 by eukaryotic initiation factor 2α (eIF2α) phosphorylation. Atg12 plays an important role in autophagosome formation. Gene knockout of PERK inhibits autophagy, demonstrating that the PERK-eIF2α signaling pathway upregulates autophagy [41]. In addition, IRE1 can combine with tumor necrosis factor receptor-associated factor-2 (TRAF-2) and further phosphorylate JNK, thus triggering autophagy [42]. Moreover, activating transcription factor 6 (ATF6), one of the signal transduction pathways of UPR, has been reported to modulate the occurrence of autophagy in stroke, but the specific signaling mechanism is still puzzling [43].

2.4. Reactive Oxygen Species (ROS) Pathway. Oxidative stress after ischemic injury causes excessive accumulation of ROS [44], which is related to autophagy regulation [45]. ROS mediates autophagy mainly through intracellular transcription regulation [14]. Elevated ROS increases p53 levels, which activates two regulators of autophagy, Tp53-induced glycolysis and apoptosis regulator (TIGAR), and DNA damage-regulated autophagy modulator (DRAM) [46, 47]. ROS also enhances the transcription of nuclear factor-(erythroid-derived2-) like2 (Nrf2). Subsequently, Nrf2 promotes the expression of autophagy-associated protein p62 to mediate autophagy [48]. ROS stimulates forkhead box O3 (FOXO3) expression to regulate autophagy through activating LC3 and BNIP3 [49]. Furthermore, PERK is also activated by ROS in addition to UPR in its involvement of autophagy regulation [50]. HIF-1 expression is induced by accumulated ROS and stimulates autophagy through the BNIP3/BNIP3L pathway as mentioned above [36, 51]. On the other hand, Atg4, which is responsible for autophagosome membrane elongation, was also shown to be inhibited by ROS, thus supporting autophagosome formation [52]. Atg4 participates in the formation of LC3-I by exposing residues at the C terminus of LC3. Then, LC3-I combines with phosphoethanolamine (PE) to form LC3-II. Moreover, Atg4 is involved in cleavage of LC3-II [13]. It is reported that Atg4 protease activity was inhibited by ROS oxidation [53]. Inhibition of Atg4 may promote autophagy by reducing cleavage of LC3-II [45].

2.5. Additional Signaling Pathways. As mentioned previously, HIF-1 binds Bcl-2 in competition with Beclin 1 and releases Beclin 1 to induce autophagy. Unlike HIF-1, peroxisome proliferators-activated receptors (PPAR-γ) upregulate Bcl-2 expression to inhibit Beclin 1-mediated autophagy activation [20]. Nuclear factor kappa B (NF-κB), a sensitive transcription factor, has been reported to be involved in autophagy and apoptosis regulation [54]. NF-κB activates autophagy by triggering the expression of protein Beclin 1 [55, 56]. In addition, p50, a subunit of NF-κB, has been reported to inhibit mTOR activity in ischemic stroke mice models [57]. Inhibiting NF-κB and its downstream effector p53 downregulates autophagy and apoptosis, consequently alleviating ischemia/reperfusion injury [58].

3. Autophagy in Stroke

Autophagy plays an integral role in the physiological and pathological processes of ischemic stroke through several pathways. Dozens of studies suggest that autophagy is activated after ischemia/reperfusion [17, 20, 59]. Yan et al. demonstrated autophagy activation by detecting the number of autophagosomes using electron microscopy. They observed that the LC3 protein levels in the ischemic penumbra of the cerebral cortex of mice increased between 3 to 24 hours following MCAO reperfusion [59]. Similarly, another study found that LC3 expression increased significantly in the ischemic penumbra after 1 hour of ischemia and continued for 5 hours without reperfusion [60]. Interestingly, the apoptotic protein cleaved caspase-3 was also elevated, and its dynamic changes were similar to those of autophagy, suggesting the coexistence of autophagy and apoptosis in the cerebral ischemic penumbra [61]. However, whether the activation of autophagy promotes neuronal survival or death has been debated. Some studies suggest that induced autophagy after stroke provides a source of cellular energy for survial by degrading damaged material. Others suggest that overactivated autophagy may aggravate stroke injury by damaging normal cells and causing autophagic cell death (type II programmed cell death) in addition to apoptosis.

3.1. Beneficial Effect of Autophagy in Ischemic State after Stroke. Changes in the intracellular environment, such as mitochondrial dysfunction, oxidative stress, endoplasmic reticulum stress, and apoptosis, may aggravate neurological dysfunction after ischemia and reperfusion. Apoptosis is a type I programmed cell death that is tightly regulated.

Proapoptotic genes are activated in ischemic conditions to initiate the apoptotic pathway. Zhang et al. discovered that astragaloside IV could decrease neuronal apoptosis by activating autophagy in HT22 cells after OGD/R [62]. In addition, ezetimibe has proved to alleviate infarct volume and neurobehavioral deficits in middle cerebral artery occlusion (MCAO) rats. The neuroprotective and antiapoptotic effects of ezetimibe were diminished after intervention with the autophagy inhibitor 3-MA [63]. These data suggest that activation of autophagy after ischemia and reperfusion can reduce neuronal damage by decreasing apoptosis. Rapamycin induces autophagy by inhibiting mTOR. Wu et al. found that rapamycin decreased infarction volumes and improved neurologic deficits [64]. It has been reported that autophagy can improve the internal conditions of the cell after ischemia by removing damaged mitochondria [65]. Li et al. also found that rapamycin-activated autophagy improved mitochondrial function and alleviated ischemic injury, and that protective effect was reversed by 3-MA [66].

3.2. Autophagy Negatively Affects Stroke Outcome. Accumulating results have suggested that autophagy activation aggravates neurological dysfunction after ischemia and reperfusion. Intraperitoneal injection of 3-MA reduced ischemic nerve injury and brain edema in permanent middle cerebral artery ischemia models [17]. Treatment with tetrahydroxystilbene glucoside (TSG), one of the essence of the *Fallopia multiflora*, also reduced infarct volume and neurobehavioral deficits in ischemia/reperfusion mice by inhibiting autophagy [67]. Zhang et al. studied the TP53-induced glycolysis and apoptosis regulator (TIGAR), which functions as a fructose-2,6-biphosphatase, to verify the role of autophagy activation after ischemia-reperfusion. They found that autophagy decreased in TIGAR-transgenic mice, as opposed to TIGAR-knockout mice. Knockout of TIGAR not only elevated autophagy but also increased infract volume and neurological deficit scores. These detrimental effects were blocked by treatment with 3-MA after ischemia/reperfusion. Thus, the neuroprotective effect of TIGAR was produced in part by inhibiting autophagy [68]. Puerarin, a traditional Chinese herb, has been demonstrated to alleviate brain dysfunction after ischemia/reperfusion by depressing autophagy protein expression via the AMPK-mTOR-ULK1 signaling pathway [8]. Similarly, Jiang and his colleagues confirmed that inhibiting excessive autophagy can reduce postischemia-reperfusion damage [69]. Luo et al. discovered that the use of dexmedetomidine could significantly reduce brain injury after ischemic stroke by inhibiting autophagy. The effect of dexmedetomidine was enhanced by 3-MA and diminished by rapamycin [70]. These data suggest that autophagy inhibition is neuroprotective.

4. Autophagy-Mediated Neuroprotection in Ischemia/Reperfusion Injury

Although the current consensus is that autophagy is a double-edged sword after ischemia-reperfusion, a number of neuroprotective strategies targeting neuronal autophagy have been discovered, including neuroprotective drugs, ischemic preconditioning, electroacupuncture, hyperbaric oxygen preconditioning, and nucleic acid therapies. These are summarized in Table 1.

4.1. Neuroprotective Agents on Autophagy. Today, pharmacological development remains the primary focus of ischemic stroke research. As mentioned above, ezetimibe attenuates neuronal apoptosis via autophagy activation after MCAO in rats [63]. Ezetimibe administration decreased infarct volumes, neurological deficits, and cerebral cholesterol levels at 24 hours after MCAO. They also noted that Beclin 1 immunopositive cells increased in ischemic rats, while 3-MA reversed the neuroprotection provided by ezetimibe. Traditional Chinese medicines have been shown to have therapeutic effects by regulating autophagy. Puerarin has proved to alleviate brain dysfunction after ischemia/reperfusion by depressing autophagy protein expression via the AMPK-mTOR-ULK1 signaling pathway [8]. Ginkogolide K (GK) pretreatment has been reported to induce autophagy under ischemia, promoting astrocyte proliferation and migration after reoxygenation [71]. Ginsenoside Rb1 (GRb1) ameliorates brain damage and increases autophagy after ischemia/reperfusion [72]. Similarly, triptolide treatment was reported to decrease apoptosis following ischemia, in association with induced autophagy [73]. In another study, rapamycin showed potential neuroprotective effects in both permanent middle cerebral artery ligation (pMCAL) and embolic clot middle cerebral artery occlusion (eMCAO). Infarct volumes measured via TTC staining after eMCAO and pMCAL indicated rapamycin-reduced injury lesions and upregulated autophagy [64, 66, 74]. Moreover, metformin is reported to lessen the risk of stroke by enhancing autophagy [19], while nicotinamide phosphoribosyl transferase (NAMPT) promotes cell survival by regulating autophagy after cerebral ischemia [75]. Overall, conferring neuroprotection through targeting autophagy with drug therapy is feasible.

4.2. Nondrug Therapies on Autophagy

4.2.1. Electroacupuncture (EA). EA was reported to be protective against cerebral ischemic injury [91, 92]. Recently, it was observed that EA treatment reduces cell apoptosis after ischemia [93, 94]. The neuroprotective effect of EA and its relation to autophagy have been assessed by Huang et al. [76]. EA is involved in the autophagy initiation, vesicle nucleation, and autophagosome maturation, in addition to autophagolysosome degradation. It was also shown that EA treatment influences autophagy flux by regulating the expression of autophagy-related proteins including the ULK1 complex, Beclin 1, and mTOR [77, 78]. However, it is unclear whether EA promotes or suppresses autophagy. In addition, different EA parameters such as the selection of acupoints, duration of stimulation, and the timing of ischemia/reperfusion have different effects against neuronal ischemic/reperfusion injury.

Table 1: Neurotherapeutics targeting autophagy after I/R.

Interventions	Key findings	References
Pharmacological interventions		
Traditional Chinese medicine (ginsenoside Rb1, puerarin, ginkogolide K, triptolide, and ezetimibe)	(i) Ginsenoside Rb1 ameliorated neuronal injury and increased autophagy after I/R (ii) Puerarin reduced ischemic brain damage by inhibiting autophagy through the AMPK-mTOR-ULK1 signaling pathway (iii) GK pretreatment induced autophagy under ischemia and promoted astrocyte proliferation and migration after reoxygenation (iv) Triptolide decreased apoptosis and induced autophagy, thus conferring neuroprotection (v) Ezetimibe attenuated neuronal apoptosis by activating autophagy and reduced cerebral cholesterol levels	[8] [63] [71] [72] [73]
Rapamycin	(i) Rapamycin reduced infarct sizes and cell death in both permanent MCAL and embolic MCAO (ii) Rapamycin may attenuate stroke injury lesion sizes and upregulate autophagy	[64] [66] [74]
Metformin	(i) Acute metformin preconditioning lessened the risk of stroke by enhancing autophagy	[19]
Nampt	(i) Nampt induced autophagy and promoted cell survival after cerebral ischemia	[75]
Nonpharmacological interventions		
Electroacupuncture	(i) EA is involved in the initiation of autophagy, vesicle nucleation, and maturation of autophagosomes, in addition to the degradation of autophagolysosomes (ii) Treatment with EA may influence autophagy activity through regulating autophagy-related proteins	[76] [77] [78] [79]
Cerebral ischemic pre-/postconditioning or remove ischemic conditioning	(i) Ischemic preconditioning alleviates cerebral I/R injury by activating autophagy, therefore improving neurologic functions (ii) RIPoC decreased infarct volume, neurological deficits, and cell apoptosis after I/R through regulating autophagy	[80] [81] [82] [76] [83] [84]
Hyperbaric oxygen preconditioning (HBO)	(i) HBO preconditioning preserved the integrity of the lysosomal membrane and formed autolysosomes in transient focal cerebral ischemia to activate autophagy (ii) HBO-mediated autophagy after cerebral I/R was also found to be neuroprotective	[85] [86] [87]
Nucleic acid therapies		
miR-497 miR-30d-5p miRNA-30a	(i) Cerebral ischemia can lead to abnormal changes in miRNA expression levels involved in the etiology and pathology of stroke (ii) miR-30a negatively regulates the 3'UTR of Beclin 1 to inhibit autophagy, and miR-30d-5p regulates autophagy in a similar way (iii) Suppression of miR-497 could increase neuronal autophagy activity to alleviate ischemia injury	[1] [88] [89] [90]

4.2.2. Ischemic Preconditioning and Postconditioning (IPC). IPC confers neuroprotection by increasing the tolerance to fatal ischemic exposure, which has been shown to be associated with autophagy [95, 96]. The results of Sheng's group showed that the number of autophagosomes in neurons increased with the induction of LC3 immunopositivity in the ischemic preconditioning model. 3-MA, an autophagy inhibitor, reversed and weakened ischemic preconditioning-induced autophagy activation and protective effects [79]. These findings indicate that enhanced autophagy contributes to neuroprotection induced by ischemic preconditioning, as demonstrated recently [80–82]. Moreover, an in vitro study confirmed that ischemic preconditioning induces autophagy activation through the AMPK pathway [97]. In addition, changes in autophagy activity are implicated in the resistance to cerebral ischemia conferred by remote ischemic postconditioning. Guo et al. found that remote limb ischemic postconditioning (RIPoC) induced autophagy-related protein expressions when compared with the ischemia/reperfusion group. Inhibition of autophagy through pharmacological means not only abolished the effect of conditioning against ischemia but also reversed the antiapoptotic effect [83]. On the other hand, Chen et al. revealed that the protective effect of RIPoC was related to the inhibition of autophagy activation [84]. These contradictory results may be due to the different influences of ischemia time and means of conditioning on autophagy activity in animal models. Taken together, ischemic pre- and

postconditioning may induce neuroprotection through the regulation of autophagy.

4.2.3. Hyperbaric Oxygen Administration (HBO). HBO is an effective method in the treatment of brain trauma in clinical practice. Currently, researchers have found that it also has a therapeutic effect in ischemic injury [98]. Although the potential mechanisms remain unclear, much attention has been given to the relationship between autophagy and HBO [99, 100]. In an MCAO model, autophagy was involved in the tolerance to cerebral ischemia conferred by HBO [60]. In this study, the authors discovered that HBO reduced cerebral damage through the enhancement of autophagy-related proteins LC3-II and Beclin 1. 3-MA reduced the HBO-induced neuroprotective effect, suggesting that activated autophagy is one of the mechanisms of HBO administration. In addition, HBO preserved the integrity of the lysosomal membrane and promoted the formation of autolysosomes in transient focal cerebral ischemia rats. Cystatin C (CysC) is a determinant for neuroprotection in HBO therapy as it promotes cerebral autophagic flux after ischemia [85]. HBO-induced autophagy in cerebral ischemia/reperfusion was also found to be neuroprotective by Wang and colleagues [86]. In contrast, a recent article by Chen et al. reported that HBO conferred neuroprotection by autophagy inhibition [87]. HBO should be further studied as a promising nonpharmacological and noninvasive treatment.

4.2.4. Nucleic Acid Therapies. MicroRNAs (miRNAs) are composed of 20–25 endogenous, noncoding, single-stranded RNA molecules. They regulate target genes' expressions and can modulate cell proliferation, differentiation, apoptosis, and metabolism [101]. Recent studies suggest that cerebral ischemia leads to abnormal changes in miRNA expression levels, which are involved in the etiology and pathology of sequelae after stroke. Dharap et al. demonstrated that 24 miRNAs were increased, while 23 other miRNAs were decreased following stroke [88]. These altered miRNAs may modulate genetic expression, which suggests that miRNA may be a potential therapeutic target to reduce cerebral injury through an autophagy-mediated mechanism [90]. Wang et al. found that miR-30a expression was downregulated, while autophagy expression was upregulated in the in vivo and in vitro ischemia/reperfusion model. It has been confirmed that the downregulation of miR-30a abolished ischemia injury by Beclin 1-mediated autophagy. miR-30a negatively regulates Beclin 1 expression through recognizing the 3′-untranslated region (3'UTR) of Beclin 1 [1]. Similarly, miR-30d-5p, which regulates the 3'UTR of Beclin 1, is presumed to promote neuronal death in hypoxic-ischemic (HI) rats by inhibiting autophagy [89]. Chen et al. observed that the suppression of miR-497 increased neuronal autophagy and alleviated ischemia injury, especially in young rats [90]. Taken together, these findings indicate that miRNA expression after stroke may be involved in neuroprotection through autophagy.

5. Conclusion

Current studies consistently report elevation of autophagic flux following ischemia/reperfusion. However, the role of autophagy after acute ischemia and reperfusion remains uncertain, especially in regard to the precise functions that mediate cell survival or cell death. Overall, autophagy may act through the "Goldilocks" principle: excessive or inadequate induction of autophagy may be maladaptive, while a specific level of autophagy may be beneficial. Moreover, the beneficial or detrimental effects of autophagy may be dependent upon the severity or length of ischemia. Further research is warranted to assess how autophagy activation is beneficial. There is consensus that signaling pathways associated with autophagy comprise potential therapeutic targets for novel and neuroprotective strategies. Multimodal targeting of autophagy at different time points may serve as an effective method in the treatment of stroke.

Data Availability

The datasets used and analyzed during the current study are available from the corresponding author on reasonable request.

Conflicts of Interest

The authors declare that they have no conflicts of interest.

Acknowledgments

This work was partially supported by the National Nature Science Foundation of China (81871838) and the Beijing Tongzhou District Financial Fund and the Science and Technology Plan of Beijing Tongzhou District (KJ2020CX002 and KJ2019CX004).

References

[1] P. Wang, J. Liang, Y. Li et al., "Down-regulation of miRNA-30a alleviates cerebral ischemic injury through enhancing beclin 1-mediated autophagy," *Neurochemical Research*, vol. 39, no. 7, pp. 1279–1291, 2014.

[2] X. Li, S. Wen, S. Zhao et al., "Mild therapeutic hypothermia protects the brain from ischemia/reperfusion injury through upregulation of iASPP," *Aging and Disease*, vol. 9, no. 3, pp. 401–411, 2018.

[3] S. Yan, T. Li, T. Ji et al., "AMPK: potential therapeutic target for ischemic stroke," *Theranostics*, vol. 8, no. 16, pp. 4535–4551, 2018.

[4] S. Yi, Q. Dai, J. Yu et al., "Identification of IL-17A-derived neural cell type and dynamic changes of IL-17A in serum/CSF of mice with ischemic stroke," *Neurological Research*, vol. 39, no. 6, pp. 552–558, 2017.

[5] B. Liu, A. Kost, and D. Kasprowska, "Neuronal autophagy in cerebral ischemia - a potential target for neuroprotective strategies?" *Pharmacological Reports*, vol. 64, no. 1, pp. 1–15, 2012.

[6] S. Zhou, B. Qiao, X. Chu, and Q. Kong, "Oxymatrine attenuates cognitive deficits through SIRT1-mediated autophagy in ischemic stroke," *Journal of Neuroimmunology*, vol. 323, pp. 136–142, 2018.

[7] K. Wei, P. Wang, and C.-Y. Miao, "A double-edged sword with therapeutic potential: an updated role of autophagy in ischemic cerebral injury," *CNS Neuroscience & Therapeutics*, vol. 18, no. 11, pp. 879–886, 2012.

[8] J. F. Wang, Z. G. Mei, Y. Fu et al., "Puerarin protects rat brain against ischemia/reperfusion injury by suppressing autophagy via the AMPK-mTOR-ULK1 signaling pathway," *Neural Regeneration Research*, vol. 13, no. 6, pp. 989–998, 2018.

[9] M. Goyal, B. K. Menon, W. H. van Zwam et al., "Endovascular thrombectomy after large-vessel ischaemic stroke: a meta-analysis of individual patient data from five randomised trials," *The Lancet*, vol. 387, no. 10029, pp. 1723–1731, 2016.

[10] K. Dippel and D. S. Liebeskind, "Wake-up stroke: dawn of a new era," *Brain Circulation*, vol. 2, no. 2, pp. 72–79, 2016.

[11] A. P. Jadhav and T. G. Jovin, "Endovascular therapy for acute ischemic stroke: the standard of care," *Brain Circulation*, vol. 2, no. 4, pp. 178–182, 2016.

[12] M. Zhang, Y.-N. Deng, J.-Y. Zhang et al., "SIRT3 protects rotenone-induced injury in SH-SY5Y cells by promoting autophagy through the LKB1-AMPK-mTOR pathway," *Aging and Disease*, vol. 9, no. 2, pp. 273–286, 2018.

[13] K. R. Liu and D. J. Klionsky, "An overview of autophagy: morphology, mechanism, and regulation," *Antioxidants & Redox Signaling*, vol. 20, no. 3, pp. 460–473, 2014.

[14] P. Wang, B.-Z. Shao, Z. Deng, S. Chen, Z. Yue, and C.-Y. Miao, "Autophagy in ischemic stroke," *Progress in Neurobiology*, vol. 163-164, pp. 98–117, 2018.

[15] S. N. Weis, A. P. Toniazzo, B. P. Ander et al., "Autophagy in the brain of neonates following hypoxia-ischemia shows sex- and region-specific effects," *Neuroscience*, vol. 256, pp. 201–209, 2014.

[16] S. Zhan, D. Chakraborty, A. Bhowmik, and M. K. Ghosh, "Cerebral ischemic stroke: cellular fate and therapeutic opportunities," *Frontiers in Bioscience (Landmark Edition)*, vol. 24, pp. 435–450, 2019.

[17] Y.-D. Wen, R. Sheng, L.-S. Zhang et al., "Neuronal injury in rat model of permanent focal cerebral ischemia is associated with activation of autophagic and lysosomal pathways," *Autophagy*, vol. 4, no. 6, pp. 762–769, 2008.

[18] A. Han, A. Langhagen, and S. Steiger, "Focal cerebral ischemia induces upregulation of Beclin 1 and autophagy-like cell death," *Neurobiology of Disease*, vol. 29, no. 1, pp. 132–141, 2008.

[19] T. Jiang, J.-T. Yu, X.-C. Zhu et al., "Acute metformin preconditioning confers neuroprotection against focal cerebral ischaemia by pre-activation of AMPK-dependent autophagy," *British Journal of Pharmacology*, vol. 171, no. 13, pp. 3146–3157, 2014.

[20] K. Wang, D. Xu, F. Li, S. Chen, and Y. Li, "The progress of neuronal autophagy in cerebral ischemia stroke: mechanisms, roles and research methods," *Journal of the Neurological Sciences*, vol. 400, pp. 72–82, 2019.

[21] S. Martens, "A division of labor in mTORC1 signaling and autophagy," *Science Signaling*, vol. 11, no. 559, 2018.

[22] B. Shi, M. Ma, Y. Zheng, Y. Pan, and X. Lin, "mTOR and Beclin1: two key autophagy-related molecules and their roles in myocardial ischemia/reperfusion injury," *Journal of Cellular Physiology*, vol. 234, 2019.

[23] S. Noorolyai, N. Shajari, E. Baghbani, S. Sadreddini, and B. Baradaran, "The relation between PI3K/AKT signalling pathway and cancer," *Gene*, vol. 698, pp. 120–128, 2019.

[24] I. Yudushkin, "Getting the Akt together: guiding intracellular Akt activity by PI3K," *Biomolecules*, vol. 9, no. 2, 2019.

[25] A. Toker and S. Marmiroli, "Signaling specificity in the Akt pathway in biology and disease," *Advances in Biological Regulation*, vol. 55, pp. 28–38, 2014.

[26] S. Alers, A. S. Loffler, S. Wesselborg, and B. Stork, "Role of AMPK-mTOR-Ulk1/2 in the regulation of autophagy: cross talk, shortcuts, and feedbacks," *Molecular and Cellular Biology*, vol. 32, no. 1, pp. 2–11, 2012.

[27] R. Ke, Q. Xu, C. Li, L. Luo, and D. Huang, "Mechanisms of AMPK in the maintenance of ATP balance during energy metabolism," *Cell Biology International*, vol. 42, no. 4, pp. 384–392, 2018.

[28] P. Weisová, D. Dávila, L. P. Tuffy, M. W. Ward, C. G. Concannon, and J. H. M. Prehn, "Role of 5′-adenosine monophosphate-activated protein kinase in cell survival and death responses in neurons," *Antioxidants & Redox Signaling*, vol. 14, no. 10, pp. 1863–1876, 2011.

[29] D. Garcia and R. J. Shaw, "AMPK: mechanisms of cellular energy sensing and restoration of metabolic balance," *Molecular Cell*, vol. 66, no. 6, pp. 789–800, 2017.

[30] W. Chen, X. Xi, S. Zhang et al., "Pioglitazone protects against renal ischemia-reperfusion injury via the AMP-activated protein kinase-regulated autophagy pathway," *Frontiers in Pharmacology*, vol. 9, p. 851, 2018.

[31] D. G. Hardie, "Why starving cells eat themselves," *Science*, vol. 331, no. 6016, pp. 410-411, 2011.

[32] K. Inoki, T. Zhu, and K.-L. Guan, "TSC2 mediates cellular energy response to control cell growth and survival," *Cell*, vol. 115, no. 5, pp. 577–590, 2003.

[33] L. Wang, D. Yuan, J. Zheng et al., "Chikusetsu saponin IVa attenuates isoprenaline-induced myocardial fibrosis in mice through activation autophagy mediated by AMPK/mTOR/ULK1 signaling," *Phytomedicine*, vol. 58, p. 152764, 2019.

[34] D. M. Wu, D. B. Shackelford, D. F. Egan et al., "AMPK phosphorylation of raptor mediates a metabolic checkpoint," *Molecular Cell*, vol. 30, no. 2, pp. 214–226, 2008.

[35] Y. Mihaylova, J. Wang, and J. Feng, "The neuroprotective effects of curcumin are associated with the regulation of the reciprocal function between autophagy and HIF-1alpha in cerebral ischemia-reperfusion injury," *Drug Design, Development and Therapy*, vol. 13, pp. 1135–1144, 2019.

[36] Y. Mo, Y. Y. Sun, and K. Y. Liu, "Autophagy and inflammation in ischemic stroke," *Neural Regeneration Research*, vol. 15, no. 8, pp. 1388–1396, 2020.

[37] N. Lu, X. Li, R. Tan et al., "HIF-1alpha/Beclin1-Mediated autophagy is involved in neuroprotection induced by hypoxic preconditioning," *Journal of Molecular Neuroscience*, vol. 66, no. 2, pp. 238–250, 2018.

[38] Y. Sun, Y. Zhu, X. Zhong, X. Chen, J. Wang, and G. Ying, "Crosstalk between autophagy and cerebral ischemia," *Frontiers in Neuroscience*, vol. 12, p. 1022, 2018.

[39] Z. Qi and L. Chen, "Endoplasmic reticulum stress and autophagy," *Autophagy: Biology and Diseases*, vol. 1206, pp. 167–177, 2019.

[40] V. P. Nakka, P. Prakash-Babu, and R. Vemuganti, "Crosstalk between endoplasmic reticulum stress, oxidative stress, and autophagy: potential therapeutic targets for acute CNS injuries," *Molecular Neurobiology*, vol. 53, no. 1, pp. 532–544, 2016.

[41] Y. Kouroku, E. Fujita, I. Tanida et al., "ER stress (PERK/eIF2 alpha phosphorylation) mediates the polyglutamine-induced LC3 conversion, an essential step for autophagy formation,"

Cell Death & Differentiation, vol. 14, no. 2, pp. 230–239, 2007.

[42] W. Chen, Y. Sun, K. Liu, and X. Sun, "Autophagy: a double-edged sword for neuronal survival after cerebral ischemia," *Neural Regeneration Research*, vol. 9, no. 12, pp. 1210–1216, 2014.

[43] Z. Yu, H. Sheng, S. Liu et al., "Activation of the ATF6 branch of the unfolded protein response in neurons improves stroke outcome," *Journal of Cerebral Blood Flow & Metabolism*, vol. 37, no. 3, pp. 1069–1079, 2017.

[44] R. Rodrigo, R. Fernandez-Gajardo, R. Gutierrez et al., "Oxidative stress and pathophysiology of ischemic stroke: novel therapeutic opportunities," *CNS Neurol Disord Drug Targets*, vol. 12, no. 5, pp. 698–714, 2013.

[45] J. Huang, G. Y. Lam, and J. H. Brumell, "Autophagy signaling through reactive oxygen species," *Antioxid Redox Signal*, vol. 14, no. 11, pp. 2215–2231, 2011.

[46] F. Pietrocola, V. Izzo, M. Niso-Santano et al., "Regulation of autophagy by stress-responsive transcription factors," *Seminars in Cancer Biology*, vol. 23, no. 5, pp. 310–322, 2013.

[47] D. Crighton, S. Wilkinson, J. O'Prey et al., "DRAM, a p53-induced modulator of autophagy, is critical for apoptosis," *Cell*, vol. 126, no. 1, pp. 121–134, 2006.

[48] A. Puissant, N. Fenouille, and P. Auberger, "When autophagy meets cancer through p62/SQSTM1," *American Journal of Cancer Research*, vol. 2, no. 4, pp. 397–413, 2012.

[49] P. K. Mahalingaiah and K. P. Singh, "Chronic oxidative stress increases growth and tumorigenic potential of MCF-7 breast cancer cells," *PLoS One*, vol. 9, no. 1, Article ID e87371, 2014.

[50] A. Avivar-Valderas, E. Salas, E. Bobrovnikova-Marjon et al., "PERK integrates autophagy and oxidative stress responses to promote survival during extracellular matrix detachment," *Molecular and Cellular Biology*, vol. 31, no. 17, pp. 3616–3629, 2011.

[51] S. F. Nabavi, A. Sureda, A. Sanches-Silva et al., "Novel therapeutic strategies for stroke: the role of autophagy," *Critical Reviews in Clinical Laboratory Sciences*, vol. 56, no. 3, pp. 182–199, 2019.

[52] L. Li, J. Tan, Y. Miao, P. Lei, and Q. Zhang, "ROS and autophagy: interactions and molecular regulatory mechanisms," *Critical Reviews in Clinical Laboratory Sciences*, vol. 35, no. 5, pp. 615–621, 2015.

[53] R. Scherz-Shouval, E. Shvets, E. Fass, H. Shorer, L. Gil, and Z. Elazar, "Reactive oxygen species are essential for autophagy and specifically regulate the activity of Atg4," *The EMBO Journal*, vol. 38, no. 10, 2007.

[54] M. Zeng, X. Wei, Z. Wu et al., "NF-kappaB-mediated induction of autophagy in cardiac ischemia/reperfusion injury," *Biochemical and Biophysical Research Communications*, vol. 436, no. 2, pp. 180–185, 2013.

[55] T. Copetti, F. Demarchi, and C. Schneider, "p65/RelA binds and activates the beclin 1 promoter," *Autophagy*, vol. 5, no. 6, pp. 858-859, 2009.

[56] N. Zhang and Y. Zhao, "Other molecular mechanisms regulating autophagy," *Advances in Experimental Medicine and Biology*, vol. 1206, pp. 261–271, 2019.

[57] W. L. Li, S. P. Yu, D. Chen et al., "The regulatory role of NF-kappaB in autophagy-like cell death after focal cerebral ischemia in mice," *Neuroscience*, vol. 244, pp. 16–30, 2013.

[58] J. Pan, X. Li, F. Guo, Z. Yang, L. Zhang, and C. Yang, "Ginkgetin attenuates cerebral ischemia-reperfusion induced autophagy and cell death via modulation of the NF-kappaB/p53 signaling pathway," *Bioscience Reports*, vol. 39, no. 9, 2019.

[59] T. Nitatori, N. Sato, S. Waguri et al., "Delayed neuronal death in the CA1 pyramidal cell layer of the gerbil hippocampus following transient ischemia is apoptosis," *The Journal of Neuroscience*, vol. 15, no. 2, pp. 1001–1011, 1995.

[60] W. Yan, H. Zhang, X. Bai, Y. Lu, H. Dong, and L. Xiong, "Autophagy activation is involved in neuroprotection induced by hyperbaric oxygen preconditioning against focal cerebral ischemia in rats," *Brain Research*, vol. 1402, pp. 109–121, 2011.

[61] Y. H. Deng, H. Y. He, L. Q. Yang, and P. Y. Zhang, "Dynamic changes in neuronal autophagy and apoptosis in the ischemic penumbra following permanent ischemic stroke," *Neural Regeneration Research*, vol. 11, no. 7, pp. 1108–1114, 2016.

[62] Y. Zhang, Y. Zhang, X. F. Jin et al., "The role of astragaloside IV against cerebral ischemia/reperfusion injury: suppression of apoptosis via promotion of P62-LC3-autophagy," *Molecules*, vol. 24, no. 9, 2019.

[63] J. Yu, X. Li, N. Matei et al., "Ezetimibe, a NPC1L1 inhibitor, attenuates neuronal apoptosis through AMPK dependent autophagy activation after MCAO in rats," *Journal of Experimental Neurology*, vol. 307, pp. 12–23, 2018.

[64] M. Wu, H. Zhang, J. Kai et al., "Rapamycin prevents cerebral stroke by modulating apoptosis and autophagy in penumbra in rats," *Annals of Clinical and Translational Neurology*, vol. 5, no. 2, pp. 138–146, 2018.

[65] Z. Shen, Y. Zheng, J. Wu et al., "PARK2-dependent mitophagy induced by acidic postconditioning protects against focal cerebral ischemia and extends the reperfusion window," *Autophagy*, vol. 13, no. 3, pp. 473–485, 2017.

[66] Q. Li, T. Zhang, J. Wang et al., "Rapamycin attenuates mitochondrial dysfunction via activation of mitophagy in experimental ischemic stroke," *Biochemical and Biophysical Research Communications*, vol. 444, no. 2, pp. 182–188, 2014.

[67] F. Yu, W. Xue, L. Dong, X. Hu, D. Huang, and K. Wang, "Tetrahydroxystilbene glucoside suppresses NAPDH oxidative stress to mitigate apoptosis and autophagy induced by cerebral ischemia/reperfusion injury in mice," *Evidence-Based Complementary and Alternative Medicine*, vol. 2019, Article ID 3913981, 9 pages, 2019.

[68] D. M. Zhang, T. Zhang, M. M. Wang et al., "TIGAR alleviates ischemia/reperfusion-induced autophagy and ischemic brain injury," *Free Radical Biology and Medicine*, vol. 137, pp. 13–23, 2019.

[69] W. W. Jiang, B. S. Huang, Y. Han, L. H. Deng, and L. X. Wu, "Sodium hydrosulfide attenuates cerebral ischemia/reperfusion injury by suppressing overactivated autophagy in rats," *FEBS Open Bio*, vol. 7, no. 11, pp. 1686–1695, 2017.

[70] C. Luo, M. W. Ouyang, Y. Y. Fang et al., "Dexmedetomidine protects mouse brain from ischemia-reperfusion injury via inhibiting neuronal autophagy through up-regulating HIF-1alpha," *Frontiers in Cellular Neuroscience*, vol. 11, p. 197, 2017.

[71] Y. Zhang and J. M. Miao, "Ginkgolide k promotes astrocyte proliferation and migration after oxygen-glucose deprivation via inducing protective autophagy through the AMPK/mTOR/ULK1 signaling pathway," *European Journal of Pharmacology*, vol. 832, pp. 96–103, 2018.

[72] T. Lu, Y. Jiang, Z. Zhou et al., "Intranasal ginsenoside Rb1 targets the brain and ameliorates cerebral ischemia/reperfusion injury in rats," *Biological & Pharmaceutical Bulletin*, vol. 34, no. 8, pp. 1319–1324, 2011.

[73] Y. Yang, K. Gao, Z. Hu et al., "Autophagy upregulation and apoptosis downregulation in DAHP and triptolide treated

cerebral ischemia," *Mediators of Inflammation*, vol. 2015, Article ID 120198, 12 pages, 2015.

[74] K. M. Buckley, D. L. Hess, I. Y. Sazonova et al., "Rapamycin up-regulation of autophagy reduces infarct size and improves outcomes in both permanent MCAL, and embolic MCAO, murine models of stroke," *Experimental & Translational Stroke Medicine*, vol. 6, p. 8, 2014.

[75] P. Wang, Y. F. Guan, H. Du, Q. W. Zhai, D. F. Su, and C. Y. Miao, "Induction of autophagy contributes to the neuroprotection of nicotinamide phosphoribosyltransferase in cerebral ischemia," *Autophagy*, vol. 8, no. 1, pp. 77–87, 2012.

[76] Y. G. Huang, W. Tao, S. B. Yang, J. F. Wang, Z. G. Mei, and Z. T. Feng, "Autophagy: novel insights into therapeutic target of electroacupuncture against cerebral ischemia/reperfusion injury," *Neural Regeneration Research*, vol. 14, no. 6, pp. 954–961, 2019.

[77] Z. Ting, Z. Jianbin, and H. Luqi, "Protective effect of electroacupuncture on neurons autophagy in perfusion period of cerebral ischemia," *Neuroscience Letters*, vol. 661, pp. 41–45, 2017.

[78] Y. Xing, M. Zhang, W. B. Li, F. Dong, and F. Zhang, "Mechanisms involved in the neuroprotection of electroacupuncture therapy for ischemic stroke," *Frontiers in Neuroscience*, vol. 12, p. 929, 2018.

[79] R. Sheng, L. S. Zhang, R. Han, X. Q. Liu, B. Gao, and Z. H. Qin, "Autophagy activation is associated with neuroprotection in a rat model of focal cerebral ischemic preconditioning," *Autophagy*, vol. 6, no. 4, pp. 482–494, 2010.

[80] D. Y. Xia, W. Li, H. R. Qian, S. Yao, J. G. Liu, and X. K. Qi, "Ischemia preconditioning is neuroprotective in a rat cerebral ischemic injury model through autophagy activation and apoptosis inhibition," *Brazilian Journal of Medical and Biological Research*, vol. 46, no. 7, pp. 580–588, 2013.

[81] C. Gao, Y. Cai, X. Zhang et al., "Ischemic preconditioning mediates neuroprotection against ischemia in mouse hippocampal CA1 neurons by inducing autophagy," *PLoS One*, vol. 10, no. 9, Article ID e0137146, 2015.

[82] J. Su, T. Zhang, K. Wang, T. Zhu, and X. Li, "Autophagy activation contributes to the neuroprotection of remote ischemic perconditioning against focal cerebral ischemia in rats," *Neurochemical Research*, vol. 39, no. 11, pp. 2068–2077, 2014.

[83] H. Guo, L. Zhao, B. Wang et al., "Remote limb ischemic postconditioning protects against cerebral ischemia-reperfusion injury by activating AMPK-dependent autophagy," *Brain Research Bulletin*, vol. 139, pp. 105–113, 2018.

[84] G. Z. Chen, X. Y. Shan, X. S. Li, and H. M. Tao, "Remote ischemic postconditioning protects the brain from focal ischemia/reperfusion injury by inhibiting autophagy through the mTOR/p70S6K pathway," *Neurological Research*, vol. 40, no. 3, pp. 182–188, 2018.

[85] Z. Fang, Y. Feng, Y. Li et al., "Neuroprotective autophagic flux induced by hyperbaric oxygen preconditioning is mediated by cystatin C," *Neuroscience Bulletin*, vol. 35, no. 2, pp. 336–346, 2019.

[86] Y. C. Wang, S. Zhang, T. Y. Du, B. Wang, and X. Q. Sun, "Hyperbaric oxygen preconditioning reduces ischemia-reperfusion injury by stimulating autophagy in neurocyte," *Brain Research*, vol. 1323, pp. 149–151, 2010.

[87] C. Chen, W. Chen, Z. Nong et al., "Hyperbaric oxygen alleviated cognitive impairments in mice induced by repeated cerebral ischemia-reperfusion injury via inhibition of autophagy," *Life Sciences*, vol. 241, Article ID 117170, 2020.

[88] A. Dharap, K. Bowen, R. Place, L. C. Li, and R. Vemuganti, "Transient focal ischemia induces extensive temporal changes in rat cerebral microRNAome," *Journal of Cerebral Blood Flow & Metabolism*, vol. 29, no. 4, pp. 675–687, 2009.

[89] F. Zhao, Y. Qu, J. Zhu et al., "miR-30d-5p plays an important role in autophagy and apoptosis in developing rat brains after hypoxic-ischemic injury," *Journal of Neuropathology & Experimental Neurology*, vol. 76, no. 8, pp. 709–719, 2017.

[90] X. Chen, S. Lin, L. Gu et al., "Inhibition of miR-497 improves functional outcome after ischemic stroke by enhancing neuronal autophagy in young and aged rats," *Neurochemistry International*, vol. 127, 2019.

[91] H. Zhao, Y. Lu, Y. Wang et al., "Electro acupunture contributes to recovery of neurological deficits in experimental stroke by activating astrocytes," *Restorative Neurology and Neuroscience*, vol. 36, no. 3, pp. 301–312, 2018.

[92] T. Wen, X. Zhang, S. Liang et al., "Electroacupuncture ameliorates cognitive impairment and spontaneous low-frequency brain activity in rats with ischemic stroke," *Journal of Stroke and Cerebrovascular Diseases*, vol. 27, no. 10, pp. 2596–2605, 2018.

[93] Y. Xing, S. D. Yang, M. M. Wang, F. Dong, Y. S. Feng, and F. Zhang, "Electroacupuncture alleviated neuronal apoptosis following ischemic stroke in rats via midkine and ERK/JNK/p38 signaling pathway," *Journal of Molecular Neuroscience*, vol. 66, no. 1, pp. 26–36, 2018.

[94] Y. Xing, M. M. Wang, Y. S. Feng, F. Dong, and F. Zhang, "Possible involvement of PTEN signaling pathway in the anti-apoptotic effect of electroacupuncture following ischemic stroke in rats," *Cellular and Molecular Neurobiology*, vol. 38, no. 8, pp. 1453–1463, 2018.

[95] W. J. Yan, H. L. Dong, and L. Z. Xiong, "The protective roles of autophagy in ischemic preconditioning," *Acta Pharmacologica Sinica*, vol. 34, no. 5, pp. 636–643, 2013.

[96] X. D. Ma, J. N. Song, M. Zhang, J. Y. An, Y. L. Zhao, and B. F. Zhang, "Advances in research of the neuroprotective mechanisms of cerebral ischemic postconditioning," *International Journal of Neuroscience*, vol. 125, no. 3, pp. 161–169, 2015.

[97] T. Jiang, J. T. Yu, X. C. Zhu et al., "Ischemic preconditioning provides neuroprotection by induction of AMP-activated protein kinase-dependent autophagy in a rat model of ischemic stroke," *Molecular Neurobiology*, vol. 51, no. 1, pp. 220–229, 2015.

[98] J. Ding, D. Zhou, M. Sui et al., "The effect of normobaric oxygen in patients with acute stroke: a systematic review and meta-analysis," *Neurological Research*, vol. 40, no. 6, pp. 433–444, 2018.

[99] Q. Hu, A. Manaenko, N. Matei et al., "Hyperbaric oxygen preconditioning: a reliable option for neuroprotection," *Medical Gas Research*, vol. 6, no. 1, pp. 20–32, 2016.

[100] C. Hentia, A. Rizzato, E. Camporesi et al., "An overview of protective strategies against ischemia/reperfusion injury: the role of hyperbaric oxygen preconditioning," *Brain and Behavior*, vol. 8, no. 5, Article ID e00959, 2018.

[101] N. Henninger and Y. Mayasi, "Nucleic acid therapies for ischemic stroke," *Neurotherapeutics*, vol. 16, no. 2, 2019.

Hindawi
Evidence-Based Complementary and Alternative Medicine
Volume 2020, Article ID 5415813, 8 pages
https://doi.org/10.1155/2020/5415813

Research Article

Effect of Catgut Embedment in Du Meridian Acupoint on Mental and Psychological Conditions of Patients with Gastroesophageal Reflux Disease

Zhengjie Luo,[1] **Xuanming Hu**,[2] **Chaoming Chen**,[2] **Lvqun Zhu**,[3] **Wenyan Zhang**,[3] **You Shen**,[3] **and Jirou He**[3]

[1]*Department of Rehabilitation Medicine, Third Affiliated Hospital of Soochow University & Changzhou First People's Hospital, Changzhou 213003, Jiangsu, China*
[2]*Department of Acupuncture, Nanjing Hospital of Chinese Medicine, Affiliated to Nanjing University of Chinese Medicine, Nanjing 210001, Jiangsu, China*
[3]*Nanjing University of Chinese Medicine, Nanjing 210029, Jiangsu, China*

Correspondence should be addressed to Chaoming Chen; czm6704@163.com

Received 21 June 2020; Revised 2 August 2020; Accepted 3 August 2020; Published 23 September 2020

Guest Editor: Feng Zhang

Objective. To observe the influence of the catgut-embedding method in Du Meridian acupoint on the mental and psychological state of patients with gastroesophageal reflux disease (GERD) and analyze its possible mechanism. *Methods*. According to the random number table, 60 patients with GERD were randomly divided into groups of acupoint catgut embedding and Western medicine, 30 cases in each group. The acupoint group was given catgut embedment in the positive reaction points along the Du Meridian, while the Western medicine group received lansoprazole tablet. They were both treated for six weeks. Scores of Gastroesophageal Reflux Disease Questionnaire (GerdQ), Zung's Self-Rating Anxiety Scale (SAS), Zung's Self-Rating Depression Scale (SDS), and Health-Related Quality of Life Scale for GERD (GERD-HRQL) were measured before and after treatment to analyze and evaluate the differences of symptom scores and mental and psychological conditions between the two groups. *Results*. (1) The scores of GerdQ, GERD-HRQL, SAS, and SDS in the two groups both significantly decreased after treatment ($P < 0.05$), and those of the acupoint group were much lower than the Western medicine group ($P < 0.05$). (2) The total effective rate was 90.00% in the acupoint group and 53.33% in the Western medicine group, with a statistically significant difference ($P < 0.05$). (3) The correlation coefficients r between the GerdQ score and scores of SAS and SDS were 0.563 and 0.322, respectively, and those between the GERD-HRQL score and scores of SAS and SDS were, respectively, 0.506 and 0.435. *Conclusion*. (1) The main symptoms of GERD patients, such as acid reflux and heartburn, mental and psychological condition, and quality of life, were all improved in the two groups, but the efficacy in the acupoint group is superior to that of the Western medicine group. (2) The clinical symptoms and scores of patients' quality of life are positively correlated with the degree of their anxiety and depression. (3) The acupoint catgut-embedding method can effectively regulate the anxiety and depressive symptoms of patients, which complements the efficacy of proton-pump inhibitors and benefits a wider range of population.

1. Introduction

The mental and psychological factors can affect the pathogenesis, diagnosis, and prognosis of gastroesophageal reflux disease (GERD) [1]. They are the important causes of high sensitivity of esophagus viscera, which stimulate the brain to generate signals that travel down to the esophagus and gastrointestinal tract, causing gastrointestinal reactions and abnormal gastric acid secretion and worsening the symptoms of the digestive tract. Long-term suffering of clinical symptoms, in turn, can aggravate patients' anxiety and depression, leading to autonomic nerve dysfunction. The imbalance between sympathetic and parasympathetic nerves reduces the contraction force of digestive tract circular fold muscle, which further slows down gastric contraction rate,

decreases migrating motor complex (MMC) function, and regurgitates stomach acid to the esophagus, eventually generating the reflux esophagitis [2, 3]. Current studies have shown that acupuncture has an accurate therapeutic effect on both the gastrointestinal somatization symptoms caused by psychosocial diseases and the psychosocial symptoms generated together with gastrointestinal diseases, and its efficacy is better than Western medicine in improving some symptoms [4, 5]. The catgut-embedding therapy, an important part of external treatment methods of traditional Chinese medicine, stimulates acupoint with a longer effect than simple acupuncture. It is simple and safe in operation, which can balance *yin* and *yang*, dredge *qi* and blood by stimulating acupoint based on syndrome differentiation of meridians and collaterals so as to reduce symptoms and improve patients' quality of life. The previous study of our research group has proved that acupuncture and catgut embedment in Du Meridian acupoint have better effects on GERD than oral administration of proton-pump inhibitor (PPI) [6, 7]. On this basis, this study discussed the influence of Du Meridian acupoint catgut embedding on the psychosocial factors of GERD, objectively evaluated its therapeutic effect on the disease, and analyzed its mechanism of improving patients' psychosocial symptoms, in order to support the application and promotion of Du Meridian catgut-embedding therapy in the future.

2. Clinical Data

2.1. General Information. This study was approved by the Hospital Ethics Committee. In this study, 60 patients diagnosed with GERD in the Acupuncture and Moxibustion Department of Nanjing Hospital of Chinese Medicine, the Acupuncture, Moxibustion and Tuina Department of Jiangdong Community Health Service Center, and the National TCM Physician Outpatient Department affiliated to Nanjing University of Chinese Medicine from March 2018 to March 2019 were enrolled, and they or their immediate family members have signed the informed consent. According to the random number table, the subjects were randomly divided into the acupoint catgut-embedding group (30 cases) and the Western medicine group (30 cases). There were 14 males and 16 females in the acupoint group, aged 23–75 years and averaged 50.77 ± 15.73, with a disease duration of 0 to 30 years, averaged 5.42 ± 6.31. In the Western medicine group, there were 11 males and 19 females, aged 19–72 years and averaged 47.30 ± 14.83, with a disease duration of 0 to 20 years, averaged 4.42 ± 5.40. The differences in gender, age, and course of disease between the two groups had no systematic significance ($P > 0.05$) and were comparable. Among the 60 included GERD patients, 5 were identified by electronic gastroscopy as Barrett's esophagus (BE), 22 were identified as erosive esophagitis (EE), 20 were chronic gastritis, and the rest 10 and 3 cases were identified as chronic superficial gastritis and chronic atrophic gastritis, respectively.

2.2. Diagnostic Criteria. It refers to *the Montreal definition and classification of gastroesophageal reflux disease* (2006) [8] and the *Guidelines for the diagnosis and management of gastroesophageal reflux disease* (2013) [9]: (1) symptoms of heartburn, gastric acid reflux, noncardiac chest pain, and upper abdominal pain occurred for more than 4 weeks. (2) Erosive esophagitis or Barrett's esophagus is found by endoscopic examination. (3) For patients with obvious symptoms but having no organic changes under the gastroscope, if the symptoms were alleviated after oral administration of proton-pump inhibitor (PPI), they will be confirmed with GERD.

2.3. Inclusion Criteria. Inclusion criteria include (1) people showing in consistence with the diagnostic criteria; (2) age from 18 to 75 years; (3) at least one of the four typical GERD symptoms occurring with a duration longer than 4 weeks; and (4) those who voluntarily signed the informed consent and actively cooperate with the treatment.

2.4. Exclusion Criteria. Exclusion criteria include (1) patients outside the inclusion criteria; (2) patients accompanied by gastrointestinal bleeding or intestinal metaplasia under gastroscope; (3) acute abdominal patients with rebound pain according to abdominal examination; (4) those with connective tissue diseases and blood system diseases; (5) those intolerant to endoscopic examination; (6) pregnant and/or lactating women; and (7) those with severe hemorrhagic diseases.

2.5. Reasons for Loss of Contact and Corresponding Measures. These include the patients dropping out of the study or abandoning treatment during the study. The solution was to supplement the patient participants into the research group in proportion to 1 : 1.

2.6. Complying with the Study Principle of Blindness. The researchers were divided into four groups: the first group randomly assigned subjects; the second was responsible for performing the treatment; the third collected data; and the fourth was responsible for data collation, statistical analysis, and article writing. The four groups separately implemented their tasks.

3. Treatment Methods

3.1. Western Medicine Group. The patients were given lansoprazole tablets (Keyilin, 15 mg × 14 tablets, produced by Sichuan Hairong Pharmaceutical Co., Ltd., National Drug Approval Code H20065186), oral administration, 1-2 tablets (15–30 mg) per day for 6 weeks.

3.2. Acupoint Group. Acupoint selection: Baihui (DU 20), Dazhui (DU 14), the positive response points to tenderness in the thoracic dorsal segment of Du Meridian (TDSDM). Exploration of positive tenderness points: before treatment, the patient lies in a prone position, fully exposing the back,

and both upper limbs are relaxed and naturally placed at the sides of the body. The operator should stand on the right side of the patient and place the right index finger pulp in the depression under the spinous process in the middle of the patient's back. The patient is then examined from the depression under the T1 spinous process to T9 spinous process depression with continuous and uniform pressure. At the same time, the operator will ask the patient whether there is pain, sour and swelling, and other discomforts, and where the discomfort exists is marked as a positive point, while those without pain or unable to clearly tell are considered as negative points. If a patient has a history of lumbago and back pain, the operator should acquire the details of his or her medical history and perform a physical examination or imaging examination for further exclusion, to avoid making mistakes in the study results due to wrong positive points [10]. The positive points along the Du Meridian were selected for catgut embedment, together with Baihui (DU 20) and Dazhui (DU 14). If there were no positive response points, Zhiyang (DU 9), Lingtai (DU 10), Shendao (DU 11), Dazhui (DU 14), and Baihui (DU 20) would be used as the substitute.

Operation process (Figure 1): after cleaning and disinfecting the hands of the operator and the patient's fully exposed back, open the disposable bending plate, disposable embedding needle, absorbable protein thread, and metal tweezer and wear disposable sterile medical gloves. Then, pull out the embedding needle core about 2 cm and use the metal tweezer to place the protein thread into the needle tube from the needle tip. The operator held the embedding needle with one hand and lifted and pinched the skin on the back with the other hand to insert needles 0.1–0.3 inches from the acupoints selected at an angle of about 45° (between the needle body and the patient's back). After that, slowly push the needle inward until it entered the interspinous ligament in the gap between the spinous processes, slightly deeper than the length of the protein thread. Then, pull it back slightly to the subcutaneous soft tissues and perform twirling, lifting, and thrusting methods until the local muscles had obvious soreness, numbness, heaviness, and distension. Afterwards, push the needle core while pulling back the needle tube to embed the protein thread into the subcutaneous soft tissues. For thread embedment in Baihui (DU 20), the needle was inserted into the subgaleal loose connective tissues at an angle of 15–30° (between the needle body and the scalp). The protein thread should not be exposed outside the epidermis. Every time before thread embedding, it is necessary to check whether there was a nodule around Baihui (DU 20) caused by incomplete absorption of protein thread. If it exists, Baihui (DU 20) will not be used for thread embedment [10]. After pulling out the needles, the operator should press the needle holes immediately with sterile cotton balls for 5–10 minutes, covering sterile dressing and fixed with adhesive tape for 24 hours. The patient could not take a shower within 24 hours. The method was performed once every two weeks for a total of 3 times (Day 0, Weeks 2 and 4). The observation indexes were evaluated before the first treatment (Day 0) and on the 6th week (Day 42) after the third treatment was finished.

4. Curative Effect Observation

4.1. Observation Indexes. The two groups both underwent assessment twice before and after the treatment using scales of GerdQ, SDS, SAS, and GERD-HRQL for efficacy evaluation. The patients in the two groups were surveyed with a questionnaire before treatment (Day 0). The Western medicine group was treated with lansoprazole orally for 6 weeks and received the second assessment on the 42nd day. The acupoint group underwent the second and third catgut-embedding treatment on the 14th and 28th days, respectively, and they also received the second assessment on the 42nd day.

4.1.1. GerdQ. Patients were asked to recall their symptoms for the last week to fill the GerdQ, including scoring of positive symptoms, negative symptoms, and positive impacts. The maximum cumulative score of the six questions was 18. The total score ≥8 supports the diagnosis of GERD. Scores of the three items were counted up to get the final score. The higher the score, the more serious the disease condition was.

4.1.2. SDS. A total of 20 topics were included, using a 4-grade scoring method set according to the occurrence frequency of the main symptoms. The scores of all questions were added together and multiplied by 1.25, and the integer part was the standard score. The maximum score was 100, and over 53 indicated the existence of depression. The higher the score, the more serious the patient's depression was.

4.1.3. SAS. A total of 20 topics were selected, using a 4-grade scoring method set according to the occurrence frequency of the main symptoms. The scores of all questions were added together and multiplied by 1.25, which was rounded to the nearest whole number to get the standard score. The maximum score was 100 and over 50 indicated the presence of anxiety. The higher the score, the more serious the patient's anxiety was.

4.1.4. GERD-HRQL. Patients were scored with GERD-HRQL, including heartburn, dietary habits, dysphagia, flatulence, and medication, from 0 to 5 points by reference to the severity of those symptoms. The higher the score, the greater the impact on the patient's quality of life and the lower the quality of life.

4.2. Clinical Efficacy Determination. The effective rate of GerdQ score calculated by nimodipine scoring method: (a) cure: curative effect index = 100%; (b) marked effect: curative effect index ≥80%; (c) effective: curative effect index ≥50% and <80%; and (d) invalid: curative effect index <50%. Total effective rate = (number of cured cases + number of markedly effective cases + number of effective cases)/total number of cases × 100%.

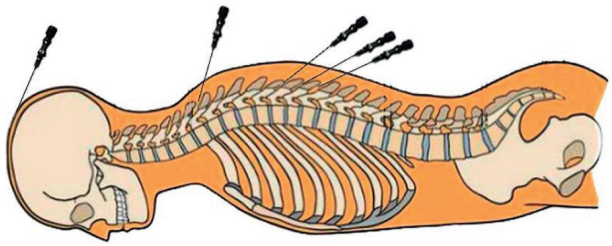

Figure 1: An example of the thread-embedding operation on the back.

4.3. Statistical Processing. In this study, IBM SPSS 23.0 was used for data collation and analysis. The measurement data were expressed as mean ± standard deviation, and the mean comparison of those with normal distribution between the two groups was evaluated by an independent sample *t*-test, while the comparison of those with nonnormal distribution was evaluated by rank-sum test. Pearson's correlation coefficient was used for correlation analysis. The count data was expressed by the case number. Chi-square test was used to compare the distribution of classification data among different groups. $A = 0.05$ was considered as the statistical basis.

4.4. Results and Analysis

(1) The results of electronic gastroscopy of 60 GERD patients showed that 27 cases had esophageal mucosal damage (5 cases of BE and 22 cases of EE), accounting for 45% while another 33 cases did not have (including 20 cases of chronic gastritis, 10 cases of chronic superficial gastritis, 3 cases of chronic atrophic gastritis). Before the clinical trial, patients without esophageal mucosal damage (accounting for 55%) showed significantly reduced reflux symptoms in the oral PPI testing, for which they were diagnosed as nonerosive reflux disease (NERD), as shown in Table 1.

(2) The differences in scores of GerdQ, SAS, SDS, and GERD-HRQL of the two groups were not statistically significant before treatment ($P > 0.05$), and there was comparability between the two groups. After treatment, those scores in the two groups all decreased with a significant difference before and after treatment ($P < 0.05$), indicating that the treatment methods used in the two groups are both effective on GERD. The scores of symptoms and quality of life of the acupoint group after treatment were significantly lower than those of the Western medicine group ($P < 0.05$), suggesting that the effect in the acupoint group is superior to that of the Western medicine group, as shown in Table 2.

(3) Correlation analysis was expressed by Pearson's correlation coefficient. The correlation coefficient *r* values of GerdQ score with scores of SAS and SDS were 0.563 and 0.322 respectively, and the *r* value of GERD-HRQL score with scores of SAS and SDS were, respectively, 0.506 and 0.435, suggesting that the clinical symptoms and quality of life of GERD patients were positively correlated with the degree of anxiety and depression, as shown in Table 3 and Figures 2 and 3.

(4) Comparison of efficacy at the end of the treatment between the two groups using the chi-square test. The curative effect was 90.00% in the acupoint group and 53.33% in the Western medicine group after treatment, showing a statistically significant difference between the two groups. The rate of the marked effect and the total effective rate in the acupoint group were significantly higher than those of the Western medicine group ($P < 0.05$), as shown in Table 4.

5. Discussion

5.1. Relationship between Du Meridian and Anxiety and Depression. Du Meridian is closely related to the brain since it passes from the uterus to the top of the head along the posterior median line, as described in the Chapter "Yingqi" of *Huangdi Neijing: Lingshu*. The brain is the house of the original spirit and the center of consciousness and thought. According to TCM theories, meridians can be applied to treat diseases located along their running routes; thus, the acupoint of Du Meridian can be used to treat brain-related diseases, such as depression and other mental diseases. Du Meridian governs all other *yang* meridians (hand and foot tai*yang* meridians, hand and foot *shaoyang* meridians, and hand and foot *yangming* meridians); therefore, *yang qi* can supplement the brain and marrow by flowing through the running route of Du Meridian, providing the "material basis" the brain needs to maintain physiological functions. However, if *yang qi* cannot flow upward or the meridians and collaterals are obstructed, the *qi* flow of Du Meridian will be blocked and fail to transport essence to nourish the brain, which may lead to mental diseases such as depression and anxiety. Therefore, the smooth qi flow of Du Meridian is a key factor affecting the normal functions of brain governing mind and consciousness. In addition, since Du Meridian is connected with the bladder meridian of foot *taiyang*, the back-transport points (BL 13, BL 15, BL 18, BL 20, and BL 23) are closely related to the *zang-fu* organs (lungs, heart, liver, spleen, and kidney); the dysfunction of the *zang-fu* organs can lead to emotional dysfunction. In addition, the bladder meridian of foot *taiyang* is connected with Du Meridian through qi and blood, so the corresponding back-transport points or points of Du Meridian are suggested to treat depression and anxiety. They can also exert the effects of regulating functions of *zang-fu* organs related to emotional disorders, such as liver, heart, pericardium, spleen, and kidney (which are different from the organs in Western medicine). Moreover, since liver meridian of foot *jueyin* converges with Du Meridian at the top of head, acupoint of Du Meridian can also be used for dredging liver *qi*. It can also be applied to calm the mind.

Among patients with depression or gastrointestinal diseases, positive reaction points may occur in the TDSDM. Zhang and Wang [10] found that in patients with depression, the occurrence rate of tenderness reaction in the thoracic dorsal segment of Du Meridian reached over 80%. Moreover, the probability of positive points of tenderness

Table 1: Gastroscopy results of 60 patients.

	Barrett's esophagus (BE)	Erosive esophagitis (EE)	Chronic gastritis	Chronic superficial gastritis	Chronic atrophic gastritis
Total (60 cases)	5	22	20	10	3
Percentage	8.33	36.67	33.33	16.67	5

Table 2: Comparison of the two groups in different indicators before and after 6 weeks of treatment ($x(-) \pm s$).

	The acupoint group	The Western medicine group	t	P
GerdQ-Day 0	14.77 ± 3.05	14.73 ± 2.05	0.050	0.961
GerdQ-6th week	3.03 ± 2.46	6.93 ± 2.08	-6.632^{***}	0.000
t	16.464^{***}	15.625^{***}		
P	0.000	0.000		
GERD-HRQL-Day 0	26.23 ± 5.75	25.80 ± 4.54	0.324	0.747
GERD-HRQL-6th week	8.57 ± 4.38	14.80 ± 4.65	-5.347^{***}	0.000
T	15.140^{***}	11.863^{***}		
P	0.000	0.000		
SAS-Day 0	63.00 ± 8.16	63.10 ± 6.25	−0.053	0.958
SAS-6th week	15.53 ± 3.78	38.50 ± 8.27	-13.831^{***}	0.000
T	27.366^{***}	12.606^{***}		
P	0.000	0.000		
SDS-Day 0	59.70 ± 6.08	59.53 ± 6.95	0.099	0.922
SDS-6th week	32.10 ± 5.9	38.17 ± 8.27	-3.270^{**}	0.002
T	21.549^{***}	9.754^{***}		
P	0.000	0.000		

$^{**}P < 0.01$; $^{***}P < 0.001$.

Table 3: Correlation analysis of the scores in the two groups.

		GerdQ	GERD-HRQL	SAS
GERD-HRQL	r	0.532^{***}	1	
	P	0.000		
SAS	r	0.563^{***}	0.506^{***}	1
	P	0.000	0.000	
SDS	r	0.322^{*}	0.435^{**}	0.326^{*}
	P	0.012	0.001	0.011

$^{*}P < 0.05$; $^{**}P < 0.01$; $^{***}P < 0.001$.

occurring under the spinal process of T3 (DU 12) to T7 (DU 9) was the highest. According to clinical observation, this study found that the tenderness points in TDSDM of GERD patients were highly consistent with those of depression patients. The detection of these positive reaction points importantly guides the clinical diagnosis and treatment of depression and gastroesophageal reflux disease with acupuncture and moxibustion [4].

5.2. Discussion on the Mechanism of Acupoint Catgut-Embedding Regulating the Mental and Psychological State of GERD Patients

5.2.1. Mechanism of Du Meridian Acupoint Catgut Embedding in the Treatment of GERD. Studies have shown that acupuncture can improve the loose lower esophageal sphincter (LES) of GERD patients by regulating the neuroendocrine-immune network, promote gastrointestinal motility, inhibit the secretion of gastric acid, and protect the gastric mucosa. It has a definite effect on the improvement of mental and psychological disorders such as depression and anxiety [11]. In terms of improving loose LES, acupuncture takes effect by enhancing its resting pressure and regulating gastrin and motilin to strengthen antireflux defense barrier [12, 13]. In terms of promoting gastrointestinal motility, acupuncture takes effect by regulating the level of the vasoactive intestinal peptide in digestive system diseases [14]. In terms of inhibiting gastric acid secretion and protecting gastric mucosa, acupuncture affects gastric acid secretion by regulating the changes of media concentration in the autonomic nervous system, gastrointestinal hormones, intestinal nervous system, and gastrointestinal mucosal tissues [15]. In terms of regulating psychological disorders, Pilkington [16] believes that acupuncture may play an anti-anxiety role by regulating signaling substances such as central serotonin, norepinephrine, dopaminergic, or hypothalamic-pituitary-adrenal axis (HPA axis) related hormones.

Acupoint catgut-embedment, an innovative extension of acupuncture treatment which broadens the application range of acupuncture, achieves the efficacy by harmonizing *yin* and *yang*, balancing functions of *zang-fu* organs, unblocking meridians and collaterals, regulating *qi* and blood, tonifying deficiency and purging the excess, and reinforcing healthy *qi* and dispelling pathogens, as well as taking advantage of the effects of needle retaining and catgut embedding. From the perspective of Western medicine, acupoint catgut-embedment can repair nerve functions and

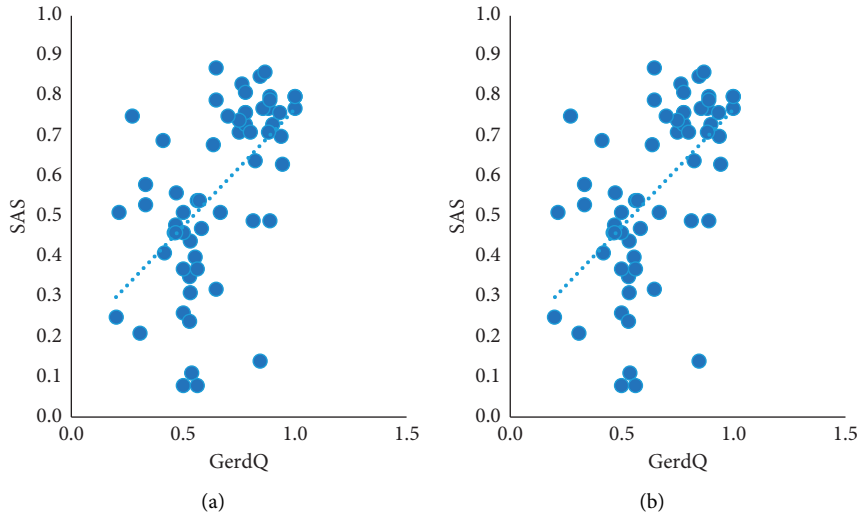

Figure 2: Scatter chart of correlation analysis between GerdQ score and scores of SAS and SDS.

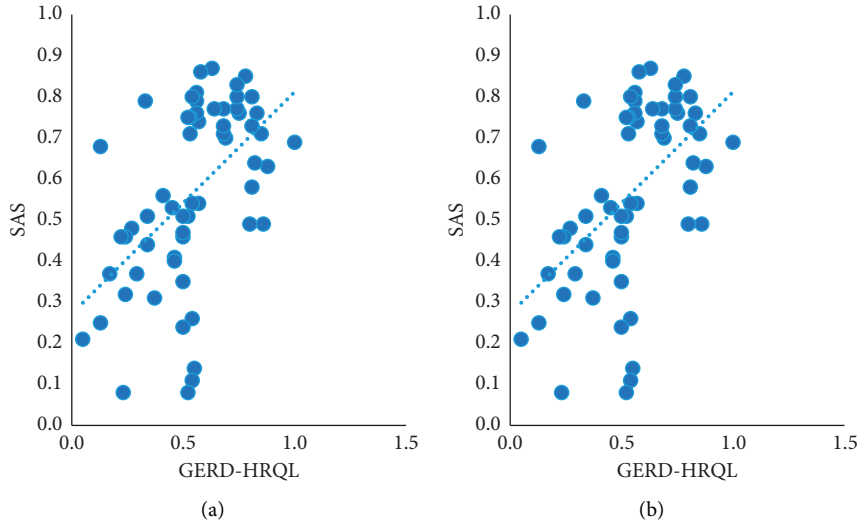

Figure 3: Scatter chart of correlation analysis between GERD-HRQL score and scores of SAS and SDS.

Table 4: Comparison of clinical efficacy between the two groups.

	Markedly effective (case)	Effective (case)	Invalid (case)	Rate of marked effect (%)	Total effective rate (%)
The acupoint group	15	12	3	50.00	90.00
The Western medicine group	3	13	14	10.00	53.33
Statistical value	11.429	0.069	9.932	11.429	9.932
P	0.001	1.000	0.003	0.001	0.003

regulate nerve conduction and reflex, improve human immune function and local microcirculation, inhibit the production of inflammatory factors, reduce cell apoptosis, and regulate cytokines to accelerate metabolism [17]. It can not only exert the effects similar to that of the ordinary acupuncture but also promote continuous treatment by prolonging the stimulation duration, which is particularly suitable for multisystem chronic diseases. To some extent, it may reduce or replace the use of Western medicine. In addition to regulating the neuroendocrine-immune network, catgut-embedding therapy in acupoint of Du Meridian also treats GERD by improving the resting pressure of

LES, preventing its transient loose, improving its ability to clear gastric acid, enhancing the resistance and repair function of gastroesophageal mucosa, accelerating the emptying of the gastrointestinal tract, promoting the gastrointestinal migrating motor complex (MMC), and reducing the sensitivity of human internal organs so as to improve its antireflux defense mechanism, thus inhibiting the occurrence of reflux.

5.2.2. Mechanism of Catgut Embedment in Acupoint of Du Meridian on Mental and Psychological Regulation. Although there are no disease names of "depression" and "anxiety" in traditional Chinese medicine, they can be categorized into the range of "depression syndrome," "visceral agitation (hysteria)," "lily disease," and "insomnia" according to their characteristics. Acupuncture may regulate symptoms of anxiety and depression associated with digestive diseases by regulating the gut-brain axis, a network connecting the brain and the intestine through the autonomic nervous system and the neuroendocrine system of the HPA axis [18]. The gut-brain axis is basically composed of the central nervous system (CNS), autonomic nervous system (ANS), and enteric nervous system (ENS) [19]. Among them, CNS directly regulates gastrointestinal motility and secretion and ANS coordinates the brain and intestines through sympathetic and parasympathetic afferent and efferent neurons while ENS, mainly including the intercostal nerve and submucosal nerve plexus, plays an independent role in regulating intestinal movement and secretion [20]. The neuroendocrine network that links the three nervous systems to the brain is known as the gut-brain axis. This is how the brain interacts with the gut so as to regulate mood.

According to clinical observation, catgut embedment in Du Meridian acupoint may improve psychological disorders and relieve symptoms of anxiety and depression by regulating the dysfunctional gut-brain axis, thus adjusting the emotions of GERD patients. On the other hand, the catgut-embedding therapy in this study improved and cured symptoms of gastric acid reflux and heartburn, thus relieving symptoms of anxiety and depression and improving patients' psychological state and quality of life.

In conclusion, catgut-embedding therapy in acupoint of Du Meridian can effectively adjust the anxiety and depression symptoms, making up for the shortage of PPI and benefiting a wider range of patients. It can also reduce or replace the use of Western medicine for GERD patients accompanied by anxiety or depression and effectively improve physical and psychological symptoms.

6. Limitations and Prospects

There are some limitations in this clinical study. (1) With relatively small sample size, the scores of clinical symptoms and anxiety and depression scales may be easily affected by the subjective factors of patients. (2) This study lacks more objective evaluation indexes such as the comparison in esophageal dynamics and esophageal pH examination before and after treatment. (3) Limited by experiment conditions, the standard pressure measuring device was unavailable to determine the range and degree of the positive reaction points, which may cause errors due to the uneven press or overexertion of researchers.

24-hour pH monitoring of the esophagus is currently considered as one of the best examination methods and gold standards for GERD. There are certain limitations in this study due to diagnosing GERD solely through symptoms and electronic gastroscopy, without using the 24-hour esophagus pH monitoring restricted by conditions. In the following study, our team will explore the correlation of the results of 24-hour pH monitoring of the esophagus and symptoms with anxiety and depression in patients with GERD, and the effect of acupuncture treatment on pH values of the esophagus of GERD patients.

The symptoms of GERD are related to mild mental disorders (depression and anxiety). Although the results of this study show a direct improvement effect of acupoint catgut-embedding therapy on anxiety and depression of GERD patients, it is not convincing enough without setting a placebo group of acupuncture to eliminate the influence of subjective factors of patients. In the future, we will carry out further related studies to provide more evidence on the effects of acupoint catgut-embedding therapy on anxiety and depression of GERD patients.

Acupuncture and catgut-embedding therapy are effective methods to treat GERD. Further studies are needed to discuss the mechanism of how they take effects by regulating the gut-brain axis. Due to the limited time of clinical research, the levels of gastrointestinal hormones before and after catgut embedding were not monitored, and the relationship between them and the mental state was not discussed. In the later period, our research team will conduct research on the correlation between TDSDM and the gut-brain axis to explore the biological effect of catgut-embedding therapy on the neuroendocrine system of GERD patients, so as to provide a new theoretical basis for its clinical application in GERD.

Data Availability

The data used to support the findings of this study are included within the article.

Conflicts of Interest

The authors declare that they have no conflicts of interest.

Acknowledgments

This work was supported by the Youth National Natural Science Foundation of China (81904279) and the Science and Technology Project of Jiangsu Provincial Bureau of Traditional Chinese Medicine (YB2017041).

References

[1] S. E. Kim, N. Kim, S. Oh et al., "Predictive factors of response to proton pump inhibitors in Korean patients with

gastroesophageal reflux disease," *Journal of Neurogastroenterology & Motility*, vol. 21, no. 1, pp. 69–77, 2015.

[2] Y. Qu, W. Wang, X. Zhang et al., "The relationship between psychological factors and the incidence of refractory gastroesophageal reflux disease," *Chinese Journal of Gastroenterology and Hepatology*, vol. 24, no. 12, pp. 1445–1447, 2015.

[3] X. Gao, "Clinical features and influence factors of patients with gastroesophageal reflux disease," *Chinese Journal of Gastroenterology and Hepatology*, vol. 23, no. 11, pp. 1267–1270, 2014.

[4] M. Lu and J. Zhang, "Clinical observation of 60 cases of depression complicated with gastrointestinal symptoms treated by acupuncture and western medicine at the tenderness point on dorsal segment of du meridian," *Journal of Traditional Chinese Medicine*, vol. 58, no. 23, pp. 2028–2031, 2017.

[5] H. Tian, L. Wang, Q. Zhou et al., "Clinical evaluation of acupuncture treatment of insomnia with depression and anxiety," *Journal of Traditional Chinese Medicine*, vol. 57, no. 22, pp. 1929–1933, 2016.

[6] D. Zhang, C. Yu, W. Xiang et al., "Clinical observation of gastro-esophageal reflux treated by catgut-embedding underneath the acupoints of governor vessel," *Journal of Clinical Acupuncture and Moxibustion*, vol. 33, no. 8, pp. 38–41, 2017.

[7] J. Feng and C. Chen, "Clinical research in governor vessel daogi needing method for treatment of non-erosive reflux disease," *Lishizhen Medicine and Materia Medica Research*, vol. 27, no. 1, pp. 138–140, 2016.

[8] N. Vakil, S. V. van Zanten, P. Kahrilas, J. Dent, and R. Jones, "The montreal definition and classification of gastroesophageal reflux disease: a global evidence-based consensus," *The American Journal of Gastroenterology*, vol. 101, no. 8, pp. 1900–1920, 2006.

[9] P. O. Katz, L. B. Gerson, and M. F. Vela, "Guidelines for the diagnosis and management of gastroesophageal reflux disease," *American Journal of Gastroenterology*, vol. 108, no. 3, pp. 308–328, 2013.

[10] J. Zhang and L. Wang, "Clinical study on the distribution of tenderness points on dorsal segment of du meridian in depressed patients," *Jiangsu Journal of Traditional Chinese Medicine*, vol. 39, no. 3, pp. 16–18, 2007.

[11] S. Pan, J. Li, Y. Li et al., "Overview of the clinical and mechanism of acupuncture treatment of gastroesophageal reflux disease," *Journal of Clinical Acupuncture and Moxibustion*, vol. 33, no. 1, pp. 79–83, 2017.

[12] Y. Qi, X. Yan-Dong, M.-x. Zhang et al., "Effect of electroacupuncture stimulation at Zusanli acupoint (ST36) on gastric motility: possible through PKC and MAPK signal transduction pathways," *BMC Complementary and Alternative Medicine*, vol. 14, no. 1, p. 137, 2014.

[13] M. Tatewaki, M. Harris, K. Uemura et al., "Dual effects of acupuncture on gastric motility in conscious rats," *American Journal of Physiology-Regulatory, Integrative and Comparative Physiology*, vol. 285, no. 4, pp. R862–R872, 2003.

[14] J.-H. Jang, D.-J. Lee, C.-H. Bae et al., "Changes in small intestinal motility and related hormones by acupuncture stimulation at Zusanli (ST 36) in mice," *Chinese Journal of Integrative Medicine*, vol. 23, no. 3, pp. 215–220, 2017.

[15] E. Noguchi, "Mechanism of reflex regulation of the gastroduodenal function by acupuncture," *Evidence-Based Complementary and Alternative Medicine*, vol. 5, no. 3, pp. 251–256, 2008.

[16] K. Pilkington, "Acupuncture therapy for psychiatric illness," *International Review of Neurobiology*, vol. 111, pp. 197–216, 2013.

[17] J. Huo, J. Zhao, Y. Yuan et al., "Research status of the effect mechanism on catgut-point embedding therapy," *Chinese Acupuncture & Moxibustion*, vol. 37, no. 11, pp. 1251–1254, 2017.

[18] N. A. Koloski, M. Jones, J. Kalantar, M. Weltman, J. Zaguirre, and N. J. Talley, "The brain-gut pathway in functional gastrointestinal disorders is bidirectional: a 12-year prospective population-based study," *Gut*, vol. 61, no. 9, pp. 1284–1290, 2012.

[19] C.-H. Bao, C.-Z. Dou, B. Xu, H.-R. Liu, and H.-G. Wu, "Brain-gut interactions and inflammatory bowel disease: implications for acupuncture and moxibustion treatment," *World Chinese Journal of Digestology*, vol. 21, no. 23, pp. 2300–2307, 2013.

[20] M. Lu and J. Zhang, "Treatment of depression from gastrointestinal tract," *Journal of Qingdao University(Medical Sciences)*, vol. 52, no. 6, pp. 746–748, 2016.

Hindawi
Evidence-Based Complementary and Alternative Medicine
Volume 2020, Article ID 7481813, 11 pages
https://doi.org/10.1155/2020/7481813

Research Article

Effect of Electroacupuncture at GV20 on Sleep Deprivation-Induced Depression-Like Behavior in Mice

Xiaohong Xu[1], **Peng Zheng**[2], **Hongyan Zhao**[3], **Bailin Song**[1] **and Fuchun Wang**[1]

[1]*Changchun University of Chinese Medicine, Changchun 130117, China*
[2]*Jilin Provincial Hospital of Traditional Chinese Medicine, Changchun University of Chinese Medicine, Changchun 130021, China*
[3]*Institute of Basic Theory of Chinese Medicine, China Academy of Chinese Medical Science, Beijing 100700, China*

Correspondence should be addressed to Peng Zheng; zhengpeng7877@163.com

Received 4 June 2020; Revised 20 July 2020; Accepted 22 July 2020; Published 21 August 2020

Guest Editor: Feng Zhang

Accumulating evidence suggests that sleep deprivation (S-Dep) is a critical risk factor for depression. Electroacupuncture (EA) treatment has been reported to ameliorate posttraumatic stress disorder- (PSTD-) like behavior and enhance hippocampal neurogenesis. However, whether EA treatment has any beneficial effect on S-Dep-induced depression-like behavior is still unknown. In the present study, we focused on whether EA at Baihui (GV20) can ameliorate the deterioration effect of S-Dep in mice. Mice were randomly divided into normal, S-Dep, S-Dep + EA, and S-Dep + sham EA groups. Cognitive behavior test and in vitro assay were performed separately to avoid the influence of behavior test on synaptic transmission and protein expression. Depression-like behaviors were determined by forced swimming test (FST), tail suspension test (TST), and Morris water maze (MWM). Neurogenesis was identified by BrdU, DCX, and NeuN immunofluorescence staining. In vitro long-term potentiation was detected by high frequency stimulation (HFS) at Schaffer collateral-CA1 synapses in hippocampal slices. Brain-derived neurotropic factor (BDNF) and tropomyosin receptor kinase B (TrkB) protein expression level were assayed by western blot. Our results indicated that D-Sep mice demonstrated depression-like behaviors determined by prolonged immobility duration in FST and TST; D-Sep mice also manifested spatial memory retention deficit in MWM. Furthermore, EA treatment ameliorated D-Sep-induced depression-like behaviors and spatial memory retention deficit. Mechanically, EA treatment alleviated neuron progenitor cell proliferation and differentiation, ameliorated the field excitatory postsynaptic potentials (fEPSPs) slope impaired by S-Dep, and elevated BDNF/TrkB protein expression. Taken together, our data suggested that EA treatment has a protective effect on S-Dep-induced depression-like behavior and cognitive impairment, which may be through regulating BDNF/TrkB protein expression.

1. Introduction

Sleep, which has been discovered as a state of consolidation of newly formulated memory, is crucial for learning new information and mental performance [1]. Sleep loss or insomnia has been proven to contribute to hippocampal-dependent cognition deficits and depression-like behavior; the underlying mechanisms include disruption of synaptic plasticity at electrophysiology and molecular levels as well as at a structural level [2]. Long time potentiation (LTP) is a form of synaptic plasticity adopted as an in vitro biological model of learning and memory. Ample evidence has demonstrated that sleep deprivation can have detrimental effects on memory formation and LTP induction [3–5]. BDNF, a member of the neurotrophin family, is a significant modulator in synaptic plasticity and memory formation. BDNF needs to bind to its high-affinity protein kinase receptor, TrkB, to exhibit its biological effect [6].

Acupuncture, a traditional therapy originating from ancient China, is an alternative and complementary medicine that has long been known to have therapeutic effect on various neurodegenerative diseases including depression [7]. Abundance studies indicated that acupuncture or electroacupuncture treatment ameliorates cognitive impairment

and improves hippocampal-dependent synaptic plasticity. GV20 is located above the apex auriculate, on the midline of the head. Clinically, acupuncture at GV20 has been widely used in neuropsychological diseases including depression, anxiety, Parkinson's disease, and neurasthenia, although the underlying mechanism is still not fully illustrated. Acupuncture stimulation at GV20 has been proven to improve scopolamine-induced cognitive impairment and alleviate BDNF expressions [8]. A former study demonstrated that acupuncture at GV20 produced instant sedative effect and altered electroencephalogram α and β waves frequencies in a model of sleep deprivation [9]. EA at GV20 and Shenting (GV24) attenuated the expression of monoamine neurotransmitters and IL-1 beta in the hypothalamus after sleep deprivation in rats with focal cerebral ischemia/reperfusion injury [10].

EA treatment or pretreatment has been shown to modulate ESPS-induced anxiety-like behaviors and prevent hippocampal neurogenesis disruption in a rat model of PTSD [11, 12]. However, the effects of EA at GV20 on S-Dep-induced hippocampal synaptic plasticity impairment and depression-like behavior have remained elusive. The present study investigated the effects of EA at the GV20 acupoints on S-Dep mice by depression-related behavior test, neurogenesis detection, LTP induction, and BDNF/TrkB signaling protein assay.

2. Materials and Methods

2.1. Animals. Male BALB/c mice aged 2–3 month were obtained from the Experimental Animal Research Center of Hubei (Wuhan, China). The animals were housed in a 12 h light-dark cycle (07 : 00–19 : 00) and had free access to food and water. The room temperature was maintained at $23 \pm 1^{\circ}$C. All mice were adapted to the environment for 1 week before the experiment. The mice were randomly divided into 4 groups: normal group, S-Dep group, S-Dep + EA group, and S-Dep + sham EA group, with each group containing 34 mice (Figure 1). The normal group did not receive any treatment but were immobilized by hand with gentle plastic restraints just as the treatment groups. After S-Dep and EA treatment, a subset of animals were used for behavior test ($n = 10$/group), LTP induction ($n = 8$/group), and biochemical analysis ($n = 6$/group). All experimental procedures complied with the guidelines of the Principles of Laboratory Animal Care and the legislation of the People's Republic of China for the Use and Care of Laboratory Animals.

2.2. Sleep Deprivation Model. The multiple-platform apparatus was adopted to establish sleep deprived mice as previously described [13]. In short, animals were placed in a chamber with multiple small platforms (diameter: 3.5 cm) which was 1 cm above water. When animals entered rapid eye movement (REM) sleep, their muscle tone diminished and the animals fell into the water, waking them up and preventing them from going to sleep. For normal mice, the small platforms were replaced with larger ones (diameter: 13 cm), allowing them to enter REM sleep without falling into water. S-Dep was induced for 48 h in this experiment.

2.3. Electroacupuncture Stimulation. EA treatment was taken once daily during the 48 h of S-DEP. The EA stimulus was continued for 30 min with insertion to a depth of 5 mm at Baihui (GV 20). A previous study had found that EA at the intensity of 2 mA and 100 Hz (pulse width: 0.2 ms, duration: 10–30 min) has significant analgesic effect in mice [14]; in light of this study, biphasic square pulse (2 mA, 0.2 ms) with high frequency, 100 Hz, was administered through a medical EA apparatus (Qingdao Xinsheng instrument, Qingdao, China). The needles (0.25 mm × 25 mm) were purchased from Suzhou Hualun Medical Appliance Co., Ltd. (Suzhou, China). In the Sham EA treatment group, acupuncture needles were inserted superficially into the acupoints without electrical stimulation. At the end of the last EA treatment, mice were subjected to behavioral, electrophysiological, and immunochemical assays separately.

2.4. Tail Suspension Test. TST was used to analyze depressive-like behavior as previously described [16]. A short piece of paper adhesive tape (about 6 cm) was attached along half the length of the tail (about 3 cm). The mouse's head was about 20 cm above the floor. The test was carried out for 6 min, during which mouse immobility time was recorded, with the absence of initiated movements defined as immobility. The first 2 min activity was considered pretreatment period, and the duration of immobility was video-recorded during the final 4 min.

2.5. Forced Swimming Test. Three hours after the TST, mice were placed in a cylinder container (diameter, 25 cm; height, 50 cm) containing fresh water (temperature $24 \pm 1^{\circ}$C) for 6 min, and behavior activity was video-recorded. The first 2 min was considered to be pretest swim and was excluded from the analysis. Immobility duration of the last 4 min was counted.

2.6. Morris Water Maze. MWM was adopted to evaluate spatial-related working memory as previously described [15]. The experiments were conducted in a tank (124 cm in diameter) filled with water (32 cm in depth). The water was made opaque by white nontoxic paint, and temperature was kept at $22 \pm 1^{\circ}$C during the experiment. Mice were trained to find a cylindrical platform (10 cm in diameter). The MWM test was divided into two phases, the training phase and the exploring phase. Each mouse performed four trials daily for 5 days during the training phase; the mice were allowed to swim for 60 s to find the hidden platform. If mice successfully reached the platform within 60 s, they were allowed to stay there for 15 s, if they failed, they were manually put on the platform. The exploring test was conducted on the 7th day after the last EA treatment while the platform was removed. The traces of exploring, time spent in the target quadrant, and number of times of crossing platform in the exploring session were analyzed.

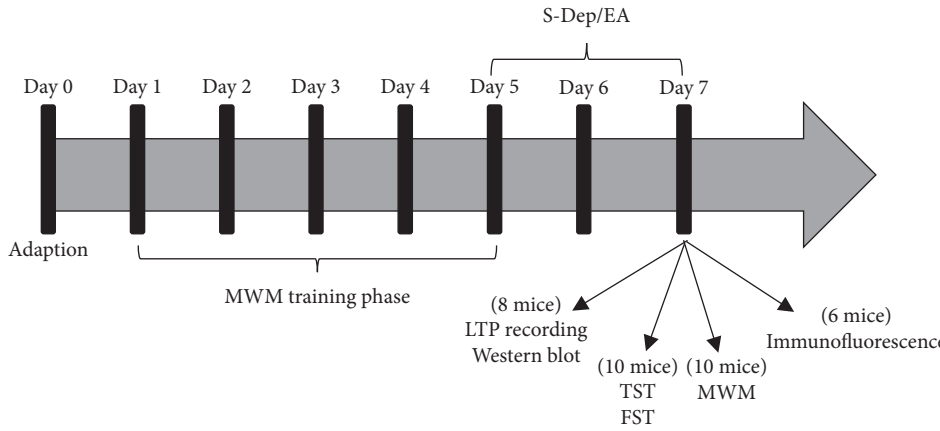

Figure 1: Schematic illustration of the experimental procedure. All mice were assigned into four groups: normal, S-Dep, S-Dep + EA, and S-Dep + sham EA group. A set of mice containing 10 mice were exposed to MWM training phase test during 5 consecutive days, followed by 48 h of S-Dep and EA or sham EA treatment once daily; on the 7th day after the last EA treatment, mice were used for exploring phase test. Another set of mice containing 10 mice underwent TST and FST; 3 h recovery time was given after TST. Two separated sets of mice from each group were sacrificed after S-Dep and EA/sham EA treatment for LTP/western blot or immunofluorescence.

2.7. LTP Recording. Eight mice from each group were sacrificed after final EA treatment. Brains were immediately removed and placed in ice-cold oxygenated artificial cerebrospinal fluid (ACSF) containing (in mM) 100 sucrose, 60 NaCl, 4 KCl, 8 $MgCl_2$, 1.3 NaH_2PO_4, 30 $NaHCO_3$, 5 D-glucose, and 0.5 $CaCl_2$ (pH 7.2–7.4) saturated with carbogen (95% O_2–5% CO_2). The left side of brains was placed in liquid nitrogen for the western blot, and the right side was used for LTP recording. Coronal hippocampal slices (300 μm) were cut using a vibratome (VT1000S, Leica, Germany) in ice-cold oxygenated cutting solution. Recording solution contained (in mM) 125 NaCl, 2 $CaCl_2$, 2.5 KCl, 1 $MgCl_2$, 25 $NaHCO_3$, 1.25 NaH_2PO_4, and 25 D-glucose (pH 7.2–7.4). LTP experiment was conducted using a bipolar stimulating electrode, stimulus electrode was located at Schaffer collateral, and recording electrode was positioned at radium stratum in CA1. The stimulus intensity was set to evoke 40–50% of the maximal amplitude of fEPSPs. fEPSPs were recorded every 30 s, and LTP was induced by a tetanic stimulus at 100 Hz for 2 s. Baseline responses were recorded for 20 min, followed by the continued recording of the fEPSPs for 60 min.

2.8. Immunofluorescence. After the finial EA treatment, 6 mice from each group were sacrificed and perfused with PBS followed by 10% formalin. Then the brain samples were cut into 20 μm slices coronally. From each brain, three slices were selected including the DG of hippocampus for staining. The slices were blocked by 0.3% BSA and 0.3% Triton X-100 to block nonspecific binding, then incubated with primary antibody of BrdU, NeuN, and doublecortin (DCX) for 24 h at 4°C, followed by incubating with secondary antibody of Alexa Fluor 488 donkey anti-rabbit IgG (1 : 1000, Invitrogen, Thermo Fisher Scientific) and Alexa Fluor 594 goat anti-mouse IgG (1 : 1000, Invitrogen, Thermo Fisher Scientific) for 2 h at room temperature. Images were captured under a fluorescence microscope (ECLIPSE 90i, Nikon, Japan).

2.9. Western Blot Analysis. The hippocampus tissues were isolated and lysed in 100 μl Radioimmunoprecipitation Assay (RIPA) buffer (Thermo Fisher Scientific, Waltham, MA) plus protease inhibitors. The protein concentration was quantified by the Bicinchoninic Acid Protein Assay Kit (Beyotime Biotechnology, Shanghai, China). Total protein (50 μg) was processed for 12% SDS-PAGE and transferred onto PVDF membranes (Millipore, Billerica, MA). Blots were blocked by 5% nonfat milk and immunoblotted with anti-BDNF (1 : 2000, Abcam), anti-TrkB (1 : 300, Cell Signal), and anti-GAPDH (1 : 1000, Abcam). The membranes were incubated with the horseradish peroxidase-conjugated secondary antibody for 1 h at room temperature. The protein bands were detected using ECL and analyzed by Image-Pro Plus 6.0.

2.10. Statistical Analysis. GraphPad Prism 7.0 software was used to perform all analyses. Data are presented as mean ± SD. Data were analyzed using two-sample Student's *t*-test for two group comparisons, and two-way analysis of variance (ANOVA) was conducted for comparison between multiple groups. The significance threshold was set to p values < 0.05.

3. Results

3.1. EA Reversed Depression-Like Behavior Induced by S-Dep. FST and TST were both classic behavior test models for depression-like symptoms. The immobility time in FST was markedly elevated in S-Dep group (121.50 ± 8. 94 s) compared with normal group (76.56 ± 7. 12 s), which was reversed by EA treatment (81.35 ± 6. 95 s). However, sham EA treatment (117.36 ± 7. 91 s) has no significant influence on the immobility time compared with the S-Dep group (Figure 2(a), all $p < 0.01$). In accordance with the FST results, the immobility time in TST was significantly increased in the S-Dep group (97.58 ± 6. 15 s) and sham EA group (95.20 ± 5. 74 s) compared with the normal group (58.64 ± 5.71 s); EA

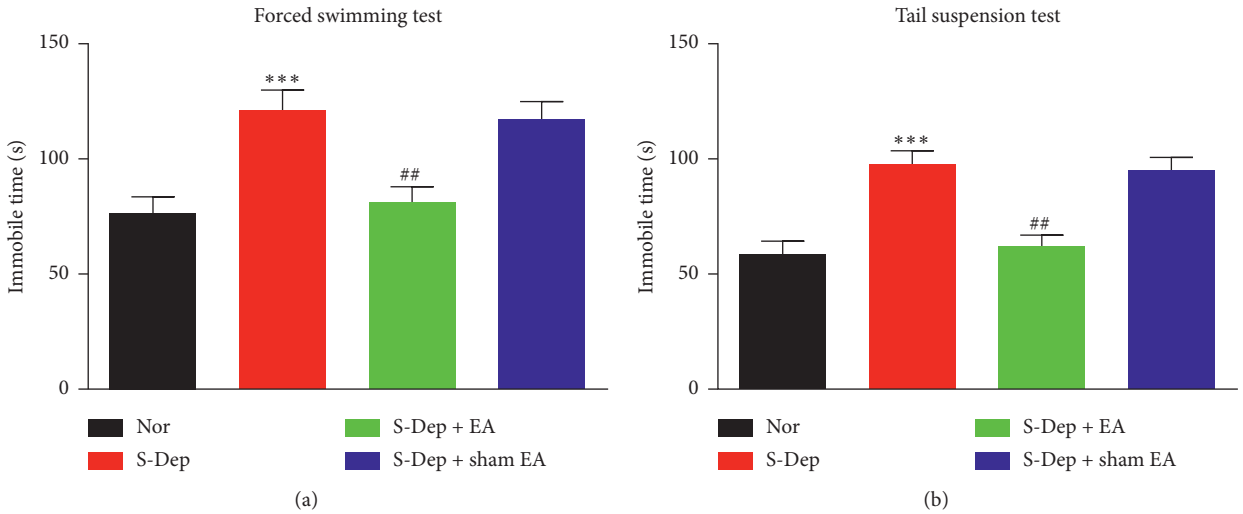

Figure 2: EA reversed depression-like behavior induced by S-Dep. The immobility time on FST (a) and TST (b). Data were presented as the mean ± SD, $n = 10$; $^{***}p < 0.001$ vs. normal group; $^{\#\#}p < 0.01$ vs. sleep deprivation group.

treatment (62.12 ± 4. 93 s) counteracted S-Dep induced rise of immobility time (Figure 2(b), all $p < 0.01$). These data suggest that EA treatment ameliorates S-Dep-induced depression-like behavior.

3.2. EA Mitigated Spatial Memory Retention Deficits Induced by S-Dep. We further investigated the effect of EA treatment on spatial memory retention by MWT. The traces of activity by mice were shown in Figure 3(a). Spatial memory retention ability was significantly impaired by S-Dep, as indicated by increased times of crossing the platform (Figure 3(b), $p < 0.001$) and less time spent in the target quadrant (Figure 3(c), $p < 0.001$) in the exploring phase. However, EA treatment dramatically ameliorated the memory retention ability of S-Dep-induced mice. Compared with S-Dep group, times of crossing the platform were attenuated, and time spent in the target quadrant was mitigated. Taken together, EA treatment protect against spatial memory retention deficit caused by S-Dep in mice.

3.3. EA Alleviated Neuron Progenitor Cell Differentiation in the DG of Hippocampus. To determine the effect of EA treatment on neurogenesis in S-Dep induced mice, we carried out immunofluorescence staining experiment. BrdU is a marker of proliferation cells, and NeuN was used to label the mature neurons. As is shown in Figure 4(a), BrdU and NeuN double positive cells were dramatically attenuated in the D-Sep group but were elevated in the EA treatment group, while sham EA treatment had no influence on BrdU and NeuN double positive cell number (Figure 4(b), all $p < 0.01$). The above results indicated that EA treatment increased the neuron progenitor cells differentiated into neurons.

3.4. EA Alleviated Neuron Progenitor Cells Proliferation in the DG of Hippocampus. To further determine the effect of EA treatment on neurogenesis, BrdU and DCX double immunofluorescence staining were conducted in DG of hippocampus. DCX was widely adopted to label immature cells. As is shown in Figure 5(a), S-Dep attenuated BrdU and DCX double positive cell expression, which was reversed by EA treatment, but not altered by sham EA treatment (Figure 5(a), all $p < 0.01$). This study demonstrated that EA treatment facilitated neuron progenitor cell self-renewal and proliferation.

3.5. EA Abolished LTP Impairment Induced by S-Dep. To determine the effect of EA on learning and memory in synaptic transmission level, hippocampal Schaffer collateral-CA1 LTP was recorded. The fEPSPs slope was significantly impaired in the S-Dep group compared with the normal group during the period of 10–60 min after HFS, which was abolished by EA treatment, but was not changed by sham EA treatment (Figures 6(a) and 6(b), all $p < 0.05$). The mean fEPSPs slope value at the period of 50–60 min in the S-Dep group (105.68 ± 8. 95) was significantly lower than normal group (152.50 ± 9. 34) and the EA treatment group (148.72 ± 8. 83) (Figure 6(c), all $p < 0.01$). The above data suggest that EA treatment ameliorated LTP deterioration by D-Sep.

3.6. EA Reversed BDNF/TrkB Expression in S-Dep Mice. To investigate the molecular mechanism underlying protective effect of EA on S-Dep-induced cognitive impairment, western blot was conducted to detect protein expression in the hippocampus. The protein expression level of BDNF and TrkB was dramatically mitigated by S-Dep, while being obviously boosted by EA treatment. There were no significant differences in protein expression level of BDNF and TrkB in sham EA treatment group (Figures 7(a) and 7(b), all $p < 0.001$). Collectively, EA treatment abolished S-Dep-induced reduction of BDNF/TrkB protein level.

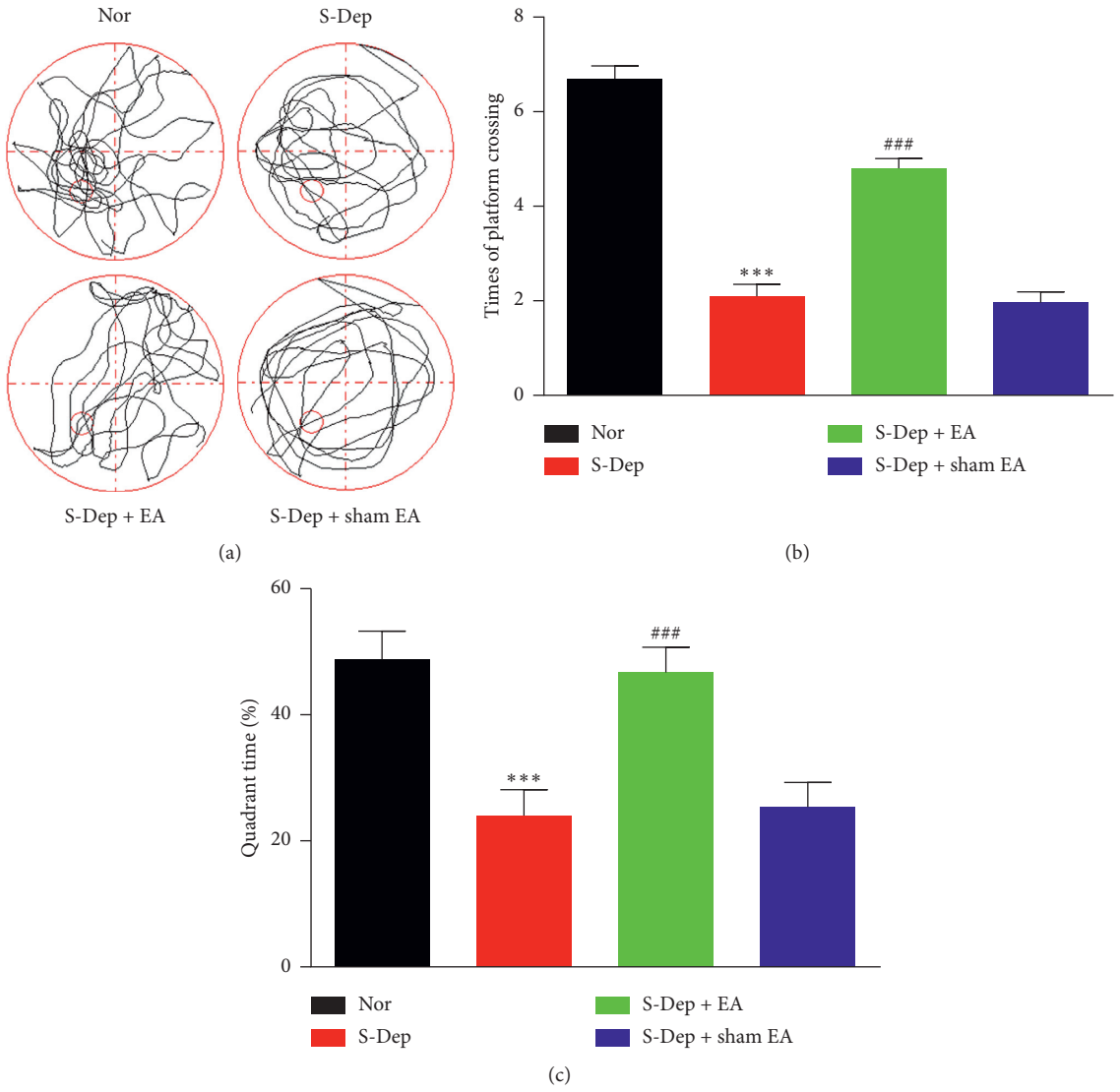

FIGURE 3: EA mitigated spatial memory retention deficits induced by S-Dep. The spatial memory retention of mice was determined by MWM. (a) Representative traces of activity of mice in the MWM. Number of times of platform crossing (b) and percentage of time spent in target quadrant (c) during the exploring phase. Data were presented as the mean ± SD, $n = 10$; $^{**}p < 0.001$, $^{***}p < 0.001$ vs. normal group; $^{\#\#}p < 0.01$, $^{\#\#\#}p < 0.001$ vs. sleep deprivation group.

4. Discussion

Acupuncture treatment has been proven to exert antidepression effects on insomnia patients and can be safely applied in insomnia treatment [17]. Stimulation at GV20 located at the top of the head is widely accepted for the cure of neuropsychiatric disorders in the clinical practice, however, the underlying molecular mechanism is controversial. The current study uses a mice model of sleep deprivation to investigate the potential mechanism of EA at GV20 acupoints on cognitive impairment. Consistent with previous studies [18], our research suggested that S-Dep for 48 h induced depression-like behavior as shown by decreased immobility time in FST and TST. After EA treatment for 2 consecutive days, the immobility durations during the FST and TST in the S-Dep + EA group were significantly lower than those of the S-Dep group, indicating an antidepression effect of EA. Further, the spatial memory retention ability was estimated by MWM. The fewer times of crossing the platform and less time spent in the target quadrant suggest a significant amelioration of spatial memory retention impairment in the S-Dep + EA group compared with the S-Dep group. In contrast, the S-Dep + sham EA group produced no significant protective effects compared with the S-Dep group. All these data suggest that EA at GV20 has a protective effect on S-Dep-induced depression. A study using a p-chlorophenylalanine-induced insomnia rat model has indicated that EA treatment facilitates melatonin secretion [19], which exerts a significant antidepression effect. Another study reported that acupuncture treatment at GV20 has a sedative effect, increases α wave frequency, and decreases β wave frequency in rats after 72 h of

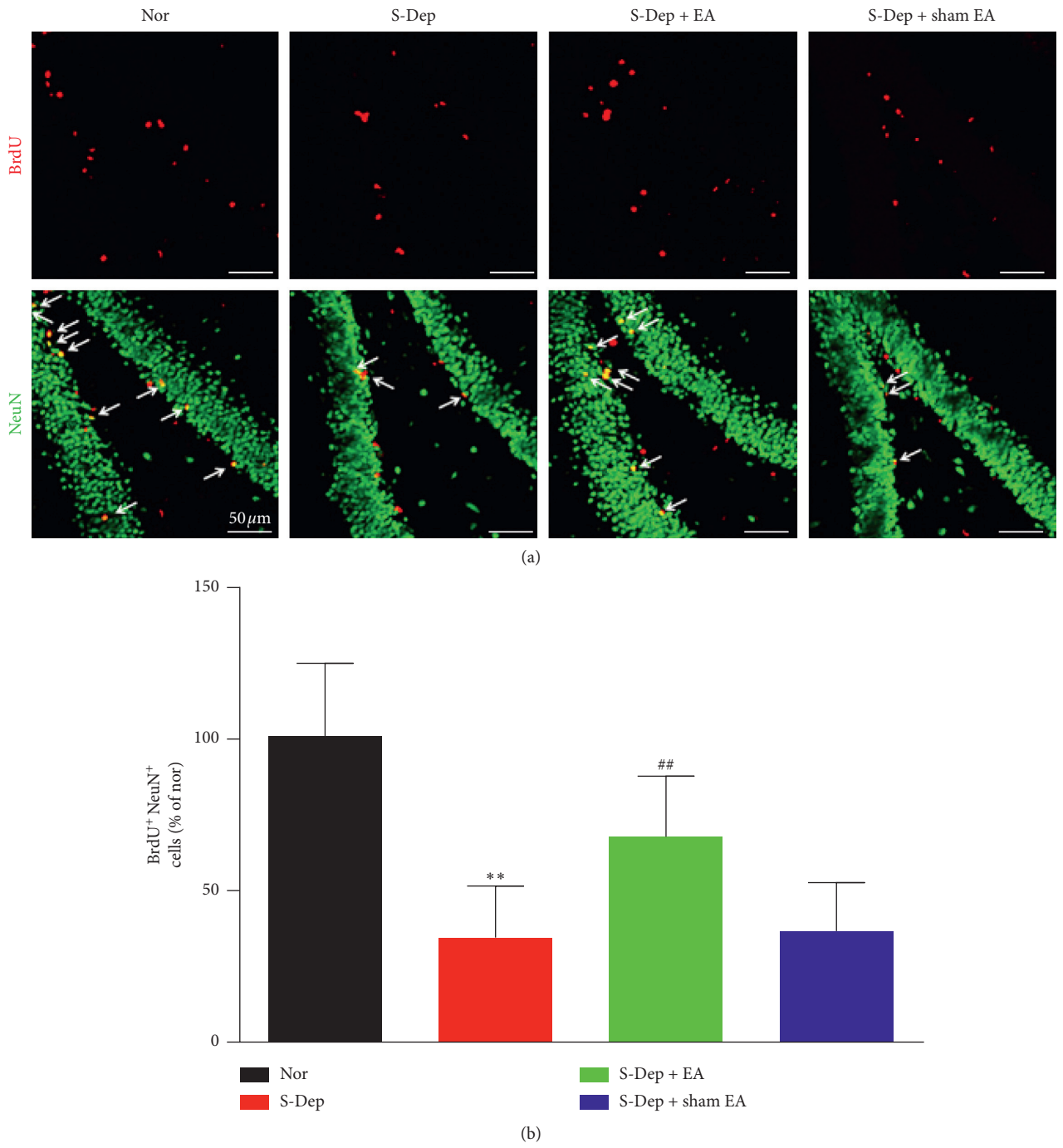

Figure 4: EA alleviated neuron progenitor cell differentiation in the DG of hippocampus. (a) Representative microphotograph of BrdU (red) and NeuN (green) double immunostaining showing matured newborn neurons in the DG. (b) Quantification of BrdU and NeuN double positive cells (yellow). Data were presented as the mean ± SD, $n = 6$; $^{***}p < 0.01$ vs. normal group; $^{\#\#}p < 0.01$ vs. sleep deprivation group.

sleep deprivation [20]. Interestingly, a previous study using 72 h sleep deprivation rat model indicated that EA at GV20 and ST36 simultaneously improved memory deficit [21], which is in accordance with our results using 48 h sleep deprivation mice model while using EA at GV20 alone. In comparison, our data extended the beneficial effect of EA for S-Dep from rat to mice and proved that EA at only acupoint GV20 could achieve this effect. Collectively, we concluded that EA at GV20 has a protective effect on S-Dep-induced depression. It is worth noting that the stimulus intensity we used in the current study resulted in a manifestation of gentle head nodding, indicating that the stimulation is well-tolerated by mice. More importantly, there is no significant behavior alteration in the first hour after EA. The amelioration of behavior test by EA appeared one hour after stimulation; this delay in EA effect may suggest that it takes time for EA

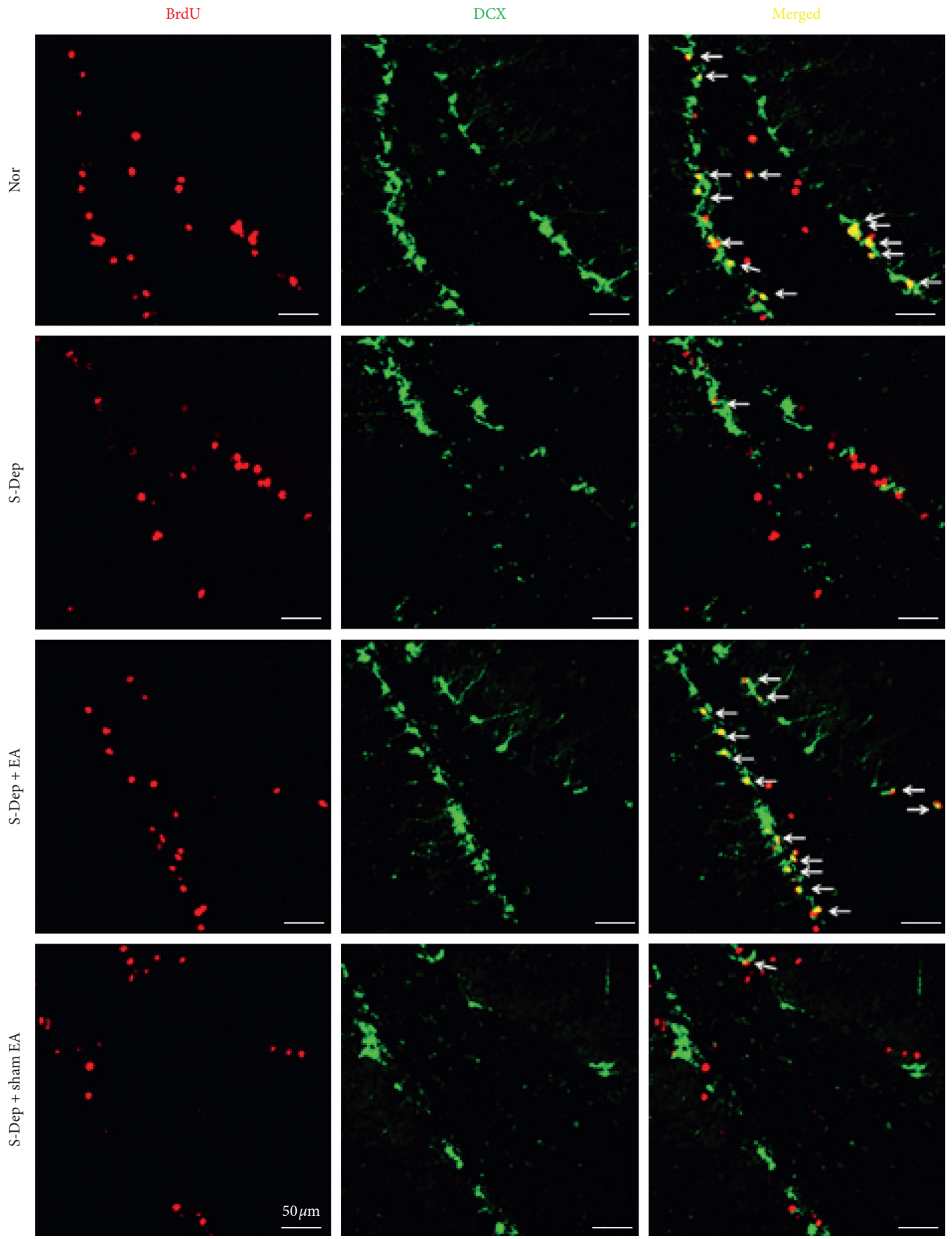

(a)

Figure 5: Continued.

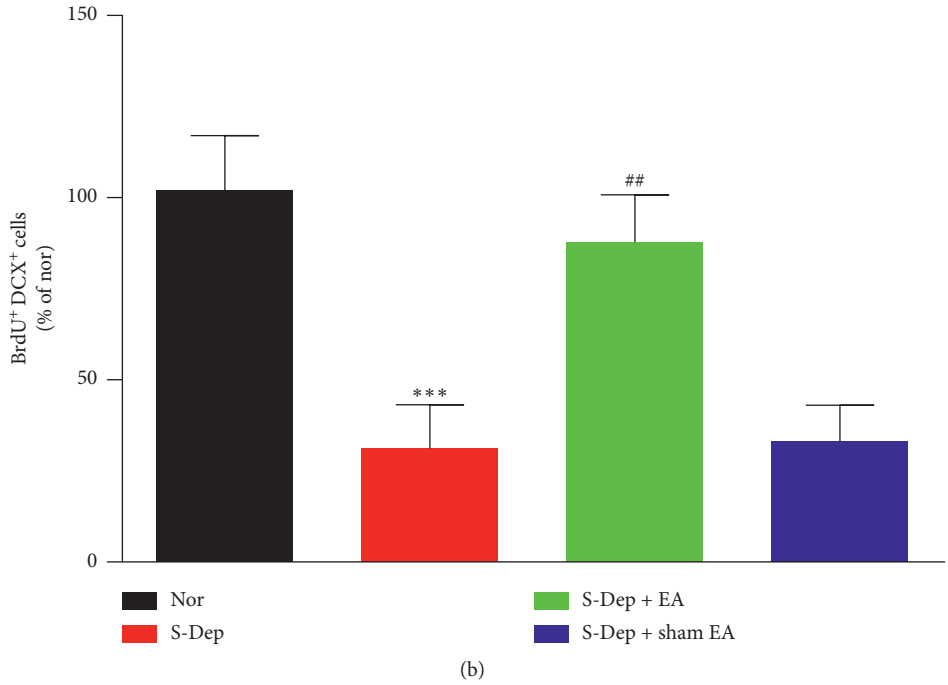

Figure 5: EA alleviated neuron progenitor cell proliferation in the DG of hippocampus. (a) Representative microphotograph of BrdU (red) and DCX (green) double immunostaining showing immature neurons in the DG. (b) Quantification of BrdU and DCX double positive cells (yellow). Data were presented as the mean ± SD, $n = 6$; $^{**}p < 0.01$ vs. normal group; $^{\#\#}p < 0.01$ vs. sleep deprivation group.

treatment to regulate neural function and network activity. Thus, we speculated that EA amelioration of sleep deprivation-induced depression-like behavior is dependent on the GV20 acupoints, rather than direct electroconvulsive shock.

Hippocampus neurogenesis has been well-documented to play a pivotal role in spatial-related memory formation and depression-like behavior; thus, we performed immunofluorescence staining to evaluate the BrdU-labeled proliferating cell and DCX-labeled immature cell expression. BrdU-positive neurons and DCX-positive cells were markedly mitigated in the S-Dep group compared with the normal group but were significantly elevated in the S-Dep + EA group. The above results demonstrated that EA treatment facilitates neuron progenitor cell proliferation and differentiation in S-Dep mice. EA at GV20 and GV14 has been reported to improve neurogenesis after stroke [22]. Taken together, we demonstrated that neurogenesis evolved in the beneficial effect of EA treatment in cognitive impairment.

LTP, a long-lasting enhancement of synaptic transmission efficacy, is widely adopted as an electrorheological mechanism for storage of learning and memory [23, 24]. Our results showed that HFS-induced potentiation of the fEPSPs slope was inhibited by S-Dep, which was reversed by EA treatment but not sham EA treatment. Our result is consistent with previous research, which indicated that acupuncture prevents the impairment of hippocampal LTP in vascular dementia rats [25].

Research has demonstrated that both EA treatment and pretreatment improved posttraumatic stress disorder-(PTSD-) like behaviors in rats [11, 12, 26]. Rather than PTSD, which is triggered by a traumatic event such as an aggressive incident or conflict situation [27], S-Dep-induced depression is closer to mild or minor stress-induced depression. Thus, we concluded that EA has a protective effect on either PTSD-induced major depression or S-Dep-induced minor depression.

BDNF plays a crucial role in synaptic plasticity and memory formation by targeting its high-affinity protein kinase receptor TrkB [28, 29]. Accumulating evidence addressed S-Dep-induced downregulation of BDNF in the hippocampus [30, 31]. 48 h S-Dep was associated with dramatically reduced BDNF expression in the CA1, CA3, and dentate gyrus (DG) of the hippocampus, accompanied by attenuated Ca^{2+}/calmodulin-dependent protein kinase II (CAMKII) and the cAMP response element binding protein (CREB) expression and mitigated CREB phosphorylation [32, 33]. LTP is mediated by distinct signaling molecules including CAMKII and phosphorylated CREB. Downregulation of CAMKII and phosphorylated CREB impaired LTP induction [34]. This in turn would decrease the expression of key target genes including BDNF, which cycles back to mediate CREB activity [35]. In the current study, we found that EA treatment prevented S-Dep-induced attenuation of BDNF and its high-affinity receptor TrkB in the hippocampus and restored LTP induction in response; therefore, we speculated that EA might play an antidepression-like effect by regulating BDNF/TrkB signaling pathway.

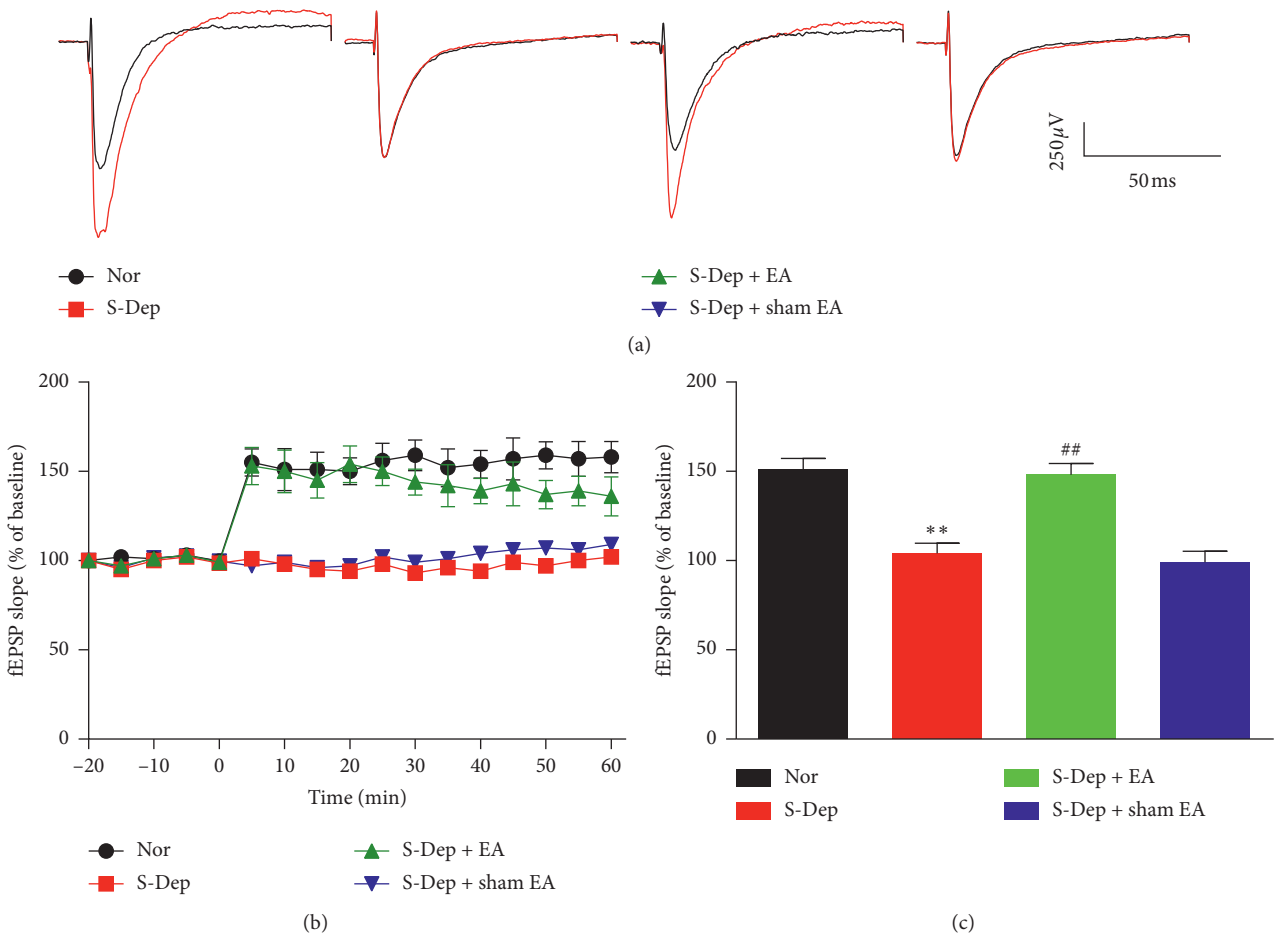

Figure 6: EA abolished LTP impairment induced by S-Dep. (a) Representative traces of the fEPSPs in the CA1 region of hippocampus before and after HFS in the Schaffer collaterals. (b) Plot of fEPSPs slope values as a percentage of baseline. (c) fEPSPs slope values were averaged from the duration 50–60 min after HFS. Data were presented as the mean ± SD, $n = 8$; $^{**}p < 0.01$ vs. normal group; $^{\#\#}p < 0.01$ vs. sleep deprivation group.

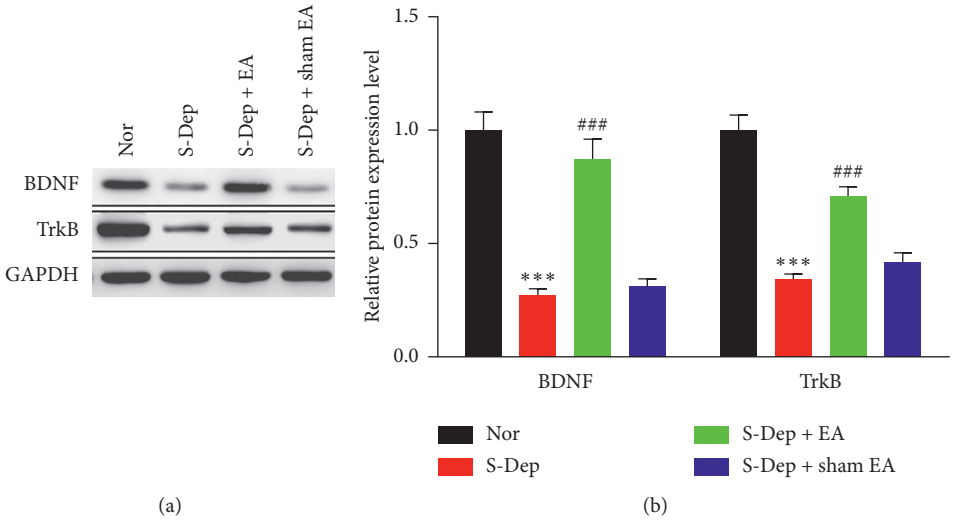

Figure 7: EA reversed BDNF/TrkB expression in S-Dep mice. Expression of BDNF and TrkB in hippocampal CA1 region was detected by western blot. (a) Western blot bands of BDNF and TrkB; GAPDH was used as an internal control. (b) Quantified protein expression level of BDNF and TrkB. Data were presented as the mean ± SD, $n = 8$; $^{***}p < 0.001$ vs. normal group; $^{\#\#\#}p < 0.001$ vs. sleep deprivation.

Data Availability

The data used to support the findings of this study are available from the corresponding author upon request.

Conflicts of Interest

The authors declare that there are no conflicts of interest regarding the publication of this paper.

Authors' Contributions

Revision of the manuscript was done by Xiaohong Xu and Fuchun Wang. Acquisition and analysis of experimental data were carried out by Xiaohong Xu. Study concept and design were the responsibility of Peng Zheng.

Acknowledgments

This work was supported by the National Key Basic Research Program of China (973 Program) (no. 2014CB543100); the Education Department of Jilin Province (no. 2016134); and the Administration of Traditional Chinese Medicine of Jilin Province (no. 2016011): Jilin Province Science and Technology Department (Therapeutic Evaluation on Traditional Chinese Medicine Comprehensive Rehabilitation Scheme of Treatment for Poststroke Limb Spasms). The authors would like to thank Professor Song Bailing for guidance on subject research.

References

[1] H. R. Joo and L. M. Frank, "The hippocampal sharp wave-ripple in memory retrieval for immediate use and consolidation," *Nature Reviews Neuroscience*, vol. 19, no. 12, pp. 744–757, 2018.

[2] R. Havekes, A. J. Park, and J. C. Tudor, "Sleep deprivation causes memory deficits by negatively impacting neuronal connectivity in hippocampal area CA1," *Elife*, vol. 5, Article ID e13424, 2016.

[3] B. Ocalan, A. Cakir, C. Koc, G. G. Suyen, and N. Kahveci, "Uridine treatment prevents REM sleep deprivation-induced learning and memory impairment," *Neuroscience Research*, vol. 148, pp. 42–48, 2019.

[4] M. Kuhn, E. Wolf, and J. G. Maier, "Sleep recalibrates homeostatic and associative synaptic plasticity in the human cortex," *Nature Communications*, vol. 7, no. 1, pp. 1–9, 2016.

[5] F. Raven, E. A. Van der Zee, P. Meerlo, and R. Havekes, "The role of sleep in regulating structural plasticity and synaptic strength: implications for memory and cognitive function," *Sleep Medicine Reviews*, vol. 39, pp. 3–11, 2018.

[6] P. Kowiański, G. Lietzau, and E. Czuba, "BDNF: a key factor with multipotent impact on brain signaling and synaptic plasticity," *Cellular and Molecular Neurobiology*, vol. 38, no. 3, pp. 579–593, 2018.

[7] C. A. Smith, M. Armour, and M. S. Lee, "Acupuncture for depression," *Cochrane Database of Systematic Reviews*, vol. 3, 2018.

[8] B. Lee, B. Sur, and J. Shim, "Acupuncture stimulation improves scopolamine-induced cognitive impairment via activation of cholinergic system and regulation of BDNF and CREB expressions in rats," *BMC Complementary and Alternative Medicine*, vol. 14, no. 1, p. 338, 2014.

[9] J. Li, X. Ran, C. Cui, C Xiang, A Zhang, and F. Shen, "Instant sedative effect of acupuncture at GV20 on the frequency of electroencephalogram α and β waves in a model of sleep deprivation," *Experimental and Therapeutic Medicine*, vol. 15, no. 6, pp. 5353–5358, 2018.

[10] Q. Y. Chang, Y. W. Lin, and C. L. Hsieh, "Acupuncture and neuroregeneration in ischemic stroke," *Neural Regeneration Research*, vol. 13, no. 4, pp. 573–583, 2018.

[11] F. Xue, S.-S. Xue, L. Liu et al., "Early intervention with electroacupuncture prevents PTSD-like behaviors in rats through enhancing hippocampal endocannabinoid signaling," *Progress in Neuro-Psychopharmacology and Biological Psychiatry*, vol. 93, pp. 171–181, 2019.

[12] C.-H Zhou, F. Xue, S.-S Xue et al., "Electroacupuncture pretreatment ameliorates PTSD-like behaviors in rats by enhancing hippocampal neurogenesis via the keap1/Nrf2 antioxidant signal pathway," *Frontiers in Cellular Neuroscience*, vol. 13, p. 275, 2019.

[13] S. Karabulut, K. Korkmaz Bayramov, R. Bayramov et al., "Effects of post-learning REM sleep deprivation on hippocampal plasticity-related genes and microRNA in mice," *Behavioural Brain Research*, vol. 361, pp. 7–13, 2019.

[14] C. Huang, Y. Wang, J.-S. Han, and Y. Wan, "Characteristics of electroacupuncture-induced analgesia in mice: variation with strain, frequency, intensity and opioid involvement," *Brain Research*, vol. 945, no. 1, pp. 20–25, 2002.

[15] L. M. P. Brod, M. G. Fronza, J. P. Vargas et al., "Involvement of monoaminergic system in the antidepressant-like effect of (octylseleno)-xylofuranoside in the mouse tail suspension test," *Progress in Neuro-Psychopharmacology & Biological Psychiatry*, vol. 65, pp. 201–207, 2016.

[16] X. y. Zhou, F. Zhang, C. j. Ying et al., "Inhibition of iNOS alleviates cognitive deficits and depression in diabetic mice through downregulating the NO/sGC/cGMP/PKG signal pathway," *Behavioural Brain Research*, vol. 322, pp. 70–82, 2017.

[17] M. E. Sorbero, K. Reynolds, and B. Colaiaco, "Acupuncture for major depressive disorder: a systematic review," *Rand Health Quaterly*, vol. 5, no. 4, 2016.

[18] F. Lopez-Rodriguez, J. Kim, and R. E. Poland, "Total sleep deprivation decreases immobility in the forced-swim test," *Neuropsychopharmacology*, vol. 29, no. 6, pp. 1105–1111, 2004.

[19] W.-Y. Huang, W.-W. Xu, and A.-N. Zhu, "Effects of electroacupuncture at auricular concha area on the circadian rhythm of melatonin secretion in p-chlorophenylalanine-induced insomnia rats," *TMR Non-drug Therapy*, vol. 3, no. 1, pp. 2–11, 2020.

[20] S.-J. Choi and D.-I. Kim, "A case report of primary ovarian insufficiency treated with Korean medicine treatment," *Korean Journal of Radiology*, vol. 32, no. 4, pp. 170–180, 2019.

[21] D. Chen, Y. Zhang, and C. Wang, "Modulation of hippocampal dopamine and synapse-related proteins by electroacupuncture improves memory deficit caused by sleep deprivation," *Acupuncture in Medicine*, vol. 2020, no. 964528420902147, 2020.

[22] Y. R. Kim, H. N. Kim, and S. M. Ahn, "Electroacupuncture promotes post-stroke functional recovery via enhancing endogenous neurogenesis in mouse focal cerebral ischemia," *PLoS One*, vol. 9, no. 2, 2014.

[23] W. C. Abraham, O. D. Jones, and D. L. Glanzman, "Is plasticity of synapses the mechanism of long-term memory storage?" *NPJ Science of Learning*, vol. 4, no. 1, pp. 1–10, 2019.

[24] S.-C. Liu, W.-Y. Hu, W.-Y. Zhang et al., "Paeoniflorin attenuates impairment of spatial learning and hippocampal long-term potentiation in mice subjected to chronic unpredictable mild stress," *Psychopharmacology*, vol. 236, no. 9, pp. 2823–2834, 2019.

[25] L.-Y. Xiao, X.-R. Wang, J.-W. Yang et al., "Acupuncture prevents the impairment of hippocampal LTP through β1-AR in vascular dementia rats," *Molecular Neurobiology*, vol. 55, no. 10, pp. 7677–7690, 2018.

[26] J.-Y. Oh, Y.-K. Kim, and S.-N. Kim, "Acupuncture modulates stress response by the mTOR signaling pathway in a rat posttraumatic stress disorder model," *Science Reports*, vol. 8, no. 1, pp. 1–17, 2018.

[27] L. E. Watkins, K. R. Sprang, and B. O. Rothbaum, "Treating PTSD: a review of evidence-based psychotherapy interventions," *Frontiers in Behavioral Neuroscience*, vol. 12, p. 258, 2018.

[28] M. Rahmani, F. Rahmani, and N. Rezaei, "The brain-derived neurotrophic factor: missing link between sleep deprivation, insomnia, and depression," *Neurochemical Research*, vol. 45, no. 2, pp. 221–231, 2020.

[29] Y. Zhi, J. Wu, S. Guo, S. Xie, and X. Zhou, "Effect of acupuncture and moxibustion on serum brain-derived neurotropic factor level, C-reactive protein, and zinc level in patients with depression," *Matrix Science Medica*, vol. 3, no. 2, p. 44, 2019.

[30] K. Schmitt, E. Holsboer-Trachsler, and A. Eckert, "BDNF in sleep, insomnia, and sleep deprivation," *Annals of Medicine*, vol. 48, no. 1-2, pp. 42–51, 2016.

[31] A. Misrani, S. Tabassum, M. Wang, J. Chen, L. Yang, and C. Long, "Citalopram prevents sleep-deprivation-induced reduction in CaMKII-CREB-BDNF signaling in mouse prefrontal cortex," *Brain Research Bulletin*, vol. 155, pp. 11–18, 2020.

[32] F. Raven, P. Meerlo, E. A. Van der Zee, T. Abel, and R. Havekes, "A brief period of sleep deprivation causes spine loss in the dentate gyrus of mice," *Neurobiology of Learning and Memory*, vol. 160, pp. 83–90, 2019.

[33] K. A. Alkadhi and I. A. Alhaider, "Caffeine and REM sleep deprivation: effect on basal levels of signaling molecules in area CA1," *Molecular and Cellular Neuroscience*, vol. 71, pp. 125–131, 2016.

[34] S. B. Baltaci, R. Mogulkoc, and A. K. Baltaci, "Molecular mechanisms of early and late LTP," *Neurochemical Research*, vol. 44, no. 2, pp. 281–296, 2019.

[35] M. A. Zagaar, A. T. Dao, I. A. Alhaider, and K. A. Alkadhi, "Prevention by regular exercise of acute sleep deprivation-induced impairment of late phase LTP and related signaling molecules in the dentate gyrus," *Molecular Neurobiology*, vol. 53, no. 5, pp. 2900–2910, 2016.